Investigation of industrial enzymatic cocktail for deconstruction of wheat bran by combining in-situ physical and ex-situ biochemical analyses

Marine Deshors

Université Fédérale
Toulouse Midi-Pyrénées

THÈSE

En vue de l'obtention du

DOCTORAT DE L'UNIVERSITÉ DE TOULOUSE

Délivré par :

Institut National des Sciences Appliquées de Toulouse (INSA de Toulouse)

Si vous êtes en cotutelle internationale, remplissez ce champs en notant : Cotutelle internationale avec "nom de l'établissement", sinon effacer ce texte pour qu'il n'apparaisse pas à l'impression

---

Présentée et soutenue par :
Marine DESHORS

le 11 juin 2018

Titre :

INVESTIGATION OF INDUSTRIAL ENZYMATIC COCKTAIL FOR DECONSTRUCTION OF WHEAT BRAN BY COMBINING IN-SITU PHYSICAL AND EX-SITU BIOCHEMICAL ANALYSES

École doctorale et discipline ou spécialité :
ED SEVAB : Ingénieries microbienne et enzymatique

Unité de recherche :
Laboratoire d'Ingénierie des Systèmes Biologiques et des Procédés (LISBP) - UMR 5504/792

Directeur/trice(s) de Thèse :

Jean Marie FRANÇOIS (PR INSA, LISBP, Toulouse, France)
Luc FILLAUDEAU (DR INRA, LISBP, Toulouse, France)

Jury :
Laurence LESAGE-MEESSEN (CR INRA, BBF, Marseille, France)
Rainer KRULL (PR, Institute of Biochemical Engineering, Braunschweig, Germany)
Guillaume DELAPLACE (DR INRA, UMET, Villeneuve d'Ascq, France)
Estelle BONNIN (IR INRA, BIA, Nantes, France)
Virginie NEUGNOT-ROUX (R&D manager, CINABio Adisseo, Toulouse, France)
Christine FRANCES (DR CNRS, LGC, Toulouse, France)
Dominique ANNE-ARCHARD (CR CNRS, IMFT, Toulouse, France)

Last-name: Deshors **First-name:** Marine
Title: Investigation of industrial enzymatic cocktail for deconstruction of wheat bran by combining *in-situ* physical and *ex-situ* biochemical analyses
Year: 2018 **Number of pages: 202**
Specialty: Microbial and Enzymatic Engineering **Place:** INSA Toulouse

ABSTRACT (EN)

Enzyme cocktails, such as Rovabio®, which is rich of hydrolytic enzymes are used as feed additives to favor degradation of non-starch polysaccharides present in wheat, a major feed in poultry industry. The deconstruction mechanism of wheat bran, part of the seed mainly composed of fiber, is still fairly unclear. This PhD aims to highlight these mechanisms using a multi-instrumented bioreactor that allowed to combine *in-situ* physical and *ex-situ* biochemical analyses. This multiscale approach stands as an alternative and original approach which is rarely considered in animal nutrition. This work highlights that Rovabio® action occurred in two concurrent process, namely fragmentation and solubilization phenomena which take place within the first 2 h after addition of the enzyme cocktail. It is then followed by a particle fragmentation which was not accompanied by any sugars solubilization. Thus, in spite of the abundant and very active hydrolytic enzyme activities in Rovabio®, the deconstruction of destarched wheat bran was however limited to 37% of w/w. At variance to Rovabio®, xylanase added alone was capable of solubilization activity (same final release of xylose and arabinose) but the fragmentation was much weaker by only disorganizing the fibrous network and hence led to particle disaggregation. Altogether, these results confirmed the importance of the enzyme mixtures which act in a synergistic manner to readily solubilize wheat bran. Our results also indicated that the limitation of Rovabio® action upon wheat bran degradation may come from physical inaccessibility of the substrate as it could be partially overcome by enhancing the substrate specific surface by a mechanical treatment and/or due to some missing or limiting enzyme activity as shown by a slight increase in solubilization following addition of some pectinases cocktails that are poorly represented in Rovabio®. Nevertheless, these complementary actions were still insufficient for complete hydrolysis of wheat bran. To conclude, this work draws attention to plant cell wall-deconstructing enzymes or active proteins which are able to attack the biomass minor structures and disorganize its network in order to increase substrate accessibility to enzymes that cleave backbone structures.

Nom de famille: Deshors **Prénom:** Marine
Titre: Etude de la déconstruction du son de blé par un cocktail enzymatique industriel en combinant des mesures physiques *in-situ* et biochimiques e*x-situ*.
Année: 2018 **Nombre de pages: 202**
Spécialité: Ingénieries microbienne et enzymatique **Lieu:** INSA Toulouse

RESUME (FR)

Les cocktails enzymatiques tels que Rovabio® sont utilisés en nutrition animale comme complément alimentaire pour aider les animaux à mieux assimiler les fibres présentes dans leur ration alimentaire composée principalement de blé en Europe. Le mécanisme de déconstruction enzymatique du son de blé, partie du grain majoritairement composée de fibres, considérées comme difficilement hydrolysables et donc assimilables reste encore incompris, c'est pourquoi ces travaux de thèse s'appuient sur l'utilisation d'un bioréacteur instrumenté combinant des analyses physiques *in-situ* et biochimiques *ex-situ* afin d'avoir un point de vue global de ce phénomène. Cette approche multi-échelle est originale car rarement considérée en nutrition animale où les études *in-vivo* sont privilégiées. Ces travaux ont ainsi permis de mettre en évidence que l'action de Rovabio® se caractérise par une première phase de fragmentation notamment des grosses particules concomitante avec une forte solubilisation. La déconstruction du son de blé se poursuit ensuite par une fragmentation mais cette fois sans aucune solubilisation de polysaccharides. L'ajout d'une xylanase seule, en tant qu'enzyme la plus active du cocktail, solubilise la même quantité d'arabinoxylane mais ne permet pas une fragmentation importante des particules, contrairement au Rovabio®. Ces résultats confirment donc l'importance de la richesse et de la diversité d'un cocktail enzymatique pour déconstruire efficacement des structures aussi complexes que le son de blé. Cependant, en dépit de cela, seulement 37%w/w de matière sèche est solubilisée, même en excès de Rovabio®. Cette incapacité du cocktail enzymatique à dégrader complètement ces fibres semblerait provenir d'une inaccessibilité des enzymes à leur substrat. Nous avons ainsi montré que le rendement d'hydrolyse enzymatique est amélioré en augmentant, mécaniquement, la surface spécifique des particules et/ ou en désorganisant l'architecture de la structure des fibres par l'ajout d'un complexe enzymatique particulièrement riche en pectinases. Néanmoins, si ces deux voies améliorent les performances du cocktail, elles ne permettent toujours pas une hydrolyse totale du son de blé. Finalement ce travail souligne l'intérêt d'enzymes ou de protéines actives capables d'attaquer les structures minoritaires du réseau lignocellulosique assurant sa résistance et sa cohésion, ce qui permet ainsi aux enzymes d'avoir un meilleur accès à leurs substrats.

REMERCIEMENTS

La réalisation de cette thèse n'aurait pas été possible sans la contribution de nombreuses personnes. Pour cette raison je voudrais adresser mes sincères remerciements à toutes les personnes qui ont participé au bon déroulement de ces 3 années.

Je voudrais tout d'abord remercier mes rapporteurs, le professeur Rainer Krull, Guillaume Delaplace et Estelle Bonnin d'avoir accepté d'examiner mon manuscrit de thèse. Merci aussi à Laurence Lesage-Messen d'avoir participé à mon jury de thèse ainsi qu'aux autres membres invités d'avoir accepté d'évaluer ce travail. Merci aux membres de mon comité de thèse : Cécile Albenne, Dominique Anne-Archard, Sébastien Dejean de m'avoir accompagné au cours de ces trois ans.

J'adresse aussi mes remerciements à M. Nicholas Lindley et à Mme Carole Molina Jouve qui a pris sa relève à la direction du Laboratoire d'Ingénierie des Systèmes et des Procédés, d'avoir permis le déroulement de cette thèse au sein de cette unité de recherche. Merci à Claude Maranges, directeur de l'école doctorale SEVAB ainsi qu'à Dominique Pantalacci pour leurs disponibilités.

Merci à Adisseo d'avoir financé cette thèse CIFRE et plus particulièrement à Olivier Guais et Marc Maestracci de m'avoir fait confiance pour ce projet et accompagné durant ces travaux de thèse. Merci à Virginie Neugnot-Roux ainsi qu'à Laurent Desrousseaux d'avoir repris le projet en cours de route et pour leurs implications.

Merci à toute l'équipe du CINAbio pour votre accueil, votre gentillesse, tous ces moments partagés et ce doux accent Belgo-Canadien qui va me suivre un moment !

Je tiens à exprimer ma plus profonde gratitude et mes sincères remerciements à mes deux directeurs de thèse Jean Marie François et Luc Fillaudeau. Jean-Marie, merci pour tous les échanges scientifiques autour de mon sujet de thèse et de m'avoir fait confiance pour la continuité de ce projet aujourd'hui. Je voudrais te remercier plus particulièrement pour ton implication dans les derniers mois de thèse notamment pour la correction de ce manuscrit et de « mon anglais ». Merci Luc d'avoir pris le temps d'approfondir mes connaissances dans tous les aspects plus « physiques » de cette thèse que je maitrisais moins ainsi que pour les nombreuses séances de formations aux techniques d'analyses envisagées.

Un immense merci à Xavier Cameleyre, « le 5ème papa » ayant encadré cette thèse pour avoir apporté à ce projet ses connaissances en enzymologie mais surtout pour avoir toujours répondu présent dès que j'ai eu besoin de son aide ou de son soutien.

Merci à toutes les personnes qui m'ont apporté leurs expertises et avec qui j'ai eu la chance de collaborer : Christine Frances, Dominique Anne-Archard, Sebastien Dejean, Claire Dumas, Pierre-Alain Hoffman et François Rizzetto. Un pensée aussi pour Audrey Arcache, Nelly Martineau et Angeline Rizzo, côté Adisseo, merci pour votre aide et pour le trafic d'enzyme! Côté LISBP merci à Florence et Lucie pour la partie analytique, merci à Eric et Carine d'avoir

été toujours disponibles en cas de soucis techniques ou informatiques et enfin merci à Marion de m'avoir épaulé au départ pour les analyses biochimiques.

Je voudrais aussi remercier mes deux stagiaires Wenxiu Hu et Salomé Plat qui ont aussi participé à ce travail notamment au niveau des analyses biochimiques.

Enfin un grand merci à mes deux équipes au LIBSP, l'EAD5 et l'EAD8 qui m'ont accueilli en garde alternée au cours de cette thèse ! Merci pour tous ces moments partagés dans un de mes 3 bureaux, à la paillasse ou lors des divers évènements de team-building dont je ne détaillerai pas les diverses anecdotes ! Merci à tout le groupe du bureau-café-aquarium dans laquelle j'ai débarqué en début de thèse : Luce, Cléa, Marie, Manon, Rozenne, Arthur et Charles, cette année ensemble a réellement été riche en aventures et en émotions en tout genre ! Merci à Catherine et Yassim pour les sorties footing où j'ai essayé tant bien que mal de vous suivre ! Une pensée aussi pour Arnaud, Florence, petite Marine, Nicolas (et ses pieds sur mon bureau !), Elodie, Yannick, Carlos, Asma, Xiaomin, Victoria, Céline, Pablo, Olivier, Cuong, Tuan, Rana, Bérengère, Julie, Louna, Susana, Lucile, Elise, William et bien sûr côté permanent Stéphane, Xavier, Sandrine, Nathalie, Eric, Carine, Julie, Elodie, César, Carole, Jean-Louis, Stéphanie et bien sûr Philippe. Côté EAD5 merci à Lucie, Claudio, Clara, Sevan, Jian, Luce, Cathy, Agustina, Nuria, Rebbeca, Ceren, Yvan, Pablo(s) pour tous ces moments partagés aussi bien au laboratoire qu'en dehors. Merci à Jean-Luc, Jean-Pascal, Hélène, Didier, Marie-Ange. Un merci particulier à Marion avec qui, en digne voisine de paillasse, j'ai partagé de longues discutions, des complaintes, des rires mais aussi finalement des sorties en tout genre et même du « bunny-sitting ». Enfin un petit mot pour Cléa, qui aura été un binôme hors-pair et sans qui beaucoup de journées n'auraient vraiment pas été les mêmes! Bref après 3 ans, 46589 aventures, 3589 pauses-café « faut que je te raconte un truc ! », 353 plats Picards avalés, 7 décorations de bureaux, 3 disputes de vieux couples, je pense que le duo Catounette & Foxynette a encore de beaux jours devant lui !

Pour finir je tiens à remercier Arnaud et ma famille pour leurs soutiens de tous les jours. Merci « aux copains » pour, comme vous me l'avait souvent dit en période de rédaction, « m'avoir permis de prendre non pas du retard mais du recul sur mon travail et avoir ainsi participé à la qualité de ce manuscrit » !

PUBLICATIONS AND COMMUNICATIONS

Publications

Marine Deshors, Olivier Guais, Virginie Neugnot-Roux, Xavier Cameleyre, Luc Fillaudeau, Jean Marie François: Deconstruction mechanism of wheat bran by enzymatic cocktail revealed by a combined in-situ physical and ex-situ biochemical study *(Submitted to Frontiers).*

International communications

Marine Deshors, Xavier CAMELEYRE, Olivier GUAIS, Luc FILLAUDEAU, Jean Marie FRANCOIS (2017): Multiscale approach for understanding the deconstruction of destarched wheat bran by an industrial enzyme cocktail. *10^{th} World Congress of Chemical Engineering, 11^{th} European Congress of Chemical Engineering and 4^{th} European Congress of Applied Biotechnology (WCCE10 + ECCE10 + ECAB4), Barcelona, Spain.*

TABLE CONTENT

LIST OF FIGURES

LIST OF TABLES

ABREVIATIONS

Abf	:	Arabinofuranosidases
AX	:	Arabinoxylan
CBM	:	Carbo-binding module
CLD	:	Chord Length Distribution
Cm	:	Dry Matter Concentration (g/L)
DLS	:	Diffraction Light Scattering
DM	:	Dry Matter
DNS	:	3,5-Dinitrosalicylic acid
D_{CE}	:	Diameter of circle equivalent (µm)
D_{se}	:	Diameter of sphere equivalent (µm)
dWB	:	Destarched wheat bran
FBRM	:	Focused Beam Reflectance Measurement
FTIR	:	Fourier Transform Infrared Spectroscopy
GH	:	Glycosyl Hydrolase
H	:	Height
HPAEC – PAD	:	High Performance Anion Exchange Chromatography – Pulsed Amperometric Detection
Kp	:	Power constant (/)
Ks	:	Metzner-Otto coefficient (/)
l_c	:	Chord length (µm)
MG	:	Morphogranulometry
Nc	:	Number of chord counted (/)
Np	:	Mixing power number (/)
Np_0	:	Mixing power number for turbulent flow (/)
NSP	:	Non-Starch Polysaccharides
NSPase	:	Non-Starch Polysaccharide hydrolases
PSD	:	Particle Size Distribution
Re	:	Mixing Reynolds number (/)
RPM	:	Rotation per minute (1/min)
tr	:	Turns
XynC	:	Endo-xylanase type C

GENERAL INTRODUCTION

GENERAL INTRODUCTION

INTRODUCTION AND CONTEXT OF THE STUDY

The aim of the digestive system is to convert feed into molecules necessary for the proper functioning of the organism. Therefore, the digestive system breakdowns feed into smaller components, until their absorption into blood flow and assimilation by the body. Poultry, pigs, rabbits or horses are monogastric animals as they have only one stomach. For poultry, digestion and nutriments absorption are efficient. Digestive system is short with a fast transit which allows to digest even concentrated feed. Currently, poultry are adapted to intensive farming and have still increased their digestive capacities. A 30 day old male broiler chicken consumes around 10 % of its live weight per day, and digest over 7 g of feed per hour. To put this in perspective, a 75 kg person would have to eat more than 450 g per hour during the 16 awake hours to have an equal food intake (Svihus, 2014). However, if monogastric digestive system is efficient, it is not optimal as 15 to 25% of feed intake are not digested (Bedford and Partridge, 2011). In animal farming, feed represents commonly the major expense (around 70% for pig and poultry) and therefore reducing this cost appears as a priority (FAO, 2017). Animal diet composition is based on wheat and barley in Europe which both contain a high level of fibers and therefore of non-starch polysaccharides (NSP). The negative impacts of NSP are well-established: (i) they are non-digestible by the monogastric, especially poultry due to their lack of specific hydrolytic enzymes, (ii) they prevent accessibility of some nutrients (starch and proteins) as these latter are trapped within the fibrous network (Bedford and Partridge, 2011), (iii) they can act as chelators of minerals such as Ca^{2+} or Fe^{2+} (Ravindran, 2013), and (iv) they may reduce nutrients adsorption due to their high molecular weight that enhance the viscosity in gut's animal (Lafond et al., 2015).

The introduction of enzymes in feed technology in Europe in the 1980's revolutionized the poultry industry. It was found that addition of enzymes such as xylanases and β-glucanases to feed had significant benefit in animal performances likely due to better uptake and assimilation of these non-digestive polysaccharides. The next major improvement in poultry nutrition came in the 1990's with the introduction of phytase enzyme as feed additives. Phytase is a type phosphatase that catalyzes the release of phosphate from phytic acid (myo-inositol hexakisphosphate) which is abundant in grains and oil seeds as a storage form of phosphorus. In the plant, phytate form complexes with minerals, proteins and starch, making them also unavailable for absorption. The usage of this enzyme responds to environmental legislations in

some countries to significantly reduce the phosphorus excretion by pigs and poultry. In addition, by improving phosphorus absorption phytase not solely provides an environmental benefit but can obviate the use of external addition of phosphorus, and hence contributes to a reduction of the feed cost (Bedford and Partridge, 2011).

In terms of growth potential, this market turns towards maize-based diets for NSPase enzyme products. The potential is huge because about 80% of global pigs and poultry feed is based on maize but only one third is supplemented by enzymes. Meantime, the increase of the world population and the higher global personal consumption of milk, egg and meat in developing countries are the market key drivers of demand. Currently, the market should attempt 1 371.03 million of dollars in 2020 with a mean compounded annual growth rate of 7.3% between 2015 and 2020 (Marketsandmarkets.com, 2015). Nowadays, the commercialized enzymatic additives target mainly fibers or phytate and have at least 5 advantages:

- Increase the availability and digestibility of starch, proteins, amino acids and minerals (phosphorus and calcium) and reduce chyme viscosity (Bedford and Partridge, 2011).
- Improve the feed nutritional constancy especially for wheat- and barley-based nutrients.
- Have a positive effect on animal health by (i) reducing the presence of polysaccharides in animal intestine that prevents the development of pathogenic bacteria, (ii) ensuring a better integrity and morphology of the intestine (Ravindran, 2013) and (iii) decreasing moisture content of excreta and thus of the litter that prevents various animal troubles and diseases.
- Decrease the quantity of excreta and the environmental impact of animal farming especially water pollution by phosphorus and nitrogen released as gas (Mottet and Tempio, 2017).
- Enzymes guaranty safety and quality in food industry as there is no trace into meat or eggs due to their digestion at the end of the digestive tract or their excretion.

Although the benefits of such enzymatic additives are well-established, their mechanisms of action to deconstruct NSP remain unclear. Considering the complexity of both enzyme cocktails and plant biomass substrates, traditional *in-vitro* methods that investigate the action of hydrolytic enzymes (either individually or in a mixture) on the NSPs solubilization in test tubes, seems to be a time-consuming work. Therefore a global approach using a multi-instrumented bioreactor to investigate *in-situ* physical deconstruction of biomass and combining with *ex-situ* biochemical measurements, appears to be an interesting strategy especially as different kind of experimental data are collected. Regarding the literature, such an approach is original in animal nutrition where *in-vivo* experiments represents 85% of the studies about enzymes cocktail efficiency (based on 321 articles studying enzyme additives in animal

nutrition). The added value of this approach is to obtain rheological (viscosity and suspension behaviour), morphogranulometric (size distribution and number of particles) and biochemical data (sugars and other components released) that can be exploited to infer relationships between macrostructure and microstructure, fragmentation and solubilization of suspended material occurring during the biomass degradation. Considering transfer limitation, this multiscale approach is also well adapted to investigate effects of any combination of enzyme mixtures. As a matter of fact, this methodology has been previously developed to investigate the deconstruction of lignocellulosic material such as paper pulp and sugarcane bagasse under semi-dilute conditions by pure or mixture of cellulolytic enzymes (Le, 2017; Nguyen, 2014). The aim of the present study is to transpose this strategy and methodology in order to investigate the deconstruction of the wheat-based feed recalcitrant fraction, as reference substrate, by a commercially available enzymatic cocktail termed Rovabio®.

OUTLINES OF THE THESIS

The thesis is structured in three parts as follows:

The first part of the manuscript (*chapter 1*) deals with a review on polysaccharide composition and structure with a specific attention to wheat bran as this was the reference matrix chosen in this work. In this first part, I also present a short overview of the large panel of enzymes able to deconstruct and degrade plant cell wall, with a specific regard to enzymes needed to solubilize NSPs. This first part is concluded by a short overview of previous studies on enzymes efficiency as feed additives in animal nutrition.

The "Results and Discussion" which constitutes the third part and the main body of the thesis section is organized in three chapters:

Chapter 2 is devoted to define and characterize a reference substrate that responds to several technical criteria, notably being highly enriched in NSPs and obviously largely used in animal feed. Our choice was therefore wheat bran which requires to be destarched as its non-negligible amount of starch was found to interfere significantly with our measurements. This chapter is also dedicated to the evaluation of the more convenient physical measurements as well as biochemical methods for biomass (sugar, protein) quantification. A specific integrated approach was set-up from macroscopic (*in-situ* physical measures) to molecular scale (biochemical measures) and adapted to the specificities of our operating conditions and reference substrate retained.

Chapter 3, reports and discusses on the mechanism by which the destarched wheat bran (dWB) is deconstructed in the presence of Rovabio Advance and compares the action of this enzyme cocktail with xylanase C as the major active NPase present in this commercial cocktail. The deconstruction process has been studied at different levels of observation, from macro scale (on-line viscosimetry); micro scale (DLS for Diffraction Light Scattering and FBRM for Focused Beam Reflectance Measurement) to molecular scale (biochemical analysis). *In-situ* viscosimetry provides information related to the liquefaction mechanisms, *in-* and *ex-situ* granulometry gave quantitative data on the evolution of particle size during enzymatic hydrolysis. The biochemical analyses provide quantitative data concerning mass balance, sugars and proteins released during the enzymatic treatment of dWB. Results of this work lead to the finding that only 30% of the whole dWB dry matter is deconstructed and solubilized by Rovabio in spite of its high content of hydrolytic enzymes, raising the question whether this limitation is physical and/or biochemical.

This question is addressed in ***the fourth chapter*** of my thesis. Experimental data showed that it was the presence of a recalcitrant fraction that explained this limitation and not the enzymes inhibition by the products of the reaction. In this chapter, we report on the finding that increasing the global surface of wheat bran particles by a milling treatment further enhanced its deconstruction and solubilisation, as well as the addition of large excess of pectinases which showed a boosting effect on sugar release. Altogether, it is anticipated from these preliminary results that we foresaw various ways to improve the Rovabio® efficiency in the deconstruction of substrates with high content of NSPs including wheat bran.

In the last part of the thesis (*chapter 5*), I provide a **general discussion** on the main results that I have obtained according to my original strategy to investigate deconstruction and solubilisation of wheat bran. I draw then several **conclusions** on the advantage of this approach to investigate the deconstruction of other substrates, as well as their hypothetic limitations. I finally provides some **perspectives** and guidelines about what could be the next steps of this work, and in particular what strategies can be applied to further enhance the potential of Rovabio in deconstructing/ solubilizing substrates containing recalcitrant polysaccharides commonly used for animal feed.

Details about the "**Materials and methods"** are presented in a supplementary chapter (***Chapter 6***).

CHAPTER 1:

LITERATURE REVIEW

CHAPTER 1. LITERATURE REVIEW

The objective of this literature review is to present an overview of the complexity in the structure and biochemistry of polysaccharides that are present in plants with a particular focus on cereal fibre structure. I will also overview the various enzymes capable and necessary to deconstruct, depolymerise and solubilize these complex polysaccharides as they represent a large source of carbon. I will finally expose the purpose of using enzyme cocktail as feed additives in animal nutrition and briefly how is investigated the efficiency of these additives on animal performances.

1.1. Wheat bran and its enzymatic degradation

Wheat (Triticum aestivum) is one of the main cereals used in human and animal nutrition. It is a major energy source of broilers feed worldwide due to its high content of starch (Amerah, 2015). However, this cereal also contains 12 to 15 % of NSPs (Knudsen, 2014; Onipe et al., 2015) which represents a recalcitrant and non-digestible fraction by animals.

1.1.1. Structure and biochemical composition of wheat bran

A wheat kernel comprises three principal fractions: 80-85% endosperm, 2.5-3.0% germ and 10-14% bran (**Figure 1-1**) (Fardet, 2017). Albumen or starchy endosperm represents a storage organ constituted by starch granules encased in a protein network mainly composed of gluten. After milling process, this part of the grain leads to wheat meal. Germ represents a small part of the grain (3%) constituting the future plant and ensuring its genetic identity. Wheat bran consisting of kernel outer layers, is a co-product from milling industry used for about 90% in animal nutrition and the remaining is used in food industry as breakfast cereals (Hossain et al., 2013).

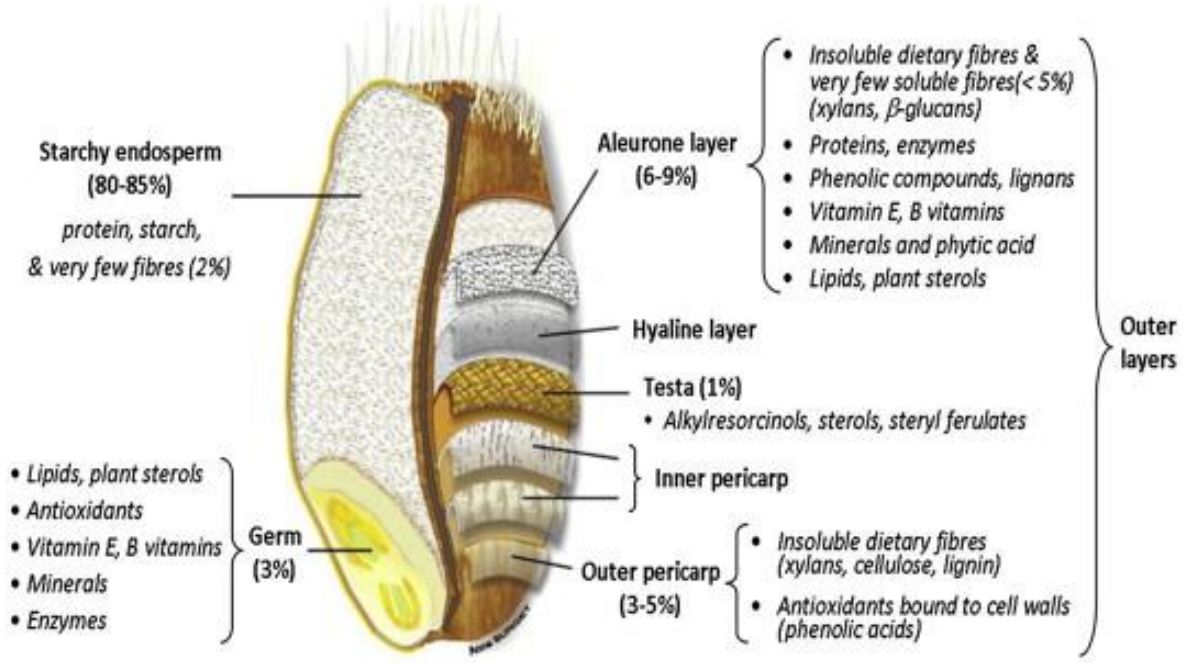

Figure 1-1. Wheat kernel structure *(Onipe et al., 2015), adapted from Surget & Barron (2005) and Brouns et al. (2012) with permission.*

Wheat bran is a superposition of several envelops constituting a physical and chemical protective barrier for endosperm and germ (Antoine et al., 2003). Three distinct layers are identified: aleurone, testa and pericarp (**Figure 1-2**). Aleurone also called protein husk is the innermost layer of bran and is composed of large living cells surrounded by a thick cell wall made of lignin, proteins, lipids, phenolic compounds and also containing vitamins, minerals and phytic acid (Prückler et al., 2014). Testa is a multi-layered complex material mainly composed of lignin and containing one or two layers of compressed cells enriched with lipids and phenolic acids. The pericarp is divided into outer and inner layers containing insoluble fibers and bounded phenolic acids (Parker et al., 2005). Walls of the outer layers cells are thick, hydrophobic and are mainly composed of cellulose and hemicelluloses (mainly xylan) with an important content of lignin (Knudsen, 2014).

A global composition of wheat grain and wheat bran is reported in the **Table 1-1**. In general, wheat bran is composed of approximatively 57 % of carbohydrates, 13-18% of protein, 3.5% of fat and 12% of water. These values can differ according to analytical methods, milling technology, cultivar variety and growing area (Apprich et al., 2014; Prückler et al., 2014).

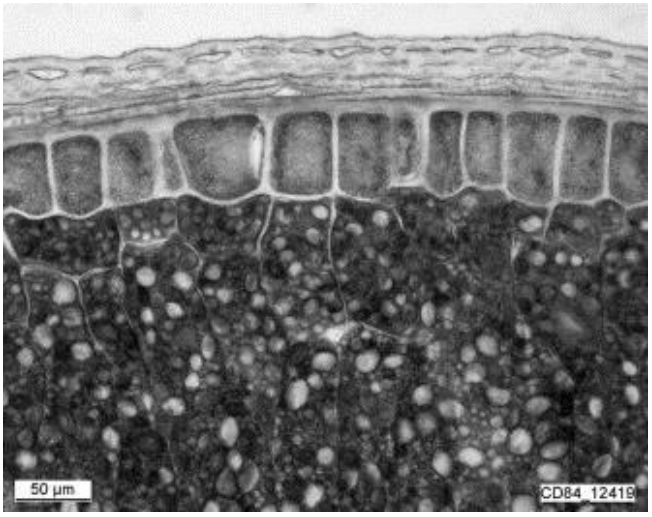

Figure 1-2. Histological section of wheat kernel *(Apprich et al., 2014)*

Table 1-1. Wheat bran composition (Apprich et al., 2014; Fardet, 2017; Heuzé et al., 2016, 2015)

Compound	**Content in whole grain [%DM]**	**Content in wheat bran [%DM]**
Sugars		
- Monosaccharides	0.26 - 1.30	0.14 - 0.63
- Sucrose	0.60 - 1.39	1.8 - 3.4
Starch	61.8 – 74.9	13.0 - 38.7
Fibers		
- Total	9.0 - 17.3	35.7 - 53.4
- Cellulose	2.1 - 2.8	6.5 - 9.9
- Hemicelluloses	8.6	20.8 - 33.0
Total arabinoxylan	1.2 - 6.8	5.0 - 26.9
Total β-glucan	0.2 - 1.2	1.1 - 2.6
- Lignin	0.9 - 2.8	2.5 – 4.8
Protein	8.9 – 19.2	13.4 - 21.1
Fat	0.9 - 2.9	2.0 - 6.4
Ash	1.2 - 3.1	3.4 - 8.1

Fibres correspond to the non-starch polysaccharides (NSP) and lignin content of the grain. These NSPs are a highly heterogeneous material with a complex structure in plant cell wall representing about 46% of its dry mass and containing arabinoxylan, cellulose and β-glucan at ratio of about 70, 24 and 6% (Maes and Delcour, 2002).

1.1.2. Plant cell wall structure and composition

One of the main characteristic of terrestrial plant cell is to be surrounded by a strong wall. Plant cell wall provides support and shape for the plant but also constitutes a protective barrier against environment and pathogenic organisms. It is a structure metabolically active allowing

exchange of molecules and signals (Burton et al., 2010; Scheller and Ulvskov, 2010). The plant wall is composed of polysaccharides, proteins and in some cases of phenolic compounds. This polysaccharide composition consists of hemicelluloses, cellulose and pectin whose association /interaction depends on plant species and tissues (see below). Upon growth arrest, some plant cells develop a secondary wall which gives them additional strength and resistance. Phenolic compounds, notably lignin, represent 30% of this secondary wall (Scheller and Ulvskov, 2010).

1.1.2.1. Plant cell wall structure

Plant cell wall components interact to each other resulting in a complex macrostructure (**Figure 1-3**). Cellulose represents the rigid frame, making microfibril structure and hemicelluloses are the crosslinking polysaccharide of the wall (Wertz, 2011). Structural similarity between cellulose and hemicellulose components promotes a strong non-covalent association between the cellulose microfibrils and hemicelluloses network. Hemicelluloses are also bond to other cell wall components such as protein, lignin and phenolic compounds by either covalent bounds, hydrogen bonds, ionic interactions or hydrophobic interactions (Sun et al., 2000). Pectin acts as the cement of the structure and fills in the remaining space (Cosgrove, 2000). For plant cells with a secondary wall, lignin provides a strong barrier by bounding cellulose to hemicellulose, which prevent enzyme penetration inside the structure (Dashtban et al., 2009).

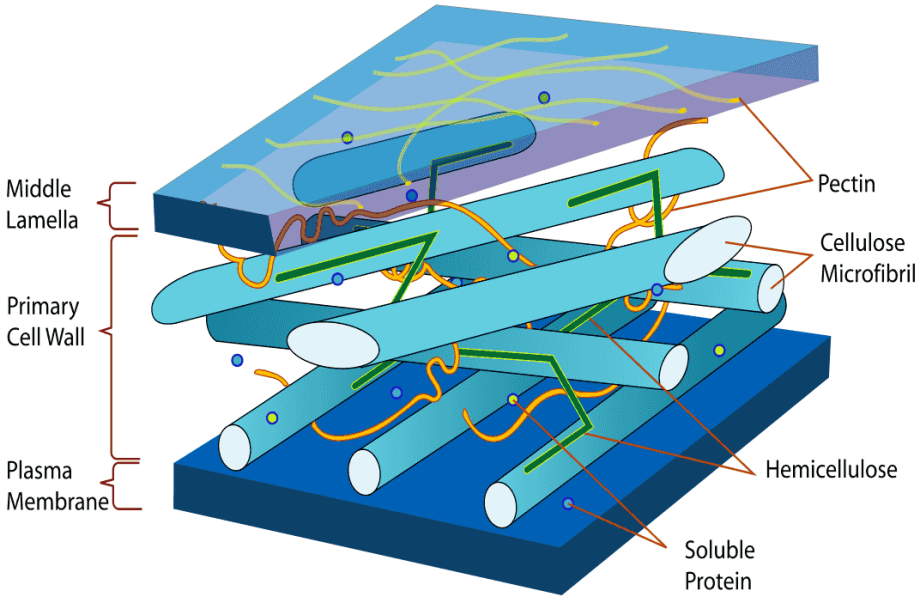

Figure 1-3. Plant cell wall structure

1.1.2.2. Cellulose composition

Cellulose is a one of the main component of plant cell wall. Cellulose consists of linear β-1,4-linked D-glucose chains (up to 15 000 residues). Up to 18 of β-1,4 glucan chains are condensed by hydrogen bonds into crystalline structures, termed microfibril (Newman et al., 2013). The microfibril form is an organized network with (i) crystalline regions where microfibrils are orientated in parallel and strongly linked each other by hydrogen bonds, hydrophobic interactions or Van der Waal's forces and (ii) amorphous regions where microfibrils are less organized (Dashtban et al., 2009).

1.1.2.3. Hemicellulose composition

The term hemicelluloses describes polysaccharides from higher plants extractible with alkaline solutions (Schulze, 1891). Hemicelluloses are branched polymers with low-molecular-weight and a degree of polymerization between 80 and 200 (Peng et al., 2012). Polysaccharides which compose this gel-like matrix are structurally complex and present an important heterogeneity in terms of sugars composition as reported in **Figure 1-4** (Burton et al., 2010). Monomers of C5 (xylose and arabinose), C6 (glucose, mannose, galactose, galacturonic acid) and C7 carbon (4-*O*-methylglucuronic acid) can be found in the composition of the hemicellulosic polymers (Wertz, 2011). These polymers have a backbone composed of β-1,4-D-pyranose residues which could be substituted by side residues of sugar monomers (Scheller & Ulvskov, 2010). Various groups are distinguished according to backbone composition and the nature of side residue(s): xylan, glucuronoxylan, arabinoxylan, glucomannan, xyloglucan…

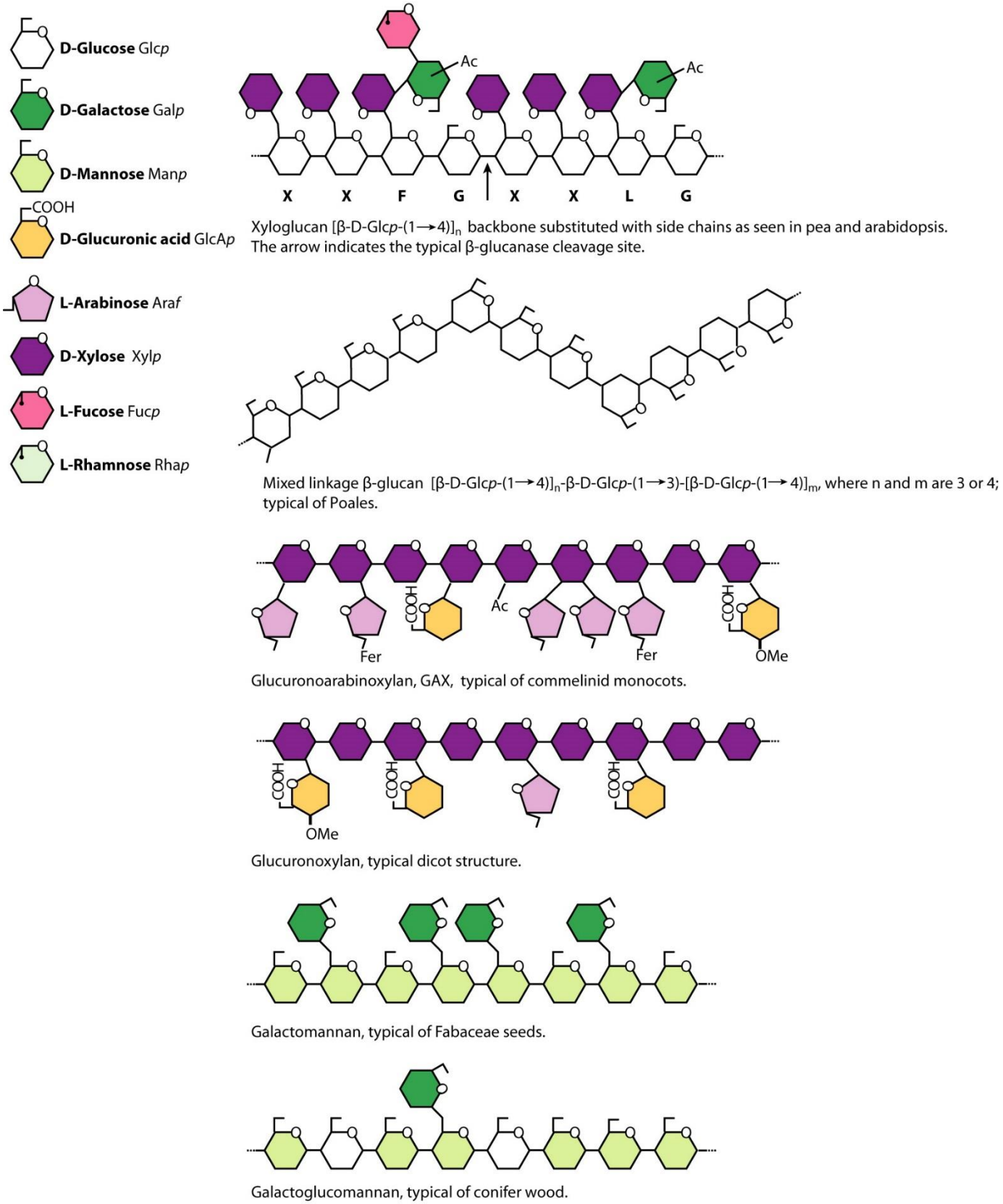

Figure 1-4. Heterogeneity in structure of cell wall hemicelluloses in plants *(Scheller and Ulvskov, 2010)*

- **Xyloglucans**

Xyloglucans are a component of the primary wall of many plants able to cross-link cellulose microfibrils via hydrogen bounds (Peng et al., 2012). This type of polysaccharide has a cellulosic β-1,4-glucan backbone substituted with α-1,6-linked xylose residues. These polymers are made of repetitive units and a special one-letter code is used to describe their structures: G refers to a non-substituted glucose, X to a glucose bound to a xylose side residue and L and F refer to glucose with a xylose side residues substituted by β-1,2-linked galactose or α-1,2-linked fucose residues respectively (**Figure 1-5**) (Scheller and Ulvskov, 2010). While typical xyloglucan oligosaccharides motifs are XXXG, XLXG, XXFG, XLLG et XLFG (Von Schantz et al. 2009), the major ones in plants cell wall are XXXG et XXGG with 75% and 50% of substituted glucose respectively (de Vries et al., 2001). The motif XXXG is thus the most abundant in most of the terrestrial plants (Wertz, 2011).

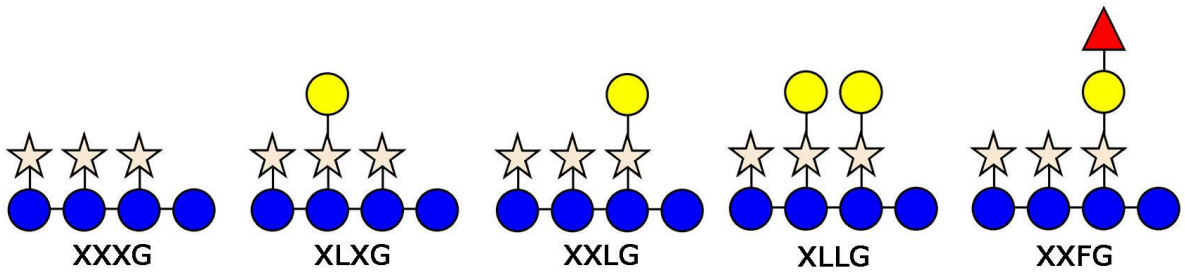

Figure 1-5. Xyloglucan building block. *The building blocks are composed of glucosyl units (blue circle) joined together by β-1,4-linkages, to which α-1,6-linked xylosyl units (orange star) may be added. Galactose (yellow circle) and fucose (red triangle) are incorporated into these structures via β-1,2- and α-1,2-linkages, respectively (von Schantz et al., 2009)*

- **Xylans**

Xylans are a heterogeneous group of polymers having a common backbone of β-1,4-linked xylose residues with a wide variety of side residues, except homoxylan which refers to unsubstituted xylan . The degree of polymerization xylan backbones depends on the nature of the plants. Xylan backbone can be substituted in C2, C3 or both by α-1,3-linked arabinofuranose residues. Other substituents can be glucuronic acid and 4-*O*-methylated derivatives that exhibit α-1,2-linkages (Burton et al., 2010) to the C2 of xylose backbone, as well as by an acetyl group in C2 and/or C3 position. Hence, arabinoxylan, glucuronoxylan and glucuronoarabinoxylan are referring to xylan backbone with arabinose, glucuronic acid and both types of sugars substitution respectively. Glucuronoxylans and glucuronoarabinoxylans have a degree of polymerization of about 200 and from 50 to 185 monomers, respectively (Wertz, 2011).

Contrary to xyloglucans, xylans do not have a regular structure based on the repetition of oligosaccharide subunits. Physical properties such as viscosity or solubility are strongly affected by the type and nature of the side chains that decorate the linear polymeric chains (Ebringerová et al., 2005). Xylans are linked to lignin as its arabinose side residues could be esterified with hydroxycinnamic acids of lignin such as ferulic or p-coumaric acids. These linkages between lignin and polysaccharides confers their solidity to the plant walls and their recalcitrance to enzymatic degradation (Wertz, 2011).

- **Galacto(gluco)mannans**

Mannans have a backbone of β-1,4 linked D-mannose residues while glucomannans have a backbone of both D-mannose and D-glucose residues which are also β-1,4-linked. These two types of backbones could be α-1,6-linked to D-galactose residues and then called galactomannans and galactoglucomannans. Galact(gluco)mannans are frequently acetylated (Scheller and Ulvskov, 2010; Wertz, 2011).

- **β-glucans**

Glucans are unbranched chains of D-glucosyl residues bound by β-1,3- or β-1,4-linkages. In plant primary-wall, these β-glucans have a major role in cell expansion and their compositions depend highly on growth status (Burton et al., 2010).

1.1.2.4. Pectins

Pectin is a highly heterogeneous polymer present in hemicellulose network which contributes to the mechanical strength, porosity, adhesion and stiffness of the cell wall (Burton et al., 2010). Pectin backbones consist of galacturonic acids or have an alternance of galacturonic acid and rhamnose in their main chain (**Figure 1-6**). Four types can be distinguished: homogalacturonan, xylogalacturonan, rhamnogalacturonan I and rhamnogalacturonan II linked to each other by covalent linkages (Burton et al., 2010).

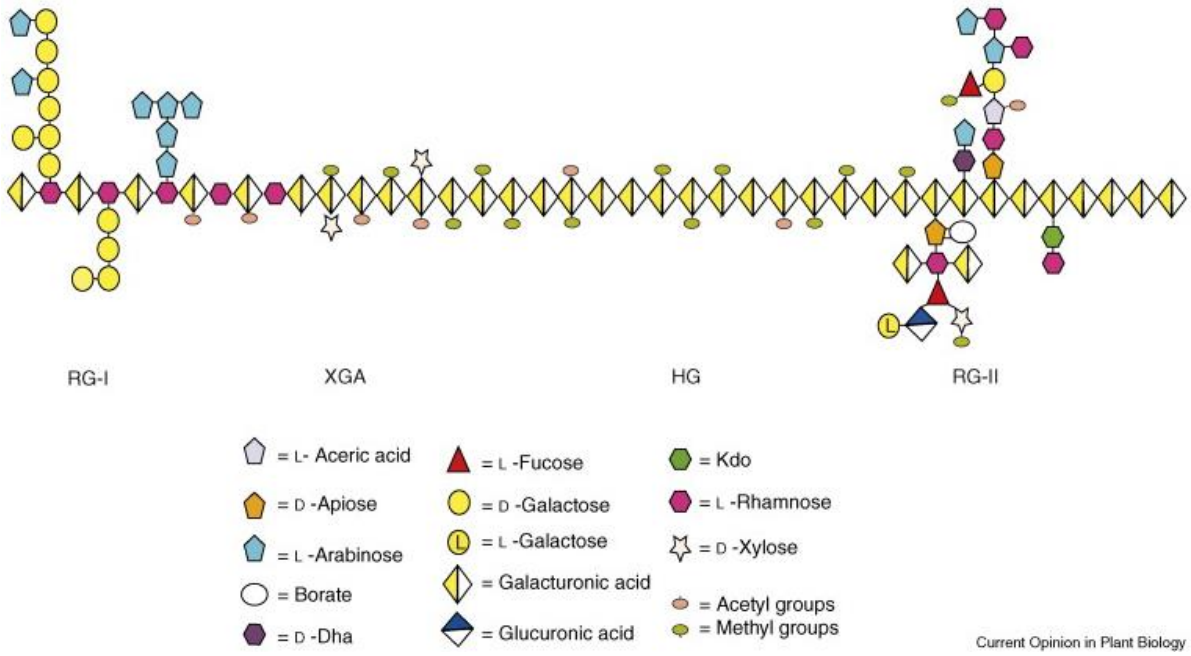

Figure 1-6. Schematic pectin structure showing the four pectin polysaccharides homogalacturonan (HG), xylogalacturonan (XGA), rhamnogalacturonan I (RG-I) and rhamnogalacturonan II (RG-II) linked to each other *(Mohnen, 2008)*

1.1.2.5. Lignin composition

The term lignin derives from the Latin word 'lignum', which means wood. Lignin is the third major component of plant cell wall and the most abundant renewable aromatic polymer on Earth (Dashtban et al., 2009). This polymer is mainly present in plant secondary wall, making plant cells rigid and impermeable (Wertz, 2010). Chemically, it is a cross-linked macromolecular material derived from oxidative coupling of monolignols, mainly hydroxycinnamyl alcohols (Pollegioni et al., 2015). It is composed of non-phenolic (80-90%) and phenolic structures, which are mainly *p*-coumaryl, coniferyl and synapyl alcohols (**Figure 1-7**). Lignin has been identified as a limiting factor in enzymatic degradation of plant cell wall. It furthermore shows a plant-specific composition, with molecular weight and linkage motifs varying according to plant species and environmental factors. Wheat bran consists of only about 4% of lignin (Brillouet and Mercier, 1981; Chotěborská et al., 2004; Lequart et al., 1999).

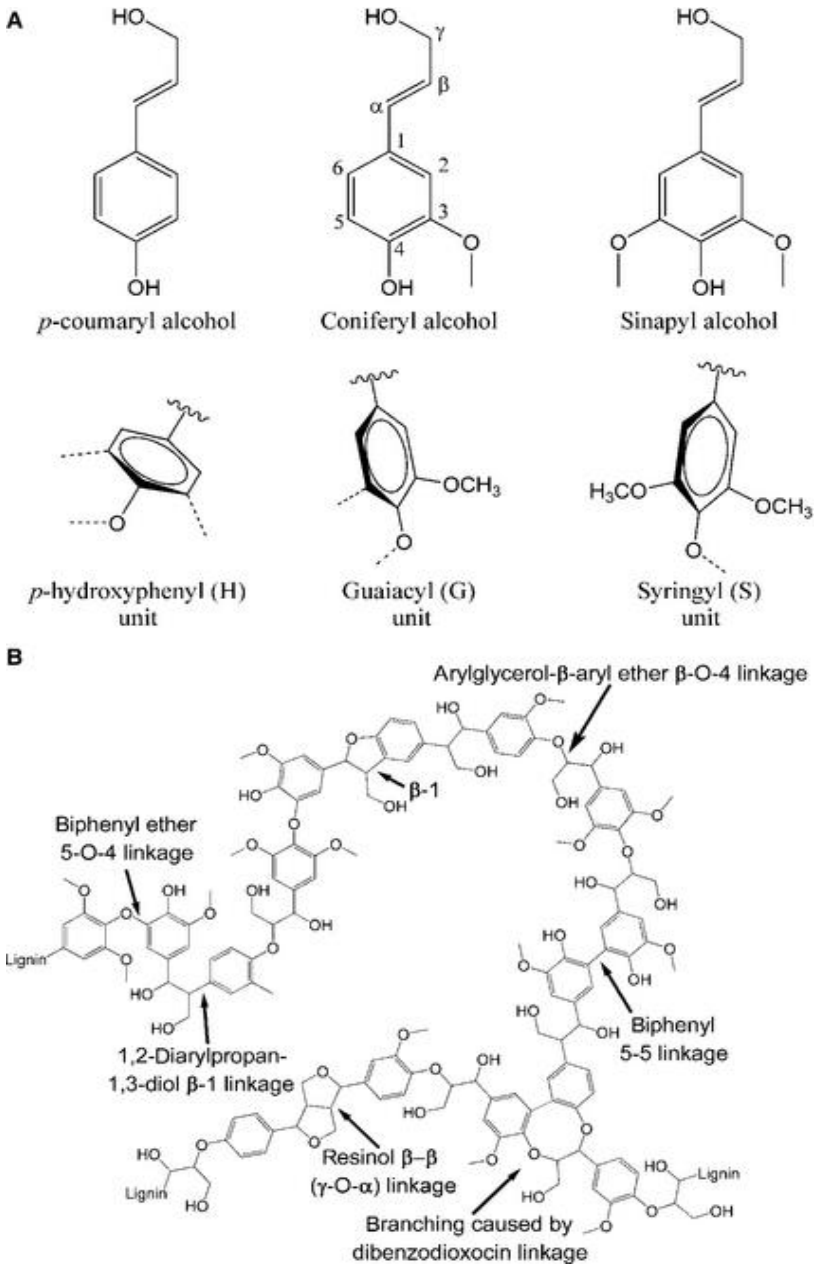

Figure 1-7. Structure of primary lignin monomers (A) and corresponding structural units in lignin (B) *indicated as p-hydrophenyl (H), guaiacyl (G) and syringyl (S) units (B) (Pollegioni et al., 2015)*

1.1.3. Enzymes for deconstruction of the plant fibers

Degradation, deconstruction and dissolution of plant fibers into its simple sugar components require a wide diversity of "hydrolytic" enzymes due to the heterogeneity and complexity of the structure of these complex polysaccharides. These enzymes are part of a larger group of enzymes named carbohydrates active enzymes (CAZYmes – www.cazy/org). They are responsible for the assembly, modification and breakdown of oligo- and polysaccharides (Lombard et al., 2014). The CAZY enzymes classification was done according to catalytic modules and functional domains of these numerous enzymes acting on carbohydrates. Five groups are distinguished, namely: glycosyl hydrolases (GH),

glycosyltransferases (GT), polysaccharides lyases (PL), carbohydrate esterases (CE) and auxiliary activities (AA). The enzymes involved in the degradation of the different polymers present in plant cell wall belongs to GHs, PLs, CEs and AAs families.

GHs hydrolyse the glycosidic linkage between two carbohydrates, or a carbohydrate and a non-carbohydrates moiety. GHs are globular proteins with a catalytic domain (CD) which is sometimes associated with a carbohydrate binding module (CBM). CBMs have different ligand specificities and several functions. They are able to accelerate the reaction by keeping the enzymes near to their target substrates. Some CBMs, which appear to be responsible for disrupting fiber structure, increase the degradation capacity of enzyme catalytic domain (Boraston et al., 2004; Shoseyov et al., 2006). PLs cleave uronic acid contained in plant polysaccharides and CEs catalyse the -O- or the -N-acetylation of substituted sugar residues (CAZYmes – www.cazy/org). The AAs include the lytic polysaccharide monooxygenases and ligninolytic enzymes. In the following sections, enzymes involved in the degradation of the different plant cell wall components will be further described.

1.1.3.1. Enzymes to degrade cellulose

Three classes are involved in cellulose degradation: endoglucanases (GH5, 7, 12, 45), cellobiohydrolases (exoglucanases) (GH6, 7) and β-glucosidases (GH1, 3). Endoglucanases hydrolyze cellulose into glucooligosaccharides by cleaving through glucose backbone. These enzymes initiate the degradation of the structure by attacking the amorphous regions and producing new free ends chains which make the macrostructures more accessible for cellobiohydrolases (Dashtban et al., 2009). Cellobiohydrolases preferentially hydrolyze reducing ends, releasing cellobiose and oligosaccharides. It has been reported that cellobiohydrolases can act both on reducing and non-reducing ends of cellulosic chains, which allows a synergy between opposite-acting enzymes (van den Brink and de Vries, 2011). Cellobiohydrolases are considered to be important enzymes to hydrolyze the crystalline regions of cellulose (Liu et al., 2011). Cellobiose, the end product of cellobiohydrolases, is a competitive inhibitor of these enzymes which can limit their ability to degrade cellulose (Dashtban et al., 2009). After endo- and exo-cleavages of cellulose, β-glucosidases degrade the remaining oligosaccharides into monomeric glucose. These enzymes can be sensitive to inhibition by glucose but this depends on the microbial origin of the enzyme (van den Brink and de Vries, 2011). **Figure 1-8** presents the complementary actions of enzymes to deconstruct cellulose.

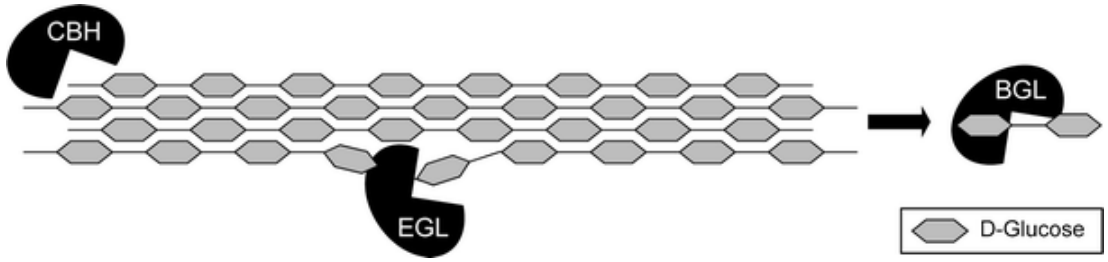

Figure 1-8. Schematic structure of cellulose with cellulolytic enzymes. *BGL is for β-glucosidase,* CBH *for cellobiohydrolases and* EGL *for β-1,4-endoglucanase (van den Brink and de Vries, 2011)*

1.1.3.2. Enzymes to degrade hemicellulose

Hemicellulose is a heterogeneous group of complex structures composed of various type of backbones and branches. It consists of xylan, galacto(gluco)mannan and xyloglucan structures plus the pectin heteropolysaccharides. Deconstruct this heterogeneous network requires thus various complementary enzyme activities which could be separate into backbone degrading enzymes and accessory/ auxiliary enzymes (**Figure 1-9**).

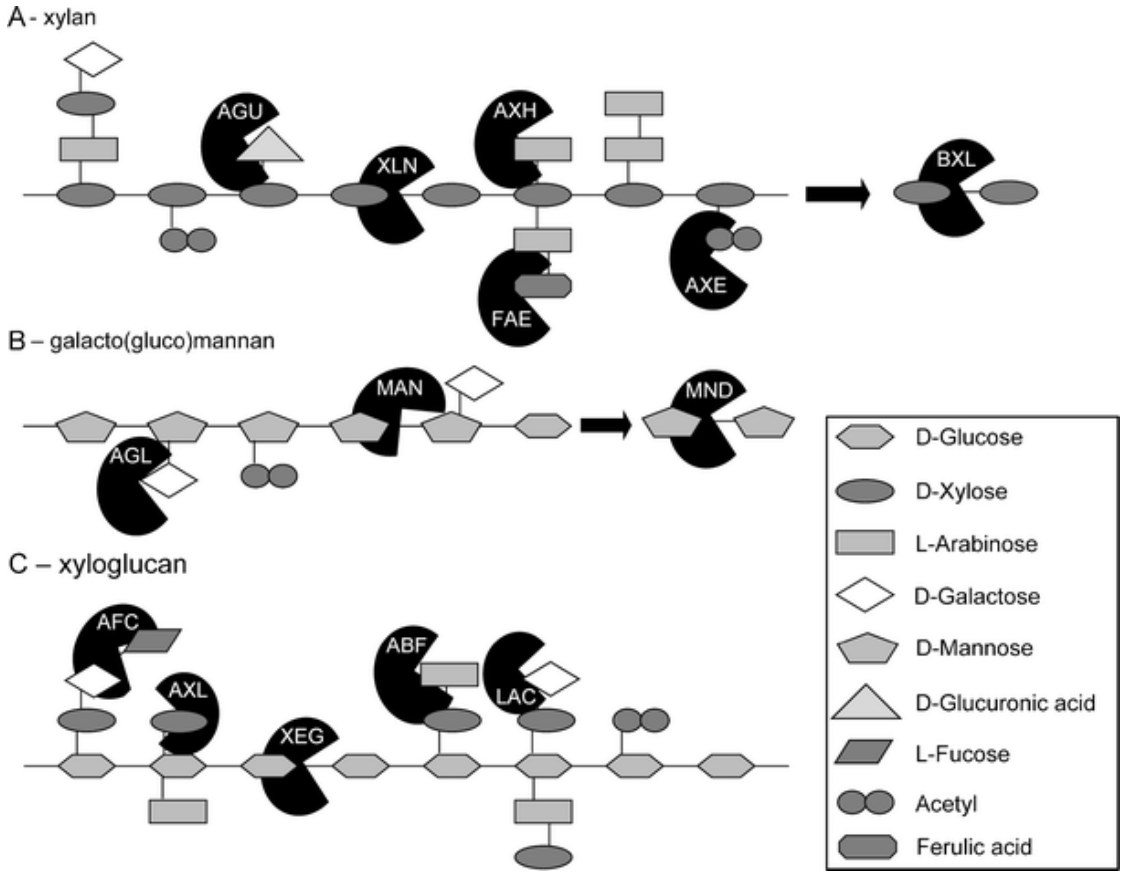

Figure 1-9. Schematic structure of the three hemicelluloses: xylan (A), galacto(gluco)mannan (B) and xyloglucan (C), with hemicellulolytic enzymes. *ABF is for α-arabinofuranosidase, AFC for α-fucosidase, AGL for α-1,4-galactosidase, AGU for α-glucuronidase, AXE for acetyl (xylan) esterase, AXH for arabinoxylan α-arabinofuranohydrolase, AXL for α-xylosidase, BXL for β-1,4-xylosidase, FAE for feruloyl esterase, LAC for β-1,4-galactosidase, MAN for β-1,4-endomannanase, MND for β-1,4-mannosidase, XEG for xyloglucan-active β-1,4-endoglucanase and XLN for β-1,4-endoxylanase* ***(van den Brink and de Vries, 2011)***

1.1.3.2.1. Backbone degrading enzyme

- **Degradation of xylan backbone**

The β-1,4-endoxylanases that belong to GH10 and GH11 families cleave xylan backbone into smaller oligosaccharides. Certain endoxylanases cut randomly between unsubstituted xylose residues, while the activity of others strongly depends on the presence of side-chains residues neighboring the attacked residues. Among different xylanases, GH10 shows better performance than family 11 even though GH11 has better kinetic activity on various xylan substrates (Hu and Saddler, 2018). In fact, GH10 xylanases have a broader substrate specificity than GH11 family. GH10 xylanases degrade xylan backbones or other xylose linear chains even with a high degree of substitutions but also smaller xylo-oligosaccharides (Biely et al., 2016). While GH11 has a lower accessibility than GH10 to the xylan backbone especially with acetyl group substitution. In addition, the GH10 was also demonstrated to be more thermostable than GH11 in the hydrolysis system (Hu and Saddler, 2018). The difference in their substrate specificity can be explained by the fact that GH10 catalytic domain is a TIM-barrel fold structure while GH11 one is a β-jelly roll structure (Henrissat and Bairoch, 1993). Finally, the released xylooligosaccharides are hydrolyzed into monomers by β-xylosidases, the second type of hydrolase attacking the β-1,4-xylosidic linkage.

- **Degradation of galacto(gluco)mannan backbone**

The degradation of galacto(gluco)mannan backbones requires the action of β-endomannanases which released mannooligosaccharides. The ability of these enzymes to degrade the mannan backbones depends on several factors such as the number and the distribution of side residues linked to the main-chain and the ratio of glucose to mannose. Enzymes are broadly more active on galactomannans with a low degree of backbone substitution (de Vries et al., 2001). However the negative impact of side residues is reduce if these substitutions are all on the same backbone side (McCleary and Matheson, 1983). β-mannosidases are exo-acting enzymes and release mannose from the non-reducing end of mannooligosaccharides.

- **Degradation of xyloglucan backbone**

The degradation of xyloglucan backbone requires two kind of enzymes: β-1,4-endoglucanases and β-glucosidases. Xyloglucan-active endoglucanases, also named xyloglucanases, cleave the xyloglucans backbones into glucose. Some β-1,4-endoglucanase families are active on both cellulose and xyloglucan backbones whereas other ones are specific to one type of backbone

(van den Brink and de Vries, 2011). Finally, β-glucosidases hydrolyze the released glucooligosaccharides into glucose.

- **Degradation of pectin backbone**

Pectin backbone hydrolysis requires two classes of carbohydrate active enzymes: glycoside hydrolases and polysaccharides lyases (**Figure 1-10**).

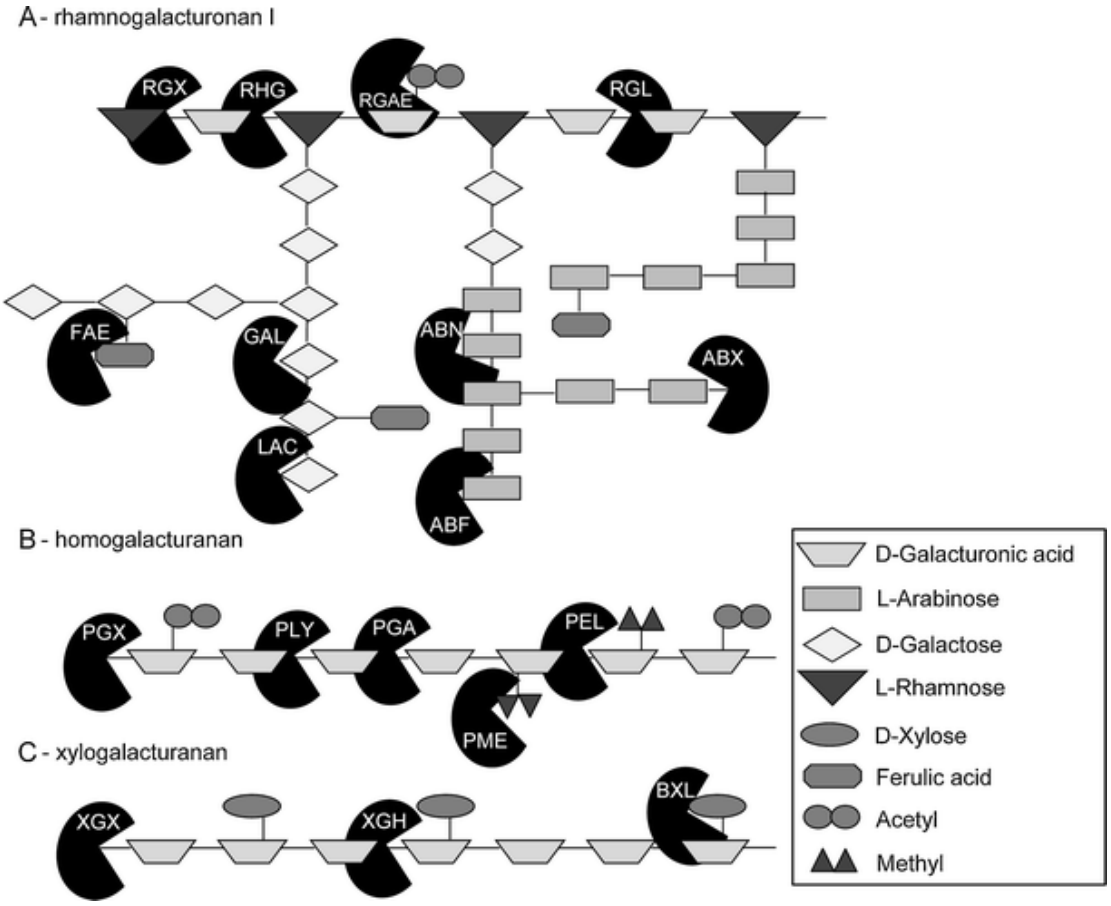

Figure 1-10. Schematic structures of three pectins structures, rhamnogalacturonan I (A), homogalacturonan (B) and xylogalacturonan (C), with pectinolytic enzymes. *ABF is for α-arabinofuranosidase, ABN for endoarabinanase, ABX for exoarabinanase, BXL for β-1,4-xylosidase, FAE for feruloyl esterase, GAL for β-1,4-endogalactanase, LAC for β-galactosidase, PEL for pectin lyase, PLY for pectate lyase, PGA for endopolygalacturonase, PGX for exopolygalacturonase, PME for pectin methyl esterase, RGAE for rhamnogalacturonan acetyl esterase, RGL for rhamnogalacturonan lyase, RHG for endo-rhamnogalacturonase, RGX for exo-rhamnogalacturonase, XGH for endoxylogalacturonase and XGX for exoxylogalacturonase (van den Brink and de Vries, 2011)*

The structural differences between the hairy and smooth regions of pectin backbones impact the glycoside hydrolases involved in their degradation. Endo- and exo-polygalacturonases cleave the α-1,4-glycosidic bounds between α-galacturonic acids in the main chain of the smooth regions while the more intricate hairy-region is further attacked by several classes of enzymes: endo- and exo-rhamnogalacturonases, xylogalacturonase, α-rhamnosidases,

unsaturated glucuronyl hydrolases and unsaturated rhamnogalacturonan hydrolases (de Vries et al., 2001). In the hairy regions, rhamnogalacturonan hydrolases act either with endo- or exolytic mechanism to cleave the α-1,2-glycosidic linkages between L-rhamnose residues and D-galacturonic acid. Endo-rhamnogalacturonases activity is severely hindered by the presence of acetyl residues on the main chain and requires the presence of rhamnogalacturonan acetyl esterases for an efficient hydrolysis of rhamnogalacturonan main chain (de Vries et al., 2000). Exo-rhamnogalacturonases release D-galacturonic acid residues from the non-reducing ends of rhamnogalacturonan chains but not of homogalaturanans (van den Brink and de Vries, 2011).

Pectin, pectate and rhamnogalacturonan lyases cleave the α-1,4-linked D-galacturonic acid residues from smooth region of pectin main chain resulting in the formation of unsaturated reducing-ends. Pectin lyases prefer substrates with a high degree of methyl esterification, while pectate lyases prefer backbone with a low esterification degree. Moreover, pectate lyases require the presence of Ca^{2+} ions for catalysis (de Vries et al., 2001). Rhamnogalacturonan lyases cleave within the hairy regions of pectin and are positively stimulated by Ca^{2+}. This enzyme activity is also positively affected by the presence of galactose side chains but negatively impacted by the presence of arabinose side chains and acetyl residues (de Vries et al., 2001).

1.1.3.2.2. Accessory/ auxiliary enzymes

To completely degrade hemicellulose structure, all the substitutions on hemicellulose backbones have to be released as some of them may hinder action of the hydrolytic enzymes described above. Enzymes that are active on these side-chains residues are called accessory enzymes. Some of them cleave the linkages between the main-chain and side residues, whereas other ones cleave internal or terminal linkage of side chains.

- **Arabinofuranosidases, arabinofuranohydrolases and endo-, exo-arabinases**

L-α-Arabinofuranosidases (Abf) are devoted of activity that cleaves L-arabinose residues that substitute xyloglucan and (arabino-) xylan. They are exo-type enzymes that can hydrolyze (1→2), (1→3), and (1→5) α-L-arabinofuranosidic bonds in L-arabinose-containing hemicelluloses such as arabinoxylan and L-arabinan (Saha, 2000). A former classification based on the mode of action and substrate specificity classified these accessory enzymes, namely in type-A as not active on polymers, type-B as active on linear and branched polymers and the arabinoxylan arabinofuranohydrolases type (AXH) as specifically active on arabinoxylans (Beldman et al., 1997). Nowadays, The CAZY nomenclature (CAZYmes –

www.cazy/org) of Abfs are now grouped into 4 families GH43, GH51, GH54 and GH62. This nomenclature allows evolutionary and structural analyses of the protein and is based on amino acid sequence similarities. The link between the two classification methods is that AbfA, AbfB, and AXH correspond to family GH51, GH54, and GH62, respectively. The Abf from the GH43 family has been also denoted AXH due to its activity on arabinoxylan (De La Mare et al., 2013; Guais et al., 2010). One should notice, however, that this linkage between enzyme activity and amino acid sequence classification is an oversimplification due to the complexity that exists within the various Abfs, as for instance two enzymes of the same family can exhibit different substrate specificities (Guais et al., 2010).

Endo- and exo-arabinases are also important accessory enzymes which are specific to pectin degradation. Endoarabinases hydrolyse the α-1,5-linkages of arabinan polysaccharides present in pectin side chains. Although some Abf can also do it, these enzymes significantly enhance arabinan degradation and positively influence the action of Abf (Martens-Uzunova and Schaap, 2009). Abfs are unable to liberate arabinose that is esterified with phenolic acids or acetylated (Biely et al., 2016)

- **Xylosidases**

α-D-xylosidases can release α-linked xylose residues from xyloglucan. All these enzymes are highly specific to α-linked xylose residues but differ with respect to the other type of glycoside they can hydrolyse: *p*-nitrophenyl-α-D-xylanopyranoside, isoprimeverose (α-xylosyl-(1-6)-glucose) or other derived from xyloglucan (de Vries et al., 2001).

- **α- and β-D-galactosidases**

The removal of α-linked D-galactose residues on xylan and galactomannan backbone requires the action of α-galactosidases. β-galactosidases release terminal galactose residues from galactan side chains of pectin. The presence of terminal β-1,4 D-galactose residues in xylan, xyloglucan and galactoglucomannans suggest that β-galactosidases also participate in the degradation of these polysaccharides (van den Brink and de Vries, 2011).

- **Endo- and exogalactanases**

Galactan side-chains of pectin are hydrolysed by endogalactannases, exogalactannases and β-galactosidases. Endogalactanases hydrolyse galactan polysaccharides into galactobiose and galactose. Differences between various endogalactanases are based on their ability to hydrolyse β-1,3-, β-1,4- or β-1,6-linkages between galactose residues. Three types of endogalactanases

are required to completely hydrolyze the two types of arabinogalactans in the pectin side chains, but so far mainly β-1,4-endogalactannases have been reported (de Vries et al., 2001).

- **α-glucuronidases**

Glucuronic acid and its 4-*O*-methyl esters can be removed from xylan main-chain by α-glucuronidases. Although these enzymes have substrates specificities (short oligosaccharides or polymeric xylan), α-glucuronidases are mainly active on small xylooligosaccharides and thus their activities dependent on the action of endoxylanases. Therefore a strong synergy has been reported between α-glucuronidases and endoxylanases or β-xylosidases (de Vries et al., 2000).

- **Feruloyl and p-coumaroyl esterases**

Feruloyl- and *p*-coumaroyl esterases are able to hydrolyse the ester bonds between hydroxycinnamic acids, ferulic acid or *p*-coumaric acids and sugars residues. Various type of enzymes have been identified based on their physical properties and their substrate specificities. Four functional sub-classes of feruloyl esterases termed types A, B, C and D have been distinguished based on their substrate specificities and their enzyme protein sequences (Crepin et al., 2004). Feruloyl esterases are able to released ferulic acid from xylan and xylan-derived oligosaccharides but also from pectin (de Vries et al., 2001). A strong synergy is reported between feruloyl esterases and xylanases (Gopalan et al., 2015; Wong, 2006). These esterases are more effective in releasing ferulic acid with a GH11 xylanase and diferulic acid with a GH10 xylanase (Faulds et al., 2006). A synergy between xylanases, arabinofuranosidases and feruloyl esterases is also reported, especially during sequential reactions (accessory enzymes prior to xylanase addition) which prevents the steric hindrance effect (Lei et al., 2016). Studies characterizing pectin degradation highlight the synergies between feruloyl esterases and arabinofuranosidases or endoarabinases (Kroon and Williamson, 1996).

- **Acetyl- and methylesterases**

Acetyl- and methylesterases release acetyl and methyl residues from various polysaccharides of plant cell wall. Acetylxylan esterases release acetyl from xylan backbone and are highly active on polymeric substrates which is important for an efficient degradation of xylan backbone by endoxylanases (de Vries et al., 2001). Acetylglucomannan esterases are highly active on acetylated galacto(gluco)mannan but could also act on acetylated xylan. They act synergistically with endo-β-1,4-mannanase on polymeric and oligomeric substrates through glycosidic linkages cleavage and deacetylation (Biely, 2012). Smooth regions of pectin contain

also acetyl and methyl esters which are removed by pectin acetylesterases and pectin methylesterases. These enzymes influences the ability of polygalacturonases and pectin lyases to degrade pectin backbones (de Vries et al., 2001). Finally rhamnogalacturonan acetylesterases are essential for the action of rhamnogalacturonan hydrolases which are active on pectin main chain (de Vries et al., 2000).

1.1.3.3. Enzymes to degrade lignin

Lignin is the most resilient component of plant cell wall to hydrolysis and various enzymes are required, among others: manganese peroxidases (MnP), lignin peroxidases (LiP) and laccases. Laccases oxidize the phenolic compounds of lignin and reduce the oxygen released to water while both peroxidases catalyse a variety of oxidative reactions that depend on the presence H_2O_2 and could require a redox mediator to catalyse the oxidative depolymerisation of lignin (Pollegioni et al., 2015; Woolridge, 2014).

It has been widely accepted that these oxidative enzymes are too large to penetrate into the cell wall. A prior attack of the polysaccharides or lignin by free radicals is required to open the structure and make enzyme penetration easier. Three different ways to generate free radicals have been reported including cellobiose dehydrogenases or chelators (Call and Mücke, 1997; Dashtban et al., 2009). These oxidative enzymes could have a negative impact on plant cell wall degradation as some enzymes like xylanase are sensible to oxidative stress and could be inactivated. However, xylanases can be adsorbed into fibers network and thus seems to be more resistant to these oxidative damages (Várnai et al., 2011; Woolridge, 2014).

1.1.3.4. Swollenins, non-hydrolytic: non catalytic proteins

The swollenin gene was originally isolated from *Trichoderma reesei* as it showed sequence similarity with the plant cell wall expansin encoding genes. These latter proteins are thought to disrupt hydrogen bonding between cell wall polysaccharides without hydrolysing them. Swollenin protein has an N-terminal CBM connected by a linker region to an expansin-like domain (Saloheimo et al., 2002). This protein was reported to be able to disrupt cell wall structure (especially cellulose) without producing detectable reducing sugars (Saloheimo et al., 2002), even though there has been some reports attesting of a small release of sugars by pure swollenin (Andberg et al., 2015; Zhou et al., 2011). More recent works have highlighted the capacity of the swollenin to fragment big cellulose agglomerates and to render rough and amorphous Avicel surfaces (Eibinger et al., 2016; Jäger et al., 2011; Santos et al., 2017). It has been suggested that swollenin can weaken hydrogen bonds in amorphous regions of cellulose

and in hemicellulose, which promotes fibers fragmentation by enhancing slippage between cell wall components (Gourlay et al., 2015; Jäger et al., 2011; Saloheimo et al., 2002). Also, by opening fibers structure, swollenin make hydrolytic enzymes more accessible to their substrates. As a matter of fact, a high synergy has been measured on hydrolysis of cellulose in the presence of both cellulases and swollenin (Kang et al., 2013; Wang et al., 2010, 2011; Zhou et al., 2011). The degree of synergy is even more pronounced for xylanases GH10 and GH11 (Gourlay et al., 2013; Santos et al., 2017), when acting on hemicellulose. Moreover, it was shown that a 95 fold increase in the amount of swollenin in a fungal enzyme cocktail enhanced by 2 times the hydrolytic efficiency of this enzyme cocktail on *Miscanthus gigantheus* biomass (Rocha et al., 2016). Swollenin could also enhances ferulic acid released acting concomitantly with ferulic acid esterases (Levasseur et al., 2006).

1.2. Overview of enzyme additives in animal nutrition

1.2.1. Enzymatic feed additives in animal nutrition

1.2.1.1. Animal nutrition and feed additives

Animal diet composition is based on wheat and barley in Europe which both contain a high levels of non-starch polysaccharides (NSPs). It is well-established that NSPs act as anti-nutritional factors because (i) they are non-digestible by monogastric, especially poultry due to a lack of specific hydrolytic enzymes in animal gut (ii) they prevent accessibility of some nutrients (starch and proteins) as these latter are trapped within the fibrous cell walls (Bedford and Partridge, 2011), (iii) they can act as chelators of minerals such as Ca^{2+} or Fe^{2+} (Ravindran, 2013), and (iv) they may reduce nutrients adsorption due to their high molecular weight that enhance the viscosity in the digestive tract (Lafond et al., 2015). Phytate is another anti-nutritional factor present in animal feed, while it contains a high amount of phosphoryl moieties linked with other compounds such as minerals, proteins or starch that is useful in feed animal. Therefore, the supply of hydrolytic enzymes such as xylanases and β-glucanases in 80^{th} and phytase in the 90^{th} in animal feed has shown significant benefit in the growth yield likely due to better feed assimilation by animals.

The use of enzymes as feed additives have at least 4 advantages. Firstly, they increase the availability and digestibility of starch, proteins, amino acids and minerals (phosphorus and calcium) in feed intakes and reduce chyme viscosity in bird's gut. This leads to an increase of the animal production yield for a same feed ratio (i.e. amount or quality of meat/egg per kilo of feed ingested termed feed conversion ratio) and in a reduction of the feed costs. This reduction

is the conjunction of the use of less expensive products in feed together with supplement of enzyme that allows their better digestibility (Bedford and Partridge, 2011). Enzymes are incorporated into feed following two strategies: either enzymes are added to a basic feed formulation and thus increasing animal performances, or feed is reformulated to ensure the same animal performances at lower price. A second advantage of enzymes as feed additives is to improve the feed nutritional constancy by increasing the digestibility of the recalcitrant fraction which was previously randomly hydrolysed by the animal digestive system. This is particularly the case for wheat- and barley-based feed which can be highly variable in their metabolizable values. Thirdly, these feed additives have a positive effect on animal health. By increasing the absorption of nutrients, enzymatic additives reduce their presence in animal intestine and thus prevent the development of pathogenic bacteria. Another consequence of this higher nutrient absorption is a better integrity and morphology of the intestine (Ravindran, 2013); Moreover, related to high viscosity gut, wet litter was also a common problem, leading to relatively high incidences of hock burns and breast blisters which reduce carcass quality and marked value of the bird. These enzymes decrease digesta viscosity and thus moisture content of excreta of the litter, which prevents various animal troubles and diseases (Bedford and Partridge, 2011). As a fourth advantage, the higher feed adsorption leads to decrease the quantity of excreta and therefore the environmental impact of animal farming. This is particularly true for water pollution by phosphorus and for nitrogen released as gas (Mottet and Tempio, 2017). Finally, enzymes are digested and absorbed at the end of the digestive tract or excreted and thus leave no traces into meat or eggs. This meet the needs for safety and quality in food industry.

1.2.1.2. Enzymatic feed additives: range of product and specifications

To improve feed digestibility and thus animal performances, three types of enzymes are required as feed additives in animal nutrition: carbohydrate active enzymes, proteases and phytases. In addition due to the reactional environment, these enzymatic products have to respond to particular specifications.

- **Glycosyl hydrolase (GH)**

In animal nutrition these enzymes are usually categorized into those targeting starch or non-starch polysaccharides (NSP). Starch digestibility varies according to its composition, granule size, structure resistance and encapsulation (Bedford and Partridge, 2011). The main exogenous

enzymes breaking down resistant starch are amylases which allow monogastric to extract more energy from feed (Bedford and Partridge, 2011).

NSPases hydrolyse non-starch polysaccharides (NSP) which are a complex and heterogeneous group of polysaccharides found in plant cell walls. NSP can be either soluble or non-soluble and are considered as strong anti-nutritional factor for monogastrics as explained previously. The two main NSPases used in animal nutrition are xylanases and β-glucanases. Xylanases hydrolyse arabinoxylan, particularly prevalent in cereal grains and their co-products. For example wheat bran consists of 70%$_{DM}$ of arabinoxylan and only 24 and 6%$_{DM}$ of cellulose and β-glucan respectively (Maes and Delcour, 2002). However, β-glucans are prevalent in barley and oat, therefore NSPases should be used regarding animal feed composition (Knudsen, 2014). Other NSPases currently used in animal nutrition, but to lesser extent, are β-mannanases, pectinases and α-galactosidases. Altogether these enzymes are commonly used as enzyme cocktails naturally product by lignocellulose-degrading fungi.

- **Proteases**

Proteases target storage proteins particularly contained in leguminous plant like soybean. Storage proteins can be bind to energy-rich starch and therefore proteases can help to release it which can be then digested by the animal (Bedford and Partridge, 2011).

- **Phytases**

Phosphorus is important for animal bone development and metabolic process. Phytate is the storage form of phosphorus in plant seeds. Phytate forms complexes with minerals (such as calcium or phosphorus), proteins and starch making them unavailable for absorption (Bedford and Partridge, 2011). Pig and poultry do not have endogenous phytases and thus are not able to breakdown these phytate-linkages. Phytase also reduces the risk of water pollution due to the excess of phosphorus in animal excreta (Mottet and Tempio, 2017).

- **Enzymes cocktail specifications for animal digestive system**

During the digestion, feed travels through the numerous compartments of the animal digestive system and is subjected to various environmental conditions which depend on animal species, feed composition, type of diet and rate of animal feed intake (continuous or intermittent feeding system). These conditions affect the efficiency of exogenous enzymes according to their optimal reaction conditions. Only the poultry anterior digestive system, located before the intestine will be scrutinized in this PhD work. In fact NSPases, which have mostly an optimal

pH between 4 and 5 (Bedford and Partridge, 2011), are mainly active there due to the acidic pH. This area of interest is composed of two main compartments for enzymatic reactions: the crop and the gizzard. The crop is a storage organ where feed can be moistured and fermented due to the presence of bacteria (Classen et al., 2016). Gizzard is the poultry muscular stomach while proventriculus is the secretory one. In the gizzard, feed are mixed with hydrochloric acid and pepsinogen secreted by the proventriculus and are grinded (Svihus, 2014). Temperature, pH, substrate moisture and retention time are parameters that critically influence the enzymatic reactions in animal digestive system.

Poultry have a body temperature of 41 ° C and most of the enzymes marketed today have an optimal temperature between 45 and 65 °C (Bedford and Partridge, 2011), making this parameter not limiting for enzymes hydrolysis. A second important factor is the substrate moisture content. If it is not problem in the gizzard, thanks to the gastric juices secreted by the proventriculus, it can become a limiting factor in the crop (Svihus, 2014). Indeed, even if feed is gradually moistened in the crop, one hour is necessary to reach 50% of humidity (Svihus et al., 2010). Thirdly, feed retention time of the poultry anterior digestive system varies widely and can be highly limiting. Regarding retention time, poultry digestion time is usually within 2 h - 2.5 h as evaluated by the excretion of a non-digestible labelled marker (Tuckey et al., 1958). In the crop, which is a storage organ, feed residency time is highly variable and can even go to zero if the gizzard is empty. On average, feed stays about 50 minutes in the crop (Danicke et al., 1999). In the gizzard, the mean retention time is 1 h for a standard commercial feeds but it can go up to 2 h if feed consists of more structured compounds (Svihus, 2014). Finally, NSPases optimal pH is between 4 and 5. In the crop wide pH variations are observed: in most of the time pH is higher than 6 while in some case it is between 4.5 and 5.9 and in the gizzard pH is between 1.9 and 4.5 with an average value of 3.5 (Svihus, 2014).

1.2.1.3. Rovabio®, a commercialized enzyme cocktail as feed additive

Rovabio Excel is an enzymatic cocktail produced by *Talaromyces versatilis* (renamed from *Penicillium funiculosum* after genome sequencing) used as animal feed additive. Proteomic analysis of this enzyme cocktail revealed more than 50 proteins, among which several glycosylhydrolytic, hemicellulolytic and proteolytic enzymes were identified and confirmed by the genomic sequence of this fungal specie (Guais et al., 2008) (Adisseo, personal communication). The list of the enzymatic activities identified in Rovabio® Excel is presented in the **Table 1-2**.

Table 1-2. List of enzymes present in Rovabio® Excel (Guais et al., 2008**,** Adisseo internal data)

Protein name	**Protein family**	
Acetyl xylan esterase	CE 5	
Alkaline protease		
Alpha-1,2-mannosyltransferase	GT 1	
Alpha-galactosidase	GH 27	
Alpha-glucuronidase	GH 67	
Alpha-L-rhamnosidase	GH 78	
Alpha-mannosidase	GH 47	
Alpha-xylosidase	GH 31	
Arabinofuranosidase	GH 62	
Aspartic protease		
Avicelase III		
Beta-1,3-glucanosyltransferase	GT 3	
Beta-1,4-xylosidase	GH 3	
Beta-1,6-glucanase	GH 5	
Beta-galactosidase	GH 35	
Beta-glucosidase	GH 3	
Beta-xylosidase	GH 3	
Carboxypeptidase		
Catalase		
Cellobiohydrolase I	GH 7	
Cellobiohydrolase II	GH 6	
Cellulase	GH 5	
Dextranase	GH 49	
Endo-1,4-beta-galactanase	GH 53	
Endo-1,4-xylanase	GH 11	
Endo-1,4-xylanase B	GH 11	
Endo-1,4-xylanase D	GH 10	(Lafond et al., 2011)
Endoglucanase	GH 5	
Endopolygalacturonase	GH 55	
Exo-beta-D-glucosaminidase	GH 2	
FAD binding monooxygenase		
Ferulic acid esterase A	CE 1	
Feruloyl esterase B	CE 1	
GDP-mannose 4,6-dehydratase		
Glucoamylase	GH 15	
Glutaminase A		
Laccase		
Lipase		
Manganese peroxydase precursor		
Neutral endopolygalacturonase	GH 28	
Oxidoreductase		
Polygalacturonase	GH 28	
Polyketide synthase		
Rhamnogalacturonase	GH 28	
Steroid monooxygenase		
Swollenin		
Type I phosphodiesterase/		
Nucleotide pyrophosphatase		
Ubiquitin-conjugating enzyme		
Xylanase/cellobiohydrolase	GH 7	

Table 1-3. Overview of in-vivo studies evaluating the efficiency of Rovabio® Excel

Diet	Results	Reference
Cotton seed, sunflower or rapeseed meal	Increase broiler performances	(Abudabos et al., 2017)
Sorghum and soybean meal	Increase broiler performances	(Aftab, 2009)
Mix of wheat, barley, corn, wheat bran and soybean meal	Increase pig performances	(Cozannet et al., 2012)
Corn and soybean meal	Increase hens performances (in phase 2)	(Gunawardana et al., 2009)
Corn, wheat, and soybean meal	Increase broilers performances	(Lee et al., 2010)
Corn and soybean meal	Increase pig performances	(Lu et al., 2016)
Corn and soybean meal	Increase broiler performances	(Lu et al., 2013)
Wheat, corn and barley	Increase layers performances	(Tekeli et al., 2014)
Barley, wheat and soybean	Increase saws and progeny performances during lactation	(Walsh et al., 2012)
US broiler industry environment	Increase broiler performances	(West et al., 2007)
Corn, soybean and distillers dried grains with soluble	No effect with broilers	(Min et al., 2009)
Sunflower, corn and soybean	No effect with young broilers	(Mushtaq et al., 2006)

Rovabio® Excel is a multi-specie, multi-ingredient and multi-application solution that appears to be the most versatile enzymatic product available on the market. It expands the range of raw materials that can be used in feed formulation, enables the use of greater levels of certain essential raw materials and is effective in both poultry and swine. It is the only product in the European market to obtain 6 registrations: broilers, layers, turkeys, ducks, pigs and piglets. It can be used with two strategies: (i) feed supplementation with no change to ingredient composition or (ii) feed cost reduction through the adjustment of specifications, taking into account the nutritional content of Rovabio®. This last strategy allows to reach to 85, 65 and 140 kcal per feed kg of metabolizable energy for wheat and soybean, corn and soybean and barley and soybean based diet respectively (http://feedsolutions.adisseo.com/en/rovabio-excel-the-versatile-enzyme/). An overview of the *in-vivo* studies demonstrating the efficiency or the limits of Rovabio® is presented in the **Table 1-3**.

In-vitro studies using the TNO gastrointestinal model (TIM-1) confirmed that Rovabio® Excel supplementation improved wheat digestibility: up to 3.9% based on organic matter, 9.7% based in total glucose and 47.2% based on reducing end increase (results dependant on wheat cultivar). However, an enzyme activity reduction was highlighted during

digestion progression which could be attribute to enzyme degradation by digestive proteases or to a limitation in substrate (Lafond et al., 2011). Another study with the TNO demonstrated the ability of Rovabio® Excel to solubilized 75% of arabinoxylan in wheat flour (from 65 to 85% upon wheat cultivar), 30% of arabinoxylan in wheat bran with 1.1 $U_{xylanase\ visco}$/g and up to 51.2% with 55 $U_{xylanase\ visco}$ per g of feed (Maisonnier-Grenier et al., 2006). The predominant role of AX on the rheological properties of chyme was also illustrated. In conclusion, although this enzyme cocktail contains a wide range of enzyme activities, its *in-vivo* action is apparently limited as it was enabled to hydrolyse all the NSP content.

1.2.2. Studies on enzymatic feed (NSPase-type) additives in animal nutrition

1.2.2.1. In-vivo studies

In-vivo studies consist of testing feed additives directly on animals. Enzymatic products are added to the feed given to animals and various zootechnic parameters are measured. These studies have been initiated in the 90's and still are continuing because of the growth of feed additive market and thus of the investments in Research and Development. These zootechnic parameters can refer to animal performances including feed intake, feed conversion ratio, body weight gain, meat quality, number of egg, egg quality, etc. Other physiological parameters are also recorded which include carcass characteristic, blood composition, intestine morphology, gut microbiota (Luo et al., 2009; Nahas and Lefrancois, 2001; Osei and Oduro, 2000; Yasar and Forbes, 2000). External parameters influencing animal health such as litter moisture (Cengiz et al., 2012; Seskeviciene et al., 1999; Shirzadi et al., 2009) are also determined. In some studies digesta samples are taken all along the animal digestive tract to characterize the progression of feed degradation. Analysis of digesta samples combines biochemical measurements with the samples chemical composition (Fuente et al., 1998, 1995; Lamp et al., 2015; van der Klis et al., 1995) and physical measurements such as supernatant viscosity or particle size (Choct et al., 1995; Fuente et al., 1998; van der Klis et al., 1995; Yasar and Forbes, 2000).

1.2.2.2. In-vitro studies

Two types of *in-vitro* approaches are identified: the development of specific protocols or apparatus in order to mimic animal digestive systems and the development of biochemical or physical analyses in order to characterize feed enzymatic deconstruction.

- **Protocols and apparatus mimicking monogastric digestive system**

Methods have been developed to predict metabolizable or digestible energy by trying to reproduce *in-vitro* digestive system (entirely or partially) of monogastrics using:

- TIM-1 (TNO gastrointestinal model) a dynamic gastrointestinal digestive system,

- Static *in-vitro* digestion protocols.

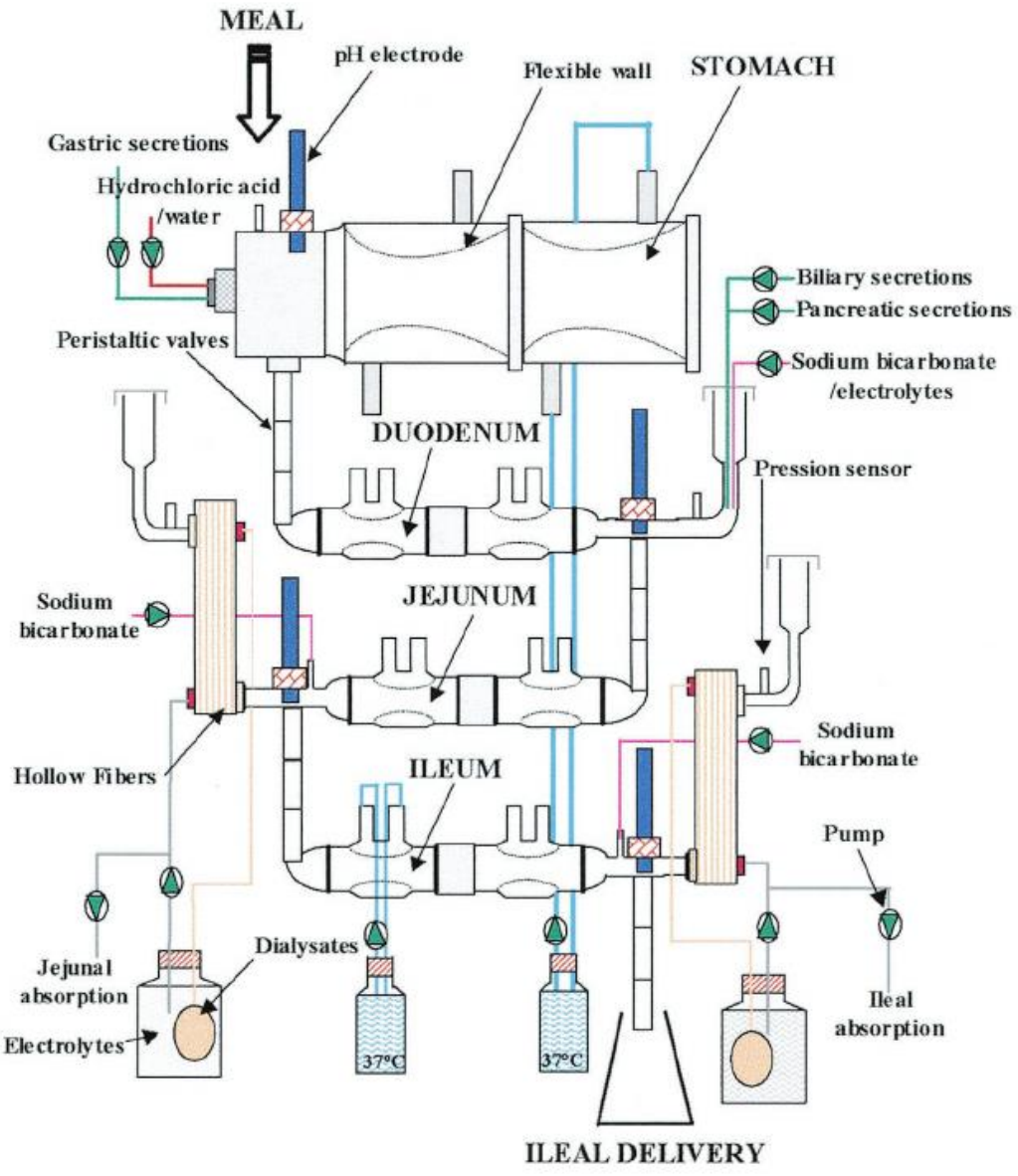

Figure 1-11. Schematic diagram of the gastrointestinal digestion model (TIM-1) *created in the 1990's in the Netherlands* (Lafond et al., 2015)

The patented *in-vitro* gastrointestinal model TIM offers rapid insights into the release, the solubility and the availability for absorption of nutrients within the gastrointestinal tract. This

well-validated and accurate system to estimate *in-vivo* values and represents a cost-effective alternative for animal trials. TIM-1 was created in the 1990's in the Netherlands and artificially mimics human or animal digestive system: stomach and small intestine. The system is presented in the **Figure 1-11**. It consists of a dynamic succession of computer-controlled compartments that reproduce the conditions of the monogastrics digestive system: temperature, pH, concentration of bile salts or other digestive enzymes, retention time, kinetics of passage of the chyme and absorption of low molecular weights and water (Minekus et al., 1995). In recent years, several studies were carried out using this model to understand fibers degradation and digestion and the effect of enzyme supplementation (Fässler et al., 2006; Haraldsson et al., 2005; Lafond et al., 2015, 2011; Maisonnier-Grenier et al., 2006).

For static *in-vitro* digestion method, two main protocols exist. The first one reproduces the ileal feed digestion while the second mimics the total digestive system. Same methodologies are used for both protocols: feed and enzymes additives are placed in flasks and incubated under the successive conditions of the digestive tract compartments (temperature, pH, molarity, endogenous enzymes, agitation and reaction time). Ileal digestion is carried out in two stages, reproducing the conditions of the stomach and small intestine (Boisen and Fernández, 1995). Prediction of total tract energy digestibility consists of a three-steps enzymatic incubation corresponding to stomach, small intestine and large intestine (Boisen and Fernández, 1997). These approaches were validated through comparisons between these *in-vitro* predicted values and values derived from: *in-vivo* studies (Noblet and Jaguelin-Peyraud, 2007; Wilfart et al., 2008), TNO's model TIM-1 (Meunier et al., 2007) or predictions based on feed chemical composition (Spanghero and Volpelli, 1999; Yegani et al., 2013).

- **Biochemical analyses**

Enzymatic activities, pure or in combination, can be characterized by monitoring substrate consumption, product released (monosaccharides, oligosaccharides, proteins…), reducing sugars or chemical composition of feed before and after enzymatic hydrolysis. These *in-vitro* enzymatic analyses are usually carried out taking into account parameters specific to those of animal digestive tract and with or without the endogenous enzymes present in their digestive system (Almirall and Esteve-Garcia, 1995; Ao et al., 2008; Aulrich and Flachowsky, 2001; Inal et al., 2000; Simbaya et al., 1996; Smeets et al., 2014; Tapingkae et al., 2008; Tervilä-Wilo et al., 1996; Vahjen and Simon, 1999; Vahjen et al., 2005).

- **Physical and biophysical analyses**

Digesta viscosity reduction is a major benefit of enzymatic feed additives which participate to improve intestinal nutrients absorption and therefore viscosity is an important parameter to evaluate enzyme efficiency. Supernatant viscosity is the main measurement used to monitor digesta viscosity evolution both for *in-vitro* (Inal et al., 2000; Li et al., 2004; Makhdum et al., 2013; Malathi and Devegowda, 2001) and *in-vivo* sampling. For an animal nutrition application, only one study measuring viscosity of the entire NSPs suspension (not only of the supernatant) during enzymatic treatment was found (Alloui-Lombarkia et al., 2003). It has been demonstrated that *in-vitro* viscosity assay may predict *in-vivo* digesta viscosity in the intestine and also animal final body weight for poultry fed with rice-based aliment supplemented with a xylanase (Bedford and Classen, 1993). More recently, also based on *in-vitro* viscosity assays, a multipurpose feed enzyme analyser was developed and allows to predict accurately the efficacy of exogenous enzymes in poultry digestion. Results provide a strong correlation ($r \geq 0.97$) between animal performances and the logarithm of xylanase quantity added to feed or the logarithm of viscosity evolution *in-vitro* (Zhang et al., 2000). However for wheat-based feed, results vary widely with sometimes very low correlations while it is well established that enzyme additives are effective on wheat (Brufau et al., 2006).

Optical microscopy and fluorescence microscopy have been used to investigate the fiber structure evolution in response to enzymatic treatment (Li et al., 2004; Parkkonen et al., 1997; Tervilä-Wilo et al., 1996). Hydration properties and initial particle size are also monitored to highlight, for example wheat bran cage effect: soluble nutriments trapped into fiber network (Aulrich and Flachowsky, 2001).

1.3. Conclusions of the literature review and objectives of the thesis

Wheat is a major source of energy in animal diets and its major component are starch and proteins, whereas NSP derived from the cell wall account for only 3-8 % of the total mass of the grain (Saulnier et al., 2007). This NSP content is well-known to have anti-nutritional properties and to be recalcitrant to digestion. As it can impact animal performances, enzymatic cocktails enriched in enzyme activities able to degrade these NSPs such as Rovabio® (Guais et al., 2008) were proposed as feed additives in order to counteract these potential negative effects. However, apart from some *in-vivo* works and *in-vitro* studies focusing only on numerous enzymes, the action of Rovabio® upon complex matrix degradation remains unclear. Therefore

characterizing the global action of this industrial enzyme cocktail upon wheat bran deconstruction is challenging.

A state of the art, about the various strategies found in animal nutrition to understand the efficiency of an alike enzyme cocktail, shows clearly a predominance of *in-vivo* studies which focus on animal performances. The few *in-vitro* approaches found in the literature focus on biochemical analyses and only some of them used basic physical analyses such as supernatant viscosity or optical microscopy. Considering the complexity of wheat bran structure and of Rovabio® enzymes cocktail, studying the cocktail activities, enzyme per enzymes, is obviously too long and non-pertinent. Therefore a global approach that characterizes the action of Rovabio® on a complex polysaccharide matrix such as wheat bran, by combining biochemical and physical analyses appears to be interesting, with a particular attention to the degradation of the recalcitrant fraction (mainly NSP fraction of the substrate). Furthermore, this strategy allows to easily evaluate the impact of adding one enzyme at a time to the Rovabio cocktail.

A comparable experimental setup had been develop to understand the saccharification step in biofuel production which allows the deconstruction of biomass into fermentable sugars. In fact, to ensure a high bio-conversion rate important factors have to be controlled as mixing system, transfers limitation or inhibition by end-products. To characterize their impacts on enzymatic hydrolysis yield, well-instrumented pilots were used combining physical and biochemical measurements. A well-equipped experimental setup has been successfully developed to investigate deconstruction of lignocellulosic-based biomass for biorefinery purposes (Le, 2017; Nguyen, 2014). The aim of the present study is to adapt this methodology for the deconstruction of the wheat-based feed recalcitrant fraction, as reference substrate, by a commercially available enzymatic cocktail termed Rovabio® with in mind the following scientific questions:

- ⇨ How Rovabio® is acting on complex substrates such as wheat bran? What are the mechanisms taking place during the deconstruction of wheat bran with Rovabio® treatment?
- ⇨ What are the factors (physical and/or biochemical) that limit the efficiency of Rovabio® in the deconstruction of wheat bran NSPs?
- ⇨ How the Rovabio® efficiency on wheat bran deconstruction can be improved?

An overview of all the experiments carried out in this respect is presented in the **Annex 1**.

CHAPTER 2:

DEVELOPMENT AND VALIDATION OF A MULTISCALE ANALYSIS TO CHARACTERIZE THE DECONSTRUCTION OF NON-STARCH POLYSACCHARIDES FROM WHEAT BRAN BY AN ENZYME COCKTAIL

CHAPTER 2. DEVELOPMENT AND VALIDATION OF A MULTISCALE ANALYSIS TO CHARACTERIZE THE DECONSTRUCTION OF NON-STARCH POLYSACCHARIDES FROM WHEAT BRAN BY AN ENZYME COCKTAIL

2.1. Introduction

Characterizing the deconstruction mechanisms of complex biological material such as wheat bran is challenging as it requires to combine *in-situ* physical with *ex-situ* biochemical analyses. Our strategy is to exploit a multiscale approach successfully developed to investigate the deconstruction of lignocellulosic-based biomass for biorefinery purposes using a pure or a mix of cellulases (Le et al., 2017; Nguyen et al., 2013).

In a first step, we had to choose an appropriate substrate widely employed in animal diet and containing an important amount of NSP. We drew our choice to wheat bran as it is the part of the grain cereals containing 36 to 53% of NSPs and yet between 13 to 40% of starch which may possibly interfere with physical (viscosity, morphogranulometry) measurements. Thus, to address the interference problem of starch in our experimental set up in a more direct way, we also used wheat meal which is mainly composed of starch.

The second step was to set up the experimental strategy, using physical and biochemical methods, to characterize the deconstruction of the chosen substrate at various ratio enzyme/substrate of Rovabio Brussel. The *in-situ* physical method was to employ an on-line viscosimeter to characterize the rheological behaviour of the initial suspension (without enzyme) and its evolution during enzymatic treatment. To complement this macroscopic analysis, diffraction light scattering (DLS), morphogranulometry (MG) and focus beam reflectance measurement (FBRM) were used to characterize the deconstruction process of wheat bran at the microscopic level. Then biochemical methods were set up to quantify the sugars and other minor compounds that were released during wheat bran enzymatic hydrolysis. A mass balance along the enzymatic treatment was applied to ensure the reliability and accuracy of our biochemical methods.

2.2. Materials and methods

2.2.1. Substrates and enzymes

Wheat meal, named "Farine de blé pâtissière T45", was a commercial French biological wheat flour type T45 (Moulin des moines, Châtenois, France). It was stored in its paper bag at room temperature.

Two types of wheat bran, with two different granulometries, were used. **Wheat bran N°1** is a product, named "Westhove wheat bran fine", purchased from Limagrain (ref E20678, 15 KG, batch 0 180, February 2015) which corresponds to wheat bran heat-treated by the Limagrain Farigel process. It was stored in its paper bag at room temperature. **Wheat bran N°2**, with higher granulometry, was obtained from "La Minoterie de la Save" (Grenade sur Garonne, France) and destarched by lixiviation (Raynal-Ioualalen, 1996) and then called "**destarched wheat bran**" (dWB). One batch (~3.5 kg) of WB was suspended in water with a ratio Liquid/Solid=10. Four consecutive washes were applied in a stirred tank (V=40 L) at 350 RPM and 40 °C during 15 min for the first one and 10 min for the following ones. Between each wash, the suspension was clarified by decantation and the supernatant containing the solubilized starch (called "starch milk") was removed. Then fresh water was added to maintain a constant solid/liquid ratio. WB was finally rinsed by percolation (bag filter with a cut-off of 50 µm), dried with incoming compressed air and stored at -18 °C. The amount of NSPs in this material estimated after acid hydrolysis (see below) was estimated to 71% of the dry mass.

Maize fibre (SOFABRAN 184-400) was purchased from Limagrain. Fibre was obtained by a genuine process of grinding, separation and stabilisation from maize coming from a few conventional selected varieties of homogeneous mixture.

Wheat bran insoluble arabinoxylan (ref 9040-27-1), arabinoxylan medium viscosity (ref 40302), **β-glucan** (ref 31202) and **xyloglucan** amyloid from tamarin seed (ref 00401) were purchased from Megazyme (Ireland) and stored at room temperature.

Arabinose, galactose, glucose, xylose and mannose used as HPAEC standards were obtained from Fluka, Applichem Pancreac, Supelco, Sigma and Sigma respectively. All these products have a purity higher than 99.0% except for glucose which is higher than 99.9%.

Rovabio® Brussel (simplified by Rovabio thorough the text) is an enzymatic cocktail secreted by *Talaromyces versatilis* fungus commercialized by Adisseo SAS (Commentry, France, http://feedsolutions.adisseo.com/en/). The cocktail contains a large amount of various glycosylhydrolases herewith termed NSPases including xylanases, β-glucanases, pectinases and cellulases. Aa alike enzymatic cocktail termed Rovabio Excel, had been characterized by a

global proteomic analysis in a previous work (Guais et al., 2008). The activity of this cocktail has been determined by an internal standard procedure and is expressed in viscosity units of xylanase per mL of arabinoxylan suspension ($U_{xylanase\ visco}$/mL). This activity corresponds to the fluidity reduction of 1 unit (dimensionless) per minute under the analysis conditions. The total activity of Rovabio Brussel corresponded to 44 505 $U_{xylanase\ visco}$/g (density of 1.09). The 'global' enzymatic activity of endo 1,4-β-xylanase in the cocktail can be also determined by the 3,5-dinitrosalicylic acid (DNS) colorimetric method (McKee, 2017) using a solution of 1,5% of birchwood xylan as the substrate in 75 mM NaAcetate buffer pH 4.0. The ratio between viscosity units and by xylanase activity is around 9 (V. Neugnot-Roux, unpublished data).

Spirizyme® from Novozyme, is a commercial gluco-amylases cocktail with an activity about 750 AGU/g (amyloglucosidase unit defined as the amount of enzyme that will liberate 0.1 µmol/min of p-nitrophenol from p-nitrophenol-alpha-glucopyromoside at pH 4.3 and 50 °C) (Mangat et al., 2010).

A heat-stable α-amylase was obtained from Sigma-Aldrich (ref A3306) with an enzymatic activity given between 20 000 and 60 000 U/ml. One unit will hydrolyse 1.0 mg of maltose from starch in 3 minutes at pH 6.9 at 20 °C. **An amyloglucosidase** solution from *Aspergillus niger* (ref A7095) was also obtained from Sigma-Aldrich with a minimal enzymatic activity of 260 U/mL. One unit of activity corresponds to the liberation of 1.0 mg of glucose from starch in 3 min at pH 4.5 at 55 °C.

2.2.2. Experimental pilot set-up and sampling

A general description of our experimental system is illustrated in **Figure 2-1**. It includes a double jacket glass bioreactor (diameter: 130 mm, h = 244 mm, V = 2.0 L) equipped with a home-designed impeller system associated with several *in-situ* sensors (temperature, pH, rotation speed, torque, FBRM). The impeller is composed by a three inclined blades located at 75 mm height from the bottom (diameter: 73.5 mm, angle: 45°, h = 38 mm) and a close bottom mixer including 2 large blades (diameter: 120 mm, h = 22 mm). A Haake VT550 viscometer (Thermo Fisher Scientific ref: 002-7026, 0.5-800 RPM ±0.1%, 100-30000 µN.m ±0.5 %FSD) was used to ensure mixing at specific rotation speed as well as *in-situ* torque measurements. The temperature was controlled by water circulation (combined cryostat Haake DC30-K20, -50/+200 °C ±0.01, Thermo Fisher Scientific) through the water jacket of the bioreactor. The viscometer and the cryostat were controlled by original software from Haake (RheoWin Job Manager) that also ensured real-time monitoring (temperature, torque, mixing rate). The pH of the suspension was controlled and auto-adjusted by a Biostat-B (Sartorius Stedim Biotech) via

home-designed software created in the LabVIEW environment. Finally, a focused beam reflectance sensor (FBRM-G400-Mettler Toledo) was located inside the reactor in order to measure particle chord length (l_c) and the number of particle counts per second and classes.

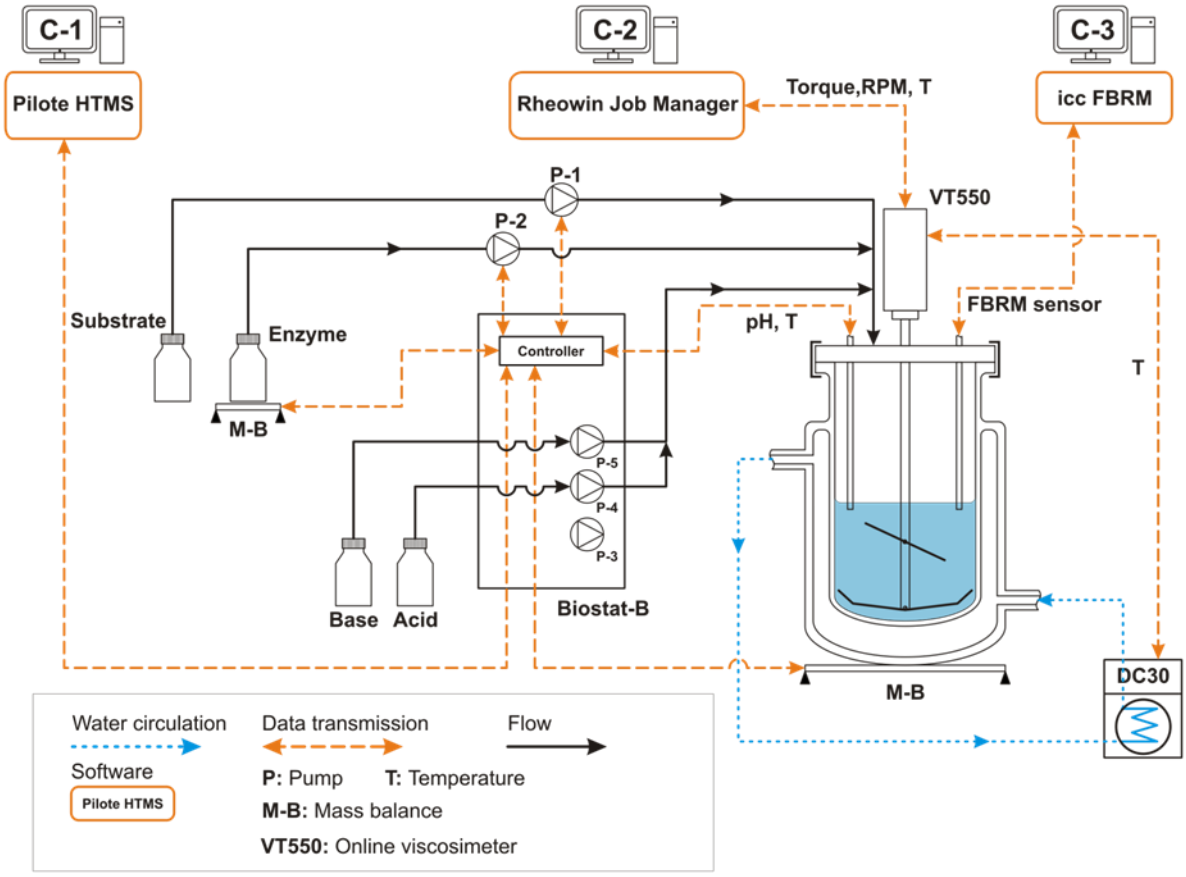

Figure 2-1. Process and instrumentation diagram of experimental setup.

Samples (12 mL, 6 per experiment) were collected during hydrolysis experiments in 25 ml Falcon conical centrifuge tubes in an ice-cold bath to readily stop the enzymatic activity. Part of the samples was centrifuged (10 min at 4000 RPM) and stored at -18 °C for biochemical analyses and the other half directly stored at 4 °C for physical analysis.

2.2.3. Chemical and biochemical analysis

Dry matter concentration. To determine sample water content, a quantity of sample (m_s) was filtered through a Whatman No1 filter paper of known weight (m_{fp}) and then washed by ≈5 mL of distilled water. The filter paper containing the sample was dried in an oven set at 60 °C and 200 mbar (Heraeus, Thermo Scientific, 0-760 mmHg, 50-150 °C) with silica gel during 4 days. The samples weight was then measured with a precision balance (Sartorius ED224S, 0.005-230 g ± 0.1 mg). The final weight was referred to m_{fin}. Water content (W) and dry matter (DM) were calculated following ***Eq. 2-1*** and ***Eq. 2-2*** (accuracy ± 0.5%):

$$W(\%) = \frac{m_s + m_{fp} - m_{fin}}{m_s} x100 \qquad \textit{Eq. 2-1}$$

$$DM(\%) = 100 - W \qquad \textit{Eq. 2-2}$$

Glucose in the supernatant was analyzed using an YSI model 2700 analyzer (Yellow Springs Instruments, Yellow Springs, Ohio, USA). The wheat bran suspension was centrifuged (4000 RPM for 10 min) to pellet the insoluble particles. For reliable measurements, supernatants should be diluted into the linear range of the instrument (0 – 2.5 g/L). The analyzer was calibrated using a single point calibration standard (2.50 g/L glucose) (YSI 2776 Standard, Yellow Springs, Ohio, USA). The apparatus provides a direct reading of the glucose concentration, expressed in g/L (see §6.3.6). The accuracy of the measurement is approximately ± 2%.

Solubilization rate corresponds to the soluble matter that is released in the supernatant during the treatment of the destarched wheat bran suspension with Rovabio. It was determined by drying 2 mL of supernatant at 105 °C on Fontainebleau sand (Ref 310-127-6) until the measured mass became stable using a Moisture Analyzer (MA 100H Moisture analyzer, Sartorius, 30 - 180 °C). These values were used to evaluate the residual dry matter concentration (Cm) remaining at different times during the enzymatic treatment of the insoluble wheat bran hydrolysis.

Sulfuric acid hydrolysis of soluble sugars released in the supernatant were carried out by the protocol described elsewhere (François, 2007) in which the first step was skipped because the sugars were already soluble. After hydrolysis, a sample was withdrawn, centrifuged (10 min at 4000 g at 4 °C) and the supernatant was diluted and filtered through 0.22 µm filters.

High-performance anion exchange chromatography (HPAEC-PAD) was carried on a ICS 3000 system (Thermofisher Scientific, Courtaboeuf, France) using a CarboPac SA10 analytical column (250 by 4 mm) with a guard column CarboPac SA10, an isocratic elution of 1 mM NaOH at 35 °C and a flow rate of 1.5 mL/min. The monosaccharide released from acid hydrolysis were converted to the equivalent polysaccharide values using the conversion factor of 0.88 for pentoses (arabinose and xylose) and 0.90 for hexoses (mannose, galactose and glucose) (Templeton and Ehrman, 1995). A correction factor of 10% due to the loss of monosaccharides during the process (estimate from experimentations presented in this chapter) was applied to the final calculation (Templeton and Ehrman, 1995; Wijaya et al., 2014; Zhou and Runge, 2014).

Protein concentration was determined by the BCA (BiCinchoninic acid Assay) kit (Pierce Thermo Scientific, Illinois, USA) (Smith et al., 1985) using bovine serum albumin as standard.

Total starch content was determined with "total starch HK" assay kit from Megazyme© (Megazyme International Ireland, Wicklow, Ireland). This method has been adopted by AOAC (Official Method 996.11) and AACC (Method 76.13.01).

2.2.4. Physical analysis

2.2.4.1. In-situ viscosity measurement

The *in-situ* viscosity was determined from real-time monitoring of torque and mixing rate. This measure requires to determine Kp and α which are two constants that only depend on the mixing system geometry and Np_0 which is the mixing power number for turbulent flows. For Newtonian fluids and in laminar flows, the product of the mixing Reynolds number (Re) by the mixing power number (Np) is constant and written as:

$$Np = Kp \cdot \frac{1}{Re} \qquad \textit{Eq. 2-3}$$

This power consumption curve $Np = f(Re)$ was characterized using Newtonian reference fluids: distilled water, glycerol, and Marcol 52 oil (Exxon Mobil). **Eq. 2-3** for laminar regime can be extended to turbulent ones (until a critical Re value) and described by a unique equation:

$$Np = \left[\left(\frac{Kp}{Re}\right)^{\alpha} + Np_0^{\alpha}\right]^{1/\alpha} \qquad \textit{Eq.2-4}$$

Experimental results on our system gave Np_0 = 0.17, α = 0.75, Kp = 115.2 and showed that a laminar regime prevailed up to Re = 41.

For a non-Newtonian fluid, **Eq.2-4** is still valid as long as a generalized Reynolds number is used. It is calculated using the Metzner-Otto concept which introduces a constant Ks that only depends on the geometrical characteristics of the mixing system (Metzner and Otto, 1957). The Ks value is determined experimentally using 0.04 - 0.1%$_{vol/vol}$ shear-thinning xanthan solutions prepared in a saturated solution of glucose and sucrose as reference fluids and has found in our system to be equal to 38.5. The concept can be extended up to transition flow (Jahangiri et al., 2001). In this study, the application of a power consumption curve to calculate suspension viscosity and establish an *in-situ* rheogram was extended to transitional

flow, which is equivalent to Re < 1000. In turbulent flow, the viscosity determination is limited by the power consumption curve up to Re = 30000 (above this value, Np is almost constant). See more details in Materials and Methods (§6.4.2).

The non-Newtonian behavior, described by the flow behavior index (n) was obtained from the slope of μ as a function of mixing rate. It was investigated every 15 minutes by adjusting mixing rates (mean shear rates) from 170 to 200 RPM for 1 min, and from 200 to 150 RPM for 1 min. All mixing rate shifts were made by linear acceleration or slowdown during 20 s. Data acquisition period was adjusted to 20 s at 170 RPM and reduced to 10 s at 150 and 200 RPM. During both steps, mean torque was calculated after stabilization.

2.2.4.2. Ex-situ morpho-granulometry (MG)

Images of particle suspension were made with a morpho-granulometer (Mastersizer G3S, Malvern Instruments Ltd. SN: MAL1033756, software Morphologi v7.21). The instrument is composed of a system of lens (magnification: from x1 to x50, particle dimension: from 0.5 to 3000 μm), an optical device (Nikon CFI60 Bright/ Dark field) and a camera (IEEE1394a, Fire Wire^{TM}, 2592x1544 pixels). Images were obtained from a 60 µL of suspension sample (diluted 1:100) deposited between cover glass and slide. A surface of 5x5 mm was analysed in dark field with a magnification x10, under the standardized operating conditions (light intensity 90, exposure time 400 ms, threshold for particle detection 30-100).

2.2.4.3. Ex-situ diffraction light scattering (DLS)

The volume-weighted particle size distribution (PSD) was determined by diffraction light scattering (DLS, Mastersizer 2000, Malvern Inst., range from 0.02 to 2000 μm, red λ = 632.8 nm and blue λ = 470.0 nm light) using Mie scattering theory. A known volume of suspension (1 to 3 mL) was added to a water circulation loop (20 °C ± 2) in order to obtain laser obscuration between 5% and 40%. The whole suspension was mixed by a Heidolph magnetic stirrer at 200 RPM while the circulation loop was maintained by a Masterflex L/S model 7553-79 at pump speed 240 RPM. The measurements of each sample were performed at three different dilution rates, in triplicate and the average data was taken. Laser diffraction analysis converts the detected scattered light (DLS) into PSD value, which is eventually assimilated to a diameter of equivalent sphere, $d_{se;}$ Volume-weighted distribution (E_v) was calculated by the Mastersizer software and could be multiplied by the suspension dry matter concentration (Cm) to take into account the loss of material due to solubilization during the enzymatic treatment.

2.2.4.4. In-situ focus beam reflectance measurement (FBRM)

Focus beam reflectance measurements (FBRM) enables *in-situ* quantification of small particles in the range < 100 µm through the estimation of the particle chord length (lc) and distribution of the chord length population (CLD). *In-situ* CLD of particles was analysed using an FBRM® G400 probe (Mettler Toledo, range: 0.1 to 1000 µm, laser light source λ = 795 nm, laser source rotation: 2 m/s). This probe was placed in the reactor and allowed real-time tracking of chord length and particle count during enzymatic hydrolysis. Thousands of individual chord lengths are typically measured each second to produce the chord length number distribution, $E_n(l_c)$, which is the fundamental measurement provided, by FBRM®. Consequently, the number-weighted CLD, $E_n(l_c)$, and the average number of chord length counted per second, N_c, are used as indicators to describe population.

2.3. RESULT PART 1: from starch interference with our approach to destarching strategy

In this part, our objective will be (i) to show the significant influence of starch content on physical measurements and (ii) to apply a destarching process based on standard procedure reported at lab and industrial scales.

2.3.1. Wheat bran hydrolysis and impact of starch content

Starch effect was highlighted through two experiments. The first one demonstrated that Rovabio has an amylolytic activity using wheat meal and the second one showed that starch degradation cannot be neglected in wheat bran viscosity assay.

Wheat flour contains at least 70%$_{DM}$ of starch and its suspension (up to 300 gdm/L) viscosity was monitored during its treatment with Rovabio Brussel. When the viscosity of the wheat flour suspension was relatively stable, which requires about 2.5 h (deviation <5% per hour), the enzymatic cocktail was added at 100 $U_{xylanase\ visco}$/g (noted T=0 h on the graph **Figure 2-2**). A rapid -3 fold decrease of viscosity was observed within 6 min after the addition of the enzyme cocktail (Figure 2-2). This result clearly indicates that Rovabio Brussel contains an important amylolytic activity which was responsible for the hydrolysis of starch, what affects wheat meal suspension viscosity.

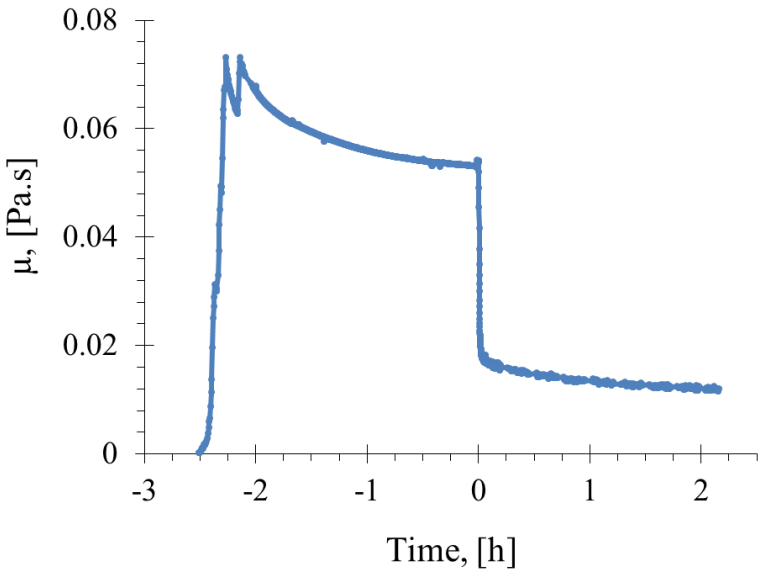

Figure 2-2. Change of the in-situ viscosity during treatment of wheat flour suspension by Rovabio (Brussel). *Operating conditions: wheat flour suspended in a potassium phosphate 0,1M at 41 °C, pH 4.0, concentration up to 300 gdm/L, Rovabio Brussel 100 $U_{xylanase\ visco}$/gdm.*

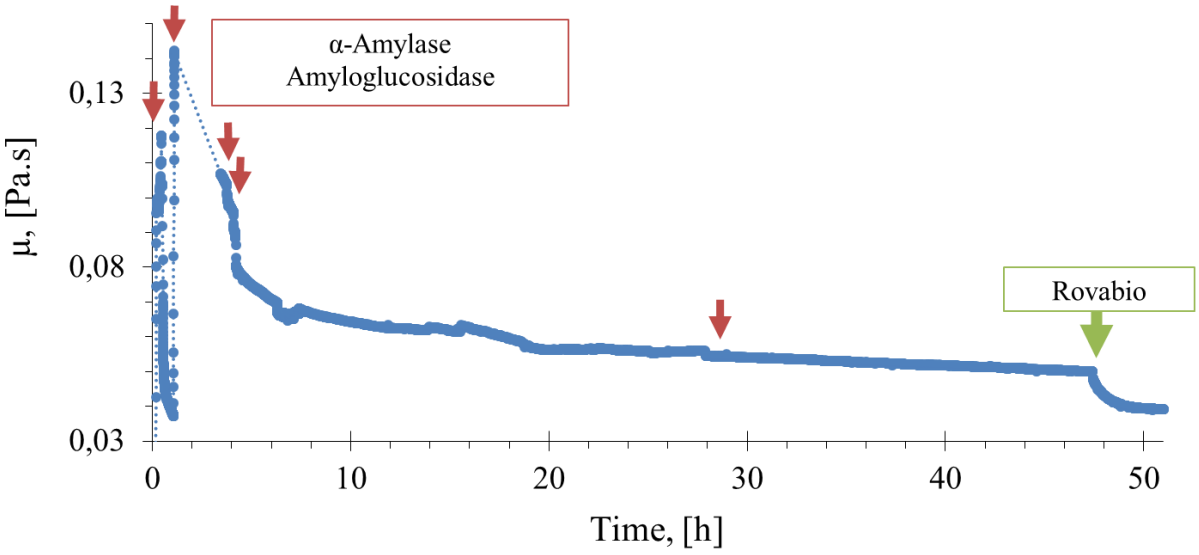

Figure 2-3. Change of the in-situ viscosity during the treatment of wheat bran suspension by α-amylase and amyloglucosidase followed by Rovabio (Brussel). *Operating conditions: wheat bran suspended in a potassium phosphate 0,1M at 41 °C, pH 4.0, concentration up to 260 gdm/L, α-amylase up to 900 U/gdm, amyloglucosidase up to 3000 U/gdm and Rovabio Brussel at about 14 $U_{xylanase\ visco}$/gdm.*

According to this result and to determine whether the degradation of starch contained in wheat bran influences viscosity measurements, we treated wheat bran suspension (wheat bran N°1, Limagrain) with pure α-amylase and amyloglucosidase which together must degrade starch into glucose. Five successive additions of these amylolytic enzymes were made at 0, 1,

2, 3 and 27 h. At each addition, 150 U/gdm and 660 U/gdm for α-amylase and amyloglucosidase was supplied to the suspension, except for the last step, for which 300 U/gdm α-amylase was provided. As shown in **Figure 2-3**, a significant decrease of viscosity was observed after the first addition of these enzymatic solutions at 0 h. Then, wheat bran was added again (up to 260 gdm/L) to ensure that suspension remains in laminar (or transitory) regime along the enzymatic treatment in order to accurately interpret suspension rheological behaviour. The three subsequent additions of enzyme, at 1, 2 and 3 h, were characterized by a sharp drop of the *in-situ* viscosity (**Figure 2-3**). Then, the suspension viscosity showed a very slow decrease that was not significantly modified by a further addition of amylase/amyloglucosidase at 27 h, suggesting that there was no starch anymore. Indeed the slow viscosity decrease was due to other effect as witnessed by the absence of glucose release during this period (data not shown). The further addition of 14 $U_{xylanase\ visco}$/gdm Rovabio Brussel at 47.5 h interestingly resulted in a net drop of viscosity which highlighted an additional deconstruction of wheat bran that could be due to destruction/mobilization of NSPs by the action of Rovabio Brussel. In conclusion, our results clearly showed the necessity to remove starch from wheat bran in order to get a careful investigation of NSP deconstruction by Rovabio.

2.3.2. Pre-treatment of the wheat bran to remove its starch content

Two types of destarching pre-treatments were considered: (i) an enzymatic treatment and (ii) a mechanical treatment consisting in successive washing of wheat bran with hot water. Enzymatic treatment is possible with pure enzymes, as previously, or with amylolytic industrial cocktail such as Spirizyme. The first option is very specific to starch but employed expensive enzymes. Consequently, enzymatic pre-treatment will be limited to a treatment with Spirizyme.

2.3.2.1. Option 1: enzymatic treatment

Spirizyme was added at about 5 AGU/gdm (amyloglucosidase activity per gdm) to wheat bran suspension (157 gdm/L) and *in-situ* viscosity was monitored as well as glucose released in the supernatant followed with the YSI method (**Figure 2-4**). A monotonic decrease of the suspension viscosity from 0.103 Pa.s at 0h to 0.089 Pa.s during 3 h after the addition of Spirizyme was found. This was accompanied by a concomitant release of glucose in the supernatant that reached about 44.7 g/L after 3 h and plateaued in the last hour (between -1 and 0 h) suggesting the end of starch degradation. Upon the addition of Rovabio at 1.1 U/gdm, the drop of viscosity showed a sudden acceleration for the next 2 h, indicating that some

components in wheat bran, other than starch and likely NSPs and proteins, are degraded by the enzymes.

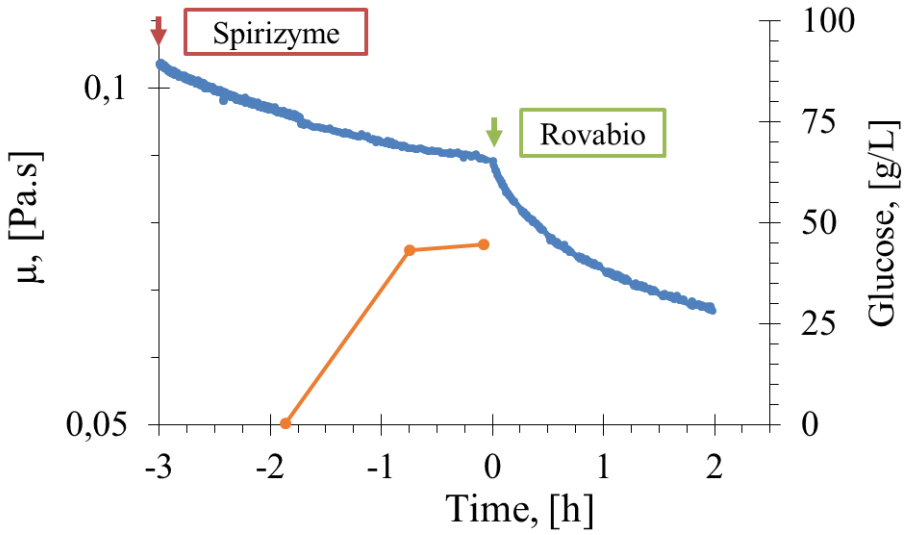

Figure 2-4. Change of *in-situ viscosity during the treatment of wheat bran suspension with Spirizyme and then Rovabio (Brussel).* *Operating conditions: wheat bran suspended in a potassium phosphate 0,1M at 41°C, pH 4.0, initial concentration 157 gdm/L, Spirizyme 5 AGU/gdm and Rovabio Brussel 1.1 Uxylanase visco/gdm.*

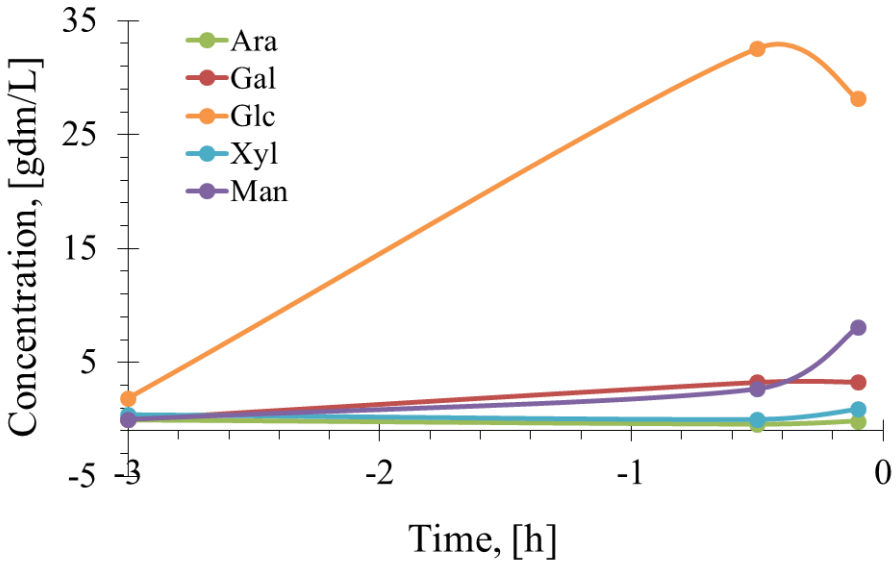

Figure 2-5. *Release of glucose (Glc), xylose (Xyl), arabinose (Ara), mannose (Man) and galactose (Gal) during treatment of the wheat bran by Spirizyme.* *Operating conditions identical to Fig.2-4. The soluble sugars were expressed as equivalent of monosaccharides*

By measuring the monosaccharides directly released in the supernatant during Spirizyme treatment, we showed that mainly glucose was found at a level of about 35 gdm/L (Figure 2-5), which corresponded to a solubilization rate about 22% of the initial amount of the

wheat bran suspension (157.5 gdm/L). This result is consistent with the 15 to 30%$_{DM}$ of starch presents in wheat bran according the milling process that is used to prepare this kind of wheat bran (Brillouet and Mercier, 1981; Chotěborská et al., 2004; Heuzé et al., 2015; Maes and Delcour, 2002). However, we found also mannose (6.5 gdm/L) and galactose (4 gdm/L) which are sugars that may arise from arabinoxylans and galactomannans present wheat bran NSPs. Therefore, this result indicated that Spirizyme solution likely contains with some galactomannanases. Due to this 'contamination', we could not envisage to treat the wheat bran with this enzymatic solution prior to test the effect of Rovabio.

2.3.2.2. Option 2: mechanical treatment

The second treatment we considered was an extensive washing of wheat bran with hot water. An overview of various protocols found in literature is given in the **Table 2-1**. We tested the method developed by Raynal-Ioualalen because it has been already shown to be very effective to remove more than 99% of the starch content in wheat bran (Raynal-Ioualalen, 1996). This process consists in 3 successive hot water washes at 40 °C with a ratio Liquid/Solid=10 and was done in a 50 L stirred tank (400 RPM). An additional washing step was appended to ensure a high starch removal. Between each washing step, the supernatant containing solubilized starch, also called "starch milk", was removed. This step was done by decanting the suspension and draining out the supernatant. Then, a final filtration step (cut-off 50 µm) removed the remaining water in the pellet by incoming compressed air (up to 3 bars). As this filtration step was done with a cut-off equal to 50 µm, wheat bran granulometry has to be larger than 50 µm. As it was not the case with the 1st wheat bran used, a new one was purchased.

Table 2-1. Overview of washing protocols to remove starch from wheat bran

	Raynal-Ioualalen 1996	**Zeitoun, 2011**	**Patent EP 0 401 117 A1 (ARD, 1990)**	**Patent FR 3 008 993 A1 (ARD, 2013)**
Granulometry		0,8 – 1,5 mm		
Water	**40 °C**	40 °C	Cold	(1st) 50 °C (2nd&3rd) 1 <pH< 3,5
Liquid/Solid	**10**	10	10 to 15	(1st) 10 (2nd&3rd) 10 to 20
Bran quantity	**5 kg (90% MS)**	25 kg		
Rotation	**400 RPM**	400 RPM		
Duration / step	**15 / 10 / 10 min**	15 / 10 / 10 min		
Filtration	**Cylindrical filter Porosity: 50 – 100 µm**	Cylindrical filter (slots 100 µm)	150 to 300 µm + pressing < $2,10^5$ Pa	
Tank capacity	**200 L**	300 L		
Spinning	**Basket centrifuge with filter bag (porosity 5 µm) 10 min at 3000 RPM**	Basket centrifuge with filter bag (porosity 5 µm) 10 min / 3000 RPM		
Drying		50 °C / 48 h		
Efficiency	**Remains starch 0,5%$_{DM}$ Extraction 40%$_{DM}$**	Starch extraction ≈ 99%	Remain 3 to 5% of starch (DM)	Remain starch < 3% DM
Other	**Water retention 5 g/g DM**	Extract matter (soluble) 50% starch + 15% proteins	Acid post treatment pH 3,5 to remove phytic acid	

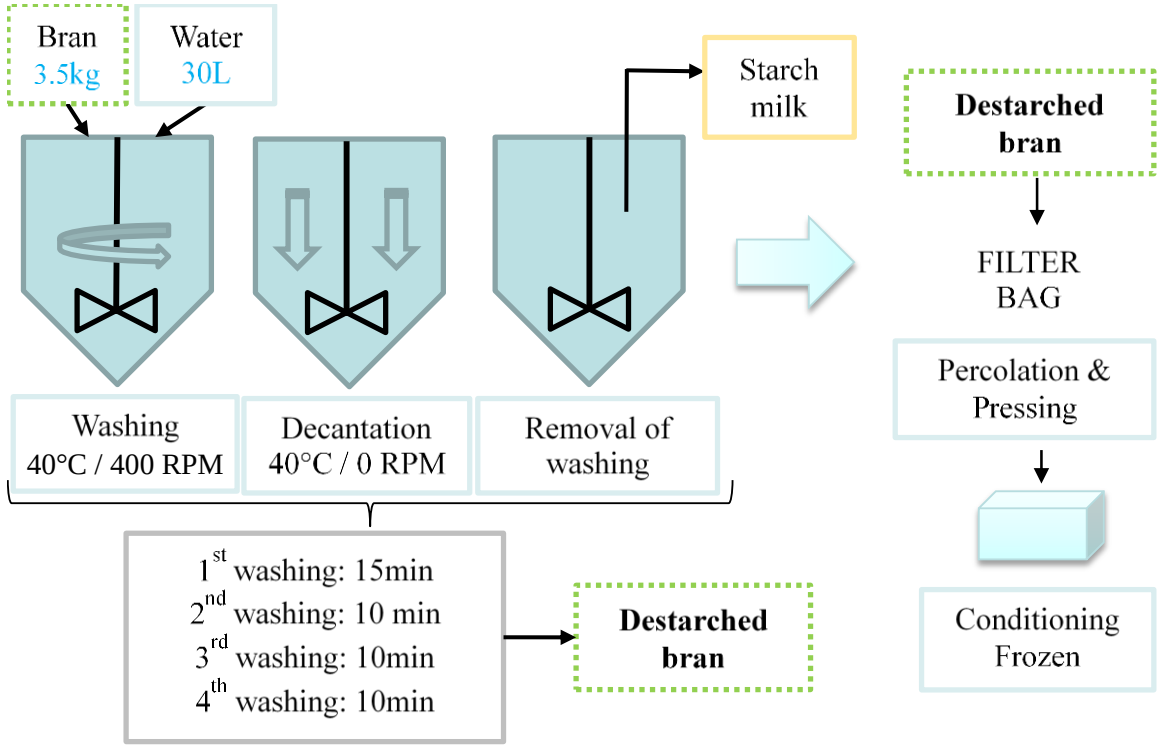

Figure 2-6. Wheat bran destarching protocol

Wheat bran for "la Minoterie de la Save" was selected as it has a higher granulometry than the previous one d(0.5)=1001 µm with a volume distribution of equivalent circle diameter, D_{CE}). This wheat bran was treated with the starch removal protocol and starch content dropped from 16.4 to 4.8 % of wheat bran DM.

To improve starch removal, we considered an additional acid water washing step at 40 °C. Wheat bran was treated with the protocol described above (**Figure 2-6**) and then suspended again in a ratio liquid/solid of 10 (22.7 g of treated wheat bran in 227 ml of water). The pH of the suspension was decreased around 2 by adding drop by drop a 2N H_2SO_4 solution for 10 minutes followed by its neutralization with a 5N NaOH solution. Then, starch content was measured in wheat bran and was found to be as low as 1.98% of its dry mass. To be sure that only starch was degraded, the supernatant from this acid washing step was submitted to acid hydrolysis and the monosaccharides released were identified and quantified by HPIC-HPAEC (**Table 2-2)**. Results show that, although glucose was the major monosaccharide released (2.2 gdm/L), other monosaccharides were also found suggesting that some "recalcitrant fibers" were also degraded by this washing step. In conclusion, the 5th acid washing has been effective in removing a great part of the remaining starch, but its action was not neutral for fibers and also released some sugars which are hallmarks of the NSP structure from wheat bran. Therefore, we restricted our protocol to four hot water washing.

Table 2-2. Monosaccharides released in the supernatant during wheat bran destarching process with an additional acid washing step, and after acid hydrolysis treatment (2N H_2S0_4 at 100°C for 2h) of the supernatant

	Arabinose	Galactose	Glucose	Xylose	Mannose
Concentration, [gdm/L]	0.14	0.19	2.20	0.53	0.02

To conclude, we showed that starch hydrolysis has an influence on the *in-situ* viscosimetry measurements and that Rovabio cocktail has a non-negligible amylolytic activity. Since our objective is to study more specifically the action of this cocktail on NSPs degradation, we successfully adapted a protocol enable to remove more than 70% of the starch that is present in wheat bran to generate our reference substrate termed destarched wheat bran (dWB).

2.4. RESULT PART 2: Development and validation of protocols and conditions for a multiscale analysis of biomass deconstruction

I will present in this part of my thesis the methods and techniques either developed or adapted from literature and that were essential to achieve the objectives described in §1.3 regarding the mechanisms of wheat bran deconstruction by Rovabio enzyme cocktail.

2.4.1. Macroscopic analysis based on *in-* and *ex-situ* viscosity measurements

Suspension viscosity encounters two major constraints: (i) the complexity of the suspension rheological behavior and its evolution related to suspension concentration and to the physico-chemical mechanical properties of particles, (ii) the technical limitations to achieve shear rate and stress measurements in accurate conditions (homogeneous suspension).

Lignocellulosic suspensions may exhibit complex rheological behaviour (Nguyen et al., 2015) and, no standard method for studying their flow behaviours does exist so far, even if several approaches have been explored (Le, 2017; Nguyen et al., 2015). Destarched wheat bran (dWB), as model substrate, contains particles of broad size and shape distribution that in suspension show a rapid decantation which may impair rheological measurements. In order to overcome these challenges, the rheological properties of this suspension were characterized by two methods: (i) *in-situ* viscometry that allows real-time monitoring of suspension viscosity during enzymatic treatment within the bioreactor and (ii) *ex-situ* rheometry under oscillation measurement condition (with serrated plane-plane module) that enables to access to yield stress as well as viscous and elastic modulus.

2.4.1.1. Initial suspension

In a preliminary step, *ex-situ* rheometry was examined under oscillation mode. Several difficulties due to sample heterogeneity and reproducibility, rapid decantation and large particles (> µm) with respect of the gap of the measurement system geometry were observed (data not show). It is remarkable to note that the largest particles D_{CE} > 1.8 mm which are almost negligible in number distribution, were directly responsible of this limitation. Therefore, we were unable to made representative measurements and *ex-situ* rheometry was excluded.

In a second step, *in-situ* viscosimetry was conducted in order to characterize the rheological behaviour of wheat bran suspension. This characterization consists in applying mixing rates from 10 to 300 RPM during 180 s per step, at 41 °C to various suspensions concentrations ranging between 20 up to 90 gdm/L (**Figure 2-7**). In some cases, the highest or the lowest mixing rates were excluded because of technical limitations (maximum torque) or settling phenomena. This analysis allowed the prediction of suspension viscosity at specific conditions of mixing rate and concentration which is valuable to design a hydrolysis process at high dry matter content. The critical concentration which points out the change between different regimes of the suspension (from dilute to semi-dilute) could be determined.

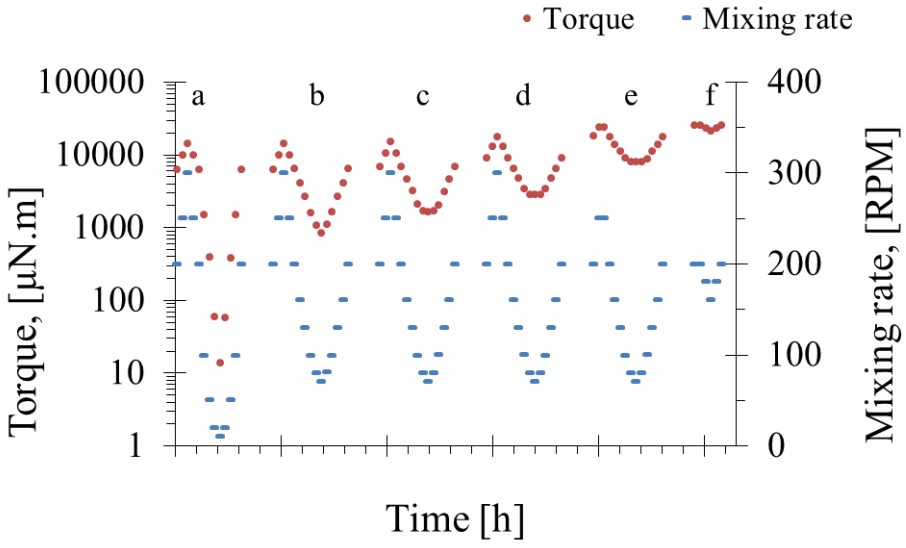

Figure 2-7. Torque and mixing rate as a function of time. *Mixing rates applied to destarched wheat bran suspension and the measured resulting torques at 0 gdm/L (a), 20 gdm/L (b), 40 gdm/L (c), 60 gdm/L (d), 80 gdm/L (e) and 86 gdm/L (f).* Operating conditions: dWB suspended in a potassium phosphate 0,1 M at 41 °C, pH 4.

From raw data (mixing rate, torque), rheograms and suspension viscosity as a function of concentration of wheat suspension were established by using the power consumption curve and applying Metzner & Otto concept (**Figure 2-8**). A Newtonian behaviour was observed for the lowest suspension concentrations (< 40 gdm/L) as the viscosity was independent to the mixing rate whereas at concentrations above 50 g/L, a shear-thinning behaviour was obtained as the viscosity decreased with an increase of mixing rate (**Figure 2-8A**). **Figure 2-8B** presents the suspension viscosity as a function of the substrate concentration for three different mixing rates (160, 200 and 250 RPM equivalent to $\dot{\gamma}$ = 104, 130 and 162 s^{-1} in laminar flow) and, as previously, illustrates two rheological behaviours depending on the suspension concentration: Newtonian below 40 gdm/L and non-Newtonian above 60 gdm/L due to the slight impact of the mixing rate upon suspension viscosity. Similar rheological behaviours using other type of lignocellulosic suspensions have been reported previously (Nguyen et al., 2013; Rosgaard et al., 2007; Viamajala et al., 2009) even if consistency and flow-behaviour indexes widely vary considering the diversity of suspended materials.

The critical concentration, $Ccrit$, marks the transition from dilute to semi-dilute suspensions as well as the appearance of a non-Newtonian behaviour. It was recognized, by applying a linear and a power-law regressions on experimental data for a chosen mixing rate (250 RPM). A *Ccrit* value at 50 gdm/L was attributed to our dWB suspension (**Figure 2-8B**) and beyond this point, a small increase in concentration led to a sharp rise in suspension viscosity. In our case, the viscosity could increase by 7 fold for a 1.5-fold increase in substrate concentration from 50 gdm/L to 75 gdm/L. This dramatic change is very likely due to particle-particle interactions: more entangled are the fibers, more resistance to the flow there is. These interactions are influenced by particle size, shape and suspension free water content (Dasari and Eric Berson, 2007; Nguyen et al., 2015; Viamajala et al., 2009).

Considering that working to extreme high solid content can hardly be investigated due to its extreme complexity, semi-dilute conditions with limited particle-particle interactions was thus considered. It corresponds to dWB suspension at 75 gdm/L, *i.e.* 1.5 times the critical concentration and was characterized by a non-Newtonian behaviour. This controlled complexity was compatible with our further objective to investigate the action of Rovabio on the wheat bran by a combined physical and biochemical approach.

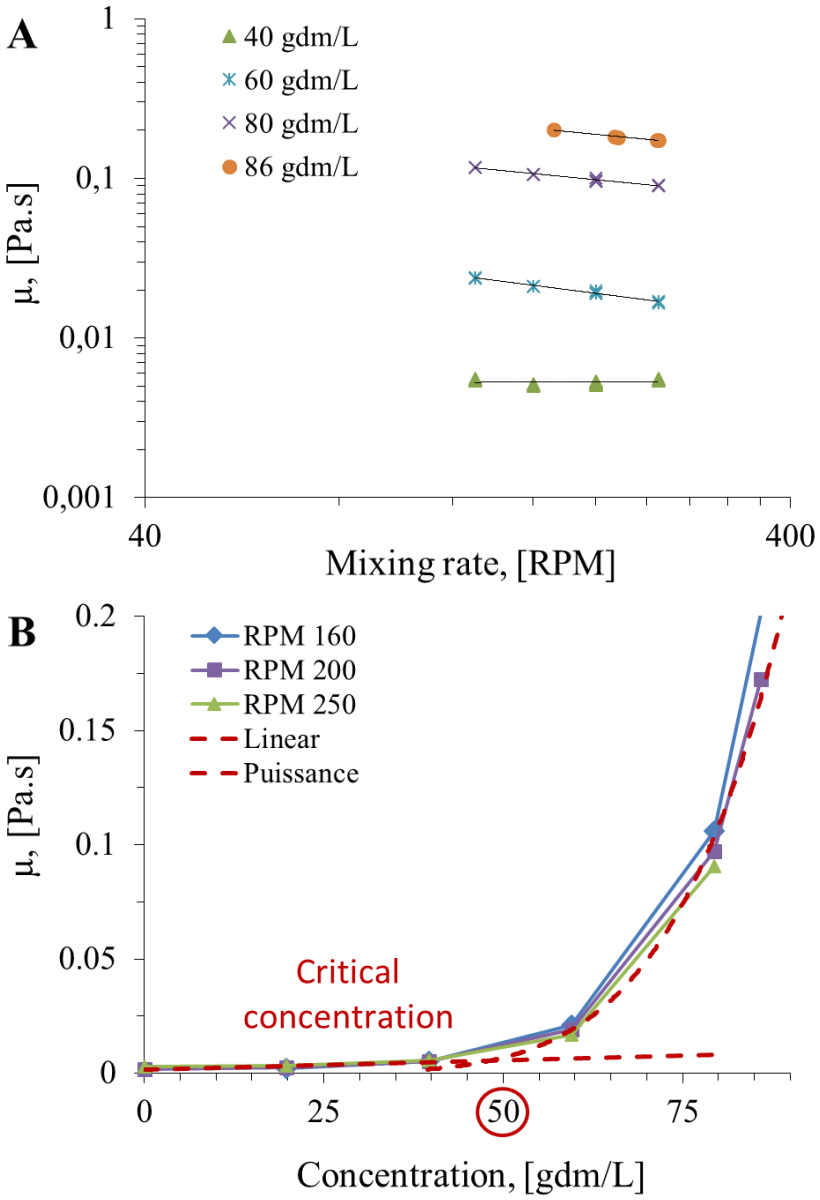

Figure 2-8: Evolution of in-situ viscosity as a function of the mixing rate applied for destarched wheat bran (dWB) suspensions at 40 gdm/L, 60 gdm/L, 80 gdm/L and 86 gdm/L (A) and as a function of the dWB suspension concentration for mixing rate of 160, 200 and 250 RPM. Operating conditions: dWB suspended in a potassium phosphate 0,1 M at 41 °C, pH 4.0.

2.4.1.2. Enzymatic treatments

Considering a suspension between 75 and 85 gdm/L and its rheological behaviour ($n \approx 0.5$, $k \approx 2$), its *in-situ* viscosity was studied at various substrate (dWB)/Rovabio ratios, from 0 to 1100 $U_{xylanase\ visco}$/gdm (**Figure 2-9A**).

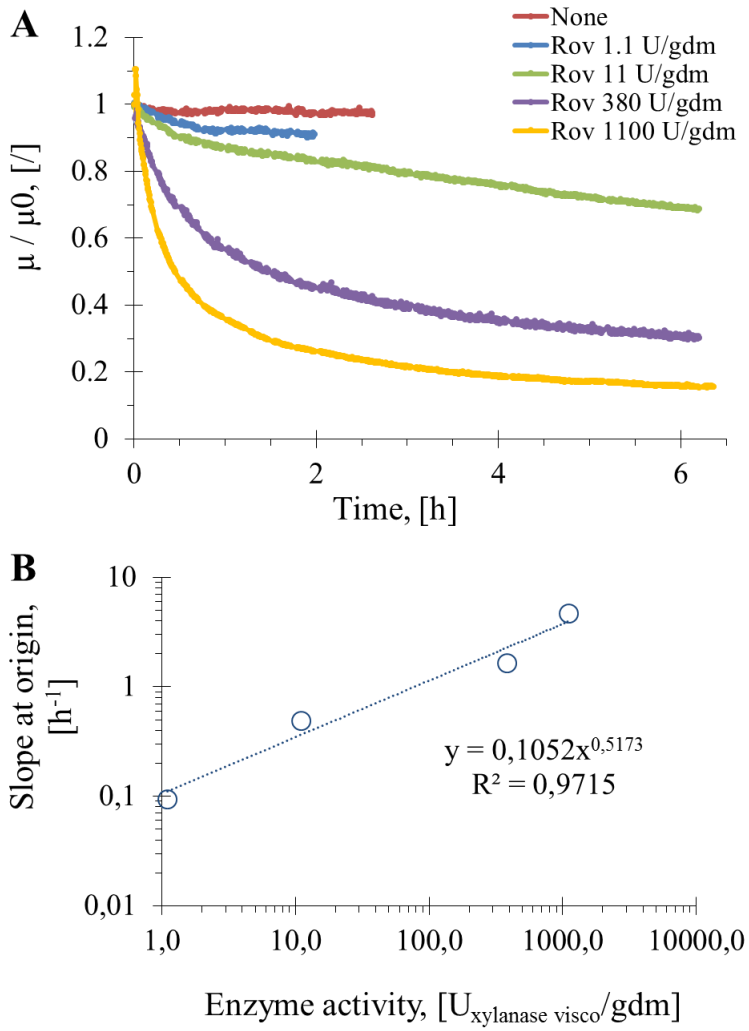

Figure 2-9. Change of the in-situ viscosity during the treatment of dWB suspension with different activity of Rovabio (Brussel) (A). *The activity of Rovabio is estimated by the xylanase viscosity value reported in the figure. The initial viscosity value was about 160 mPa.s and was normalized at t=0, so the change of viscosity was expressed relative to μ0.* ***In (B) is reported the slope at the origin of the in-situ viscosity evolution as a function of the enzyme doses used.*** *The slope at the origin was calculated within the 2 first minutes of the treatment. Operating conditions: destarched wheat bran suspended in a potassium phosphate 0,1M at 41 °C, pH 4.0, initial concentration between 75 to 85 gdm/L.*

In the absence of enzyme solution, the suspension viscosity showed a slight but steady decrease of less than 3% after 2 h. In contrast, the addition of Rovabio Brussel led to a viscosity decrease whose kinetics and magnitudes seem to closely depend on enzyme-substrate ratios. This dose-response was determined by the initial rates of viscosity reduction (curve slope at the origin) at various Rovabio activities (as units of Xylanase), showing a R^2=0.97 (**Figure 2-9B**). This rapid decrease was followed by a slowdown that eventually reached a plateau after 6 h of treatment with the highest enzymatic doses, but likely would require longer time to reach the same viscosity with lower enzyme doses (**Figure 2-9A**). For the highest enzyme dose (1100

$U_{xylanase\ visco}$/gdm), viscosity was about 27 mPa/s at the end of the 6 h of enzymatic treatment, which is far from water viscosity value at 40 °C (0.99 mPa.s) and therefore from the limit of detection. Considering an equivalent glucose concentration, a complete hydrolysis of wheat bran suspension shall result in a solution at about 82 g/L, which would have a viscosity of 1.25 mPa/s at 41 °C (Lide, 2000). Therefore, a value of 27 mPa/s for dWB suspension deconstructed with Rovabio suggested an incomplete hydrolysis of the NSP in this substrate.

Meantime, the rheological behaviour of the suspensions was examined by modulating mixing rates and using the power law model, $\mu = k \cdot \dot{\gamma}^{n-1}$, (**Figure 2-10**). In theory, Metzner & Otto concept is limited to laminar regime, which allows to estimate a mean shear rate knowing Ks. In the present work, this limit was extended to transitional regime (Re < 650) as proposed by Jahangiri, Golkar-Narenji et al. 2001. However, at the highest Rovabio activity (1100 $U_{xylanase\ visco}$/gdm), the turbulent regime was established after 1h15 and for 380 $U_{xylanase\ visco}$/gdm after 5 h of treatment. All the initial suspensions, before the enzymatic treatment, exhibited a flow behaviour index (*n*) around 0.5 reflecting a shear-thinning behaviour (**Figure 2-10B**). The treatment led to a loss of this shear-thinning properties that eventually ended up to a Newtonian behaviour with the 2 highest enzymatic doses. These results suggest that higher the enzyme dose was, greater and faster was the loss of the shear-thinning behaviour. However this analysis was no accurate enough to draw a definitive proof of this effect and should remain as tendencies.

In conclusion, access to *in-situ* viscosity of dWB suspension during its enzymatic treatment is a pertinent method to monitor on a global scale the deconstruction of such a complex material. A critical concentration, specific to our substrate, was determined at 50 gdm/L. Taking into account a working suspension at 75 gdm/L, the addition of Rovabio resulted in a fast decrease of the suspension viscosity concomitant with a loss of its shear-thinning properties. The rate of viscosity change was found to be proportional to the enzyme dose in the 2 first minutes and then slowed down, to reach a plateau at the highest Rovabio activity content. According to Dasari and Berson, 2007; Geddes et al., 2010, suspension viscosity correlates with particles size with a dominant contribution of the bigger ones, even if other properties interfere such as morphological complexity, physico-chemical surface properties or the ratio between sub-population of various size (Quemada, 2006). Thus, our next step was to examine this deconstruction at a microscopic scale with morpho-granulometric analyses.

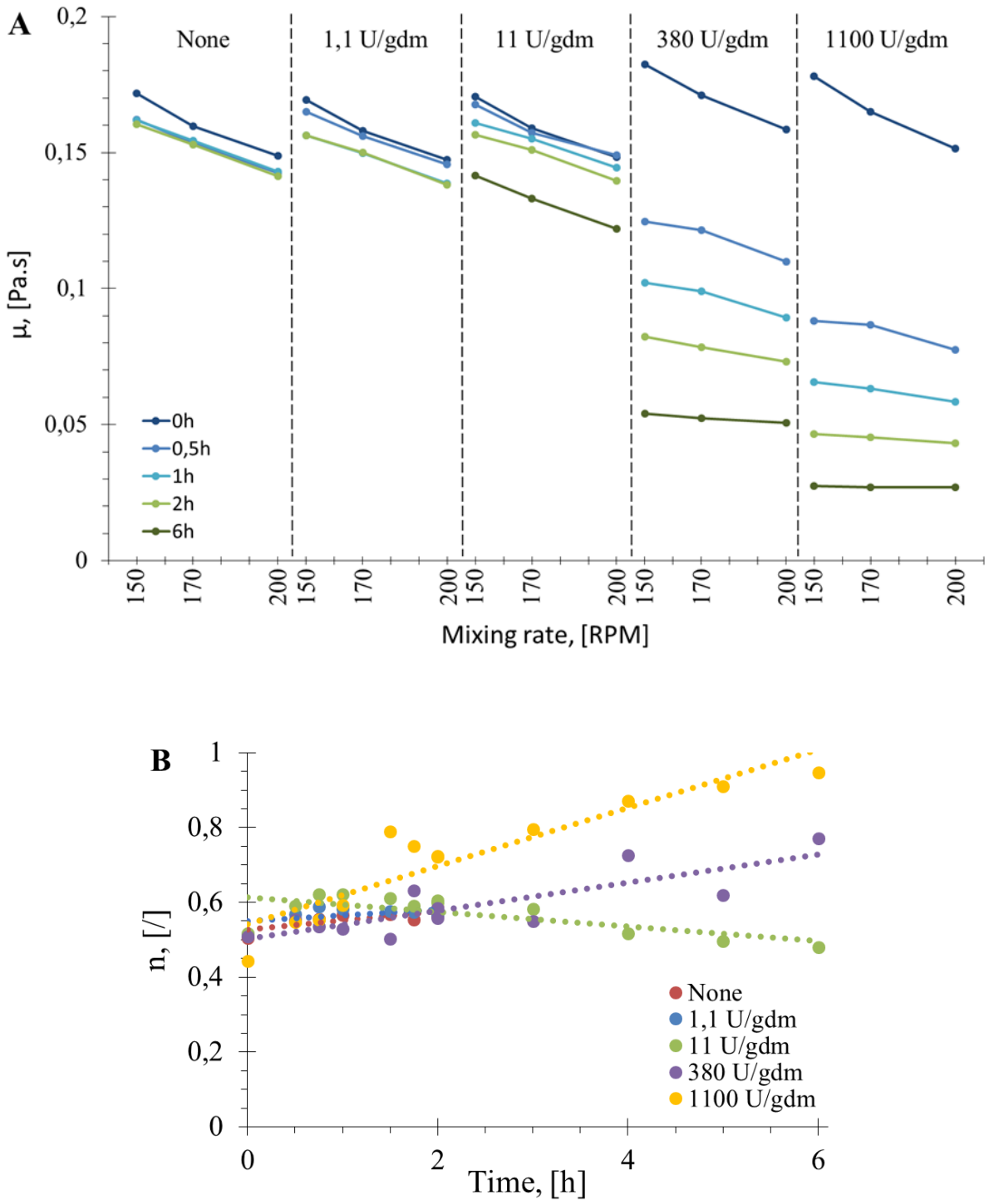

Figure 2-10. Suspension viscosity as a function the mixing rate for different hydrolysis time without enzyme (None) and treated with 11, 380 and 1100 $U_{xylanase\ visco}$/gdm (A) and flow behaviour index (n) as a function of hydrolysis time (B). *Operating conditions identical to Fig.2-9.*

2.4.2. Microscopic analyses based on particle size and morphology

2.4.2.1. Methods to analyze particle size and morphology

A broad range of methods is currently available to characterize particles size and shape, including optical microscopy, morpho-granulometric (microscopy associated with automatic image acquisition and particle analysis), dynamic light scattering, static or dynamic image analyses, tomography, scanning electron microscopy, size exclusion chromatography, resonant mass measurements, electrophoretic light scattering and focus beam reflectance measurements. With regular-shaped and spherical particles, size characterization is simple and a single method can be sufficient to analyse their morphogranulometric properties. However, characterizing and quantifying the size and shape of irregular complex material such as dWB suspension require to combine different methods. Among the existing techniques, three methods were selected and compared in this study: focus beam reflectance measurement (FBRM), morphogranulometry (MG) and dynamic laser light scattering (DLS).

Table 2-3 provides a summary of technical specifications of morphogranulometry methods reported in §6.4.3. These methods enable measurements of the size distribution profiles (either in number, E_n; or in volume, E_v) at the entire population level (statistically representative) and, each of these tools allow to investigate the particle according to a specific range of size.

Table 2-3. Specifications of the three selected techniques for the characterization of particle size

Method	**FBRM**	**DLS**	**MG**
Measurement mode	*In-situ*	*Ex-situ*	*Ex-situ*
Wavelength	795 nm	632.8 / 470 nm	White light
Sample preparation	None	Sampling Dilution	Sampling Dilution Plate preparation
Dimension	2D	3D	2D
Measured parameter	N_c, l_c	d_{se}	d_{ce} (and others)
Size range	0.1 – 1000 µm	0.01 – 2000 µm	0.1 – 4000 µm
Size distribution	E_n	E_v	E_n

The FBRM is a powerful tool for studying *in-situ* the evolution of particles size during an enzymatic reaction, or others bioprocesses. It gives information on the number distribution of particles chord length, which is sensitive to the fraction of fine population (< 100 µm for dWB). On the other hand, the DLS is based on volume distribution which highlights the contribution of coarse population. The advantage of FBRM and DLS methods is the automatized measures which minimize the measurement error and ensure a high reproducibility. However, the conversion from raw signal into final data (distribution function)

needs to be performed under restriction considering the non-spherical irregular shape of dWB particles and the mathematical model used. The last method, optical morphogranulometry (MG) consists in the direct observation of particles under microscopy and requires less theoretical assumption than FBRM or DLS. In contrast, the disadvantages of MG come from the sample preparation step (sampling and sample deposition between cover glass and slide), which could strongly affect the analyses which are far less reproducible.

2.4.2.2. Particle size analyses during enzymatic treatment

- **Morphogranulometry measurements (MG)**

The morphogranulometric analysis in wet way required several operations to prepare samples and several difficulties were encountered due to the sampling method and the sample heterogeneity and reproducibility. In addition, the large spreading of particle size distribution (from about 10 µm to 3000 µm) and the thickness of the sample observed between slide and coverslip caused difficulties to focus the image both on large and small particles. To overcome this problem various operating conditions were selected and tested with different samples:

- Dark field or bright field illumination,
- Magnification X5, x10, x25 or combination of several magnifications,
- Various light intensity and time of exposition (with dark field illumination).

However, neither parameters allow to ensure accurate measurements and these difficulties led to poorly reproducible results (data not shown). Thus, the methodology does not allow to find any significant evolution of particle size during the enzymatic treatment of dWB, even at the highest dose of Rovabio (1100 $U_{xylanase\ visco}$/gdm) (data not shown).

- **DLS measurements**

With DLS, large sample volume can be analysed and volume distribution of sphere equivalent diameter, $E_v(d_{se})$, can be determined. **Figure 2-11** presents the evolution of $E_v(d_{se})$ during dWB deconstruction by Rovabio Brussel at various enzyme-substrate ratios. The particle size did not change significantly during the treatment at the two lowest enzyme doses (**Figure 2-11A and B**). On the contrary, with 380 $U_{xylanase\ visco}$/gdm (**Figure 2-11C**), PSD showed a decrease of coarse particles population and concomitantly a slight apparition of particles with smaller sizes. After 2 h of enzymatic treatment, an opposite trend was observed with a slight rise of coarse particles and a reduction on the fine ones. At the highest dose of 1100 U/gdm (**Figure 2-11D**), same trends in PSD was observed during the 1st hydrolysis hour and then no significant changes were observed for longer treatment.

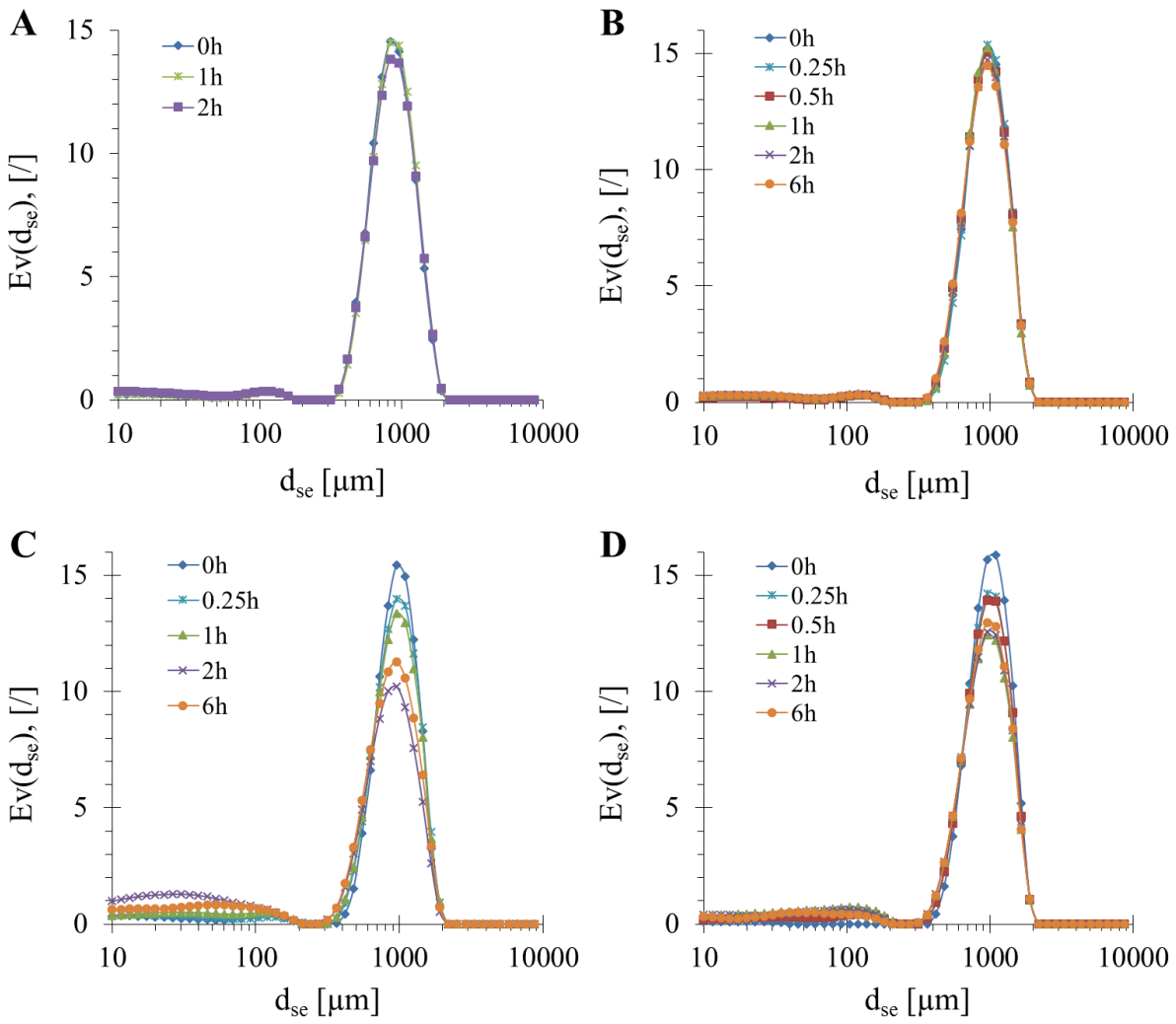

Figure 2-11. Particle size distribution evolution during the treatment of destarched wheat bran suspension in the presence of Rovabio Brussel at 1.1 U/gdm (A), 11 U/gdm (B), 380 U/gdm (C) and 1100 U/gdm (D). *The particle size distribution was assimilated to a diameter of equivalent sphere (dse). Operating conditions identical to Fig.2-9.*

The results presented above (**Figure 2-11)** suggest that the deconstruction of dWB is characterized by the equilibrium of different classes of particle size (fine and large) whose proportions vary during the treatment. We found that the decrease of the coarse particles was not compensated by an increase in smaller populations, indicating that part of these particles had been solubilized during the treatment. Solubilization phenomenon was even more significant when large particles increased at the same time that small ones decreased, as after 6 h of hydrolysis with 380 U/gdm of Rovabio (**Figure 2-11C)**. Therefore, by multiplying E_v(dse) by the dry matter content of the suspension (Cm), we should report quantitatively the evolution of PSD at different times during the treatment of the suspension with Rovabio (**Figure 2-12**).

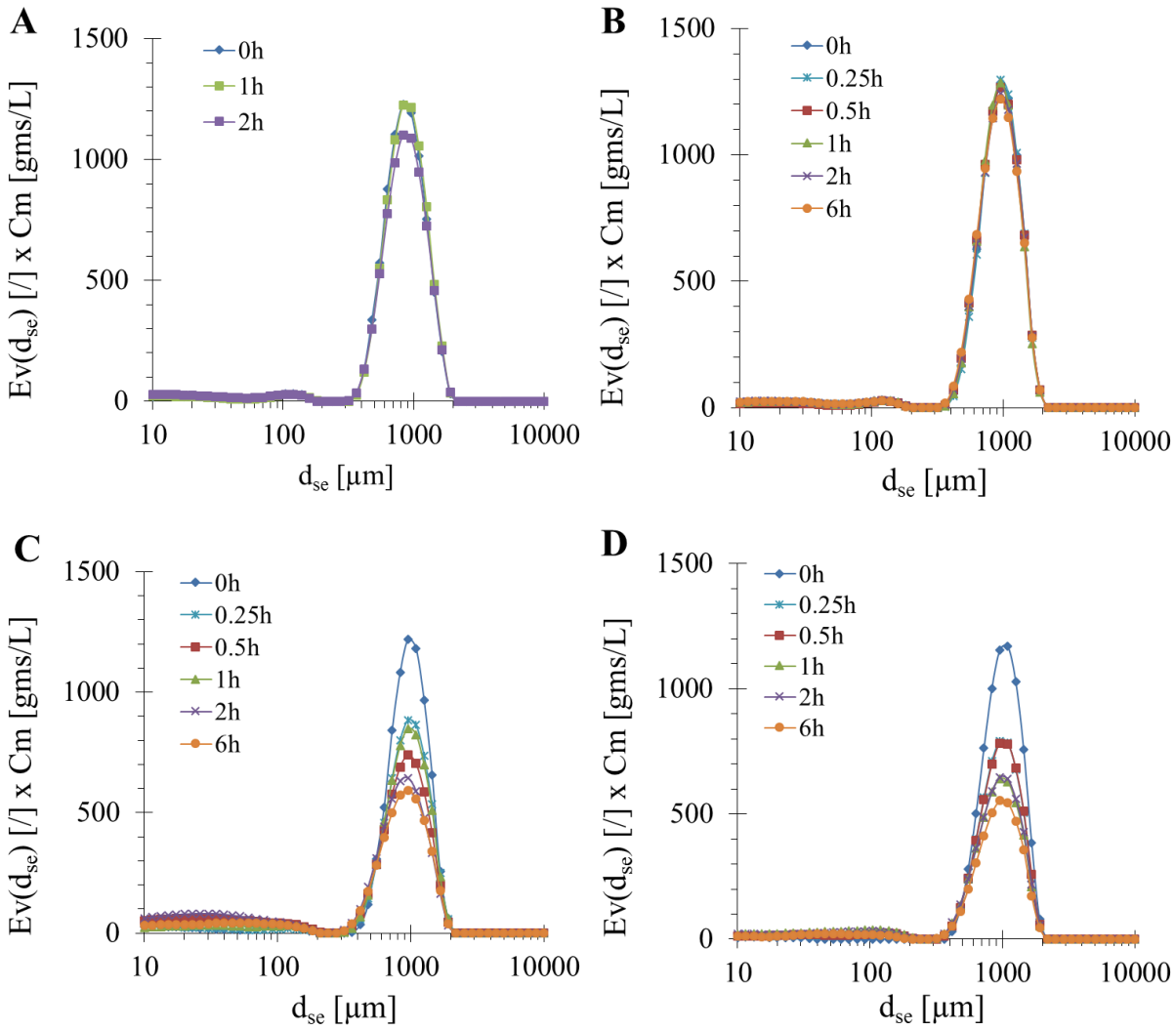

Figure 2-12. Particle size distribution plotted with the respect to the particle abundance during the treatment of destarched wheat bran suspension in the presence of Rovabio Brussel: 1.1 U/gdm (A), 11 U/gdm (B), 380 U/gdm (C) and 1100 U/gdm (D). *The particle size distribution was assimilated to a diameter of equivalent sphere (dse) and multiplyed by the concentration of wheat bran suspension (Cm) that remained at each time during the enzymatic treatment. Operating conditions identical to Fig.2-9.*

As shown previously, only a slight decrease of coarse particles population was measured with the two lowest enzyme doses (**Figure 2-12A and B**). At the two highest doses, there was a significant reduction of coarse particles population, even faster for the highest one which was not balanced by accumulation of fine population which otherwise remained almost unchanged (**Figure 2-12C and D**). This almost unchanged proportion of the finest population during the treatment suggested that the small particles originated from the fragmentation of coarse particles were entirely solubilized, which should therefore suggest that the fragmentation of these coarse particles might be the limiting step in Rovabio action on wheat bran.

- **FBRM measurements**

Since the evolution of small populations may be hidden by the coarse ones with DLS analysis as a volume distribution focus on large particles, we employed the *in-situ* FBRM measurements to monitor the evolution of these populations. *In-situ* CLD measurements provide access to two parameters: number distribution of particle chord length (lc) and number of count per second (Nc). Results expressed in number focus on the finest population as the number of coarse particles was almost negligible. **Figure 2-13** illustrates the evolution of Nc and mean lc within the dWB suspension deconstruction at various doses of Rovabio Brussel. During the treatment, the sharp evolution of suspension viscosity may induced important change in flow regime and pattern, therefore interpretation of Nc analysis will be limited to time intervals of stable viscosity (< 25% deviation). Thus, in the present work, we excluded the first 15 min of treatment with 380 and 1100 $U_{xylanase\ visco}$/gdm. The small peaks visible, especially for lower enzymatic doses (**Figure 2-13A and B**) are explained by the mixing rate shifts applied to explore the rheological behaviour which modify the suspension flow regime.

Our FBRM analysis allows to illustrate fragmentation and solubilization phenomena that take place during the treatment of dWB with Rovabio. Fragmentation is highlighted by a reduction of mean lc ($\overline{lc}$) and an increase of the number of count (Nc) whereas solubilization corresponds to a decrease of both of them. At the two lowest doses (1.1 and 11 $U_{xylanase\ visco}$/gdm), Nc increased and $\overline{lc}$ decreased within the 2 first hours of enzymatic treatment, which supports a dominant fragmentation process (**Figure 2-13A and B**). Beyond 2h with 11 $U_{xylanase\ visco}$/gdm, fragmentation was balanced by a solubilization of the finest particles resulting in constant Nc and a slower $\overline{lc}$ decrease. With 380 $U_{xylanase\ visco}$/gdm, Nc sharply increased and reached a plateau after only 45 min of treatment. Concomitantly, $\overline{lc}$ significantly decreased with a kinetic which slow down over time (**Figure 2-13C**). Considering the original assumptions, the initial particle fragmentation was, beyond 45 min, compensated by solubilization. For the highest enzyme dose, 1100 $U_{xylanase\ visco}$/gdm same particle size reduction was measured but Nc evolution was different: Nc raised significantly during 15 min and then the increase slowed down to finally decreased beyond 3 h of hydrolysis (**Figure 2-13D**). These final Nc and $\overline{lc}$ trends sustain a dominant solubilization phenomenon compared to fractionation one. Altogether these results allow to conclude that the fine particles population was fractionated under enzymatic treatment resulting in a particle size reduction and even more at a higher dose of

Rovabio. At this highest dose, the smallest subpopulation issue from fragmentation of the coarse ones was clearly solubilized as indicated by Nc which decreased.

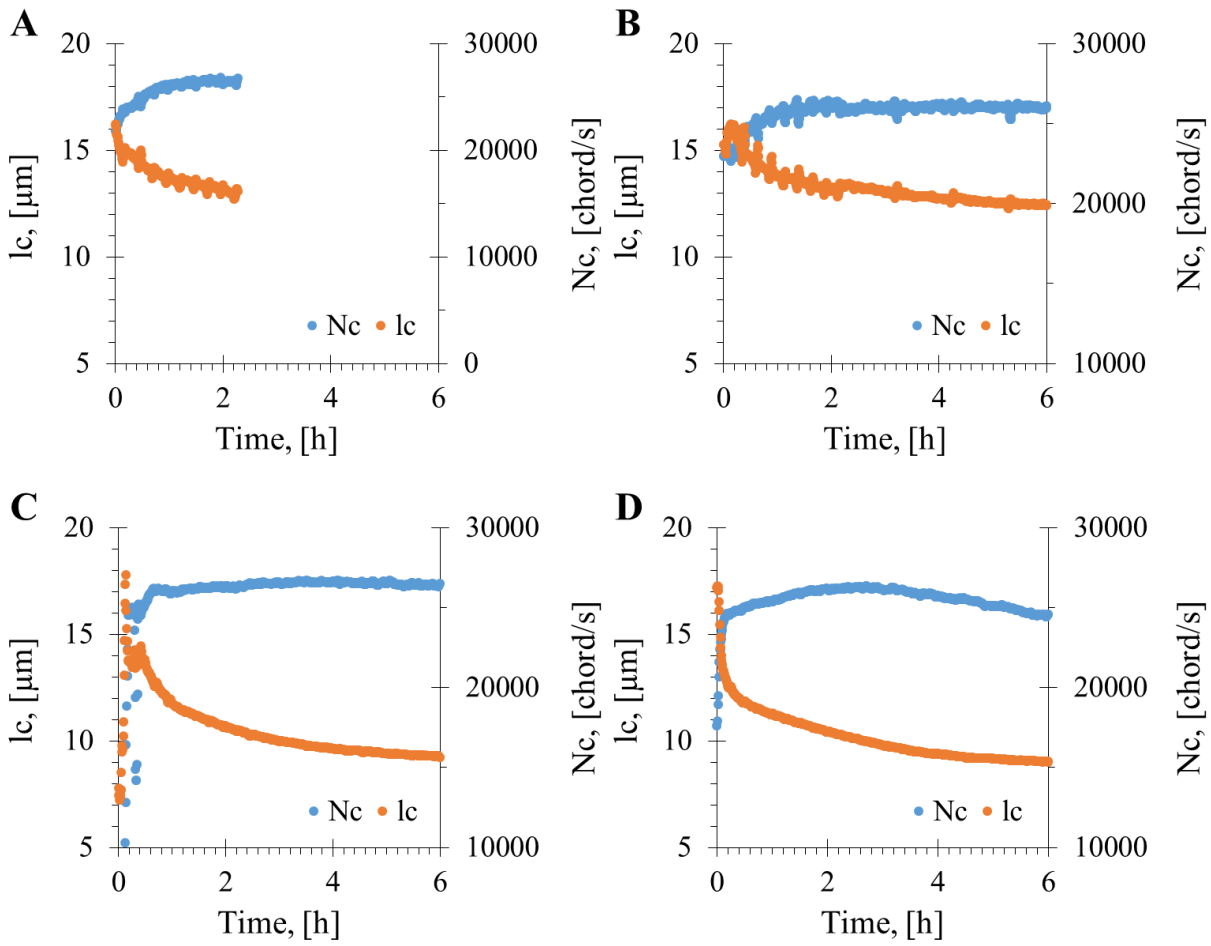

Figure 2-13. Evolution of the number of count per sec (Nc) and mean lc during wheat bran suspension hydrolysis by Rovabio Brussel at 1.1 U/gdm (A), 11 U/gdm (B), 380 U/gdm (C) and 1100 U/gdm (D). *Operating condition identical to Fig.2-9.*

To further analyse the finest population, the number distribution of chord length (lc) is reported in the **Figure 2-14**. While at low enzymatic doses (1.1 and 11 $U_{xylanase\ visco}$/gdm) CLD barely changed over the entire period of treatment (**Figure 2-14A and B**), we found that at a higher dose (380 $U_{xylanase\ visco}$/gdm), the fine population (< 100 µm) increased significantly as a consequence of a stronger fragmentation phenomenon of coarse particles (> 100µm) (**Figure 2-14C**). We have to notice that with 380 $U_{xylanase\ visco}$ /gdm, CLD was not represented in the first minutes because the CLD measurements was not correct. At the highest enzymatic dose (1100 $U_{xylanase\ visco}$/gdm), the small particles increase was concomitant with a global reduction of particle size as CLD curves shift left toward smaller sizes (**Figure 2-14D**). For all these enzymatic treatments, FBRM measurements provide the evolution of the small particles

population (< 100 µm) which could either increase due to fragmentation of coarse particles or decrease due to solubilization phenomenon. To take into account these two phenomena CLD were multiplied by Nc (**Annex 2**) and this representation led exactly to the same conclusions.

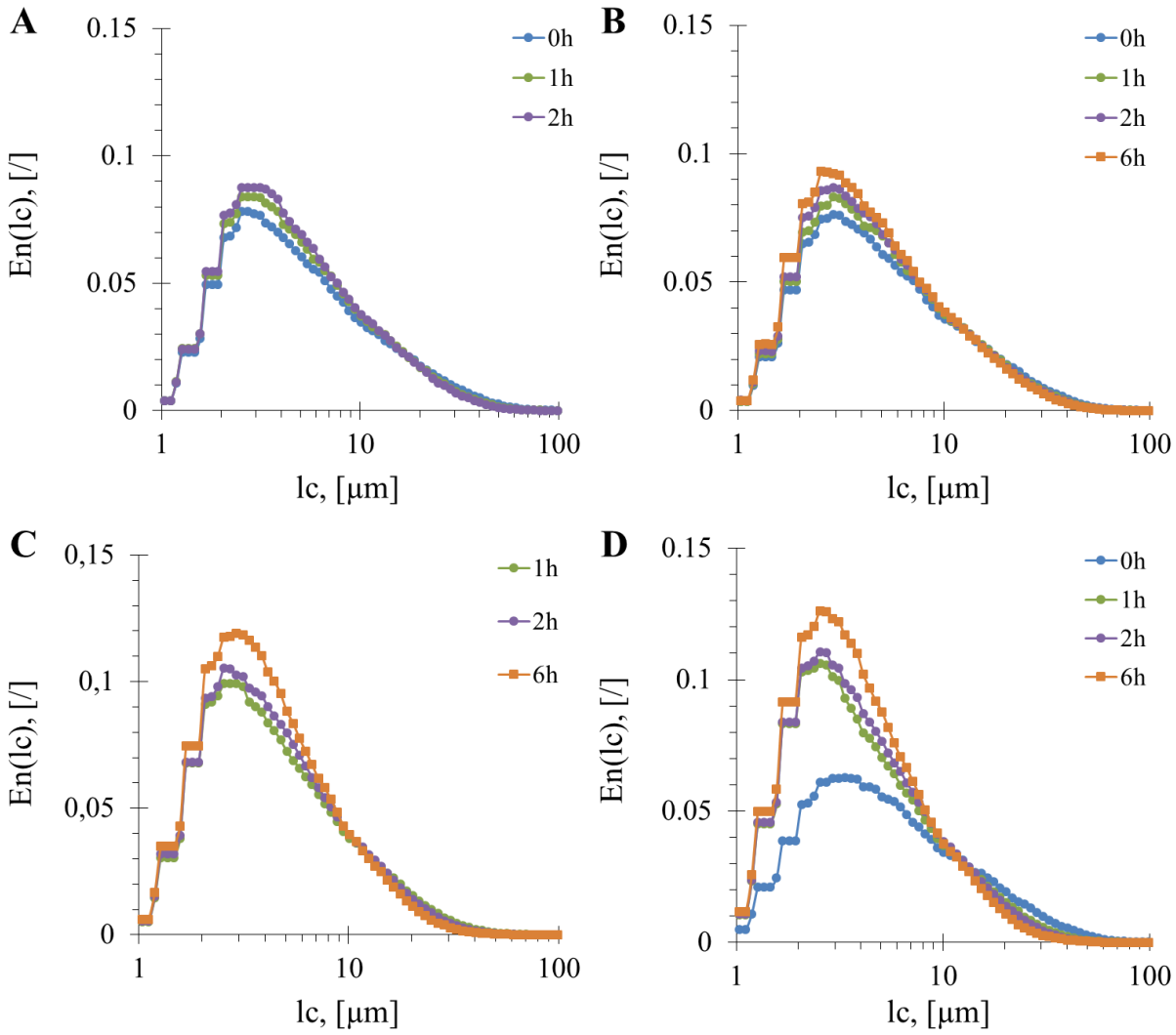

Figure 2-14: Chord length (lc) number distribution of wheat bran suspension during hydrolysis with Rovabio Brussel with 1.1 U/gdm (A), 11 U/gdm (B), 380 U/gdm (C) and 1100 U/gdm (D). *Operating conditions identical to Fig.2-9.*

Altogether FBRM and DLS measurements supported the notion that coarse particles were initially fractioned (DLS) and this fragmentation process continued with the finest population (FBRM) resulting in smaller and smaller particles. In addition, this fragmentation was concomitant with a particle solubilization which together represents the key phenomenon to explain dWB deconstruction.

2.4.3. Molecular scale: biochemical analyses

2.4.3.1. Methods for polysaccharides determination by acid hydrolysis

The quantification of solubilized 'sugars' (i.e. considered as a generic term to mean enzymatic release of complex polysaccharides into the liquid phase of the suspension) during the treatment with Rovabio is determinant to characterize dWB deconstruction. This bioconversion results in both monosaccharides and oligosaccharides release. Methods for quantification of monosaccharides by HPAEC-PAD are well established (Hell et al., 2014) while quantification and characterization of oligosaccharides are more complicated due to their complex and heterogeneous compositions. Therefore, an acid hydrolysis treatment, which can hydrolyse polysaccharides into its monomers, is a good method to determine polysaccharides composition (both as soluble released sugars or remaining in insoluble fraction) during the dWB treatment with Rovabio. Generally a concentrated acidic treatment at low temperature to solubilize insoluble sugars is followed by a second step with more diluted acid at high temperature to cleave glycosidic linkages. Oligosaccharides already soluble are only submitted to the second acid hydrolysis step. Our strategy was to look for the various acid hydrolysis conditions found in the literature and to test those which seem to be the more pertinent regarding our matrix (% of the dry mass treated) for both soluble and insoluble polysaccharides. An overview of various published protocols developed for this purpose is reported in the **Table 2-4**.

Table 2-4. Overview of acid hydrolysis conditions found in the literature

Authors	Substrate	1st hydrolysis						2nd hydrolysis		
		H_2SO_4	**Sample [g]**	**Acid [ml]**	**v/w [ml/g]**	**T°C**	**time**	**H_2SO_4**	**T°C**	**time**
(Alves et al., 2010)	Eucalyptus, bagasse and bamboo	72%	0.5	16	32	25°C	2h	40%	80°C	1h
(Wijaya et al., 2014)	Lignocellulose	65 / 70 / 75 / 80%			2	30°C	0,5h	30%	80 / 100°C	2h
(François, 2007)	fungal cell walls	72%	0.01	0.075	7.5	RT	3h	2N (9,3%)	100°C	4h
(Slavin and Marlett, 1983)	food and feces	72%	2	10 / 15 g		24 °C	3h		100 °C	2h
(Hoebler et al., 1989)	Avicel, wheat straw and bran, ect	72%	0.1	1.25	12.5	25 / 30°C	0,25 / 0,5 / 1h	2N (9,3%)	100 °C	0,5 / 1 / 1,5 / 2 / 4h
(Yoon et al., 2014)	Cellulose, willow	72%	0.07	0.8	11	30°C	1h	4%	100 / 110 / 120°C	1,25 / 1,5 / 1,75 / 2h
(Pettersen, 1984)	Wood	72%	0.2	?		30 °C	1h	3%	120°C	1h
(Pettersen, 1991)	Wood	72%	0.05	0.5	10	30 °C	1h	4%	120 °C	1h
(Milne et al., 1992)	Pine, willow, wheat straw, bagasse	72%	0.25	3	12	30°C	1h		125 °C	1h
(Saeman et al., 1954)	Wood, wood pulps	72%	0.3	3	10	30 °C	1h	4%	15 psi	1h
(Templeton and Ehrman, 1995)		72%	0.3	3	10	30°C	1h	4%	121 °C	1h
(Gao et al., 2014)	Hemicellulose		0.3	87	290			4%	121°C	1h
(Zhou and Runge, 2014)	Cotton, filter paper, starch, holocellulose	72%	0,2 / 0,3 / 0,4	3	15 - 10 - 7,5	30°C	1h	4%	121°C	1h

According to this literature overview, it appears that an acid concentration superior to 70% is required for complete hydrolysis of carbohydrates, especially crystalline cellulose (Wijaya et al., 2014) and that the first acid hydrolysis step must be carried out at 25 °C rather than at 30 °C (Hoebler et al., 1989). Strong acid condition is generally more effective than increasing temperature both to hydrolyse polysaccharides and to minimize monosaccharides degradation (Wijaya et al., 2014). Acid concentration appears thus to be the most important parameter for a high sugar released (Rahman et al., 2007; Roberto et al., 2003). In that respect a higher acid/material ratio (v/w) is favourable in case of very recalcitrant carbohydrates difficult to hydrolyse but could have a negative effect if the hydrolysis is complete due to monosaccharide degradation (Zhou and Runge, 2014). Similarly, the 2nd hydrolysis step should be kept at 100 °C in order to reduce monosaccharides degradation (Yoon et al., 2014). Based on these considerations, our experimental plan is presented in the **Table 2-5**. Commercial products used in this work: insoluble wheat AX, soluble wheat AX and soluble xyloglucan are pure at 80%, 95% and 95% respectively, therefore correction factors will be applied to take that into account.

Table 2-5. Experimental plan to test various acid hydrolysis protocols

	1st step			2nd step			Protocol n°
Substrate	Time	Temperature	Ratio $V_{acid}/W_{substrate}$	Time	Temperature	Acid concentration	
Insoluble AX Wheat bran Maize bran	1h	30 °C	10, 15	1h	121 °C	4%	**1**
	3h	RT	10, 15	1h	121 °C	4%	**2**
	1h	30 °C	7.5	1h	121 °C (autoclave)	4%	**3**
	1h	30 °C	7.5	2, 3, 4, 6h	100 °C	9.3% (2N)	**4**
	3h	RT	7.5	2, 3, 4, 6h	100 °C	9.3% (2N)	**5**
	1h	30°	7.5, 10, 15, 20	3h	100 °C	9.3% (2N)	**6**
	3h	RT	7.5, 10, 15, 20	3h	100 °C	9.3% (2N)	**7**
Soluble AX, xyloglucans	None			2, 3, 4h	100 °C	9.3% (2N)	**8**
Ara, Glc, Gal, Xyl, Man	None			2, 3, 4h	100 °C	9.3% (2N)	**9**

- **Results for insoluble polysaccharides**

Protocols 1 and 2 listed in **Table 2-5**, using 3 types of insoluble materials, *i.e.* arabinoxylan, wheat bran and maize bran, were tested to evaluate the impact of the second acid hydrolysis step at 121 °C (4% of H_2SO_4 during 1 h). Two different 1st steps (1 h at 30 °C and 3 h at room temperature, RT) were used with 2 ratios $V_{acid}/W_{substrate}$ (10 and 15). For both protocols 1 and 2, the release of monosaccharides determined by HPAEC-PAD was greater at a higher ratio $V_{acid}/W_{substrate}$ (**Figure 2-15A, B, C, D, E and F)** and following a 1st acidic hydrolysis step at RT for 3 h rather than at 30 °C for 1 h. **Figure 2-15G** presents the overall yield as the equivalent total sugar content calculated from the release monosaccharides (see materials and methods §6.3.3) after digestion by the acidic treatment for protocols 1, 2 and 3 (**Table 2-5**) at a ratio $V_{acid}/W_{substrate}$ of 15. Protocol 3 corresponds to the NREL (National Renewable Energy Laboratory, USA) reference protocol for lignocellulolytic matrix and consists in autoclaving the solution as 2nd step of acid hydrolysis. This protocol appeared to be less efficient than the two other ones as it likely caused a more important loss of sugars due to its stronger acidic conditions.

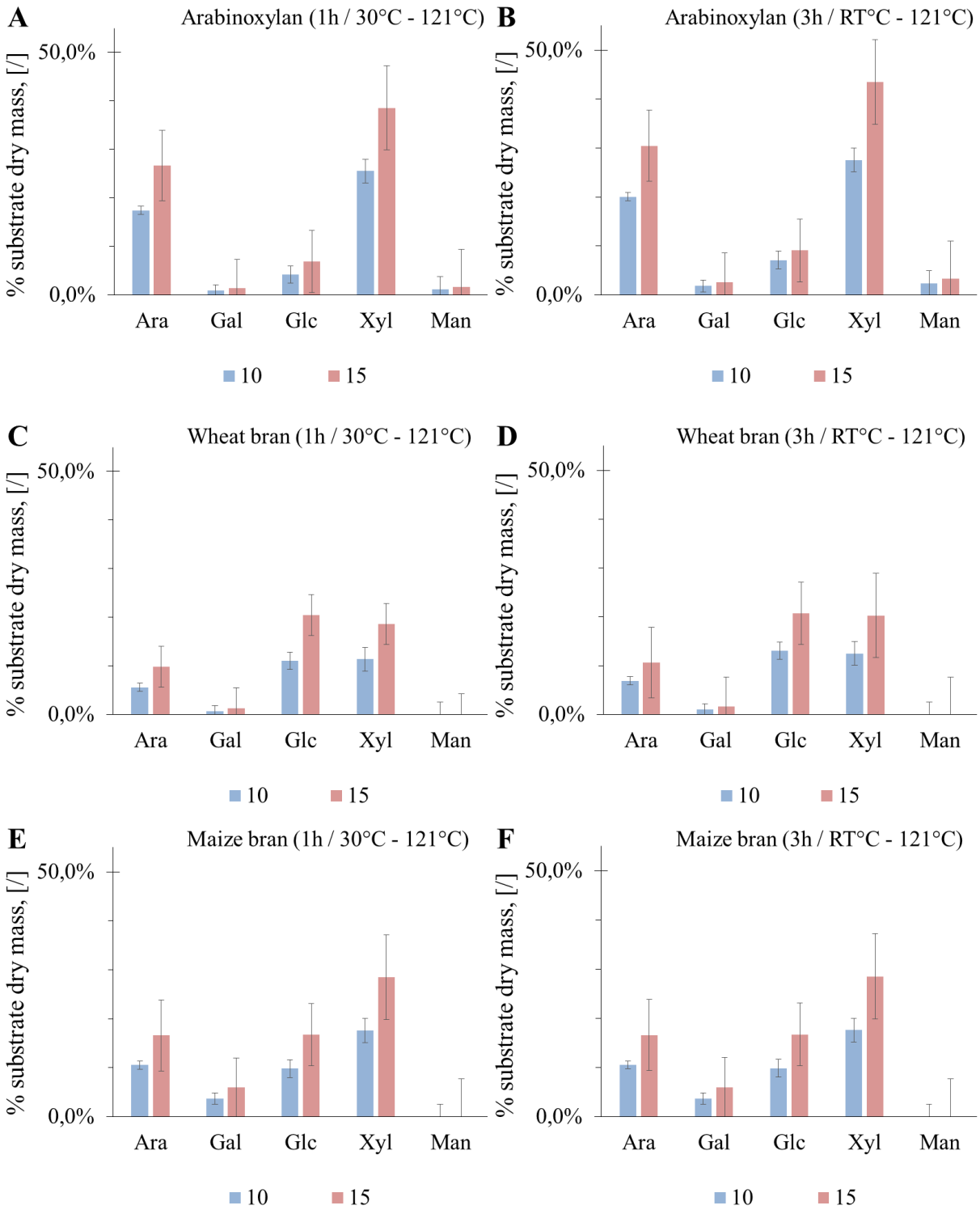
A
Arabinoxylan (1h / 30°C - 121°C)
B
Arabinoxylan (3h / RT°C - 121°C)
C
Wheat bran (1h / 30°C - 121°C)
D
Wheat bran (3h / RT°C - 121°C)
E
Maize bran (1h / 30°C - 121°C)
F
Maize bran (3h / RT°C - 121°C)
% substrate dry mass, [/]
50,0%
0,0%
Ara
Gal
Glc
Xyl
Man
10
15

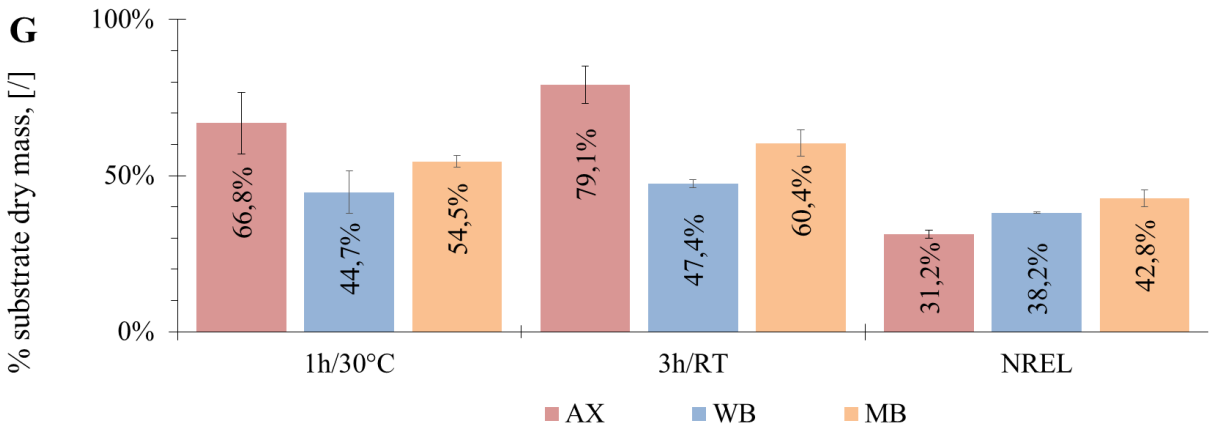

Figure 2-15. Release of arabinose (Ara), galactose (Gal), glucose (Glc), xylose (Xyl) and mannose (Man) (A, B, C, D, E, F) and the equivalent total sugar recovery (G) by various acid hydrolysis treatment (indicated at the top of each figure) of insoluble AX, WB and MB and expressed as the percentage of initial dry matter treated (% substrate dry mass). *The error bars represent the standard deviation of three independent experiments.*

Secondly, we used the protocols 4 and 5 to test a 2nd step of acid hydrolysis at 100 °C for 2, 3, 4, or 6 h (2N H_2SO_4) which followed a 1st step at 30 °C for 1 h or at RT for 3 h. **Figure 2-16** shows that increasing the duration of the 2nd step decreased xylose yield, especially for wheat bran (**Figure 2-16C and D**) suggesting in agreement with previous reports, that xylose is very sensitive to acid treatment leading to its conversion into furans derivatives (Yoon et al., 2014). On the contrary, the release of glucose moieties from the polysaccharides increased with the time of acid treatment suggesting that glucose from cellulose crystalline structure was harder to hydrolyse (**Figure 2-16A and B).** The total sugar recovery (**Figure 2-16G and F**) shows that a first step at 30 °C for 1 h provided a higher hydrolysis rate than at RT for 3 h. On the other hand, the duration of the 2nd step has an impact on the hydrolysis yield that is different between sugars. Altogether these results illustrate the difficulty to find the best protocol as each monosaccharide is more or less versatile and each structure is more or less hydrolysable. As wheat bran is our reference substrate, we decided to retain a 2nd step at 100 °C for 3 h as this one provides the best hydrolysis yield for this fiber matrix.

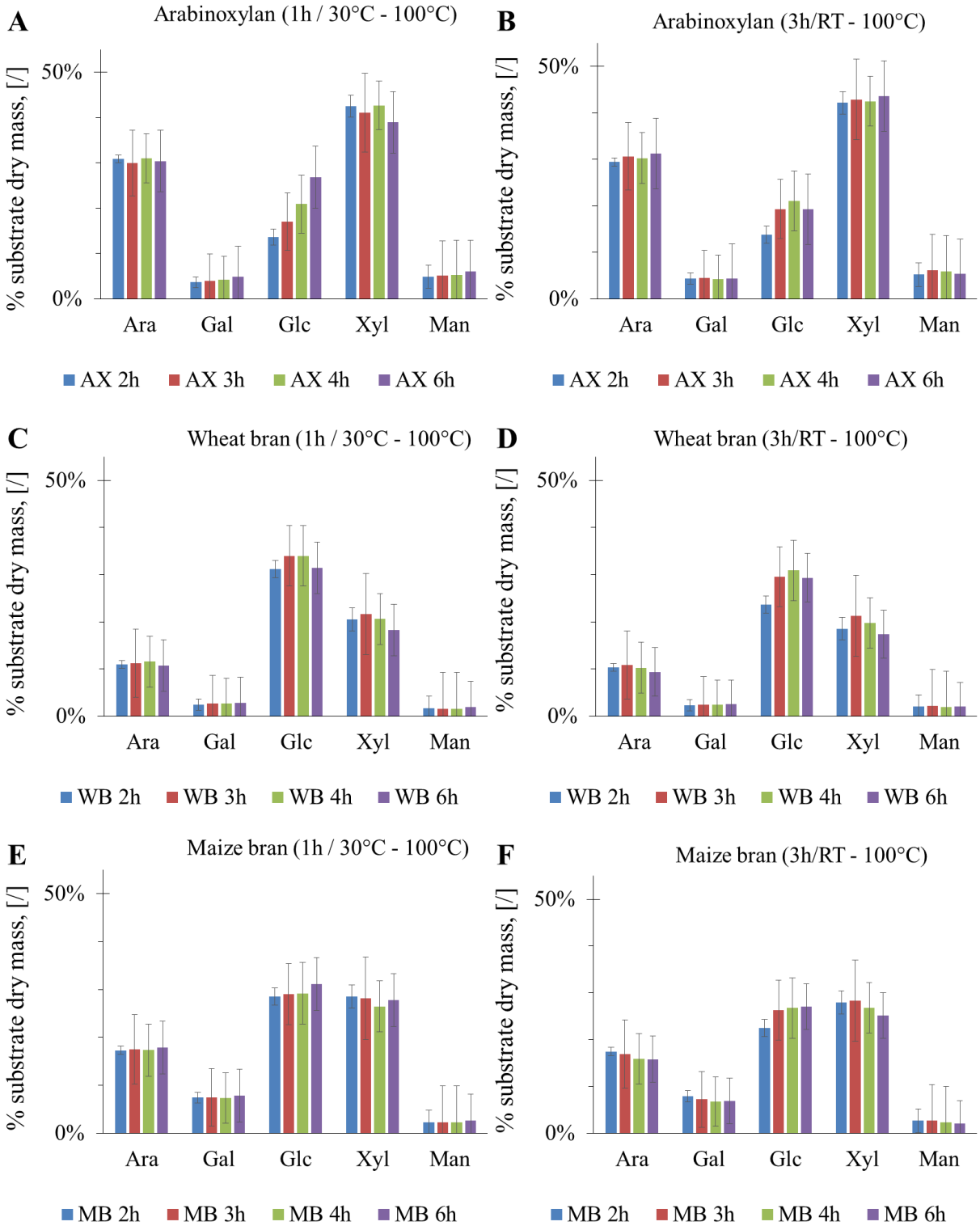
A
Arabinoxylan (1h / 30°C - 100°C)
% substrate dry mass, [/]
50%
0%
Ara
Gal
Glc
Xyl
Man
AX 2h
AX 3h
AX 4h
AX 6h
B
Arabinoxylan (3h/RT - 100°C)
% substrate dry mass, [/]
50%
0%
Ara
Gal
Glc
Xyl
Man
AX 2h
AX 3h
AX 4h
AX 6h
C
Wheat bran (1h / 30°C - 100°C)
% substrate dry mass, [/]
50%
0%
Ara
Gal
Glc
Xyl
Man
WB 2h
WB 3h
WB 4h
WB 6h
D
Wheat bran (3h/RT - 100°C)
% substrate dry mass, [/]
50%
0%
Ara
Gal
Glc
Xyl
Man
WB 2h
WB 3h
WB 4h
WB 6h
E
Maize bran (1h / 30°C - 100°C)
% substrate dry mass, [/]
50%
0%
Ara
Gal
Glc
Xyl
Man
MB 2h
MB 3h
MB 4h
MB 6h
F
Maize bran (3h/RT - 100°C)
% substrate dry mass, [/]
50%
0%
Ara
Gal
Glc
Xyl
Man
MB 2h
MB 3h
MB 4h
MB 6h

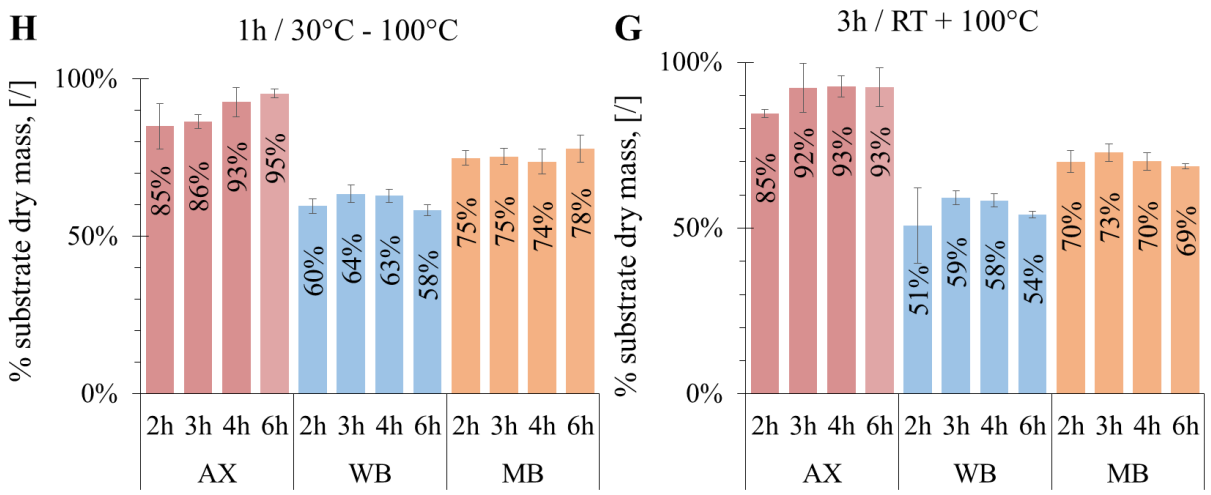

Figure 2-16. Soluble monosaccharides (A, B, C, D, E and F) and equivalent total sugar recovery (G and H) released after acid hydrolysis of insoluble AX, WB and MB and expressed as the % of the initial dry matter mass treated (% substrate dry mass). *The error bars represent the standard deviation of three independent experiments.*

Since the protocol of the 2nd step (100 °C for 3 h) is now defined, we return back to the 1st step assess to ensure an efficient solubilization rate and therefore a complete sugar hydrolysis. Thus, higher substrate concentrations were tested ($V_{acid}/W_{substrate}$) with the protocols 6 and 7 (concentrate acid for 1 h at 30 °C or 3 h at RT and then dilute acid for 3 h at 100 °C). In addition, during this 1st step, the acid suspension was vortexed every 10 min for 1h at 30 °C and every 20 min for 3 h at RT. The total sugar recovered are presented in the **Figure 2-17** and for more details, monosaccharide yields are presented in the **Annex 3**. Some hydrolysis yields of arabinoxylan were higher than 100% probably because we applied a correction factor for its 20% of this commercial product impurities but these last ones are obviously also sugars.

Solubilization of carbohydrate with protocols 6 and 7 using a $V_{acid}/W_{substrate}$ = 7.5 was roughly similar to protocols 4 and 5 (**Table 2-5**), except that adding mixing stage of the tubes during the 1st step apparently has a positive impact on overall solubilisation and on the final hydrolysis yield. More specifically, we found that mixing time to time the suspension that is in contact for 3 h at RT (protocol 5), raised the final yield from 59% to 73 % (**Figure 2-16G** and **Figure 2-17B**). Finally, the best hydrolysis yield was achieved with a 1st step at RT for 3 h including mixing stages every 20 min. We also found that a higher $V_{acid}/W_{substrate}$ ratio (10, 15 or 20 instead of 7.5) resulted in a lower hydrolysis rate, probably due to monosaccharides degradation.

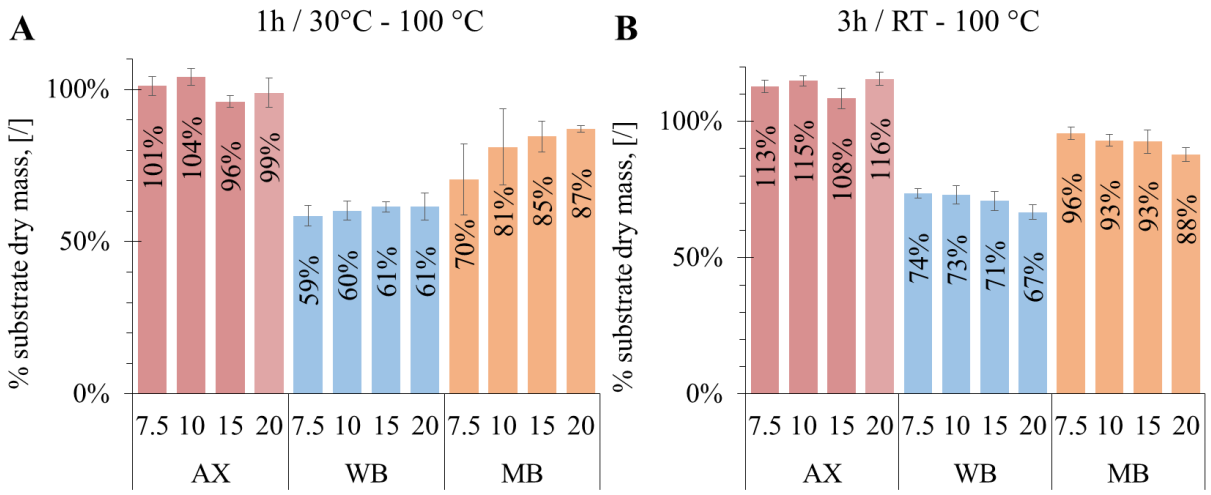

Figure 2-17. Total sugar recovery calculated from monosaccharides released after acid hydrolysis of insoluble arabinoxylan (AX), wheat bran (WB) and maize bran (MB) and expressed as the % of the initial dry matter mass treated (% intakes). *The error bars represent the standard deviation of three independent experiments.*

Altogether these results allow to define the best protocol with respect to an acid hydrolysis of polysaccharides in wheat bran: (i) Step 1: 72% of H_2SO_4 with a ratio $V_{acid}/W_{substrate}$ equals to 7.5 at RT for 3 h with mixing stages every 20 min; (ii) Step 2: dilute acid concentration to 2N at 100 °C for 3 h.

- **Results for soluble substrates**

Two soluble substrates (arabinoxylan and xyloglucan) were treated according to protocol 8 which consists in digesting the soluble sugars in a 2N H_2SO_4 solution at 100 °C for 3 or 4 h (**Figure 2-18)**. Sugar recovery could be superior to 100% due to correction factors applied for product impurities. With about 100% of sugar recovery, arabinoxylan appeared to be completely hydrolysed whichever the duration of the treatment, suggesting that no monosaccharide was degraded (**Figure 2-18A)**. With xyloglucan, an acidic treatment of 4 h was required to reach 100% of sugar hydrolysed (**Figure 2-18B**). In conclusion, for soluble oligosaccharides, acid hydrolysis protocol will consist in a 2N H_2SO_4 solution at 100 °C for 4h.

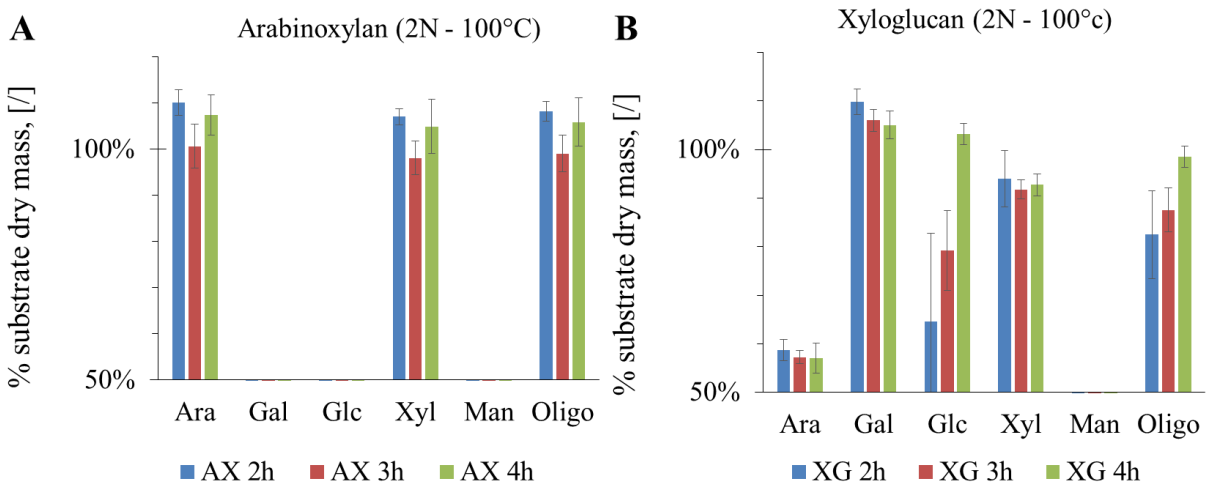

Figure 2-18. Monosaccharides released and their equivalent total sugar recovery after acid hydrolysis treatment of soluble AX (A) and soluble xyloglucan (XG) (B) and expressed as the % of the initial dry matter mass treated (% substrate dry mass). *The error bars represent the standard deviation of three independent experiments.*

- **Estimation of the correction factor**

When assessing these various methods, one has to bear in mind that acidic treatment of monosaccharides can transform them into organic acids via furan intermediates (Li and Xu, 2013; Templeton and Ehrman, 1995). This chemical alteration can therefore lead to an underestimation of sugars in the solution. However this loss could be estimated by treating monosaccharide standards under the acidic conditions chosen with the assumption that the loss of monosaccharides happened the same way in both the samples and standards. To do this, only the 2nd acid hydrolysis step was performed as monosaccharides decomposition is much lower during the primary hydrolysis step than during the second one (Khanizadeh et al., 1995; Saeman et al., 1954; Zhou and Runge, 2014).

A known amount of monosaccharide standards (arabinose, galactose, glucose, xylose and mannose) was therefore treated in 2N H_2SO_4 at 100 °C for 4 h and for 3 h. As reported in **Figure 2-19,** with two different concentrations at 10 and 100 µg/L, a roughly 10% loss of all kind of monosaccharide was obtained after 3 to 4 h in this acidic condition. Therefore, we decided to apply a correction factor of 1,1 in our calculation to take into account this sugar underestimation in both soluble and insoluble acid hydrolysis protocols. However, we have to notice that this value represents the maximal rate of monosaccharides degradation as during the acid hydrolysis polysaccharides do not be degrade into monomers in the first minutes but over the 3 h / 4 h of treatment.

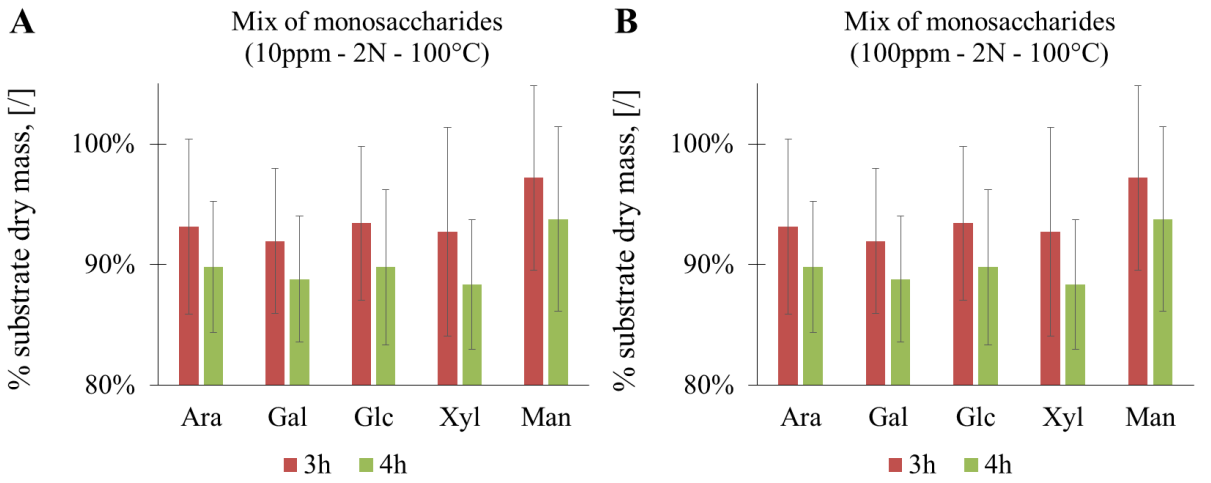

Figure 2-19. Recovery percentage of monosaccharides after their acid hydrolysis treatment at 10 ppm (A) and 100 ppm (B) and expressed as the % of the initial dry matter mass treated (% substrate dry mass). *The error bars represent the standard deviation of three independent experiments.*

2.4.3.2. Enzymatic treatment and biochemical analyses

Deconstruction of dWB by enzymes cocktail led to the release of soluble materials that can be sugars but also other components, such as proteins. As it was impossible to harvest sample in a homogeneous manner, we monitored the hydrolysis and evaluated its yield by measuring the soluble matter that was released in the supernatant during the enzymatic treatment. This quantification of soluble matter was also used to assess whether the mass balance (*i.e.* what is soluble = what has been lost from the suspension) is constant along the process. To validate our protocols, we carried out in duplicate an experiment in which the mass balance was determined before and after 2 h of dWB treatment by Rovabio Brussel at 1100 $U_{xylanase\ visco}$/gdm. One batch was centrifuged to recover and analyse the supernatant; while the other one was filtered to collect and analyse the pellet. Results are presented in the **Table 2-6**.

Table 2-6. Mass balance assessment before and after treatment with Rovabio Brussel for a total volume of 50 mL, 41 °C, pH 4 in mixed beakers.

Time, [h]	Pellet [(a)]	Supernatant [(b)]	Pellet sugar content [(c)]	Supernatant sugar content [(d)]	Supernatant protein content [(e)]
0 h	3.55 g	0.62 g	1.82 g	0.00 g	0.00 g
2 h	2.73 g	1.54 g	1.39 g	0.60 g	0.22 g
Difference	**- 0.82**	**0.91**	**- 0.43**	**0.60**	**0.22**

a. Pellet was dried and weight as described in material and methods (§6.3.1)

b. Supernatant was dried and weight as described in materials and methods (§6.3.2)

c. Sugars were estimated as equivalent oligosaccharides after acid hydrolysis (François, 2007)

d. Sugars were estimated as equivalent oligosaccharides after acid hydrolysis as described in materials and methods (§6.3.3)

e. Proteins was measured with the BCA method as described in materials and methods (§6.3.8)

Table 2-6 reports that the loss of dry matter in the pellet was inferior to the solubilized matter. However, the difference of 10% is whiten the error and therefore we can consider that the mass balance is conserved. This is confirmed by the fact that the summation of soluble sugars content after its complete hydrolysis (0, 60 g) and proteins released in the supernatant (0,22 g) is equal to the matter loss from the pellet. However, the acid hydrolysis of insoluble pellet amounted to only 0.43 g of sugar, which is 30 % less than determined in the supernatant. This result indicates that acid hydrolysis of insoluble dWB was not complete, which agrees with other works showing that acid hydrolysis of complex matrix is very difficult and could be incomplete (Zhou and Runge, 2014). In addition, the loss of dry matter was fully equal to the solubilized sugars (73.2%) plus the solubilized proteins (26.8%), which supports that the acid hydrolysis of soluble sugars was complete (**Figure 2-20**). Therefore, measurement of the solubilized matter and its sugar (after hydrolysis) and protein contents are reliable parameters that can be determined during the Rovabio treatment.

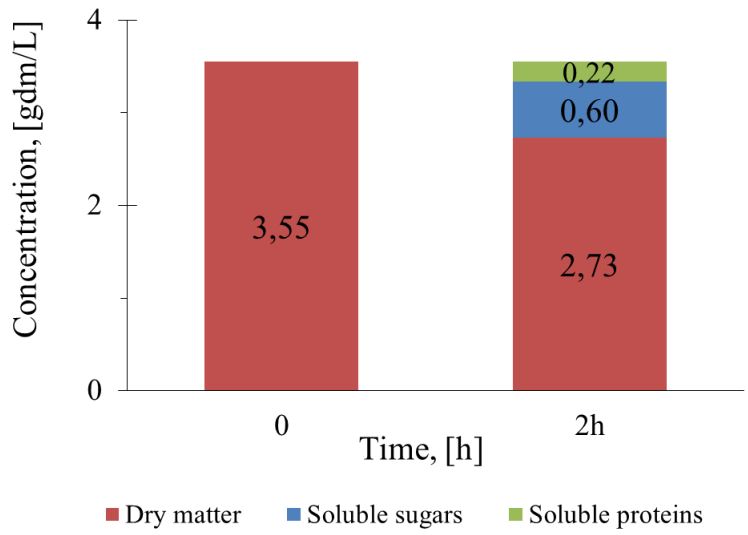

Figure 2-20. Mass balance assessment between dry matter evolution (DM) and sugars and proteins solubilized, before and after an enzymatic treatment with Rovabio Brussel, in grams of dry matter per litter. *Operating condition identical to Table.2-6.*

To validate our experimental strategy, then, we need to check whether we are able to discriminate the quantity and the kinetic of maters, especially sugar, released during the treatment of dWB by different doses of Rovabio. Upon acid hydrolysis of the supernatant from dWB treated with two doses of Rovabio, the major monosaccharides quantified by HPAEC-PAD was xylose followed by glucose and arabinose (**Figure 2-21**), which is consistent with wheat bran composition (Beaugrand et al., 2004; Brillouet and Mercier, 1981; Maes and

Delcour, 2002). It is also shown that the solubilisation was dependent on the dose of Rovabio since there was 4 times more sugars released at 6 h with a 10 fold higher Rovabio activity (in $U_{xylanase\ visco}$). The solubilization rate at the highest dose of Rovabio was very fast during the 1st hour, then slowed down dramatically between 1 and 2 h and was almost null at 6 h. This trend confirmed previous results obtained by monitoring the solubilization of insoluble AX in wheat bran with Rovabio Excel and reproducing poultry digestive system with the TNO (Maisonnier-Grenier et al., 2006). All these results illustrate our ability to quantify solubilized sugars during enzymatic treatment and clearly showed an effect of the enzyme dose on the kinetic of solubilization.

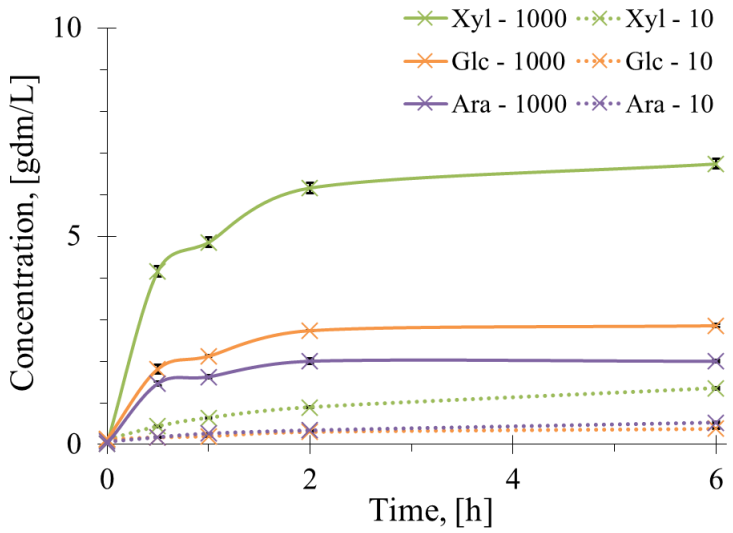

Figure 2-21. Rate of soluble sugars released during treatment of the destarched wheat bran with Rovabio Brussel. *Two different doses of Rovabio expressed as Uxylanase viscosity per g has been used , 1100 and 11 U/ gdm. Operating conditions identical to Fig.2-9. The soluble sugars were expressed as equivalent of monosaccharides glucose (Glc), xylose (Xyl), arabinose (Ara), mannose (Man) and galactose (Gal) after their chemical acid hydrolysis as described in Material & Methods. The error bars represent the standard deviation of three independent experiments.*

With biochemical analysis, our strategy consists in measuring the total matter, the sugars and the proteins solubilized along enzymatic treatment. Soluble monosaccharides will be estimated after acid hydrolysis (2N H_2SO_4 solution at 100 °C for 4 h) by HPAEC-PAD and a correction factor of 10% will be applied to fix the monosaccharides degradation into furfurans and their underestimation.

2.5. Conclusions

Rovabio Brussel has an amylolytic activity which impacts *in-situ* viscosimetry. A wheat bran destarching process based on successive hot water wash enables to reduce starch from 16.4 to 4.96% of wheat bran DM. Destarched wheat bran suspension provided shear-thinning properties and a *Ccrit* value of 50 gdm/L. With the addition of Rovabio Brussel, dWB suspension viscosity decreased proportionally to the enzyme dose, within the first minutes of treatment (macroscopic scale). Large particles were initially fractionated (DLS) and this mechanism continued within the finest population (FBRM) resulting in smaller and smaller particles measured (microscopic scale). Along the enzymatic treatment, insoluble dWB was solubilized into 73.2% of sugars and 26.8% of proteins on the $23\%_{DM}$ of dWB solubilized (molecular scale).

Our preliminary study furthermore suggests that the deconstruction of dWB by Rovabio implies a concurrent phenomenon of fragmentation as assessed by change in particle size and its number and of a solubilization as indicated by release of soluble matter into the liquid phase of the suspension

CHAPTER 3:

DECONSTRUCTION MECHANISM OF WHEAT BRAN BY ENZYMATIC COCKTAIL REVEALED BY A COMBINED IN-SITU PHYSICAL AND EX-SITU BIOCHEMICAL STUDY

CHAPTER 3. DECONSTRUCTION MECHANISM OF WHEAT BRAN BY ENZYMATIC COCKTAIL REVEALED BY A COMBINED IN-SITU PHYSICAL AND EX-SITU BIOCHEMICAL STUDY

Marine DESHORS[a, b], Olivier GUAIS[b], Virginie NEUGNOT-ROUX[b],

Xavier CAMELEYRE[a], Luc FILLAUDEAU[a, c], Jean Marie FRANCOIS[a, *].

[a]LISBP, UMR INSA-CNRS 5504 & INRA 792; F-31077 Toulouse, France,

[b]Cinabio-Adisseo France S.A.S., F-31077 Toulouse, France

[c]Fédération de Recherche FERMAT (Fluides, Energie, Réacteurs, Matériaux et Transferts), Université de Toulouse, CNRS, INPT, INSA, UPS, Toulouse, France.

* Corresponding author : Jean Marie FRANCOIS: fran_jm@insa-toulouse.fr

E-mail address:

Marine DESHORS: deshors@insa-toulouse.fr

Olivier GUAIS : olivier.guais@adisseo.com

Virginie NEUGNOT-ROUX : virginie.neugnot-roux@adisseo.com

Xavier CAMELEYRE: xavier.cameleyre@insa-toulouse.fr

Luc FILLAUDEAU : luc.fillaudeau@insa-toulouse.fr

Jean Marie FRANCOIS : fran_jm@insa-toulouse.fr

Keywords

Biomass deconstruction, enzymes cocktails, non-starch polysaccharides, *in-situ* viscosimetry, morphogranulometry, biochemistry.

Submitted to Frontiers

Abstract

Enzymatic deconstruction of complex carbohydrates is an important issue not solely for biofuel production but also in feed biotechnology. This report investigates the deconstruction of wheat bran by a well characterized enzymatic mixture termed Rovabio® and compared it to the action of xylanase C as its major hydrolytic enzyme. To this end, we applied an original methodology using a multi-instrument bioreactor that combines *in-situ* physical and *ex-situ* biochemical analyses. We showed that the deconstruction of wheat bran by Rovabio® was entailed by two concurrent events, namely particles fragmentation and solubilization that together lead in less than 2 h to a 70% drop in the suspension viscosity and a release of soluble sugars. In contrast, a weak drop of viscosity (- 25%) accompanied by a slight particle fragmentation were found in the presence of the sole xylanase C, even though the amount of xylose and arabinose released after 6 h of treatment was similar to that with Rovabio®. Altogether, and in spite of a high content and a great diversity of hydrolytic enzymes in the Rovabio® cocktail, only 30% of the initial matter was solubilized, which raises the question of the nature of this recalcitrant fraction produced and how it could be further deconstructed.

3.1. Introduction

Over the last decades, biorefining of biomass has attracted much interest due to the escalating energy crisis and environmental pollutions. Enzymatic hydrolysis of biomass is therefore becoming an extensive research area with the ultimate goal of converting polysaccharides into fermentable sugars for biofuel production and commodity chemicals (Chundawat et al., 2011; Kubicek and Kubicek, 2016; Park et al., 2016). Genome and metagenome sequencing of lignocellulose active microorganisms and microbial communities reveal the diversity of enzymes that have evolved to transform lignocellulose from wood, herbaceous plants and grasses and has led to thousands of new entries in the carbohydrate active enzyme (CAZy) database (http://www.cazy.org/) (Goacher et al., 2014). A complete deconstruction of lignocellulose to monomers by enzymes requires, in theory, the concerted activities of ligninases (manganese peroxidase, lignin peroxidase, versatile peroxidase, and laccase), endoglucanases and exoglucanases (acting on reducing and non-reducing ends of cellulose), various hemicellulases as well as accessory enzymes such as the lytic polysaccharide monooxygenases (LPMOs) or proteins such as swollenins (Gupta et al., 2016). Currently, commercial enzyme preparations available for the depolymerization of lignocellulosic materials are vaguely defined as complex mixtures that contain around 80 to 200 proteins (Goldbeck et al., 2014).

The hydrolytic efficiency of a multi-enzyme complex in the lignocellulose saccharification process depends on both the properties of individual enzymes and their ratio in the multi-enzyme cocktail (Goldbeck et al., 2014). Therefore, the specific contribution of an individual enzyme is established only after working with enzymes in a purified state, or in studies through combinatory designs or defined complex mixtures (Banerjee et al., 2010; Goldbeck et al., 2014; Kumar et al., 2009; Wang et al., 2011). These studies may actually lead to activity profiles that often poorly correlate with their true performance on industrially relevant lignocellulosic materials (Goacher et al., 2014; Van Dyk and Pletschke, 2012). Thus, what is often lacking in studies involving enzymatic deconstruction and degradation of complex substrates is a methodology that readily documents the hydrolytic abilities of enzyme systems at macroscopic (spatial disorganization of plant cell wall structure) and molecular (breakdown of polymers and oligomers) levels (Gupta et al., 2016).

The deconstruction of wheat bran will be the emphasis of this study as it is an important animal feed containing 12 to 15% of non-starch polysaccharides (Knudsen, 2014) which have a well-established anti-nutritional effect (Bedford and Partridge, 2011) and thus can be hydrolysed by industrial enzymatic cocktail termed Rovabio®, used as feed additive and well characterized at its global proteomic level (Guais et al., 2008). By mean of investigating the deconstruction of wheat bran, we here report on a so-called multi-scale approach that uses a well-equipped bioreactor and which combines *in-situ* physical *(i.e.* rheological and morphogranulometric data) with *ex-situ* biochemical (*i.e.* nature and rate of sugar solubilization) analyses to monitor, visualize and obtain quantitative data of the deconstruction/ solubilization process of this complex biomass. In addition, this methodology allows to work with a substrate having a large granulometry which prevents the impact of size reduction on sample chemistry and microstructure as well as its negative impacts of complex polysaccharide heterogeneity (Goacher et al., 2014). To better illustrate the advantage of our methodology in investigating biomass deconstruction and to show how much important is a multi-enzyme complex in this process, we have compared the action of the enzymatic cocktail Rovabio® with the endo-xylanase encoded by *XynC* (Lafond et al., 2014) which corresponds to the most active glycosyl hydrolase in this cocktail. Our multi-scale analysis not only supported the synergistic action of NSPases in the solubilization of wheat bran, but it unravelled that the deconstruction of this complex polysaccharide is entailed by a particles fragmentation not accompanied by solubilization. Moreover, yet 70% of the initial wheat bran suspension remains as insoluble fraction in spite of the high diversity of NSPases present in this industrial cocktail.

3.2. Materials and methods

3.2.1. Substrate and enzymes

Destarched wheat bran obtained following the process described in §2.2.1 was used as substrate. The amount of NSPs in this material after acid hydrolysis was estimated to 71% of the dry mass.

Rovabio® Advance (simplified by Rovabio thorough the text) is an enzymatic cocktail secreted by *Talaromyces versatilis* fungus commercialized by Adisseo SAS (Commentry, France, http://feedsolutions.adisseo.com/en/). The cocktail contains a large amount of various glycosylhydrolases herewith termed NSPases including xylanases, β-glucanases, pectinases and cellulases. An enzymatic cocktail termed Rovabio Excel with had been characterized by a

global proteomic analysis in a previous work (Guais et al., 2008). Rovabio Advance version differs from the Excel one by additional presence of xylanases and arabinofuranosidases as reported on Adisseo Web site (http://feedsolutions.adisseo.com/en/rovabio-advance-the-only-feedase/). The total activity of Rovabio Advance corresponded to 24000 $U_{xylanase\ visco}$/mL, as described in §2.2.1.

Production of recombinant endo-xylanase C encoded by *T versatilis XynC* (Lafond et al., 2014) has been subcontracted to GTP biotech company (https://fr.gtptech.com/). Briefly, it consisted of a 50 L fermentation of *Pichia Pastoris* strain GS115 that expressed *T. versatilis XynC* cloned in a pPIC9K plasmid under the strong AOX1 promoter and bearing a secretory sequence to release the protein in the supernatant. The purified enzyme showed to be pure by SDS page analysis and exhibited 30000 $U_{xylanase\ visco}$/mL.

3.2.2. Experimental pilot set-up

Our experimental set-up used to characterize enzymatic dWB deconstruction has been described in Chapter 2, §2.2.2 (see more details in §6.1.1).

During hydrolysis experiments, samples (12 mL, 6 per experiment) were collected in 25 mL Falcon conical centrifuge tubes in an ice-cold bath to readily stop the enzymatic activity. Part of the samples was centrifuged (10 min at 4000 RPM) and stored at -18 °C for biochemical analyses and the other half directly stored at 4 °C for physical analysis.

3.2.3. Chemical and biochemical analysis

Solubilization rate. It corresponds to the soluble matter that is released in the supernatant during the treatment of the destarched wheat bran and was estimated by dry weight measurements as described in §2.2.3.

Sugars determination. Released soluble sugars were first acid hydrolysed into monomers and then determined by HPAEC as described in §2.2.3.

Soluble monosaccharides that were directly released in the supernatant during the enzymatic treatment of the insoluble polysaccharide were determined by High performance anion exchange chromatography (HPAEC) as described above, but using a CarboPac PA1 analytical column (250 mm x 4 mm) with a CarboPac PA1 guard column, and an isocratic elution of 18 mM NaOH at 25 °C with a flow rate of 1 mL/min.

Protein concentration was determined by the BCA (BiCinchoninic acid Assay) assay kit (Pierce Thermo Scientific, Illinois, USA) (Smith et al., 1985) using bovine serum albumin as standard.

3.2.4. Physical analysis

In-situ viscosity measurement. The *in-situ* viscosity was determined from real-time monitoring of torque and mixing rate as described in §2.2.4.1.

Ex-situ diffraction light scattering (DLS). The volume-weighted particle size distribution (PSD) was determined by DLS as described in §2.2.4.3. Volume-weighted distribution (E_v) was calculated by the Mastersizer software and multiplied by dry matter concentration (Cm) to take into account the loss of material due to solubilization during the enzymatic treatment.

In-situ focus beam reflectance measurement (FBRM). FBRM enables *in-situ* quantification of small particles in the range < 100 µm through the estimation of the chord length (lc) and distribution of the chord length population (CLD) using an FBRM® G400 probe as described in §2.2.4.4. The number-weighted CLD, $E_n(l_c)$, and the average number of chord length counted per second, N_c, are used as indicators to describe population.

3.3. Results

3.3.1. Set-up of the experimental system and determination of the operational conditions

The originality of our study was to use multi-instrumented bioreactor (see 2.2.2 and **Figure 2-1**) that allows to analyse at different scales (*i.e.* multi-scale analysis), namely rheology, granulometry and biochemistry, the deconstruction of insoluble biomass from various origins by hydrolytic enzymes either alone, or in a mixture under well controlled operating conditions.

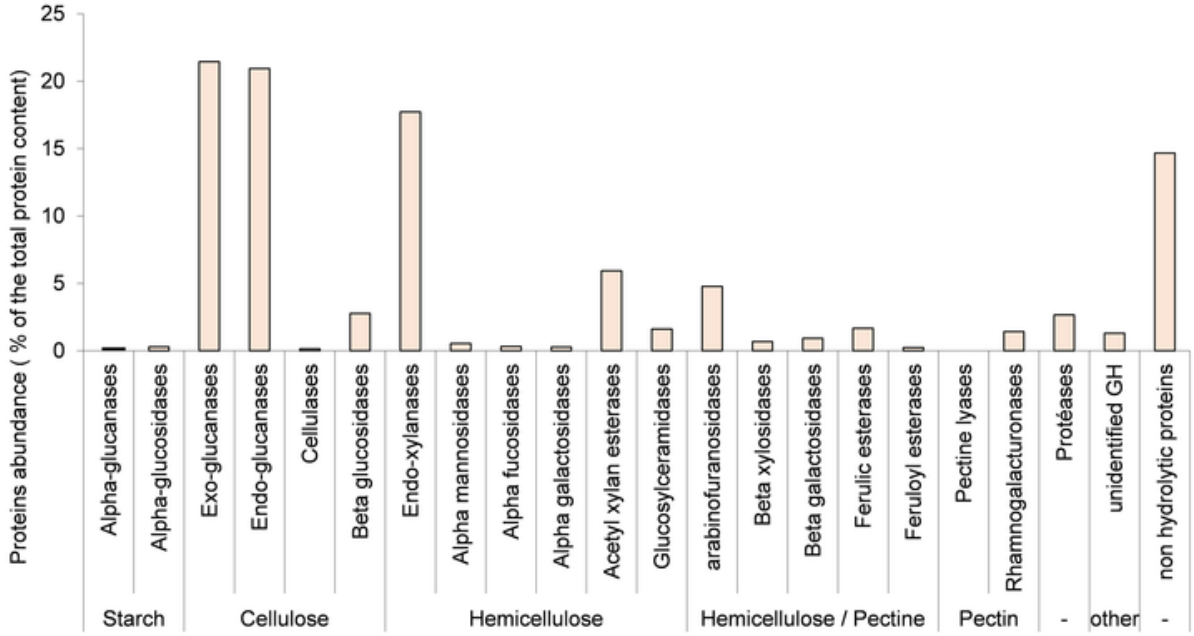

Figure 3-1. The proteomic analysis of a sample of liquid Rovabio Excel was realized by a shot gun procedure *as described in* Guais et al., 2008***.*** *The different proteins were classified into major categories according to CAZYmes classification and reported as % of the total proteins content.*

In the present study, the industrial enzymatic cocktail termed Rovabio®, whose proteomic content has been characterized (Guais et al., 2008) and which contains a large panel of various glycosylhydrolases and auxiliary enzymes (**Figure 3-1**) has been used as it is currently employed as feed additives in animal nutrition. Our purpose was to determine the efficiency of this industrial cocktail to deconstruct insoluble wheat bran and compare the action of this multi-enzyme complex with that carried out by the pure endo-xylanase (xylanase C) (Lafond et al., 2014), as the latter is the most active hemicellulolytic enzyme present in Rovabio® (Adisseo, unpublished data). Operating conditions were mimicking conditions encountered in poultry anterior digestive system which corresponds to a high dry matter (> 50 gdm/L) suspended into 100 mM potassium phosphate buffer pH 4.0 at 41 °C (Svihus, 2014). In addition, we carried out a specific procedure described previously (see §2.2.1) to remove, as much as possible, the starch present in the wheat bran because our purpose was to investigate the deconstruction of the non-starch polysaccharides components of wheat bran which are mainly arabinoxylans. We then determined the critical concentration (*Ccrit)* of the destarched wheat bran suspension that marked the transition from dilute to semi-dilute suspensions. This was done by applying various mixing rates from 10 to 250 RPM at 41 °C to destarched wheat bran suspended at concentrations ranging from 10 to 86 g/L in potassium phosphate buffer. In

agreement with literature data (Geddes et al., 2010; Nguyen et al., 2015), the viscosity and the non-Newtonian behavior of the suspension were strongly dependent on substrate concentration. A *Ccrit* value of 50 gdm/L was obtained and operational conditions were fixed at 1.5 *Ccrit* as a non-Newtonian behavior of the suspension was obtained above this value. Also, prior to treatment with Rovabio and xylanase C, the suspension was subjected to a thermal treatment by raising the temperature of the reactor up 85 °C for 1 h which was found to be sufficient to denature the known xylanase inhibitor proteins XIP (xylanase inhibitor protein) and TAXI (*Triticum aestivum* endoxylanase inhibitor) that are present in the wheat bran (Furniss et al., 2002; Juge, 2006). Upon return at 41 °C and stabilization when the viscosity of the suspension reached a stable torque value, both enzyme solutions (Rovabio® and xylanase C) were added to the destarched wheat bran suspension at an equivalent of 400 $U_{xylanase\ visco}$ of endo-xylanolytic activity per gram of dry mass. Sampling was regularly performed over a 6 h period to determine physical and biochemical parameters as further developed below.

3.3.2. Destarched wheat bran deconstruction monitored by in-situ viscosimetry

Destarched wheat bran suspended at about 74 g/L and mixed at 170 RPM gave an initial viscosity μ_0 of 0.206 Pa.s after homogenization and stabilization of the suspension. In the absence of NSPases, slight and linear decrease of viscosity (<10 %) over 6 h was observed that can be due to mechanical disaggregation of insoluble particles by the mixing system **(Figure 3-2A)**. Upon addition of Rovabio at an equivalence of 400 $U_{xylanase\ visco}$ per g, the suspension lost 50% of its initial viscosity in 1 h and 70% in 2 h following a 1^{st} order decay, then the viscosity reduction slowed down in the next 4 h to reach a loss of 73.5 % towards 0.05 Pa.s after 6 h. To verify whether the slow reduction of viscosity could result from an inhibition of Rovabio by products released in the supernatant, fresh wheat bran was suspended in the supernatant of a 6h-treated wheat bran suspension and then treated with a same dose of the a 'fresh' enzymatic cocktail. As a similar viscosity drop was obtained as shown in **Fig.3-2** (data not shown), we concluded that the slow reduction of viscosity was not due to inhibition of Rovabio but most probably due to some mechanical effects caused by the mixing system.

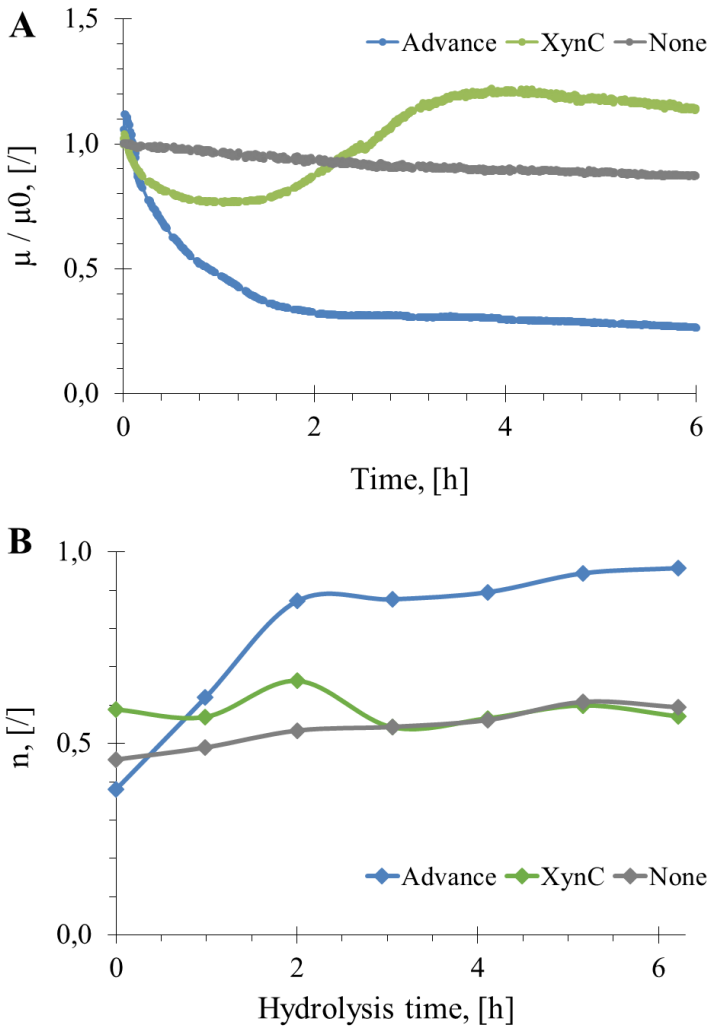

Figure 3-2. Normalized in-situ viscosity (A) and flow behavior index (B) as a function of the hydrolysis time of wheat bran suspension by Rovabio (Advance), pure xylanase C (XynC) and without enzyme (None). *Operating conditions: destarched wheat bran suspended in a potassium phosphate 0,1M at 41°C, pH 4.0, initial concentration 74 g/L, Rovabio Advance and xylanase C 400* $_{Uxylanase\ visco}$*/g.*

We then investigated the effect of pure xylanase C on this physical parameter and compared with that obtained with the complex enzymatic cocktail. As it can be seen in **Figure 3-2A**, the viscosity of the suspension decreased by only 25 % during the first hour, followed by an overtake above the initial value between 2 and 4 h (+20%) to finally stabilized at a relative viscosity that was 14% above the initial value. Taking into account that the drop in viscosity is a direct physical indication of biomass deconstruction (Dunaway et al., 2010; Nguyen et al., 2013; Wiman et al., 2011), this result confirmed the importance of a mixture of hydrolytic enzymes in this process.

The effects of Rovabio and xylanase C on the rheological behavior of the suspension were also evaluated by determining the flow behavior index (n). As these measurements are feasible under laminar and transitory regimes (Re < 700), they could be obtained with suspensions treated with Rovabio and with xylanase C all along the treatment. **Figure 3-2B** shows that only Rovabio caused a modification of the rheological behavior leading to a loss of the shear-thinning behavior, as the flow behavior index (*n*) eventually increased to near 1 after 2 h of treatment of the suspension with the enzymatic cocktail. On the contrary, with XynC, even though the suspension viscosity dropped by 25% or increase by 20% at 2 h after the treatment (see **Figure 3-2A**), a strong shear-thinning behavior was maintained *(n* ~ 0.5).

3.3.3. A granulometry analysis of destarched wheat bran deconstruction

Diffraction light scattering (DLS) and focus beam reflectance measurements (FBRM) were employed to monitor the particles size distribution and evolution during the enzyme treatment of destarched wheat bran. Based on volume distribution of d_{se}, particle class ranging from 300 to over 1100 µm was dominant ($85\%_{vol/vol}$) in amount but not in number, with the major class of particles size ($80\%_{nb/nb}$) between 5 and 50 µm based on CLD. Detailed granulometric parameters were investigated by *ex-situ* diffraction scattering (DLS) which allows to get access to particles size distribution (PSD). However, one must keep in mind that the accuracy of the DLS measurements is based on several criteria, namely that the particles must be spherical giving rise to a diameter of equivalent sphere, d_{se} and that the refractive index of these particles suspension is known and constant. As the particles in our suspension are largely non spherical and biologically heterogeneous, we get around these limitations by evaluating a volume distribution (E_v) of sphere equivalent diameter (d_{se}) as described in Material & Methods. The particles size distribution (PSD) during the treatment of destarched wheat bran with either Rovabio or xylanase C could be determined from E_v multiplied by dry matter, which takes into account the loss of insoluble fraction material due to solubilization.

As shown in **Figure 3-3**, three classes of PSD could be identified whose relative abundance was changing over the time of treatment. Class 3 defined by "d_{se}" > 300 µm was the most abundant and showed a peak decrease of 46% drop in less than 30 min after the addition of Rovabio (**Figure 3-3A**), whereas an equivalent drop required 6 h in the presence of xylanase C (**Figure 3-3B**). Moreover, the decrease of class 3 was not counterbalanced by an increase in the abundance of two other classes, which can be explained by a concomitant significant solubilization.

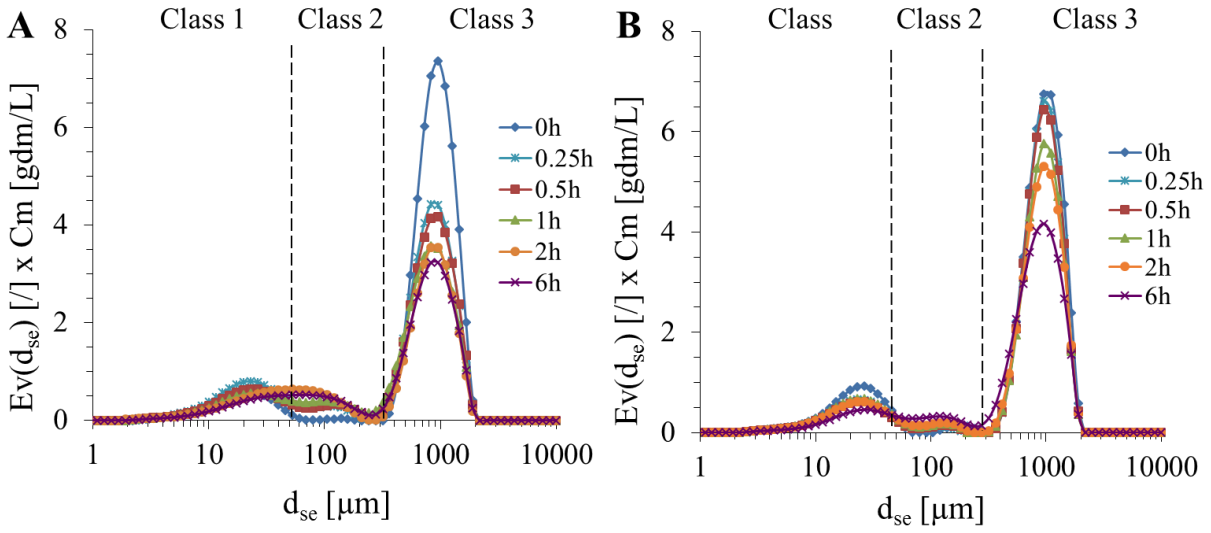

Figure 3-3. Particle size distribution during the treatment of destarched wheat bran suspension in the presence of Rovabio (A) and xylanase C (B). *The particle size distribution was assimilated to a diameter of equivalent sphere (dse) and was plotted with respect to the abundance of particle size which was obtained by multiplying Ev by the concentration of wheat bran suspension (cm) that remained at each time during the enzymatic treatment. Operating conditions identical to Fig.3-2.*

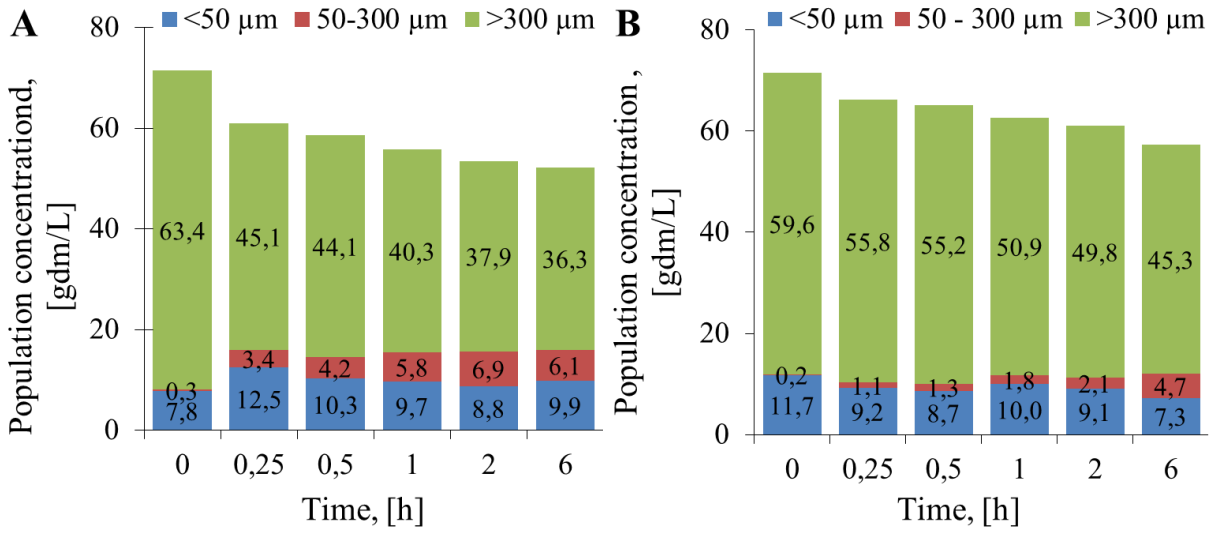

Figure 3-4. Evolution of three subpopulation concentration per class during enzymatic treatment of the destarched wheat bran by Rovabio (A) and xylanase C (B) for different hydrolysis times. *Operating conditions identical to Fig.3-2.*

To better quantify the evolution of PSD population during enzymatic treatment, we converted volumetric distributions into concentration assuming that the particle density is constant whatever the class throughout the enzymatic hydrolysis. As reported in **Figure 3-4**, the loss of 27.1 g of class 3 particles after 6 h of treatment with Rovabio, was accompanied by

only an increase of 7.9 g/L of class 1 and 2, indicating that the remaining 19.2 g/L had been released as soluble content in the supernatant. In addition, this analysis revealed that it was mainly class 2 that became enriched through the treatment with Rovabio as the abundance of class raised from 0.27 g/L to 6.1 g/L after 6 h of treatment whereas class 1 raised by only 25 % (from 7.78 g/L to 9.87 g/L). Like with Rovabio, class 3 was also the main target of xylanase C, the abundance of which decreased by about 13.3 g/L over the 6 h of treatment. However, contrary to Rovabio, class 1 also decreased by about 40 % (from 11. 83 to 7.29 g/L) whereas class 2 showed a slight increase from 1.13 to 4.72 g/L. These data pointed out again the difference between Rovabio and xylanase C in biomass fragmentation and solubilization.

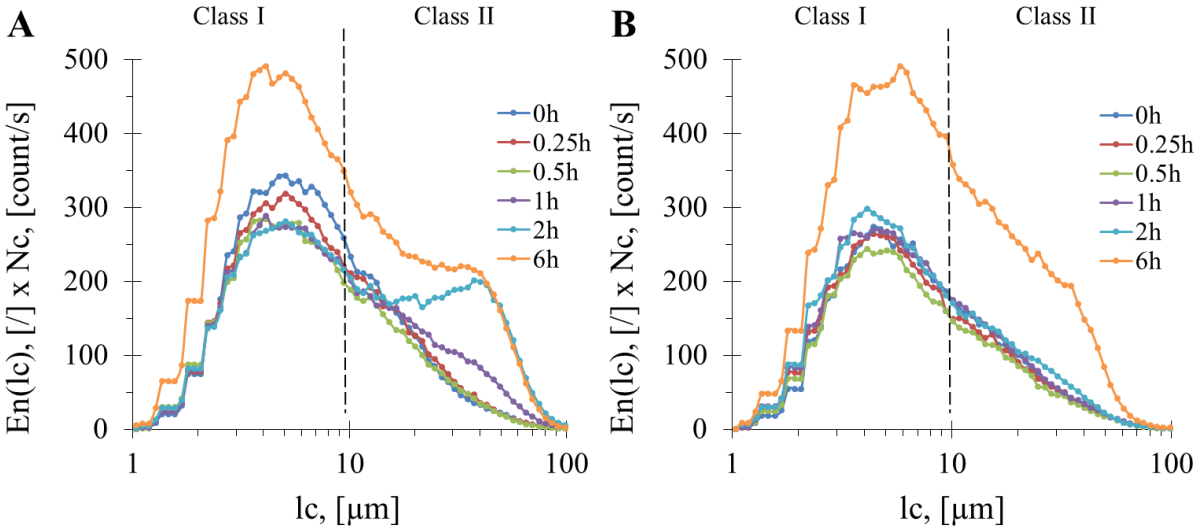

Figure 3-5. Evolution in the abundance of three population class as determined by their relative dse during the treatment of the wheat bran suspension by Rovabio (A) and xylanase C (B). *The abundance of each class in % was calculated by multiplying their dse by the dry matter concentration (Cm) remaining at each time during enzymatic treatment. Operating conditions identical to Fig.3-2.*

To complete the DLS approach that focuses on particles size > 100 µm; we employed the FBRM technique to investigate the evolution of smaller particles during enzymatic hydrolysis. With this method, we can obtain chord length (*lc*) values which are represented as number of chord length distribution $E_n(l_c)$. By multiplying $E_n(l_c)$ by the total number of particles counted per sec (*Nc*), we take into account the loss of insoluble matter by the solubilization and hence we can monitor the evolution of CLD along the treatment of destarched wheat brand with Rovabio and xylanase C. As it is reported in **Figure 3-5**, two subpopulations termed class I with 1< lc < 10 µm (centred around 4.5 µm) and class II with 10< lc <100 µm (centred around 45 µm), were identified, whose abundances increased at 6 h after treatment

with both Rovabio and xylanase C. However, we noticed a clear difference between the two treatments, as only in response to Rovabio the class II increased earlier (at 2 h of treatment), although at the end of the treatment, the proportion of this class was roughly equal (**Figure 3-6**).

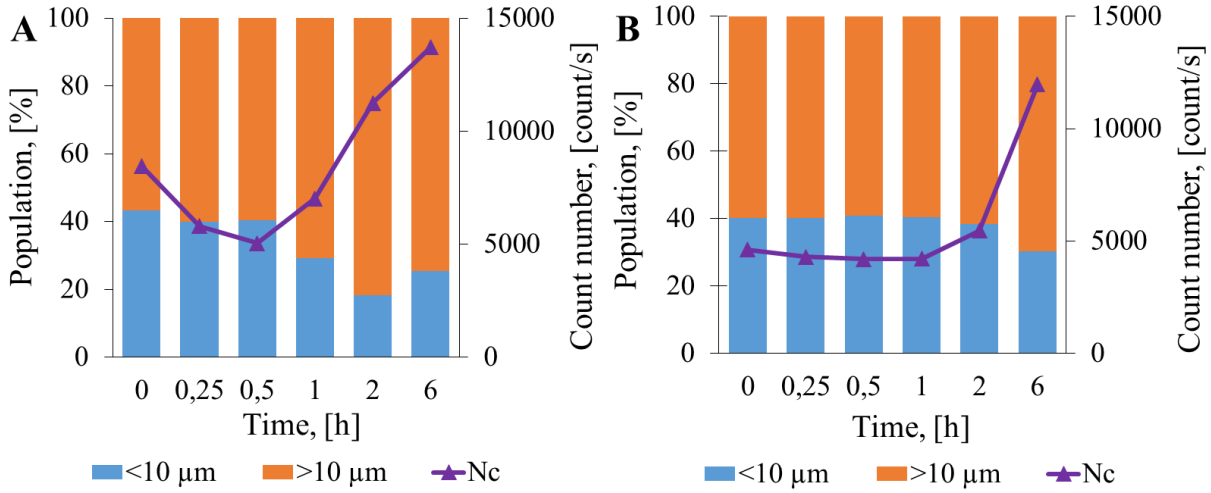

Figure 3-6. Evolution of subpopulation proportions per class and the number of count per second (Nc) during destarched wheat bran treatment with Rovabio (A) and xylanase C (B). *Operating conditions identical to Fig.3-2.*

3.3.4. Biochemical analysis of the deconstruction of destarched wheat bran

The *in-situ* analysis reported above clearly indicated that the enzymatic action of Rovabio and xylanase C caused a release of soluble material in the supernatant from insoluble destarched wheat bran. As a first approach to quantify this release of soluble matter, we determined the solubilisation rate as the total matter released during these enzymatic treatments.

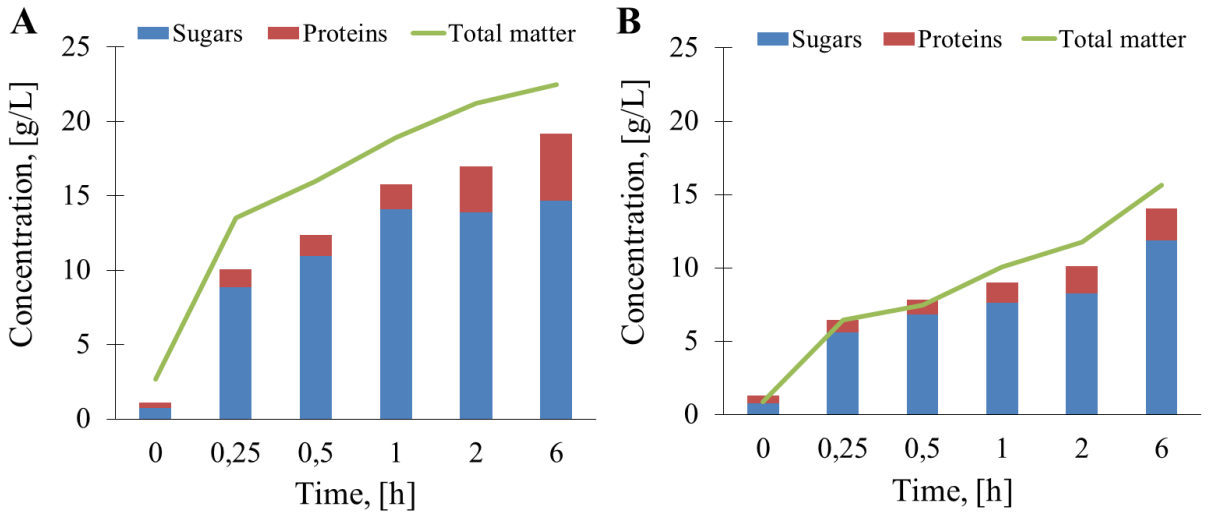

Figure 3-7. Sugars, proteins and total matter (g/L) solubilized during enzymatic treatment of the destarched wheat bran by Rovabio (A) and xylanase C (B). *Operating conditions identical to Fig.3-2.*

Figure 3-7 shows the solubilization rate was roughly 3-time faster with Rovabio than with xylanase C within the first 30 min of treatment. After this time, the kinetic of solubilization suddenly dropped but continued at a very slow rate until the end of the treatment. After 6 h, the total soluble matter released by Rovabio was round 22.5 g/l, which represented a solubilization of only 30% of the initial amount wheat bran put in the reactor, and 15.65 g/L upon incubation with xylanase C. Since the solubilization mainly corresponded to release of sugars from NSPs hydrolysis and proteins, these two components were quantified in the supernatant as described in Material & Methods. While the sum of these two components roughly matched the solubilized matter during the hydrolysis action of xylanase C (**Figure 3-7B**), the addition of soluble sugars and proteins was about 20% below the total matter solubilized by Rovabio (**Figure 3-7A**), suggesting that this treatment led to the release of other yet uncharacterized components in the supernatant. Also, we noticed that the release of sugars stopped after 1 h in the presence of Rovabio whereas it continued at a slow rate with Xylanase C. On the other hand, the proportion of proteins in the solubilized matter increased more significantly upon treatment with Rovabio than with xylanase C.

As indicated in **Table 3-1,** we showed that the treatment of the insoluble destarched wheat bran with Rovabio was accompanied by a release in the supernatant of xylose, glucose and arabinose, whereas only xylose was found during the treatment with xylanase C, at a rate that was about 6 times lower than upon Rovabio treatment. In addition, the rate of these monosaccharides released was almost linear over the first hour of incubation to slow down afterwards not because of the loss of enzyme activity but likely because of loss of accessibility to insoluble fractions. As the action of xylanase C or glycosyl hydrolases in the Rovabio not solely released monosaccharides but also soluble oligosaccharides, we treated the supernatant with sulfuric acid as described in Material & Methods to digest the released oligosaccharides and quantified their corresponding monosaccharides. The results of these experiments is illustrated in **Figure 3-8**, and showed a rapid liberation of sugars that plateaued at 1 h after Rovabio treatment, with a major proportion of xylose, followed by glucose and arabinose.

Table 3-1. Determination of monosaccharides solubilized (g/L) during treatment of destarched wheat bran by Rovabio or by XynC at equivalent activity to 400 $U_{xylanase\ visco}$/g.

	Xylose		Glucose		Arabinose	
Time, [h]	Advance	XynC	Advance	XynC	Advance	XynC
0	0.01	0.01	0.07	0.04	0.03	0.02
0.25	0.31	0.06	0.20	0.05	0.30	0.03
0.5	0.59	0.08	0.37	0.05	0.56	0.02
1	0.94	0.15	0.52	0.06	0.74	0.03
2	1.64	0.20	0.94	0.05	1.15	0.03
6	2.33	0.33	1.47	0.06	1.36	0.03

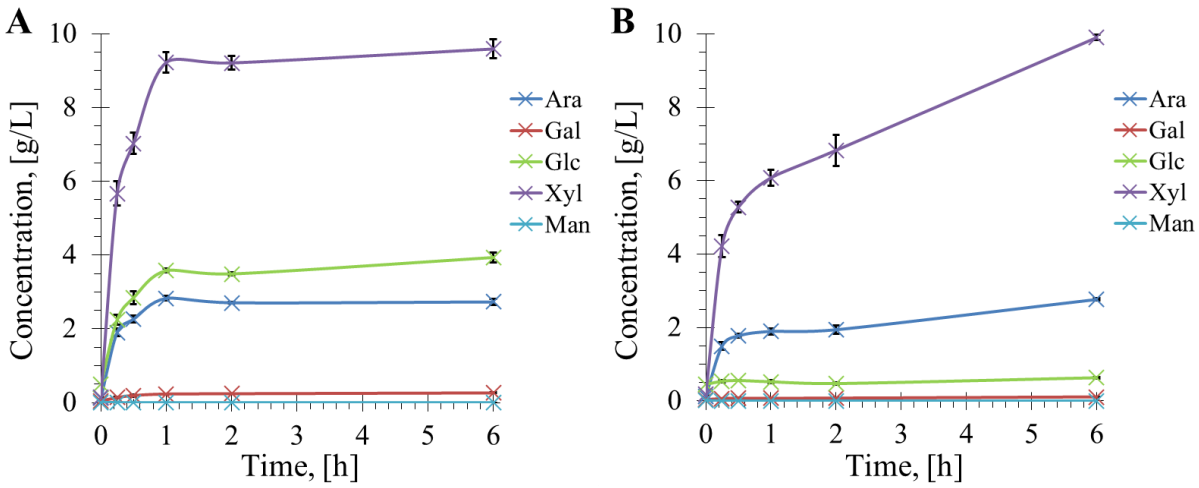

Figure 3-8. Kinetics of soluble sugars released during enzymatic treatment of the destarched wheat bran by Rovabio (A) and xylanase C (B). *Operating conditions identical to Fig.3-2. The soluble sugars were expressed as equivalent of monosaccharides glucose (Glc), xylose (Xyl), arabinose (Ara), mannose (Man) and galactose (Gal) after their chemical acid hydrolysis as described in Material & Methods. The error bars represent the standard deviation of three independent experiments.*

When compared to the monosaccharides directly released during the hydrolysis (**Table 3-1**), one can notice that the proportion of these monosaccharides in the total solubilized sugars increased with time (**Figure 3-9**). This result indicates that oligosaccharides were in majority released at the onset of the Rovabio treatment and then were later hydrolysed by hydrolytic enzymes into monosaccharides. A similar behavior of sugar solubilization during the first 2 h of treatment was observed with xylanase C alone, except that solubilized sugars were only comprised of xylose and arabinose. However, we found that xylose still continued to be released at a very slow rate upon xylanase C treatment till the end of the incubation time and probably

beyond. By comparing xylose and arabinose released, we can notice that Rovabio and xylanase C alone provide the same final amount of these pentoses after 6 h of enzymatic treatment.

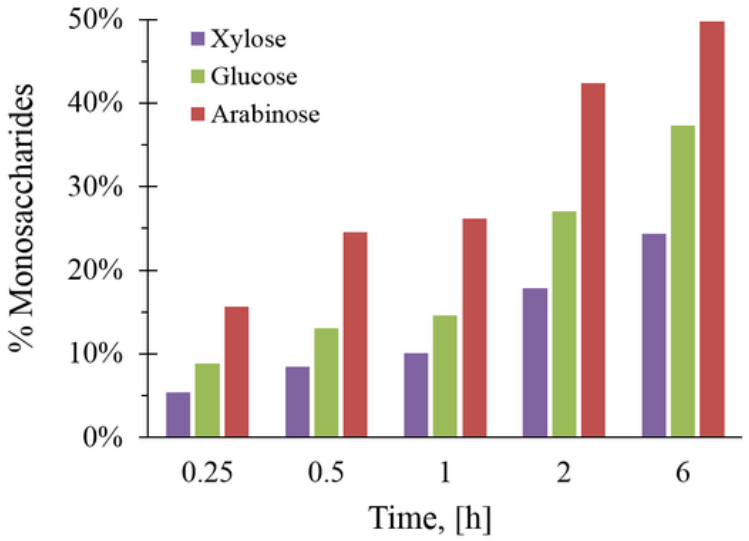

Figure 3-9. Proportion of monosaccharide in the total soluble sugars released (in opposition to oligosaccharide forms) during enzymatic treatment of destarched wheat bran by Rovabio® Advance. *Operating conditions identical to Fig.3-2.*

3.4. Discussion

With respect to traditional *in-vitro* methods that investigate the action of hydrolytic enzymes either individually or in a mixture on the NSPs solubilization from complex plant biomass in test tubes, we here made use of an instrumented pilot for *in-situ* deconstruction of destarched wheat bran by Rovabio, a commercially available enzymatic cocktail and compared the action of this complex enzymes mixture with xylanase C which is by far the most active NSPase present in this cocktail (Adisseo, unpublished data). The added value of this approach is to obtain rheological (viscosity and suspension behavior), granulometric (diameter and chord length distribution) and biochemical data (sugars and other components released) that can be exploited to infer relationships between macrostructure and microstructure fragmentation and solubilization of suspended material. This multiscale approach is also well adapted to investigate effects of any combination of enzymes mixtures with any type of suspension with a significant viscosity (>10 mPa.s) and a granulometry superior to 0.1 µm. As a matter of fact, this methodology has been previously developed to investigate the deconstruction of lignocellulosic material such as paper pulp and sugarcane bagasse under semi-dilute conditions by mixture of cellulolytic enzymes (Le, 2017; Nguyen, 2014).

The *in-situ* multiscale analysis of destarched wheat bran by Rovabio and Xylanase C brought to us two major insights. Firstly, this study revealed that the enzymatic cocktail exerts its deconstructive activity on insoluble matter in two concurrent manners: a strictly solubilization activity that releases accessible sugar moieties at the accessible solid-liquid interface of the particles and a concomitant fragmentation activity that corresponds to the breakup of particles, both action accounting for the drop of viscosity of wheat bran suspension (-50%) that takes place within 1 h after the addition of Rovabio. This rapid viscosity drop is in accordance with other studies focusing on enzymatic deconstruction of lignocellulosic suspensions in semi-dilute conditions (Dunaway et al., 2010; Nguyen et al., 2015). According to literature, suspension viscosity correlates with particles size with a dominant contribution of the biggest particles (Dasari and Eric Berson, 2007; Geddes et al., 2010) even if other properties interfere such as morphological complexity, physico-chemical surface properties or the ratio between sub-population of various size (Quemada, 2006). Hence, the significant reduction of large particles population as determined by DLS measurements can explain in great part this drop of viscosity of the wheat bran suspension treated by Rovabio. The viscosity of a suspension is also impacted by surface properties of particles such as roughness, adhesion, zeta potential, porosity, etc.(Bayod et al., 2005; Dibble et al., 2011; Nguyen et al., 2013; Viamajala et al., 2009). The solubilization activity that only hydrolysed 22 % of the insoluble NSPs in the wheat bran suspension during this 1st h of the treatment may also contribute to the drop of viscosity likely by affecting the surface properties and not by a change of the particles size. Taken together, one can conclude in agreement with previous reports (Le et al., 2017; Nguyen et al., 2013; Wiman et al., 2011) that the particle fragmentation is the dominant mechanism to explain the important viscosity drop of wheat bran suspension upon treatment with Rovabio. In contrast to the action of the enzymatic cocktail, the viscosity of the wheat bran suspension dropped by only 20% within 1 h after the addition of pure xylanase C which was followed by an overtake above initial viscosity value. The slight viscosity decrease can be attributed, as explained above, to both solubilization activity and partial fragmentation that likely arises from the endo-xylanosidic activity. However, our results showed that subpopulations particles resulting from xylanase C activity have different sizes and morphologies than Rovabio. In addition, the boost of viscosity that follows its fall after 2 h supports the nonlinear relationship between *in-situ* viscosity and PSD evolution. Indeed, difference in the proportion of large (> 300 µm) and small particles subpopulation (< 300 µm) between Rovabio (~70% large versus 30% small) and xylanase C (~80% large versus ~20% small) beyond 1 h of treatment could explain in part that

viscosity exhibits opposite trends between the two treatments. In addition, the degradation of insoluble arabinoxylans by xylanase C likely alters the interface solid-liquid area in a different manner than Rovabio. This difference could result in unspooling external fibers and an increase of surface tension and roughness, leading to greater particle interactions and higher yield stress, which together increases the viscosity of the suspension.

The requirement of enzymes mixtures to readily deconstruct complex plant matrix is clearly supported in this work using Rovabio which revealed a concomitant fractionation and solubilization of wheat bran. This efficient action can be attributed to synergistic activity of the wide range of glycosyl hydrolases with diverse and synergistic activity, together with 'auxiliary proteins' such as swollenins which are present in Rovabio. While they do not have any hydrolytic activity, they are reported to open up and disaggregate less-ordered regions of lignocellulosic substrate and to disrupt crystalline cellulose (Cosgrove, 2017; Georgelis et al., 2015). In addition, the non-catalytic carbohydrate-binding modules (CBM) that are present in either the N- or C-terminal part of the sequence of many Rovabio glycosyl hydrolase enzymes such as the arabinofuranosidases GH62 and GH54 (De La Mare et al., 2013; Guais et al., 2010) are reported to enhance substrate accessibility of these enzymes not solely through their binding to insoluble polysaccharide fibers but also by disorganizing the particles structure (Guillén et al., 2010). The importance of CBM in deconstruction of biomass is also supported by the finding that the suspension liquefaction efficiency is rather dependent on the site than the frequency of enzymatic cleavages (Szijarta et al., 2011). The potential action of these 'proteins' could account for fragmentation of particles that still continued albeit at a very low rate after 1 h up to 6 h of treatment and was characterized by lack of sugar released but by some additional solubilisation of proteins. This further solubilisation could be explained by a better accessibility of proteases to proteins covalently linked to some NSPs and by the release of proteins that are entrapped into insoluble fibers due to the cage effect of NSPs (Amerah, 2015; Aulrich and Flachowsky, 2001; Brufau et al., 2006). On the contrary, the main action of xylanase C was solubilisation which, as expected, was slower than with Rovabio, but reached after 6 h the same amount of arabinoxylans solubilized. These data supported the notion that the xylanase C is by far the most active xylanase present in Rovabio even though this cocktail contains 4 different GH11 xylanases encoded by *XynB*, *XynC*, *XynE* and *XynF* and one GH10 encoded *XynD* (Lafond et al., 2014). While xylanase C alone mostly displayed a solubilization activity, one cannot totally exclude a slight fragmentation activity that takes place after 6 h incubation as

witnessed by a sharp rise of small particles. This fragmentation can be explained by intense cleavage of arabinoxylans by the endo-xylanosidic activity that weakens the structure of the particles which thereafter are mechanically disrupted by the mixing system.

Finally, in spite of a rapid and effective action of Rovabio, only 30% of the wheat bran dry mass was solubilized leading to an insoluble fraction mostly enriched of particles at size < 300 µm. This finding raises the question of the physical and biochemical structure of this recalcitrant fraction. It is obvious that this fraction still contains a large amount of NSPs, that are apparently not accessible to Rovabio because either some key deconstructive/ destabilizing activities such as swollenin and other auxiliary enzymes are limiting or missing and/or because this fraction is physically inaccessible to the enzymatic action.

3.5. Conclusions

The *in-situ* deconstruction of insoluble wheat bran by Rovabio, a commercially available enzymatic cocktail and by pure xylanase C was investigated at a multiscale level by mean of an instrumented pilot. Our results support the notion that the rapid deconstruction implies a concomitant solubilization and fragmentation activities that requires the synergistic action of various glycosyl hydrolases and ancillary proteins. However, in spite of the presence of these numerous enzymes activities in Rovabio, the deconstruction of insoluble wheat bran was limited to 30% of solubilization, what raises the question whether this limitation in the deconstruction is of biochemical and/or physical nature. Finally, the rheology, granulometry and biochemistry study turns out to be an attractive approach to unravel the mechanism of biomass deconstruction by enzymes cocktails.

ACKNOWLEDGEMENTS

This work was supported in part by a grant support from Adisseo Company to J.M.F and L.F. The authors are grateful to D. Tuan LE and D. Tien Cuong NGUYEN for their original works in the development of the experimental set-up. We also acknowledge the technical assistance of Wenxiu HU for acid hydrolysis of sugars and HPLC methods and the fermentation platform of Toulouse White Biotechnology center for access to the FBRM probe. M.D is a recipient of CIFRE fellowship from ANRT and supported by Adisseo to carry out her Ph.D thesis.

CHAPTER 4:

WHEAT BRAN DECONSTRUCTION BY ROVABIO® CAN BE ENHANCED EITHER BY INCREASING SUBSTRATE ACCESSIBILITY OR BY THE ADDITION OF AUXILIARY ENZYMES

CHAPTER 4. WHEAT BRAN DECONSTRUCTION BY ROVABIO® CAN BE ENHANCED EITHER BY INCREASING SUBSTRATE ACCESSIBILITY OR BY THE ADDITION OF AUXILIARY ENZYMES

Abstract

As reported earlier, the deconstruction of wheat bran by Rovabio turned out to be partial, culminating with an insoluble fraction enriched in small particles at size < 300 µm, even if a very high dose of enzyme cocktail was used. Preliminary results have showed that this limitation was not due to an inactivation of the hydrolytic enzyme during the process or their inhibition by end-products released during the reaction. Thus, the accumulation of a recalcitrant -enzymatically inaccessible- fraction was the most likely explanation. We provided in this report evidence that the limited action of Rovabio to deconstruct wheat bran was due to a lack of accessibility to this insoluble fraction. On the one hand, a milling process of this insoluble recalcitrant fraction obtained after a 6 h treatment of destarched wheat bran with Rovabio, resulted in a 5.7% further solubilization upon addition of fresh enzymatic cocktail. On the other hand, a supplementation with an excess of pectinases allowed to also a further 16% solubilization of the recalcitrant fraction. The addition of pectinases was accompanied by a release of glucose what demonstrates that removing pectin increased cellulose accessibility by cellulases present in the Rovabio. Taken together, these results indicated that an enhancement of Rovabio activity can be obtained either by a physical treatment leading to an increase of the particle specific surface or by an enzymatic complementation with auxiliary enzymes that may help to brake open the recalcitrant particles.

4.1. Introduction

In animal nutrition, pigs and poultry are unable to digest 15 to 25% of their feed because of the presence of anti-nutritional factors such as non-starch polysaccharides (NSPs) that cannot be degraded due to a lack of specific enzymes. As feed is the biggest cost in animal production (FAO, 2017), industrial solutions with enzymes cocktail mainly composed of NSPases have been developed. Rovabio® is such an enzyme cocktail highly enriched with glycosylhydrolase enzymes (Guais et al., 2008) that shows beneficial effects through *in-vivo* assays by increasing animal performances (Abudabos et al., 2017; Lu et al., 2016, 2013; Tekeli et al., 2014; West et al., 2007). However plant biomass has evolved superb mechanisms for resisting assault on its structural sugars from micro-organisms or enzymes (Scheller and Ulvskov, 2010) which limits the efficiency of this bioprocess. In that respect, *in-vitro* experiments reported that only 30% of the arabinoxylan contained in wheat bran was solubilized with 1.1 $U_{xylanase\ visco}$ of the enzyme cocktail per gram of substrate (Lafond et al., 2011; Maisonnier-Grenier et al., 2006). To deeply characterize the deconstruction mechanisms of destarched wheat bran (dWB) with Rovabio®, a multi-scale approach encompassing direct and indirect physical and biochemical measurements was used in a previous work with a well-equipped bioreactor. Experimental data reported that Rovabio acts through both particles fragmentation and solubilization phenomena. However, in spite of the presence of these numerous enzymes activities in Rovabio, the deconstruction of insoluble wheat bran, even with 1100 $U_{xylanase\ visco}$/gdm, was limited to 30% of substrate solubilization. This raises the question whether this limitation in the deconstruction is physical and/or biochemical. This point will be investigated in the present work as well as different ways to enhance dWB deconstruction by Rovabio.

4.2. Materials and methods

4.2.1. Substrate and enzymes

Destarched wheat bran obtained following the process described in §2.2.1 were used as substrate. The enzymatic cocktail Rovabio® Brussel (simplified by Rovabio thorough the text) has been described in §2.2.1. The total activity of Rovabio Brussel corresponded to 44 505 $U_{xylanase\ visco}$/g (density of 1.09). Cellic® CTec2 from Novozyme® (Bagsværd, Danemark), is a commercial enzymes cocktail containing mainly glycosyl hydrolase activities (cellulases). Protein concentration of Ctec2 is 303.2 g/L (Bradford, 1976) and its xylanase activity is 8006 $U_{xylanase\ visco}$/mL (assayed with Beechwood Xylan from Megazyme at pH 5.0, 50 °C). A pectinolytic cocktail, Optizym®, was obtained from Laffort (Laffort SAS, Bordeaux, France).

Mass spectroscopy identified 7 enzymes: endopolygalacturonase, endoglucanase, endo-β-1,4-mannosidase, rhamnogalacturonate lyase, rhamnogalacturonase, avicelase and a probably endopolygalacturonase. Optizym® contains 31.7 mg of protein per g of powder (BiCinchoninic acid Assay). Ronozyme® ProAct is a protease cocktail obtained from DSM (Koninklijke DSM N.V., Heerlen, the Netherlands). This enzyme cocktail contains 73.1 mg of proteins per g of product (internal dosage, BCA).

4.2.2. Milling experimental set-up and operating conditions

4.2.2.1. Experimental set-up

Wet batch grinding experiments were carried out in an industrial stirred bead mill commercially known as LabStar and manufactured by NETZSCH with a grinding chamber of 0,6L. In this type of mill (**Figure 4-1**), the apparent volume of grinding is approximately filled up to 75 - 85% with mono-sized beads (from µm to few mm diameter). The remaining of the volume contains the suspension of particles to be ground. The beads and the suspension are strongly stirred by a central rotating agitator at a speed ranging from 1000 to 3000 RPM. The particle fragmentation results from the capture of particles inside zones of strong occurring stress when two grinding beads collide. A double jacket where cooling fluid (water and glycerol) flows, allows the control of the temperature increase due to the size reduction process. The suspension is pumped through a stirrer tank to the inlet of the grinding chamber of the stirred media mill (LabStar) with the help of flexible-tube pump. After experiencing a certain comminution in grinding chamber, the suspension leaves through a steel (Cr–Ni–steel) separating cartridge (filter) that was installed at the outlet of the grinding chamber. Then ground suspension returns to the stirred tank as the experimental set-up consists in an instrumented close-loop which, in addition, measures both the suspension pressure and its temperature before the grinding chamber and the suspension temperature after it.

4.2.2.2. Milling operating conditions

To reduce particles size of dWB 6h-treated with Rovabio® Advance, a moderate agitation speed into the grinding chamber was applied with 1500 RPM. The filling volume of the beads was fixed at 83.5% of the grinding chamber with 1.8 kg of silicate zirconium beads with a diameter from 0.9 to 1.1 mm (ZetaBeads® 1.0, NETZSCH). The steel separating cartridge has slots size of 300 µm, which agrees with the size of the used beads. The pilot pump (150 tr/h) ensures a sample circulation at 57.5 L/h. For all experiments, the temperature in the grinding chamber was kept lower than 40 °C thanks to the double jacket containing cooling

fluids. Suspension was mixed at 340 RPM in the stirred tank. During the assays, the grinding chamber was firstly filled with the grinding medium (450 mL of beads) and the process was started under water. Then dWB was quickly added into the stirred tank and grinding process started. Samples (about 5 mL) were collected in the stirred tank at 0, 4, 7, 10, 15, 20 and 40 min in order to monitor particle size evolution (DLS and MG) and to do hydrolysis assays (see below). Three runs were then performed under the same operational conditions to ensure ground matrix homogeneity and a sufficient amount of matter to run additional hydrolysis experiments.

Figure 4-1. LabStar industrial stirred bead mill (NETZSCH)

4.2.3. Experimental pilot set-up and operating conditions

Our experimental set-up used to characterize enzymatic dWB deconstruction has been described in Chapter 2 and 3. Operating conditions were mimicking conditions encountered in poultry anterior digestive system which are high dry matter suspended into 100 mM potassium phosphate buffer at 41 °C and pH 4.0 (Svihus, 2014). The working concentration of destarched wheat bran suspension was fixed at 1.5 *Ccrit* as a non-Newtonian behavior of the suspension was obtained above this value, which corresponds to 75 gdm/L. The experimental strategy consists of three parts: (i) *in-situ* viscosimetry assays, (ii) enzymatic hydrolysis combine with grinding process and (iii) enzymatic complementation of Rovabio Brussel.

4.2.4. Chemical and biochemical analyses

Dry matter concentration. For determining water content of sample during enzymatic hydrolysis, a quantity of sample (m_s) was filtered through a Whatman No1 filter paper of known weight (m_{fp}) and then washed by ≈5 mL of distilled water. The filter paper containing the sample was dried in an oven set at 60 °C and 200 mbar (Heraeus, Thermo Scientific, 0 - 760 mmHg, 50 - 150 °C) with silica gel during 4 days. The weight of samples was then measured with a precision balance (Sartorius ED224S, 0.005-230 g ± 0.1 mg). The final weight was identified m_{fin}. Water content (W) and dry matter (DM) were calculated following ***Eq. 2-1*** and ***Eq. 2-2*** (accuracy ± 0.5 %):

$$W(\%) = \frac{m_s + m_{fp} - m_{fin}}{m_s} x100 \qquad \textit{Eq. 2-1}$$

$$DM(\%) = 100 - W \qquad \textit{Eq. 2-2}$$

Solubilization rate. It corresponds to the soluble matter that is released in the supernatant during the treatment of the destarched wheat bran and was estimated dry weight measurements as described in §2.2.3.

DNS assay. Reducing sugars were estimated by dinitrosalicylic method which is based on the property of reducing sugars to reduce a colorimetric sugars detection reagent (Sumner and Howell, 1935). DNS reagent was prepared with the following protocol: 30 g of tartrate double of sodium and potassium was solubilized into 50 mL of distilled water and 20 mL of sodium hydroxide 2M were added. Then, 1 g of 3,5-dinitrosalicyclic acid were added slowly stirring continuously the solution. Finally the solution was completed with distilled water to reach 100 mL. This solution was stored in dark glass bottle at temperature below 20 °C. In the protocol 1 mL of experimental samples and 1 mL of DNS reagent were mixed. The tubes were stirred and heated 5 min at 100 °C. Then tubes were cooled into ice during 10 minutes and at room temperature during 15 minutes. Absorbance was measured at 540 nm on a spectrophotometer (Biochrom Libra S11, Harvard Bioscience, Holliston, Massachusetts, USA) with respect to a control solution consisting of 1 mL of distilled water and 1 mL of DNS. A xylose standard curve from 0 g/L to 2 g/L was prepared from the stock solution.

Sugar determination. Released insoluble or soluble sugars were first acid hydrolysed into monomers and then determined by HPAEIC as described in §2.2.3.

4.2.5. Physical analyses

In-situ viscosity measurement. The *in-situ* viscosity was determined from real-time monitoring of torque and mixing rate as described in §2.2.4.1.

Morphogranulometry (MG). Images of particle suspension were made with a morpho-granulometer (Mastersizer G3S, Malvern Instruments Ltd. SN: MAL1033756, software Morphologi v7.21). The instrument is composed of a system of lens (magnification: from x1 to x50, particle dimension: from 0.5 to 3000 µm), an optical device (Nikon CFI60 Bright/ Dark field) and a camera (IEEE1394a, Fire Wire^{TM}, 2592x1544 pixels). Images were obtained from a 60 µL of suspension sample (diluted 1:100) deposited between cover glass and slide. A surface of 5x5 mm was analysed in dark field with a magnification x10, under the standardized operating conditions (light intensity 90, exposure time 400 ms, threshold for particle detection 30-100).

Ex-situ diffraction light scattering (DLS). The volume-weighted particle size distribution (PSD) was determined by DLS as described in §2.2.4.3. Volume-weighted distribution (E_v) was calculated by the Mastersizer software and multiplied by dry matter concentration (Cm) to take into account the loss of material due to solubilization during the enzymatic treatment.

In-situ focus beam reflectance measurement (FBRM). FBRM enables *in-situ* quantification of small particles in the range < 100 µm through the estimation of the chord length (lc) and distribution of the chord length population (CLD) using an FBRM® G400 probe as described in §2.2.4.4. The number-weighted CLD, $E_n(l_c)$, and the average number of chord length counted per second, N_c, are used as indicators to describe population.

4.3. Results

4.3.1. The partial deconstruction and solubilisation of dWB by excess of Rovabio

Destarched wheat bran (dWB) was suspended at 75 gdm/L at 170 RPM and gave an initial viscosity μ_0 of 0.165 Pa.s after suspension homogenization and stabilization. This suspension viscosity remained almost constant throughout 6 h of incubation in the absence of any enzymatic solution (**Figure 4-2A**). Upon addition of Rovabio at an equivalent dose of 1100 $U_{xylanase\ visco}$/gdm, the suspension viscosity dropped by more than 60% in less than 2 h, which was followed by a dramatic falldown to stabilize at about 80% of its initial value (0.032 Pa.s) after 6 h (**Figure 4-2A and B**). To analyse enzyme activities limitation without excess of

enzymes, dWB suspension (≈ 75 gdm/L) was treated by Rovabio at 1.1 $U_{xylanase\ visco}$/gdm, which was progressively complemented to reach 380 and then 1100 $U_{xylanase\ visco}$/gdm. Substrate deconstruction was monitored following its viscosity decrease (**Figure 4-2A**) and compared to previous viscosity assays with a unique addition of Rovabio at 1.1, 380 and 1100 $U_{xylanase\ visco}$/gdm at 0h. Results showed that the cumulative enzyme addition (1100 $U_{xylanase\ visco}$/gdm added 4 times at 0, 3, 6, 20 h) allowed to reach progressively the same viscosity reduction than adding a unique enzyme dose at 0 h. However the maximal viscosity reduction was achieved after 20 h of enzymatic treatment instead of 6 h with an initial and unique enzyme addition at 1100 $U_{xylanase\ visco}$/gdm.

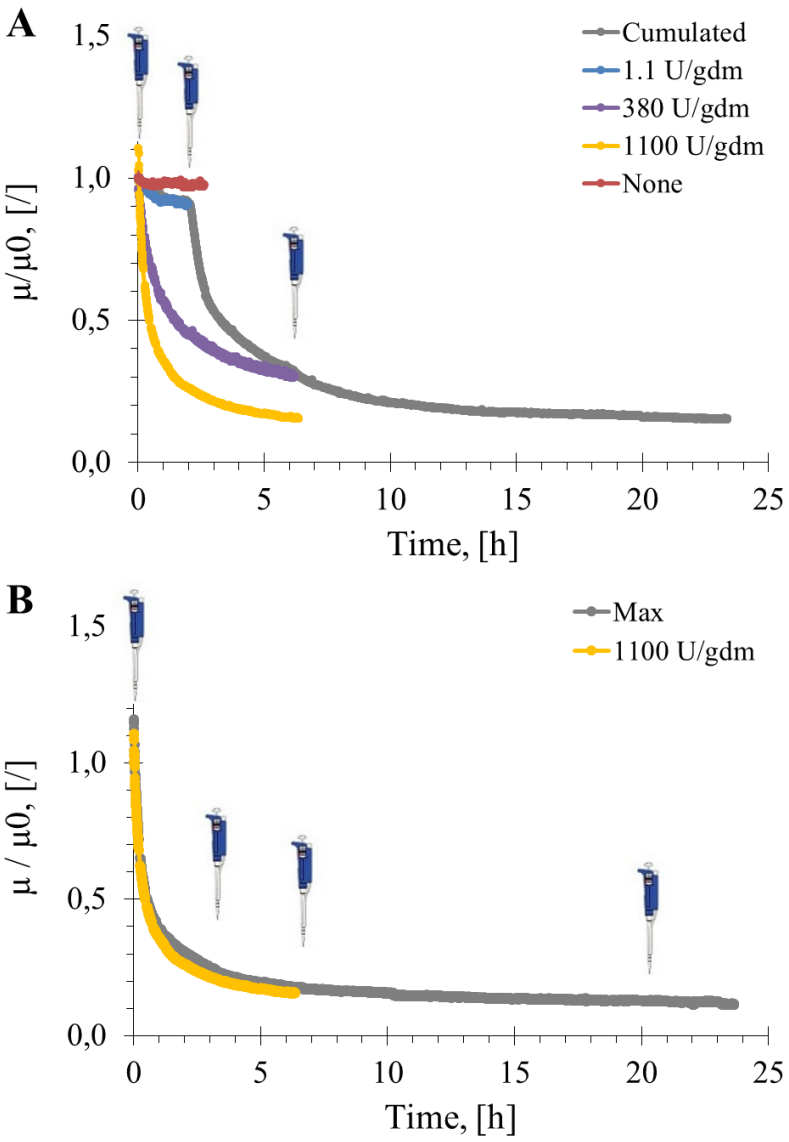

Figure 4-2. Change in the viscosity of the destarched wheat bran suspension upon cumulative addition of Rovabio (A) or of large excess of Rovabio, 4400 $U_{xylanase\ visco}$/gdm (B). *Operating conditions: destarched wheat bran suspended in a potassium phosphate 0,1M at 41 °C, pH 4.0, initial concentration about 75 gdm/L*

To verify whether the viscosity achieved is the lowest that can be reached, dWB suspension was treated with cumulative addition of Rovabio (1100 $U_{xylanase\ visco}$/gdm) at 0, 3, 6 and 20 h. As shown in **Figure 4-2B**, these additional inputs of Rovabio did not further decrease the suspension viscosity. Therefore a single enzymatic dose of 1100 $U_{xylanase\ visco}$/gdm allowed to reach the maximal viscosity reduction of dWB suspension which correspond to a loss about 80% of initial viscosity value. However the suspension viscosity, after 6 h of enzymatic treatment, was far from the viscosity of a sugar solution. In fact considering that all dWB (75 gdm/L) was hydrolyzed into glucose monomer solution, this solution should have a concentration about 82 g/L and thus a viscosity about 1.25 mPa.s at 25 °C (Lide, 2000) which highlights that dWB degradation was not complete. Therefore one or several enzyme activities may be inhibited or limited during dWB deconstruction that could be compensated by increasing enzyme loading until achieving the maximal deconstruction yield.

These data suggest that the action of Rovabio to deconstruct dWB may be stopped or hampered either by an inhibition of hydrolytic activities by end-products (merely monosaccharides sugars) released in the supernatant or by the presence of a recalcitrant fraction that is no longer accessible to hydrolytic enzymes. To test the first hypothesis, dWB was suspended in the supernatant of a 6h-treated dWB suspension with Rovabio (1100 $U_{xylanase\ visco}$/gdm) to which fresh Rovabio was added at the same dose as for the first treatment. Results reported in **Figure 4-3** show that the kinetic of viscosity reduction was comparable to the one reported earlier (**Figure 4-2**) with dWB suspended in a fresh buffer. We can therefore conclude that the inability of Rovabio to fully deconstruct and solubilize dWB is not due to presence of inhibitors released in the supernatant during the treatment. To argue that the action of Rovabio is merely limited by the presence of a recalcitrant fraction inaccessible to further deconstruction, we suspended the 6h-treated dWB matrix in a fresh phosphate buffer and treated with the same fresh enzyme dose (Rovabio 1100 $U_{xylanase\ visco}$/gdm). Only a limited decrease of viscosity from 45 mPa.s to 33 mPa.s (- 12mPa.s compared to initial viscosity of suspension around 165 mPa.s) was recorded (**Figure 4-3)** supporting the idea that the limitation of dWB deconstruction by Rovabio was due to the production of an insoluble recalcitrant fraction that was not any more accessible to enzymatic action. This recalcitrant fraction was about 47 gdm/L (**Figure 4-13**) which represented 62.7% of the initial dWB suspended and submitted to Rovabio treatment.

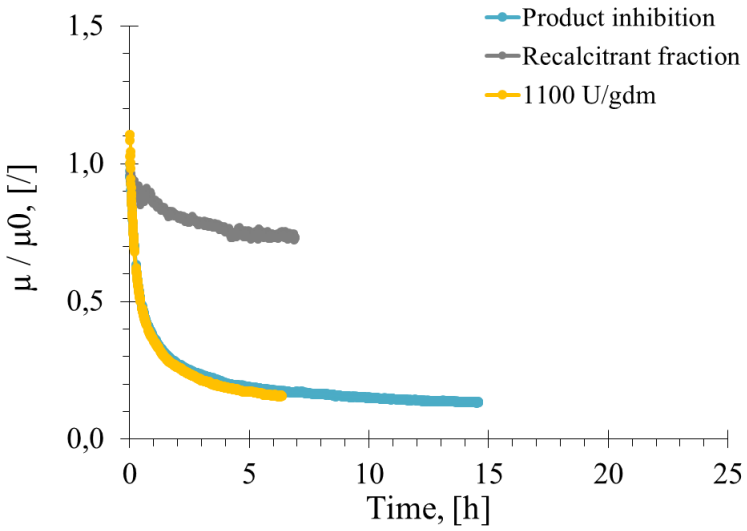

Figure 4-3. Effect of the addition of Rovabio at 1100 $U_{xylanase\ visco}$/gdm, on dWB suspended in the supernatant from a 6h-treated dWB at 1100 $U_{xylanase\ visco}$/gdm (Product inhibition) and on the recalcitrant fraction of a similar treated dWB suspended in fresh buffer (recalcitrant fraction). *Operating conditions are identical to Fig.4-2.*

4.3.2. Physical treatment to increase to substrate accessibility

4.3.2.1. Milling process

In order to improve substrate accessibility for enzymes present in Rovabio, the recalcitrant fraction that has been obtained after 6h of treatment of dWB with Rovabio, was milled using a stirred bead mill. We firstly set up milling parameters in order to significantly fractionate the insoluble recalcitrant particles but without reducing them to a powder with particles smaller than µm. We found that grinding this fraction for 40 min with a moderate agitation speed into the grinding chamber (1500 RPM), a filling volume of the beads (≈1 mm) at 83.5% of the grinding chamber and a pilot pump (150 tr/h) which ensured a sample circulation at 57.5 L/h, resulted in a particle size reduction as visualized by a fragmentation of large particles into smaller ones (**Figure 4-4A)**.

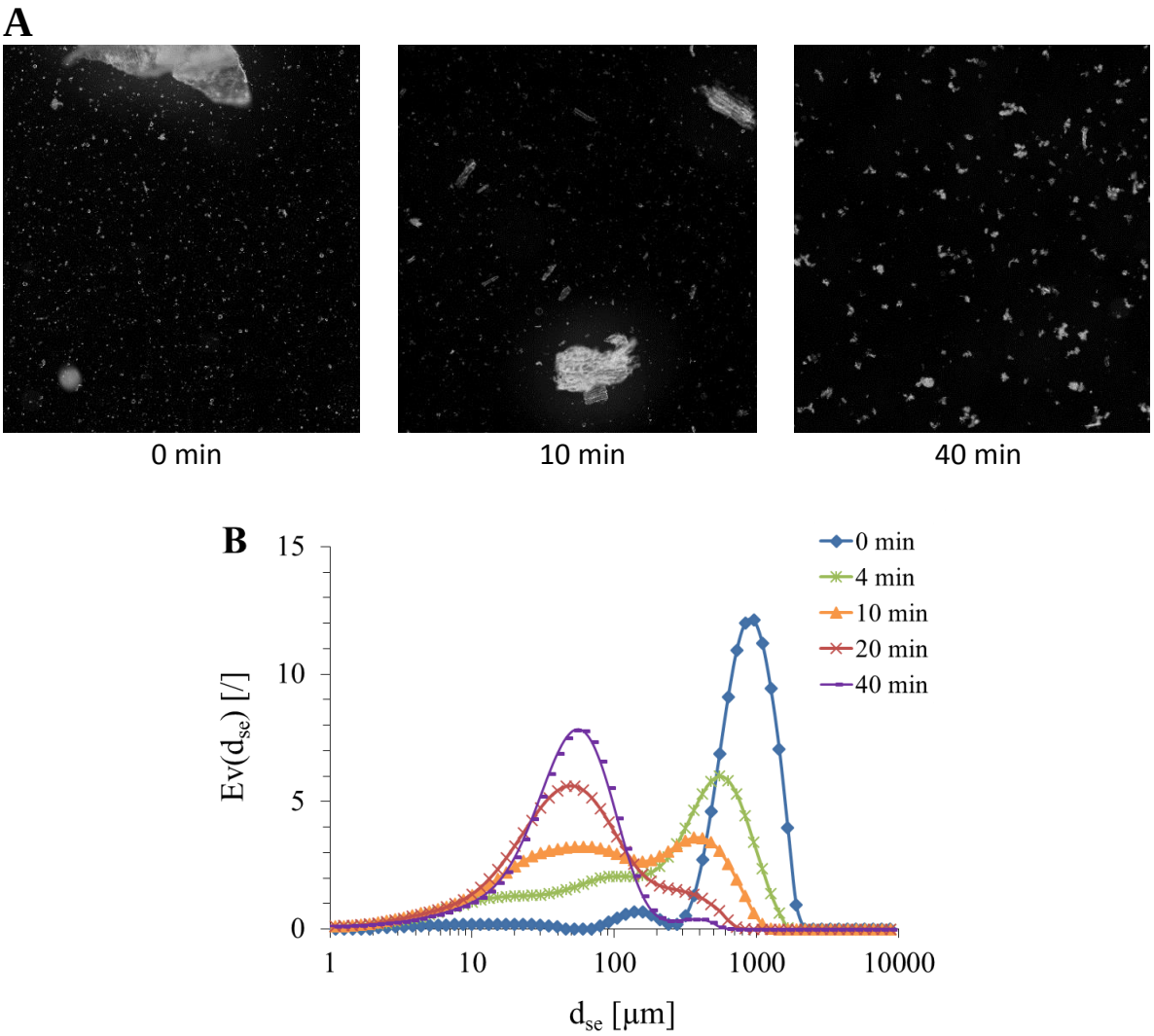

Figure 4-4. Effect of milling process on particles size of a 6h-treated destarched wheat bran treated with an excess of Rovabio (1100 $U_{xylanase\ visco}$/gdm): *Morphologi G3S images (dilution 1:100 - X10 – 5x5mm – dark field – Trouble shoot 30 – luminosity 90% and exposure time 500ms) (A) and the sphere equivalent diameter (d_{se}) volume distribution multiplied with the suspension concentration (Cm)*

The fragmented particles by this milling process were then characterized by DLS analysis, which allowed getting access to PSD and its evolution as quantify by the volume distribution of the sphere equivalent diameter, E_v (d_{se}). Results in **Figure 4-4B** showed that the recalcitrant fraction was bimodal and enriched of a major population of large particles ($D_{4,3}$=935.2 µm ± 17) that was progressively fragmented, along the milling process, passing to a bimodal distribution with an increase of finest particles ($D_{4,3}$=106.5 µm ±18), which became the predominant population after 20 min of milling treatment. In addition during this milling process, no material was solubilized (data not shown).

Samples were taken at different times of the milling process, their insoluble fraction were then treated by an excess of Rovabio Brussel (>11 000 $U_{xylanase\ visco}$/gdm) at 40 °C for 2 h and reducing sugars were measured in the supernatant by the DNS method. As shown in **Figure 4-5** the amount of sugar released increased with the time of the milling process, which suggests that the reduction of particles size resulted in a regain of enzymes accessibility. There was however no obvious proportionality between particle size reduction and sugar solubilization rate.

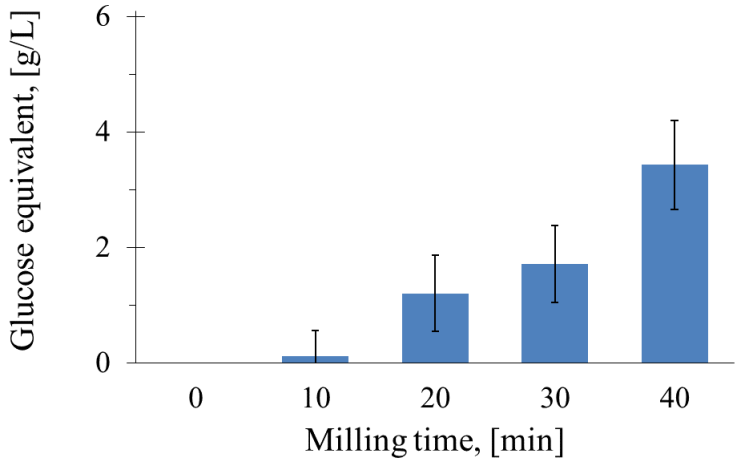

Figure 4-5. Effect of milling process on the solubilisation rate by Rovabio. *A 6h-treated destarched wheat bran treated 6 h with an excess of Rovabio was used prior to milling treatment. Suspension were harvested at different time during the milling process and treated with 11000 $U_{xylanase\ visco/gdm}$ of Rovabio for 2 h. Soluble sugars released were expressed as equivalent glucose concentration, during the enzymatic treatment of this milled substrate as a function of the milling duration (41 °C, pH4 in stirred tubes). Background signal at t=0h was subtracted from all samples and the error bars represent the standard deviation of two independent experiments.*

4.3.2.2. Enzymatic treatment of milled substrate

A 40 min duration of the milling process was chosen to ensure a sufficient particles fragmentation of the recalcitrant fraction. Three batches of 6h-Rovabio treated dWB were thus milled and the resulting pellets were washed and suspended in fresh phosphate buffer at 68 gdm/L. A stable viscosity (evolution < 5% in 5 h) required more than 20 h after re-suspension likely because some particles were agglomerated, unstructured or destabilized during the milling process and post-treatment (centrifugation). After this period, we added fresh Rovabio Excel (1100 $U_{xylanase\ visco}$/gdm) and monitored change in viscosity. As it can be seen in **Figure 4-6** a sharp decrease of viscosity was observed with a loss of 60% of the initial value of 86 mPa.s that reached a value as low as about 6 mPa.s at 6 h after the addition of the enzyme cocktail. The kinetic of viscosity change showed the same behaviour than the deconstruction of

raw dWB by an equivalent dose of Rovabio. However the final viscosity value was equal to 6 mPa.s which is still far from the viscosity value of the dWB suspension entirely hydrolysed into soluble sugars (1.25 mPa.s - see §4.3.1.) and thus some material remained insoluble and recalcitrant to the enzyme hydrolysis.

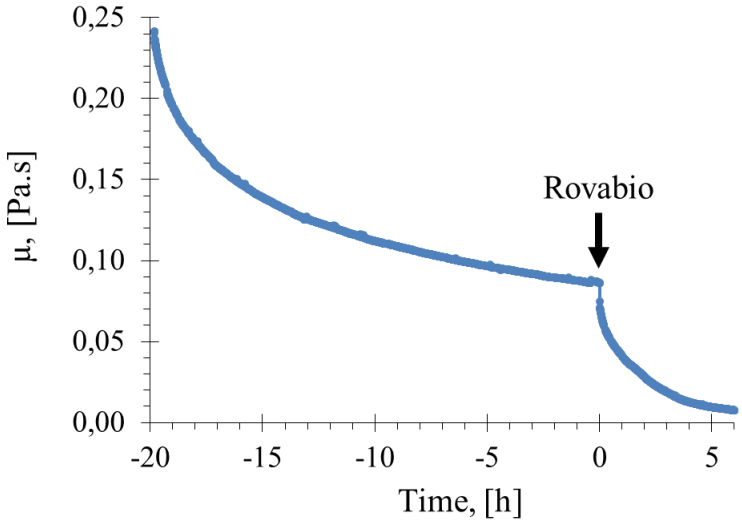

Figure 4-6. Change of viscosity of a recalcitrant fraction from dWB after resuspension in buffer and after addition of excess of Rovabio. *A 6h-treated destarched wheat bran with an excess of Rovabio (11000 Uxylanase visco/gdm) was milled, resuspended (-20 to 0h) and then treated with 11000* $U_{xylanase\ visco/gdm}$ *of Rovabio Brussel (0 to 6h). Operating conditions are identical to Fig.4-2.*

In-depth investigation of the evolution of PSD population during enzymatic treatment was achieved through DLS and is reported in the **Figure 4-7**. It is interesting to notice a change in the particles size from -20 h (volume distribution with a d(0.5) = 44.69 µm ± 3.73 when the milled fraction was just re-suspended in the buffer to 0 h (volume distribution with a d(0.5) = 34.47 µm ± 4.98 just before the addition of Rovabio. However, there was almost no solubilization during this period (**Figure 4-9**), confirming that this change in PSD was due to a reorganisation of the particle structure due to mixing. PSD evolution following the treatment of the milled fraction with Rovabio showed an overall reduction of the particle size with a drift of the median of the volume distribution to a d(0.5) = 27.6 µm ± 2.02 (volume distribution), reflecting a slight particles fragmentation and solubilization as none increase of smaller particles was reported.

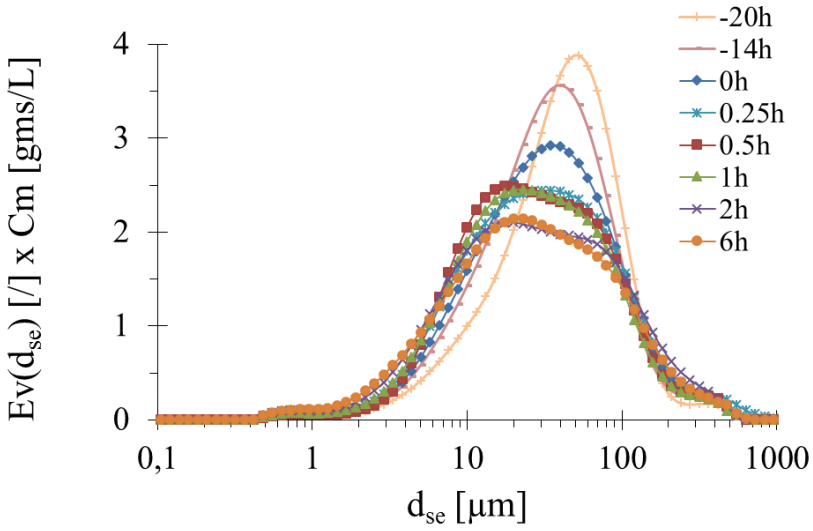

Figure 4-7: Particles size evolution during the suspending time and the hydrolysis of milled destarched wheat bran. *The particle size is reported as the number distribution of particle shepre equivalent diameter (dse) multiplied by the suspension concentration (Cm). Operating conditions are identical to Fig.4-2.*

To further analyze what occurred at the level of particles fragmentation, we employed the FBRM to monitor change in size and abundance of smaller particles during the treatment of the milled fraction with Rovabio. During suspending time, the total number of particle (Nc) and their mean chord length (lc) remained constant (data not shown). During the treatment with Rovabio, the total number of particle (Nc) followed a slightly and monotone increase, whereas the chord length decreased in a an almost exponential manner (**Figure 4-8A**). These data indicate that the particles in this recalcitrant fraction are subjected to both a fragmentation and a solubilization phenomenon. However, the finding of net increase in the abundance of smallest particle, as estimated by the chord length distribution (CLD) multiplied by Nc during the Rovabio treatment, supports the idea that the fragmentation of particles was superior to their solubilization (**Figure 4-8B**).

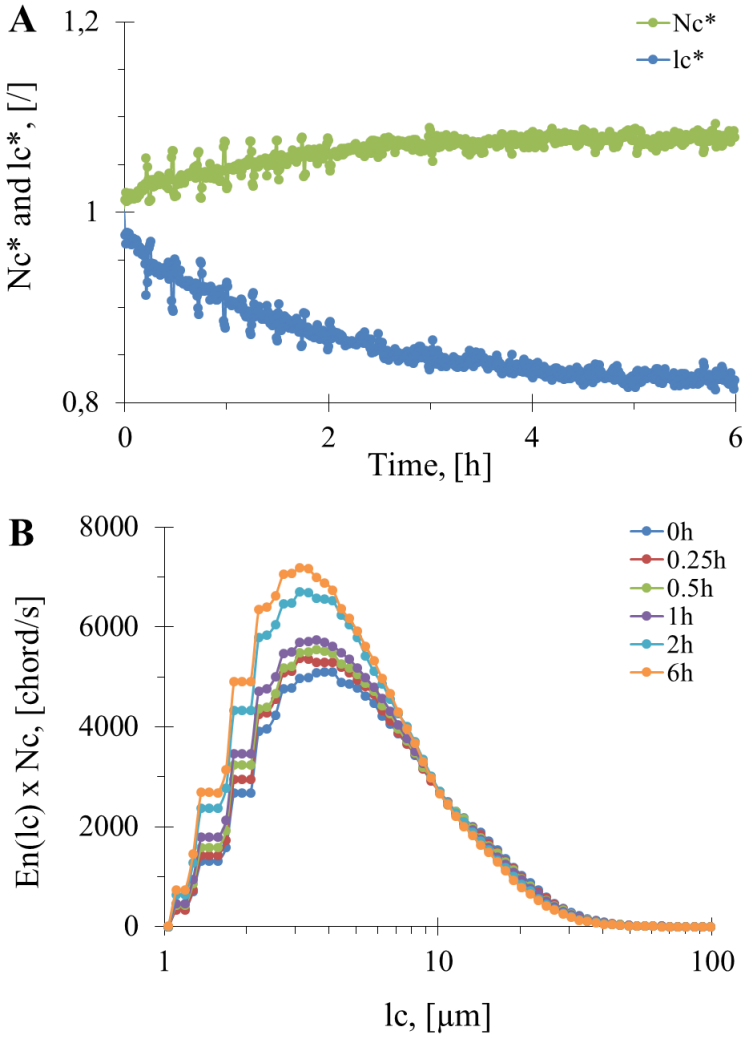

Figure 4-8. Evolution of particle size and number by focusing on the finest population during the deconstruction of milled destarched wheat bran by Rovabio Brussel. *This evolution is reported as the normalized number of count per second (Nc*) and the normalized mean chorld length (lc*) as a function of the time (A) and the number distribution of chord length multiplied by the number of particle (B). Operating conditions are identical to Fig.4-2.*

The solubilisation rate which corresponds to soluble matter released in the supernatant upon the treatment of the milled fraction with Rovabio is reported in **Figure 4-9**. As expected, there was almost no solubilization during the 20 h required to suspend and homogenize the milled fraction until it reached a relatively stable viscosity. Addition of Rovabio resulted in an immediate release of soluble matter, from 0.45 to 3.55 gdm/L within 1 h that started to slow down after 2 h. At 6 h after the addition of the enzyme cocktail, about 6.6 gdm/L of soluble matter was measured which corresponded to 9% of the initial dry mass of milled fraction (68 gdm/L). Considering raw dWB concentration, the 1st addition of Rovabio solubilized 37% of

the initial dry matter (75 gdm/L) and after the milling process, the 2nd addition of Rovabio allowed a further solubilization of 5.7% to reach 42.7% of solubilized matter.

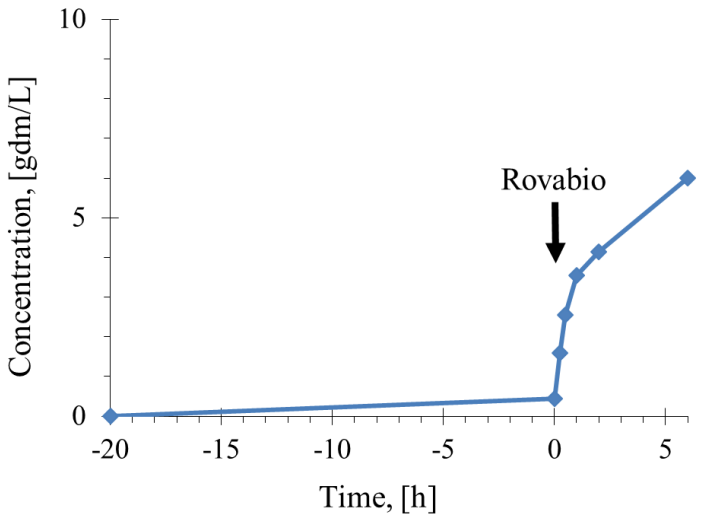

Figure 4-9. Total matter (gdm/L) solubilized during enzymatic treatment of the ground destarched wheat bran by Rovabio Brussel. *Operating conditions are identical to Fig.4-2.*

4.3.3. Enzymes complementation of Rovabio on wheat bran deconstruction

The physical treatment reported previously suggested that increasing the particles specific surface is a potential way to increase enzyme accessibility. Therefore, and in spite of the fact that Rovabio is highly enriched in a wide spectrum and complementary hydrolytic enzymes, especially xylanases and endoglucanases, it might be possible that the inability of this enzymes cocktail to solubilize wheat bran was due to the inefficient action of enzyme in helping to fragment insoluble particles and hence to augment their accessibility to hydrolytic enzymes. Numerous enzymes or proteins can potentially display this function and regarding to the wheat bran composition we selected three of them. Swollenins are expansin-like proteins and are reported to disrupt, fragment, deagglomerate cellulose crystalline structure (Gourlay et al., 2015; Jäger et al., 2011; Santos et al., 2017) and are also efficient on arabinoxylan to enhance the xylanase action (Gourlay et al., 2013; Santos et al., 2017). Pectinases are degrading enzymes specific to pectin structure which plays a peculiar role into the hemicellulose structure by filling in the remaining space into this network (Cosgrove, 2000) and proteases deconstruct the protein part of the bran . All these enzymes or active proteins represent less than 10% of the total protein content of Rovabio (Guais et al., 2008).

Since we do not have access to swollenin yet, whereas pectinases and proteases can be easily purchased from commercial sources (Optizym and Ronozyme commercial enzyme cocktails), we tested the complementation of Rovabio (after 6 h of treatment) with these latter as well as

another commercial enzyme cocktail Ctec2 rich in cellulases upon dWB deconstruction. The enzyme complementation dose was equal to 15% of the prior dose of Rovabio, based on the protein quantities of the enzyme cocktails.

4.3.3.1. Effect of enzyme complementation at macroscopic scale

As shown in **Figure 4-10**, the complementation of Rovabio (after 6 h of initial treatment of dWB) by itself as well as Optizym (pectinases), Ronozyme (proteases) or Ctec2 (cellulases) had almost no effect on the suspension viscosity even if it passed from 100 mPa.s at 0 h to 38 mPa.s after 6 h of treatment.

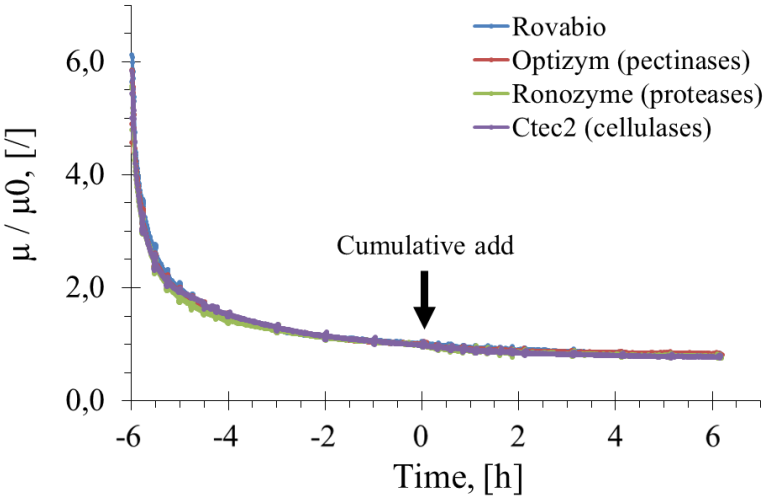

Figure 4-10. Effect of the addition of Rovabio on dWB at 1100 Uxylanase visco/gdm, then complemented at 6h of treatment by itself (Rovabio), Optizym (pectinases), Ronozyme (proteases) or Ctec2 (cellulases). *Complementation was done by a dose of 15% of the prior dose of Rovabio, based on the protein quantities of the enzyme cocktails. Operating conditions are identical to Fig.4-2.*

4.3.3.2. Effect of enzyme complementation on particles fragmentation

Using DLS we have analysed the evolution of PSD during enzyme complementation. As reported in **Figure 4-11**, a further addition of Rovabio at 6 h showed a very weak change in the particle size distribution. What we observed at 30 min after this addition was a slight increase of the large particles population (1000 µm), probably due to a weak solubilization of the fine one, that is followed by a significant decrease of these large particles with a concomitant appearance of smaller ones in the range of 100 to 250 µm that traduce a slight fragmentation phenomenon (**Figure 4-11A**). Therefore a weak dWB deconstruction was still observed during the complementation of Rovabio by itself. While addition of CteC2 had no effect at all (**Figure 4-11D**), that of the pectinases (Optizym) led to reduction of the large particle population (1000 µm) in 15 - 30 min that can be accounted by: (i) a solubilization process directly of the large

particle surface or (ii) a concomitant solubilization of the small particles resulting from coarse ones fractionation, since there was no appearance of any other particles population during this treatment (**Figure 4-11B**). On the other hand, the proteolytic cocktail Ronozyme exhibited a slight fragmentation process as suggested by the appearance of a population around 250 µm at the last hour of incubation together with a significant reduction of large particle size (**Figure 4-11C**). From these results, it is conclude that the pectinolytic cocktail has a positive effect in the deconstruction of wheat bran. However the PSD evolution during the complementation with the other enzyme cocktails showed only slight evolutions with no significant trends and therefore their interests were not clearly confirmed.

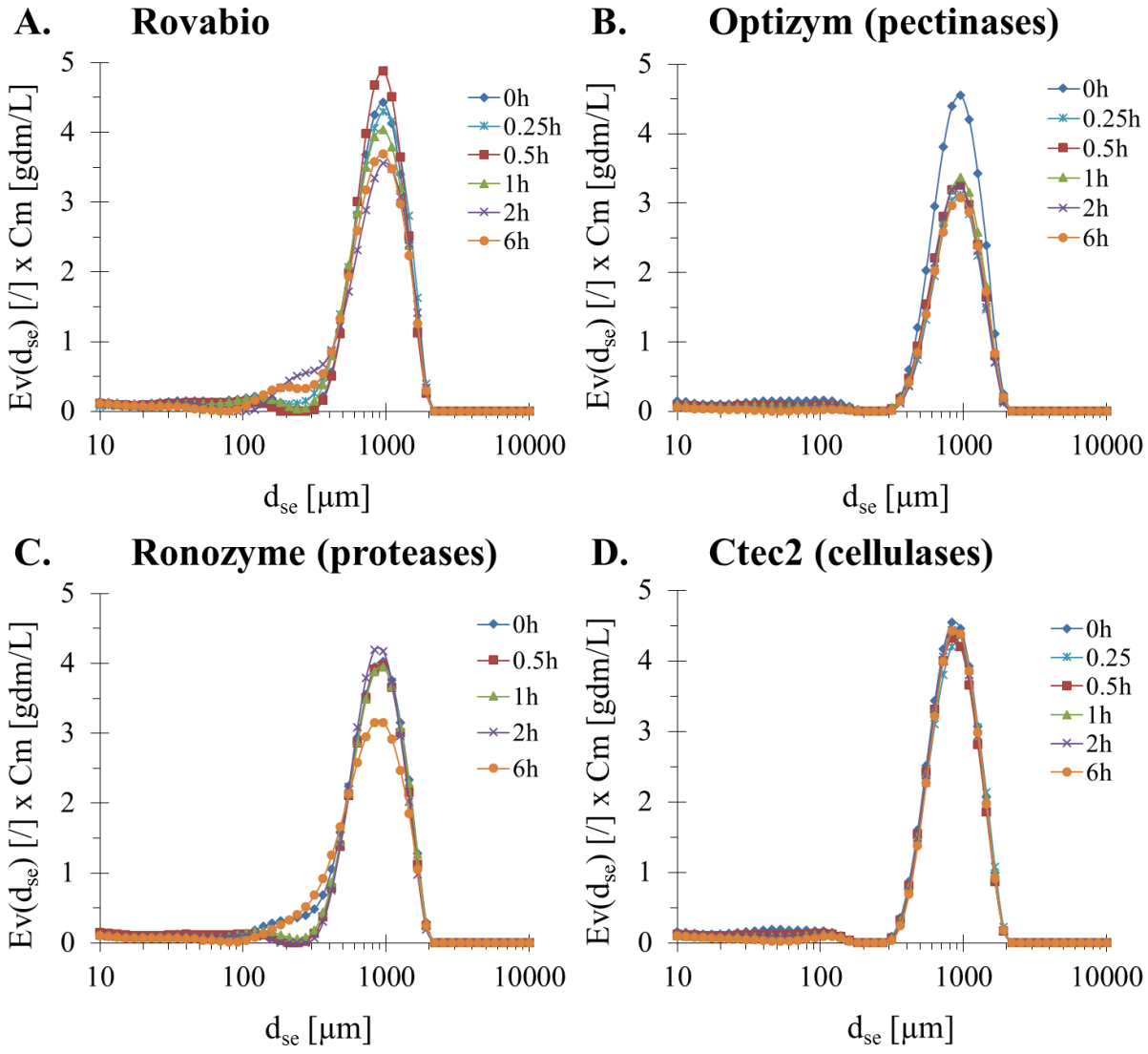

Figure 4-11. Particle size distribution during the treatment of dWB Rovabio complemented by itself (A), Optizym (pectinases) (B), Ronozyme (proteases) (C) and Ctec2 (cellulases) (D). *The particle size distribution was assimilated to a diameter of equivalent sphere (d_{se}) and was plotted with respect to the abundance of particle size which was obtained by multiplying E_v by the concentration of wheat bran suspension (Cm) that remained at each time during the enzymatic treatment. Operating conditions are identical to Fig.4-2.*

We also investigated whether the addition of these different enzyme solutions on dWB treated for 6 h with Rovabio could cause a change of small size particle population by FBRM measurements (**Figure 4-12**). This analysis highlights clearly that only the pectinolytic cocktail Optizym (**Figure 4-12B**) provided a slight CLD shift towards smaller particle sizes and a decrease of the total number of particles as shown by the decrease of the area under the curve clearly measurable at 6 h after the addition of the enzyme solution. This trend illustrates an important solubilization of the small particles which was superior to the fragmentation phenomenon highlighted previously with DLS measurements.

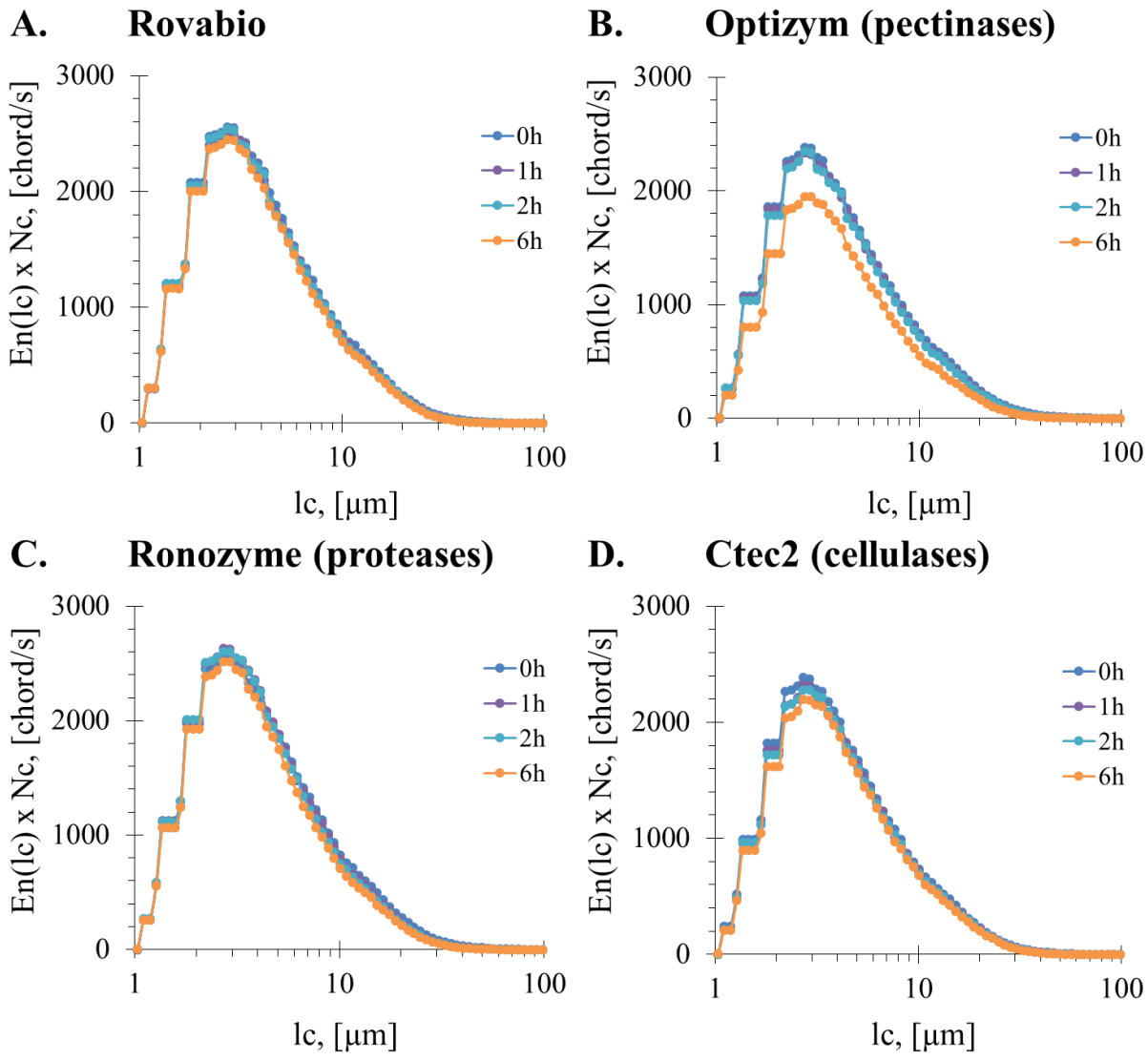

Figure 4-12. The number distribution of chord length multiplied by the number of particle during destarched wheat bran treatment with Rovabio Brussel complemented by itself (A), Optizym (pectinases) (B), Ronozyme (proteases) (C) and Ctec2 (cellulases) (D). *Operating conditions are identical to Fig.4-2.*

4.3.3.3. Effect of enzymes complementation on solubilization

Taking into account the significant reduction of large particle population mainly in response to the addition of the pectinolytic solution (Optizym) to a 6h-treated suspension of dWB with Rovabio, one can expect a consequent release of sugar in the suspension supernatant. In accordance with this assumption, we show in **Figure 4-13** a net release of soluble matter in response to the addition of pectinases solution. This solubilisation rate was about 12 gdm/L after the 6 h of pectinolytic action and when added to the 28 gdm/L of dWB solubilized within the 6 h of treatment with Rovabio, this led to an overall 53% solubilisation of dWB by the combined action of Rovabio and Optizym (40 gdm/L). As expected, no significant evolution of solubilized matter was reported with the addition of Rovabio itself, Ronozyme or Ctec2.

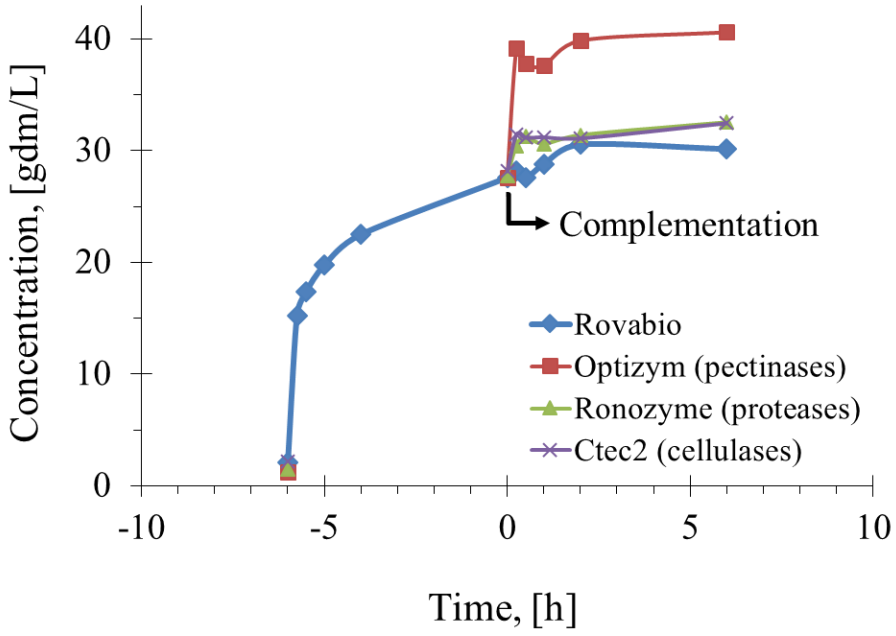

Figure 4-13. Total matter (gdm/L) solubilized during enzymatic treatment of destarched wheat bran by Rovabio Brussel (-6 to 0h) complemented by itself, Optizym (pectinases), Ronozyme (proteases) or Ctec2 (cellulases) from 0h to 6h. *Operating conditions are identical to Fig.4-2.*

Then, we quantified released sugars, after the acidic treatment of the supernatant sampled during the complementation of Rovabio by itself, Optizym (pectinases), Ronozyme (proteases) or Ctec2 (cellulases). Interestingly, we only identified glucose (**Figure 4-14**) with a concentration which raised from 5.35 gdm/L at 0h to 14 gdm/L after the 6 h of pectinolytic treatment, that closely matched (75%) within the amount of solubilized matter reported in **Figure 4-13**. All the other monosaccharide concentrations remained constant along all the enzymatic complementation.

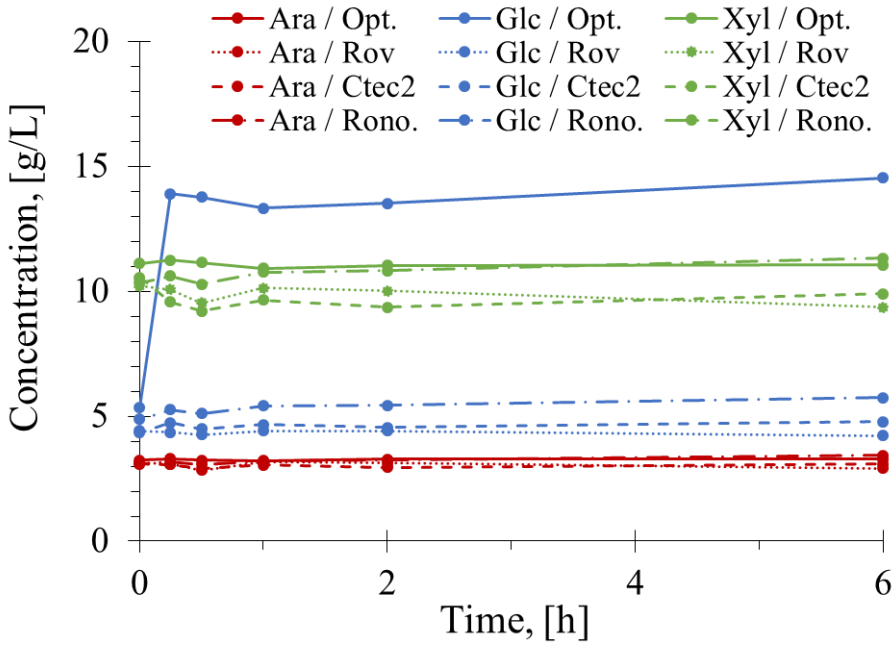

Figure 4-14. Kinetics of soluble sugars released during enzymatic treatment of the destarched wheat bran by Rovabio complemented by itself (Rov), Optizym (Opt.), Ronozyme (Rono) or Ctec2. *The soluble sugars were expressed as equivalent of monosaccharides glucose (Glc), xylose (Xyl), arabinose (Ara), mannose (Man) and galactose (Gal) after their chemical acid hydrolysis. The error bars are not reported and are inferior to 0.56 gdm/L (standard deviation of three independent samples). Operating conditions are identical to Fig.4-2.*

4.4. Discussion

A multi-scale approach encompassing direct and indirect physical and biochemical measurements was used in the present work to identify factors that restrict the action of Rovabio enzymatic cocktail to a partial 37%$_{DM}$ degradation of wheat bran NSPs. We first showed that this limitation could not be overcome by adding three times more Rovabio than the already large dose of 1100 $U_{xylanase\ visco}$/gdm. Only the initial rate of solubilization could increase with the dose of Rovabio but the deconstruction and solubilization of this feed material still remained at a maximum of 37% of the initial dry matter. We also showed that this limitation of the Rovabio action was due neither to some enzymes inactivation nor inhibition by end-products released during the process. Taken together, we concluded that the most probable reason that prevents Rovabio to completely solubilize the wheat bran NSPs, is the difficulty of these enzymes to access to their substrates, whatsoever the high variety and complementary of hydrolytic enzymes present in this cocktail. This hypothesis is actually supported by the finding that an insoluble fraction highly enriched in particles between 50 and 300 µm is accumulated along the wheat bran treatment with Rovabio as well as a smaller particles population <100 µm

in the last hour of treatment. These fractions are becoming refractory to further action of Rovabio even if a large excess of enzyme cocktail is added, suggesting that this limitation is mainly physical. The question was therefore to verify this hypothesis on the one hand, and to find ways to overcome this limitation on the other hand.

To verify that the physical accessibility to wheat bran particles is an important parameter in the action of Rovabio, we subjected the so-called recalcitrant fraction obtained after a 6 h treatment of dWB with excess of Rovabio to milling process which resulted in a reduction of particle size and hence in an almost 20 increase in the particle specific surface. Remarkably, addition of Rovabio to this milled fraction resulted in a further deconstruction of the wheat bran which was characterized by sharp viscosity reduction, a fragmentation process revealed by a decrease of the large particle population from 2 to 400 µm (DLS) as well as an increased number (about 10%) of fine particles of 1 - 40 µm size (FBRM) and by a 5.7% additional solubilisation of the initial dWB dry mass. Altogether, this experiment supports the hypothesis that a limiting factor of Rovabio action is the physical accessibility of its hydrolytic enzymes to their substrates. However, this experiment also showed that this substrate accessibility could be difficult to solve solely by physical means because, unless with an intense milling process which is energy-intensive and thus not competitive against the enzyme bio-process, there might be always a remaining, even very small particles that shall remain not solubilized.

If the accessibility to substrate is obviously physical, there might be biochemical ways to overcome this limitation which would not solely result in an increase of the specific surface through particles fragmentation but also to open somehow the particle structure. As a matter of fact, we found that pectinases solution seems to contribute to these two functions which is not the case for proteases and a cocktail enriched mainly of cellulolytic enzymes (Ctec2). Thus, only the pectinolytic enzyme cocktail was able to increase the solubilization rate together with a reduction of the particle size. Interestingly, within the action of the pectinases, glucose was found as the sole sugar released between the five main monosaccharides that comprise wheat bran: arabinose, galactose, glucose, xylose and mannose. However, it is very likely that galacturonic acids and rhamnose have been produced regarding pectin composition (Burton and Fincher, 2014) but our chromatography analytical method was not able to quantify these sugars. Nevertheless, the significant quantity of glucose released can be explained by the fact that pectin is considered as a cement of the hemicellulose network (Cosgrove, 2000) and thus removing pectin could leave the accessibility of cellulolytic enzymes to cellulose that is imprisoned into the insoluble particles. This finding supports the suggestion that the

accessibility of enzymes to their substrates can be solved by both an increase of the particle specific surface and by dedicated enzymes attack that rupture the molecular architecture of the particles, leaving better access to hydrolytic enzymes. As final remark, it is noteworthy that the pectinases solution was not really pure. Thus, to validate whether the complementation of Rovabio by pectinases would be worthy, pure pectinolytic enzymes shall be used in further experiments.

4.5. Conclusion

The factors that restrict the Rovabio enzyme cocktail to degrade wheat have been investigated in this work. The limitation of Rovabio action was attributed to the presence of a recalcitrant fraction and not to the loss of enzyme activities or inhibition of these enzymes by released products during the reaction. Increasing substrate specific surface by milling this recalcitrant fraction or complementing Rovabio with pectinases, allowed to enhance dWB deconstruction and solubilization rate. Therefore Rovabio limitation was attributed to a physical inaccessibility of the substrate which could be overcome either by a mechanical treatment (milling process) or by the addition of auxiliary enzymes (or other specific active proteins) allowing a better access to the substrate structure for the main hydrolytic enzymes such as endo-xylanases or endo-glucanases. With pectinases complementation, mainly glucose was solubilized which suggests that pectin degradation rendered accessible a new proportion of cellulose in the dWB matrix. As neither the physical nor biochemical treatment allow to reach a complete dWB solubilization, combining both could be interesting to show if this could increase even more this deconstruction.

CHAPTER 5:

GENERAL DISCUSSION, CONCLUSIONS AND PERSPECTIVES

CHAPTER 5. GENERAL DISCUSSION, CONCLUSIONS AND PERSPECTIVES

A wide variety of hydrolytic enzymes is naturally produced and secreted by microorganisms such as filamentous fungi to hydrolyse complex carbohydrates of plant biomass into simple sugars for their growth purposes. Since 80's, these enzyme cocktails are being exploited as feed additives in animal nutrition to improve digestion of non-starch polysaccharides (NSP) and thus enhance health, performances and reduce environmental impact of industrial animal production. In particular, Adisseo Company has developed a remarkable enzyme cocktail termed Rovabio that contains a wide range of hydrolytic enzymes secreted by the filamentous fungus *T. versatilis* under a specific fermentation condition (Guais et al., 2008). Several zootechnical data have reported a positive effect of these feed additives on animal performances (Abudabos et al., 2017; Lu et al., 2016, 2013; Tekeli et al., 2014; West et al., 2007). A major objective of the industrial application of these enzyme cocktails as feed additive is to know how they act on their substrates and how to improve their efficiencies at a lower enzyme cost possible, i.e. at the best ratio of each enzyme/substrate possible. The achievement of this objective rests on two main bodies: characterize the physical and biochemical composition and structure of the biomass substrate and characterize the enzymatic content and the functionality of this content with respect to its substrate. My thesis work was to provide part of the answer to the second component of the problem.

A literature review showed that most of the enzyme families present in Rovabio® and their mechanisms of action are known but synergy and cooperative activity between them on complex carbohydrates remain largely unexplored, likely because it cannot be done by a simple approach asking to assay action of each enzyme at a time and then their mix on the substrate. To circumvent this limitation, we applied a multiscale approach that combines *in-situ* and *ex-situ* physical measurements (namely change in viscosity, of morphogranulometry, etc.) with biochemical analysis to unravel the mechanism by which Rovabio® can deconstruct and solubilize complex carbohydrates. For the purpose of the thesis, as well as from the industrial partner's perspective and taking into account the easy way to manipulate the substrate, our strategy was adapted to the deconstruction of wheat bran. Moreover, the combination of physical and biochemical analysis is relatively new in animal nutrition as about 85% of the studies about enzymatic feed additive are made *in-vivo* and very few are *in-vitro* and limited to biochemical/ enzymatic studies.

A multiscale analysis was thus developed to characterize the enzymatic deconstruction of wheat bran. Rovabio® which contains a wide range of glycosyl hydrolases, shows that it has also a significant amylolytic activity which impacts viscosimetry. Since our objective is to study more specifically the action of this cocktail on NSP degradation, a pre-treatment protocol was successfully adapted to remove more than 70% of the starch that is present in wheat bran. Our new reference substrate, called destarched wheat bran (dWB), was then used to characterize Rovabio® enzymes activities through a multiscale analysis system. Destarched wheat bran suspension exhibited strong shear-thinning properties as a function of its concentration. A *Ccrit* value of 50 gdm/L, indicating the evolution to dilute Newtonian suspension to semi-dilute Non-Newtonian suspension, was identified. Then, according to this original approach, we were able to address and respond to the three following questions:

- ⇨ What are the mechanisms underlying the deconstruction of wheat bran by Rovabio®?
- ⇨ What are the limiting factors in Rovabio® in the deconstruction of wheat bran NSPs?
- ⇨ How can the efficiency of Rovabio® be improved to deconstruct wheat bran NSPs?

The deconstruction mechanism of wheat bran by Rovabio encompasses a fragmentation and solubilisation process

With the addition of Rovabio® Brussel into dWB suspension (75 gdm/L), its viscosity decreased proportionally to the enzyme-substrate ratio, within the first minutes of treatment (macroscopic scale). Large particles were initially fractioned (DLS) and this mechanism continued within the finest population (FBRM) resulting in smaller and smaller particles measured (microscopic scale). Along the enzymatic treatment, part of insoluble dWB was solubilized into 73.2% of sugars and 26.8% of proteins (molecular scale). This multiscale analysis highlights that Rovabio® action occurred thanks to the balance between fragmentation and solubilization phenomena with enzyme dose effect but kinetic slowdowns over time. Nevertheless, the combination of these two processes led to only 37% of loss of insoluble wheat bran matter into soluble matter.

Xylanase alone was capable of solubilisation activity, with a final release of xylose and arabinose that was equivalent to that obtained by Rovabio. At variance, the fragmentation activity was much weaker and likely resulted from an indirect consequence of the endo-xylanolytic activity which disorganized the fibrous network and hence led to particle disaggregation. Altogether, these results confirmed the importance of the enzyme mixture

which acts in a synergistic manner to readily solubilize wheat bran. They furthermore showed that sugar solubilisation was almost stopped after only 2 h whereas fragmentation of particles still continued to eventually lead to the production of recalcitrant insoluble fraction that was enriched of particles in the range of 50 to 300 µm. These finding suggested that either the lack of any further solubilisation was due to inactivation and/or inhibition of some key hydrolytic enzymes of the cocktail or that these enzymes are no longer accessible to their substrates, which are exemplified by these recalcitrant fraction whose physical and biochemical natures are questioned as well as how this fraction could be further deconstructed.

The accessibility of the wheat bran substrate is the main factor limiting the action of Rovabio®

Since enzyme inhibition or inactivation were excluded, the hypothesis of substrate accessibility was therefore the most likely relevant hypothesis which is further supported by the production of a recalcitrant fraction. To verify this hypothesis we firstly improved the substrate accessibility by increasing the specific surface of the dWB particles which was obtained by a milling process that resulted in the production of a homogenous population of finer particles. This mechanical treatment allowed a further wheat bran deconstruction that was traduced by a particle fragmentation as well as a higher solubilization rate (+ 5.7%). However, in practical term, it is excluded to apply a milling process to the recalcitrant fraction obtained after a treatment with excess of Rovabio. In addition, this process actually can take place naturally in the chicken gizzard which is the muscular stomach of poultry that has an important function in grinding feed material (Svihus, 2014). More broadly, this substrate accessibility could be difficult to solve solely by physical means because, unless with an intense milling process which is intensive-energy and therefore not cost-competitive, there might be always a remaining of small particles that will be solubilized only on their surfaces. Overall, these data support the notion that enhancing substrate accessibility requires a combination of an increase of the specific surface with a strong disorganization of the particle molecular architecture that can be obtained with specific enzymes or proteins.

Wheat bran deconstruction by Rovabio® can be enhanced by addition of auxiliary enzymes

As a physical mean is not compatible with an industrial use of Rovabio, we investigate whether such an increase of substrate accessibility could be obtained by a biochemical method, assuming that the Rovabio may be limited in enzymes that would provide this function. We

actually found that the addition of pectinases to a 6h-Rovabio treated dWB suspension caused a burst of both fragmentation of large particles which increase of their specific surfaces as well as a significant solubilization (+ 16%) of the resulting fine particles with a specific release of glucose as sugar moieties. The fact that glucose was released after pectinase action clearly revealed an increased accessibility of cellulases to the cellulose that is trapped in insoluble particles. All together, these results highlight the interest of using deconstructing enzymes which attack the biomass minority structures but are essential to enhance the substrate accessibility to enzymes that cleave lignocellulolytic backbone structures.

In conclusion, the present results might be of particular relevance for a better understanding of the actions of an industrial enzyme cocktail, Rovabio®. It provides deeper insights on dWB deconstruction by Rovabio® especially from an integrated approach (*in*- and *ex-situ* analysis of rheological behaviour and morphogranulometry), which is rarely considered in animal nutrition. Even if numerous enzyme activities are present in Rovabio®, the deconstruction of dWB was limited to 37%$_{w/w}$, even in excess of enzyme. Our experimental data highlighted that this limitation which appears to origin from a substrate inaccessibility, could be overcome by enhancing the substrate specific surface (mechanical treatment) and/or disorganizing its structure (enzymatic treatment). Both ways have improved performances (hydrolysis yield) but do not allow a complete hydrolysis of dWB. Finally, this work draws attention to deconstruction enzymes such as pectinases, proteases, ferulic acid esterases, LPMO (lytic polysaccharides monooxygenases), etc. as well as swollenins which are able to open the lignocellulose network in order to improve the enzyme access to their substrates.

Above all, this work demonstrates the pertinence to associate process engineering and biochemical approaches. Design of a dedicated and multi-instrumented experimental set-up coupled with a well-defined experimental strategy brought an overview of the actions of a complex enzyme mixture. In fact, the complementarity of rheometry, granulometry and biochemistry turns out to be an attractive approach to unravel the mechanisms associated with biomass deconstruction. Nevertheless some limitations in our multiscale analysis may be reported: (i) the technical limitations of our on-line viscosimeter namely the range of torque cover and the accuracy of the measurements, (ii) with a volume and a number distributions of the results, DLS and FBRM measurements are not directly comparable and (iii) none information is collected about the biochemical composition and the structure of the insoluble fraction of wheat bran along the enzymatic treatment.

Perspectives

Considering our results and our level of interpretation, numerous scientific questions are pending and merging and some suggestions for future works can be drawn.

IN THE SHORT-TERM:

- ✓ New technological developments, such as the conception of a new bioreactor, the implementation of our analytical methods or the use of alternative techniques, should allow to go further in the understanding of the biomass deconstruction through Rovabio actions. From physical standpoint, get access to the following data should be interesting:
    - Crystallinity with RMN (resonance magnetic measurements),
    - Porosity and specific surface with tomography,
    - Surface aspect and roughness with AFM (atomic force microscopy),
    - Evolution of each specific layers of the bran with fluorescent microscopy, etc.

  The investigation of mechanisms, structures and biochemistry between biopolymer up to submicron scales is essential to fill our gap of knowledge.

  From biochemical standpoint, measuring the composition of the recalcitrant fraction as well as qualifying and quantifying the oligosaccharides released in the supernatant along the enzymatic treatment could be interesting. In addition, measuring uronic acids appears also to be pertinent due to their non-negligible quantities: 10% of destarched wheat bran dry mass (Brillouet and Mercier, 1981).

- ✓ Genericity of this approach can be transpose to other matrixes used in animal nutrition (corn, soybean, barley, etc.). The limitation of Rovabio® upon other substrates can be also characterized in order to improve its efficiency. Beforehand, some considerations have to be taken into account: (i) the presence of starch which could influence physical measurement, (ii) the biochemical and physical characterization of a new substrate and the presence of enzyme inhibitors which could be released during its enzymatic treatment.

  As dWB remained not completely accessible to Rovabio, some key deconstructive/ destabilize activities such as swollenin and other auxiliary enzymes should be tested. Swollenins, which are proteins found in all filamentous fungal secretome (Eibinger et al., 2016), are able to cleave hydrogen bounding, disrupt, fragment, deagglomerate particles and render their surfaces roughness (Gourlay et al., 2015; Jäger et al., 2011; Santos et al.,

2017). Thus, the addition of a recombinant swollenin from Trichoderma harzianum increases by 147% xylanase activity on xylan hydrolysis (Santos et al., 2017), provides a synergy with xylanases with +300% of xylose released (Gourlay et al., 2013) and improves by two folds the efficiency of a fungus enzyme cocktail upon biomass treatment (Rocha et al., 2016). On the other hand the interest of ferulic acid esterases was demonstrated in the literature as they act in synergy with xylanases and arabinofuranosidases to attack arabinoxylan structures (Beaugrand et al., 2004; Lei et al., 2016). Therefore the complementation of Rovabio® with those activities could be interesting. In a similar way, deeper study about the relation between particle accessibility (specific surface) and their hydrolysis rate could provide information about the kinetic of dWB deconstruction during the enzymatic treatment. Establishment of an optimal equilibrium between enzymes loading and particle size could be relevant for feed formulation.

- ✓ With an application in animal nutrition, all collected data at laboratory scale leading to the conception of optimal enzyme cocktail have to be comforted and validated with *in-vivo* experimentations. In fact the presence of endogenous enzymes as well as specific reaction conditions in animal digestive tract could influence and modify the assessment established *in-vitro*.

IN THE LONG-TERM:

- ✓ Understanding precisely the mechanisms underlying a great deconstruction of lignocellulosic material and the role of each enzyme involved in this bioprocess could be relevant. Thanks to this investigation a model could be constructed and applied to any kind of matrix taking into account these mechanisms and the knowledge of biomass structure and composition. The ultimate goal of feed additive producers is to optimize their enzymatic cocktail efficiency, in one hand by modulating the enzymatic activity profile regarding to feed composition and in the other hand by intensifying bioprocess for fungi cultivation and secretome production.

CHAPTER 6:

COMPLEMENTARY MATERIALS AND METHODS

CHAPTER 6. COMPLEMENTARY MATERIALS AND METHODS

6.1. Set-up of the experimental and operating conditions

6.1.1. Experimental bioreactor set-up

The experimental setup includes a double jacket glass bioreactor (d = 130 mm, h = 244 mm, V = 2.0L) equipped with a home-designed impeller system associated with several *in-situ* sensors (temperature, pH, rotation speed, torque, FBRM). The mixing system consists in two classical impellers mounted on the same shaft. The first one is a three inclined blades (diameter: 73.5 mm, angle: 45 °, h = 38 mm) located at 75 mm height from the bottom to ensure mixing in the central region of reactor as well as suspension homogeneity. The second is a close bottom mixer including 2 large blades (diameter: 120 mm, h = 22 mm) to avoid substrate decantation. A Haake VT550 viscometer (Thermo Fisher Scientific ref: 002-7026, 0.5-800 RPM ±0.1%, 100-30000 µN.m ±0.5%FSD) was used to ensure mixing at specific rotation speed as well as in-situ torque measurements. The temperature was controlled by water circulation (combined cryostat Haake DC30-K20, -50/+200 °C±0.01, Thermo Fisher Scientific) through the water jacket of the bioreactor. The viscometer and the cryostat were controlled by original software from Haake (RheoWin Job Manager) that also ensured real-time data recording (temperature, torque, mixing rate). The pH of the suspension was controlled and auto-adjusted by a Biostat-B (Sartorius Stedim Biotech) via home-designed software created in the LabVIEW environment. Finally, a focused beam reflectance sensor (FBRM-G400-Mettler Toledo) was located inside the reactor in order to measure the distribution of particle chords. A global description of the whole system is illustrated in **Figure 6-1**.

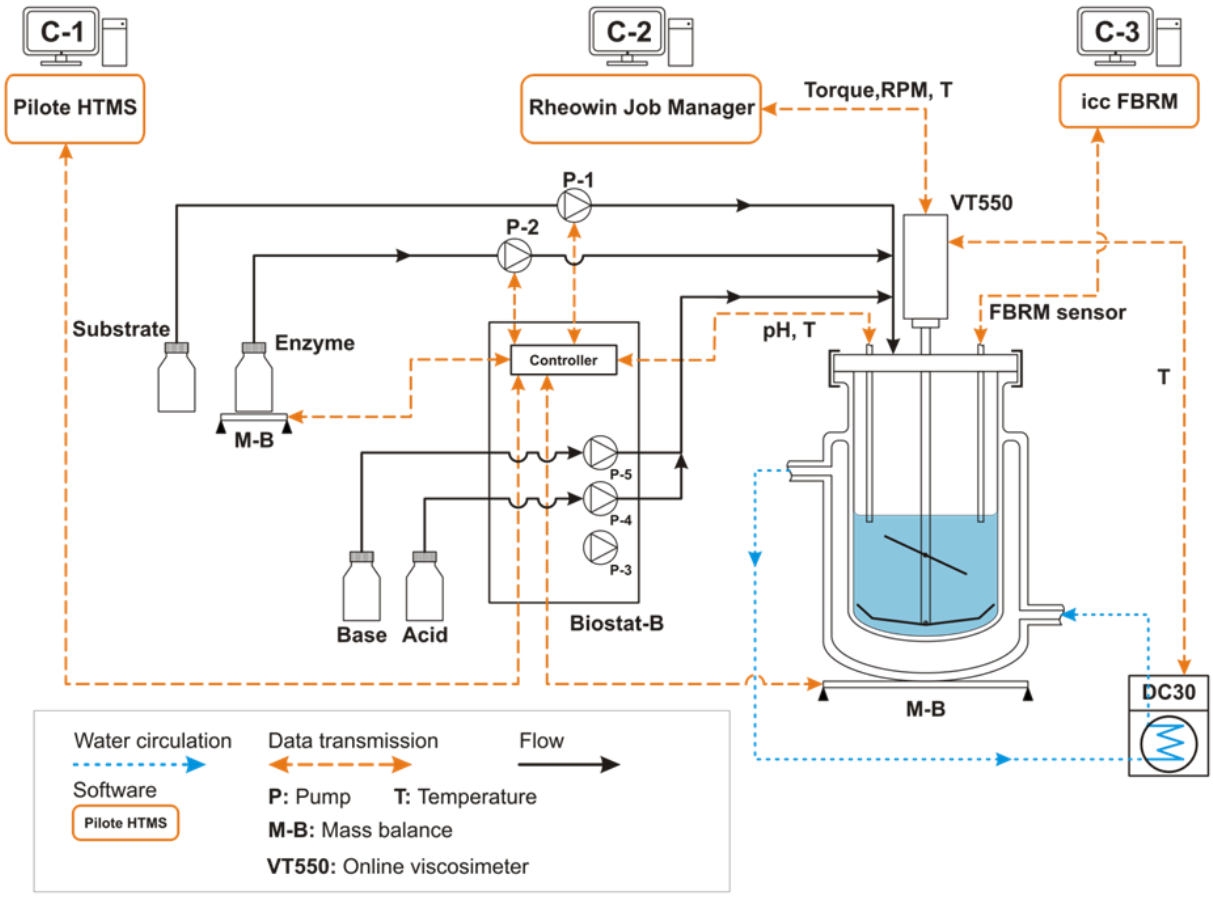

Figure 6-1. Process and instrumentation diagram of HTMS experimental bioreactor setup

6.1.2. Operating conditions

Operating conditions during enzymatic hydrolysis were conditions mimicking those encountered in poultry anterior digestive system, which corresponded to high dry matter suspended into 100 mM potassium phosphate buffer pH 4.0 and operating at 41 °C (Svihus, 2014). Potassium phosphate buffer is a solution H_3PO_4 (ref 131032.1211, Applichem Panreac) at 1.45 mM and dipotassium hydrogen phosphate, KH_2PO_4, at 100 mM (ref 26931.263, VWR chemicals). The pH of the suspension was lowered at 4 by addition of 4N sulfuric acid solution prepared from a concentrated sulfuric acid, H_2SO_4 stock solution (ref 131058.1211, Applichem Panreac).

During enzymatic hydrolysis a nominal mixing rate of 170 PRM was applied and every 15 minutes it was shifted from 170 to 200 RPM for 1 min, and then back to 150 RPM for 1 min. All mixing rate changes were made by linear acceleration or slowdown during 20 s. Data acquisition period was adjusted to 20 s at 170 RPM and reduced to 10 s at 150 and 200 RPM. During both steps, mean torque (see §6.4.2) was calculated after stabilization.

6.1.3. Sampling procedure

During hydrolysis experiments, samples (12 mL, 6 per experiment) were collected in 15 ml Falcon conical centrifuge tubes in an ice-cold bath to readily stop the enzymatic activity. A part of the samples was centrifuged (10 min at 4000 RPM) and stored at -18 °C for biochemical analyses (solubilization rate, protein dosage, monosaccharides dosage and acid hydrolysis plus released monosaccharides dosages) and the other half directly stored at 4 °C for physical analysis. To prevent any alteration of fiber properties, *ex-situ* physical analyses were considered in priority and performed within 24 h after sampling.

6.1.4. Characterization of the rheology of substrate suspension

Prior to enzymatic hydrolysis, rheological properties of lignocellulosic suspensions were characterized with suspensions at different concentrations ranging between 20 up to 90 gdm/L and using different impeller speeds (from 10 to 300 RPM) during 180 sec per step, at 41°C (see §2.4.1.1). Lowest concentration of tested suspension was suspended, 170 RPM, T = 41 °C to obtain homogeneous state. This was then followed by an ascending step of mixing rate (from 200 RPM to 300 RPM), followed by a descending step (from 300 to 10 RPM) and finally a second ascending step (from 10 to 200 RPM). For each mixing rate at given concentration, the duration of mixing was equal to 180 s. At the end of the experiment, the substrate was added to reach the chosen concentration and the protocol was repeated. Suspension viscosity for a given substrate concentration and at a specific mixing rate was deduced from the mean value of measured torque according to the method described in (§6.4.2). We established a relation between the suspension viscosity and the substrate concentration or the shear rate (equivalent to mixing rate by Metzner and Otto coefficient – Ks) as follows. For each substrate, the viscosity versus mixing rate (equivalent to shear rate) was modeled using a Power law equation and the viscosity versus concentration (for a given mixing rate) was modeled using Krieger-Dougherty or Simha relation.

6.2. Overview of enzymes and substrates

6.2.1. Enzymes

Several products, from single activity to enzyme mixture were selected and used in this study. Some were obtained from suppliers and other ones were produced by Adisseo SAS. The full listing of enzyme products is presented in **Table 6-1.**

Table 6-1. Overview of all the enzymatic products used is this study

Enzyme product	Source	Main enzymatic activity
Rovabio® *Brussel*	Adisseo SAS	NSPase [(a)]
Rovabio® *Excel*	Adisseo SAS	NSPase **(a)**
Rovabio® *Advance*	Adisseo SAS	NSPase **(b)**
Cellic® CTec2	Novozyme	NSPase **(c)**
Spirizyme®	Novozyme	Gluco-amylases
Ronozyme®	DSM	Proteases **(d)**
Optizyme®	Laffort SAS	Pectinases **(e)**
α-amylases	Sigma Aldrich	α-amylase
Amyloglucosidase	Sigma Aldrich	Amyloglucosidase
XynC	Adisseo SAS	Endo-xylanase

(a) (Guais et al., 2008)
(b) http://feedsolutions.adisseo.com/en/rovabio-advance-the-only-feedase/
(c) https://www.sigmaaldrich.com/catalog/product/sigma/sae0020?lang=fr&region=FR; (Rodrigues et al., 2015)
(d) https://www.dsm.com/markets/anh/en_US/products/products-feedenzymes/products-feed-proteaseronozymeproact.html
(e) https://www.laffort.com/en/products/enzymes/120

6.2.2. Substrates

Several substrates were used for this work and **Table 6-2** give their full list.

Table 6-2. Overview of all the substrates used is this study

Substrate	Source
Wheat meal	Moulin des moines, Châtenois, France
Wheat bran N°1	Limagrain
Wheat bran N°2	La Minoterie de la Save

Wheat bran was obtained from "La Minoterie de la Save" (Grenade sur Garonne, France) and destarched by lixiviation (Raynal-Ioualalen, 1996). One batch (~3.5 kg) of WB was suspended in water at 10 $\%_{vol/vol}$. Four consecutive washes were applied in a stirred tank (V=40 L) at 350 RPM and 40 °C during 15 min for the first one and 10 min for the following ones. Between each step, suspension is clarified by decantation and the supernatant containing solubilized starch (called "starch milk") is removed. Then fresh water was added to maintain a constant solid/liquid ratio. WB was finally rinsed by percolation (bag filter with a cut-off of 50 µm), dried with incoming compressed air and stored at -18 °C. The amount of NSPs in this material estimated after acid hydrolysis (see below) was estimated to 71% of the dry mass.

6.3. Chemical and biochemical analysis

6.3.1. Water and dry matter content

The water content of raw material used as substrate was determined by drying at high temperature and atmospheric pressure. The mass difference before and after drying represents the water content in the sample. Empty metal cup was dried 15 min in an oven at 105 °C and its mass was then quantified with a precision balance (Sartor IUs ED224S, 0.005-230 g ± 0.1mg). This mass was identified m_{cup}. A quantity of sample (m_s) was placed in this cup, dried in the oven at 105 °C during 3 h and mass was then measured with the precision balance. This final weight was identified m_{fin}. Water content (W) and dry matter (DM) were calculated following **Eq. 6-1** and **Eq. 6-2** (accuracy ± 0.5 %):

$$W(\%) = \frac{m_s + m_{cup} - m_{fin}}{m_s} x100 \qquad \textit{Eq. 6-1}$$

$$DM(\%) = 100 - W \qquad \textit{Eq. 6-2}$$

For determining water content of sample during enzymatic hydrolysis, a quantity of sample (m_s) was filtered through a Whatman No1 filter paper of known weight (m_{fp}) and then washed by ≈5 mL of distilled water. The filter paper containing the sample was dried in an oven set at 60 °C and 200 mbar (Heraeus, Thermo Scientific, 0-760 mmHg, 50-150°<kC) with silica gel during 4 days. The weight of samples was then measured with a precision balance (Sartorius ED224S, 0.005-230 g ± 0.1mg). The final weight was identified m_{fin}. Water content (W) and dry matter (DM) were calculated as previously but with m_{fp} instead of m_{cup}.

6.3.2. Determination of the solubilization rate

The solubilization rate corresponds to the soluble matter that is released in the supernatant during the treatment of the destarched wheat bran suspension with Rovabio or with purified xylanase solution. It was determined by drying 2 mL of supernatant on dry Fontainebleau sand (Ref 310-127-6) until the measured mass became stable using an infrared Moisture Analyzer (MA 100H Moisture analyzer, Sartorius, 30 - 180 °C) that featured an analytical weighing system with 0.1 mg resolution. These values (in g/L) were used to evaluate the residual dry matter concentration (Cm) remaining at different time during the enzymatic treatment of the insoluble wheat bran hydrolysis.

6.3.3. Sugar acid hydrolysis and released monosaccharides measurement

- **Acid hydrolysis**

Sulfuric acid hydrolysis of soluble sugars released in the supernatant were carried out according to protocol described in (François, 2007) in which the first step was skipped because the sugars were already soluble. Sample was centrifuged (4000 RPM 10 min) and 500 µL of the supernatant was mixed with 4N H_2SO_4 (ref 131032.1211, AppliChem Panreac) in a glass tube. Glass tube was shaken and transferred into a sand bath set at 100 °C for exactly 4 h. It was removed from the sand bath, 2.5 mL MilliQ water was added and the solution was transferred to a 50 mL falcon tube. The glass tube was then rinsed with an addition 2.5 mL MilliQ water and the two washings were pooled. The acid solution was neutralized by dropwise addition of a saturated barium hydroxide octahydrate, $Ba(OH)_2 \cdot 8H_2O$, solution at 40 g/L (ref 217573, Sigma Aldrich) until pH reached neutrality. The sulfate ions precipitated as a white $BaSO_4$ powder and white precipitate was settle down overnight at 4°C. The next day pH was checked and had to be between 6.0 and 8.0. The final volume was adjusted to 20 mL with MilliQ water and the falcon tube was then centrifuged at 4.800 g for 15 min at 4 °C. The supernatant was diluted with MilliQ water and filtered through 0.20 µm filters (Minisart RC 4, Sartorius) into glass vials (certified screw thread vials 9 mm and certified polypropylene bonded caps with septa 9 mm, Supelco) for HPAEC measurement.

- **Released monosaccharides measurement**

High-performance anion exchange chromatography (HPAEC) was carried on an ICS-3000 system (Dionex, USA) composed of:

- An autosampler (AS autosampler, Dionex).
- A pump (SP, Dionex).
- A anion trap column (IonPac™ ATC-HC, 9 mm x 75 mm, Dionex).
- A pre-column (CarboPac™ SA10 guard, 4 mm x 5 mm, Dionex).
- A column (CarboPac™ SA10, 4 mm x 250 mm, Dionex).
- A gold working electrode and pH-Ag/AgCl reference electrode (Dionex).
- An amperometric detector (ED 40, Dionex).
- A software system for data acquisition and processing (Chromatography Management System version 6.80).

Monosaccharides (arabinose, galactose, glucose, mannose, and xylose) were separated on an anion-exchange column (CarboPac SA10) using 1 mM NaOH (isocratic elution) as a mobile phase, at a flow rate of 1.5 mL/min for 10 min at 45 °C. At high pH, monosaccharides are

partially ionized, and can thus be separated by anionic exchange mechanisms. After each run, the column was regenerated with 60 mM NaOH during 10 min in order to remove compounds that may potentially contaminate the column (e.g. carbonates, peptides and amino acids). After each regeneration, the column must be equilibrated with the working concentration of the eluent (1 mM NaOH) during 25 min before the next sample injection.

The detection of each monosaccharide was performed using pulsed amperometric detection at 35 °C: the analyte was adsorbed onto the surface of a gold working electrode with a potential of 0.10 V, and later detected by an oxidation desorption process. Following the detection, an oxidative cleaning of the electrode surface was carried out by applying another potential. In this study, the potential applied for the integration was 0.10 V, and the integration time was set between 0.2 - 0.4 s.

The eluent was prepared by the dilution of a concentrated NaOH stock solution of analytical grade 46/ 51 % (w/w) (Fisher Scientific, UK) in MilliQ water (18.2 mΩ-cm resistance). A mix of arabinose, galactose, glucose, xylose and mannose used as standard solution was prepared from the stock solution with ultrapure water. Calibration standard with concentrations of 0.1, 0.5, 0.75, 1, 1.5 and 2 mg/L of each monosaccharides were prepared by diluting the stock solution at 100 mg/L in MilliQ water. In order to ensure the system stability, the calibration is made every 10 samples by analyzing 3 different standard concentrations. Then, to determine the concentration of these 10 samples, the standard curve was established on the 3 standards injected before and after these 10 unknown samples.

The measured monosaccharides, released from acid hydrolysis, were converted to the equivalent polysaccharide values using the conversion factor of 0.88 for pentose (arabinose and xylose) and 0.90 for hexose (mannose, galactose and glucose) (Templeton and Ehrman, 1995). A correction factor of 10% due to the loss of monosaccharides during the process (estimate from previous experiences, see §2.4.3.1, was applied to the final calculation (Templeton and Ehrman, 1995; Wijaya et al., 2014; Zhou and Runge, 2014).

6.3.4. Soluble monosaccharides dosage

Soluble monosaccharides (arabinose, galactose, glucose, xylose) that were directly released in the supernatant during the enzymatic treatment of the insoluble polysaccharide were determined by High performance anion exchange chromatography (HPAEC) as described above (without carbonate suppressor), but using a PA1 analytical column (CarboPac^{TM} PA1, 4 mm x 250 mm, Dionex) with a PA1 guard column (CarboPac^{TM} PA1 guard, 4 mm x 5 mm, Dionex) and an isocratic elution of 18 mM NaOH at 25 °C with a flow rate of 1 mL/min for 20

min. After each run, the column was regenerated with 200 mM NaOH and 300 mM NaOH during 17 min and equilibrated with the working concentration of the eluent (18 mM NaOH) during 20 min. Calibration standards with concentrations of 3.125, 6.25, 12.5, 25 and 50 mg/L were prepared by diluting stock solutions at 1000 mg/L of each monosaccharide in MilliQ water.

6.3.5. Starch dosage

Total starch content was determined with "total starch HK" assay kit from Megazyme© (Megazyme International Ireland, Wicklow, Ireland). This method has been adopted by AOAC (Official Method 996.11) and AACC (Method 76.13.01). Briefly and taking into account the complexity of the wheat bran matrix, the following procedure was applied.

1. As sample could contain D-glucose and maltodextrins it was washed with aqueous ethanol (80%$_{v/v}$) prior to analyse. Resistant starch was extracted by stirring the sample with 2M KOH at approximatively 4 °C, followed by neutralization with sodium acetate buffer.

2. Then a thermostable α-amylase hydrolyzed starch into soluble branched and unbranched maltodextrins (pH 5.0, 100 °C), followed by the action of an amyloglucosidase which releases glucose from maltodextrins.

$$\text{Starch} \xrightarrow{\alpha-\text{amylase}} \text{maltodextrins}$$

$$\text{Maltodextrins} \xrightarrow{Amyloglucosidases} \text{glucose}$$

3. Glucose was determined enzymatically by coupling with hexokinase which forms glucose-6-phosphate (G6P) in the presence of ATP and the later sugar is dehydrogenated into 6-phosphogluconate by a glucose-6-phosphate dehydrogenase in the presence of NADP. The measured NADPH at 340 nm is stoichiometric to the amount of glucose consumed.

$$\text{Glucose} + \text{ATP} \xrightarrow{Hexokinase} \text{G6P} + \text{ADP}$$

$$\text{G6P} + \text{NAPD}^{+} \xrightarrow{G6P-DH} \text{gluconate} - 6 - \text{phosphate} + \text{NADPH} + \text{H}^{+}$$

6.3.6. Glucose (ISY)

Glucose concentration in the supernatant was analyzed using a YSI model 2700 analyzer (Yellow Springs Instruments, Yellow Springs, Ohio, USA). The measurement is based on the detection of hydrogen peroxide (H_2O_2) released during the conversion of glucose into gluconic acid by means of an immobilized glucose oxidase:

$$\text{Glucose} + 2\ H_2O + O_2 \rightarrow \text{gluconic acid} + 2\ H_2O_2$$

The hydrogen peroxide is then oxidized at a platinum electrode to yield $2H^{+}+O_2+2e$ (electrons). The electron flow generated will give rise to an electrical current proportional to the glucose concentration in the sample. Assays were performed on suspension supernatants. The wheat bran suspension was centrifuged (4000 RPM for 10 min) to pellet the insoluble particles. For reliable measurements, supernatants should be diluted into the linear range of the instrument (0 – 2.5 g/L). The analyzer was calibrated using a single point calibration standard (2.50 g/L glucose) (YSI 2776 Standard, Yellow Springs, Ohio, USA). The apparatus provides a direct reading of the glucose concentration, expressed in g/L. The accuracy of the measurement is approximatly ± 2 %.

6.3.7. Protein assay by Bicinchoninic acid (BCA) method

Protein concentration was determined by the BCA (BiCinchoninic acid Assay) assay kit (Pierce Thermo Scientific, Illinois, USA) (Smith et al., 1985) using bovine serum albumin as standard. This method combines the well-known reduction of Cu^{2+} to Cu^{+} by proteins in an alkaline medium (the biuret reaction) with the highly sensitive and selective colorimetric detection of the cuprous cation (Cu^{+}) using bicinchoninic acid. The purple-colored reaction product of this assay is formed by the chelation of two molecules of BCA with one cuprous ion. This water-soluble complex exhibits a strong absorbance at 562 nm and can cover a large range of concentration from 20 to 2000 µg/mL.

The BCA Reagent was prepared as recommended by the supplier (Intron Biotechnology). The Bovine Serum Albumin (BSA) standard curve from 20 to 2000 µg/mL was prepared from the stock solution (2 $mg.ml^{-1}$ in water). 25 µL of each standard or unknown sample and 200 µl of BCA reagent were dropped on microplate. The reaction mixture was mixed gently and incubate in the dark during 30 min at 37 °C. Absorbance was read at 562 nm on a microplate reader (Epoch 2, BioTek instruments Inc., Winooski, VT, USA).

6.4. Physical analysis

6.4.1. Density of the substrates

The density of substrates was determined by gravimetry-volume method (proportion of substrate volume and added water volume in a volumetric flask). This density corresponds to the suspended matrix, including its initial water content (if applicable).

Firstly, the empty and dry flask (Flask Duran, type A, 100 ± 0.1 mL, 20 °C) was weighted (Sartor IUs ED822CW, 0.5 – 820 g ± 0.01 g). A quantity of substrate (3 different quantities ranging from 2 to 20 g) was added in each flask. Secondly, distilled water was injected slowly

in the flask. Before the flask volume was reached, it was gently manually shacked to avoid air bubbles and ensure the water distribution in substrate. All measurements were realized at ambient temperature (20 °C ± 2). The substrate density (± 5 %) was calculated with **Eq. 6-3:**

$$\rho_s = \frac{m_s}{V_s} = \frac{m_1 - m_0}{V_{tot} - V_w} \qquad \textit{Eq. 6-3}$$

$$V_w = \frac{m_2 - m_1}{\rho_w^{20}}$$

with ρ_s and ρ_w^{20} : apparent density and water density at 20 °C, respectively (g/mL).

m_s, m_0, m_1, m_2: substrate, empty flask, flask before and after water added mass respectively (g).

V_s, V_{tot}, V_w: volume of substrate, flask and water added respectively (mL).

The linear regression of m_s versus V_s enables to quantify the value of ρ_s.

It is necessary to calculate the intrinsic density ρ_{DM} considering the dry matter as reference. We define then:

- Dry matter content $DM = {m_{DM}}/{m_s}$ *Eq. 6-4*
- Water content $W = {m_w}/{m_s}$ *Eq. 6-5*
- Apparent density $\rho_s = {m_s}/{V_s}$ *Eq. 6-6*
- Intrinsic density $\rho_{DM} = {m_{DM}}/{V_{DM}}$ *Eq. 6-7*

where m_s; m_w and m_{DM} are masse of humid substrate, water and dry matter content, respectively ($m_s = m_w + m_{DM}$) and the substrate volume is defined as :

$$V_s = V_w + V_{DM}$$

Finally, after calculation we can establish:

$$\rho_{DM} = DM \cdot \left(\frac{1}{\rho_s} + \frac{W}{\rho_w}\right)^{-1} \qquad \textit{Eq. 6-8}$$

6.4.2. In-situ viscosity measurement

In-situ viscosimetry measurement was based on the real-time monitoring of torque and the establishment of the power consumption curve. This curve corresponds to the relationship between the power number (N_p) and the Reynold number (Re) and is established using fluids model (see below). It allows the determination of Re from Np values and then suspension viscosity can be calculate. In addition, mixing rate was periodically increased and decreased,

during enzymatic hydrolysis, to have access to the flow behavior index (*n*) and the consistency index (*k*).

- **Establishment of power consumption curve**

Power number (N_p), calculated from torque values, and Reynold number (Re) were defined as:

$$N_p = \frac{P}{\rho \cdot N^3 \cdot d^5} \qquad \textit{Eq. 6-9}$$

with $P(W) = 2 \cdot \pi \cdot \omega \cdot M$

$$Re = \frac{\rho \cdot N \cdot d^2}{\mu} \qquad \textit{Eq. 6-10}$$

Where d is the mixer diameter of the mixing systems (m), N is the mixing rate (turn/s), ρ is the volumetric mass of the dissolved material (kg/m^3) and M is the measured torque (N/m).

In laminar regime, the relationship between Re and Np is linear and can be illustrated by:

$$\boldsymbol{N_p = K_p \cdot \frac{1}{Re}} \qquad \textit{Eq. 6-11}$$

Where Kp is a constant that depends only on impeller shape and geometry for any Newtonian fluid. In pure turbulent regime and for Newtonian fluids, the dimensionless power number Np is assumed to be independent of mixing Reynolds number and equal to a constant, (N_{p0}). From experimental data, a semi-empirical model or Churchill model (**Eq. 6-12)** including laminar and transition regions were considered for the reference curve with a one-to-one relationship between Np and Re (Churchill, 1977).

$$N_p = \left[\left(\frac{K_p}{Re}\right)^{\alpha} + {N_{p0}}^{\alpha}\right]^{\frac{1}{\alpha}} \qquad \textit{Eq. 6-12}$$

This model includes Kp and α which are two constants that only depend on the mixing system geometry and Np_0 which is the mixing power number for turbulent flows. Several Newtonian fluids (with a well-known viscosity) were used to experimentally determine these constants by establishing the power consumption curve: distilled water, glycerol and Marcol 52 oil (Le, 2017). Power consumption curve is presented in **Figure 6-2.** Experimental results on our system gave Np_0 = 0.17, α = 0.75 and Kp = 115.2. From the power consumption curve, reference values, $Re_{crit\text{-}1}$ and $Re_{crit\text{-}3}$ were identified as leading to a 15% deviation of Np (**Eq. 6-**

12) from laminar (Np = Kp/Re) and turbulent (Np = Np_0) models, respectively. In addition, Re_{crit-2} = 642 was identified by the intersection of laminar and turbulent models.

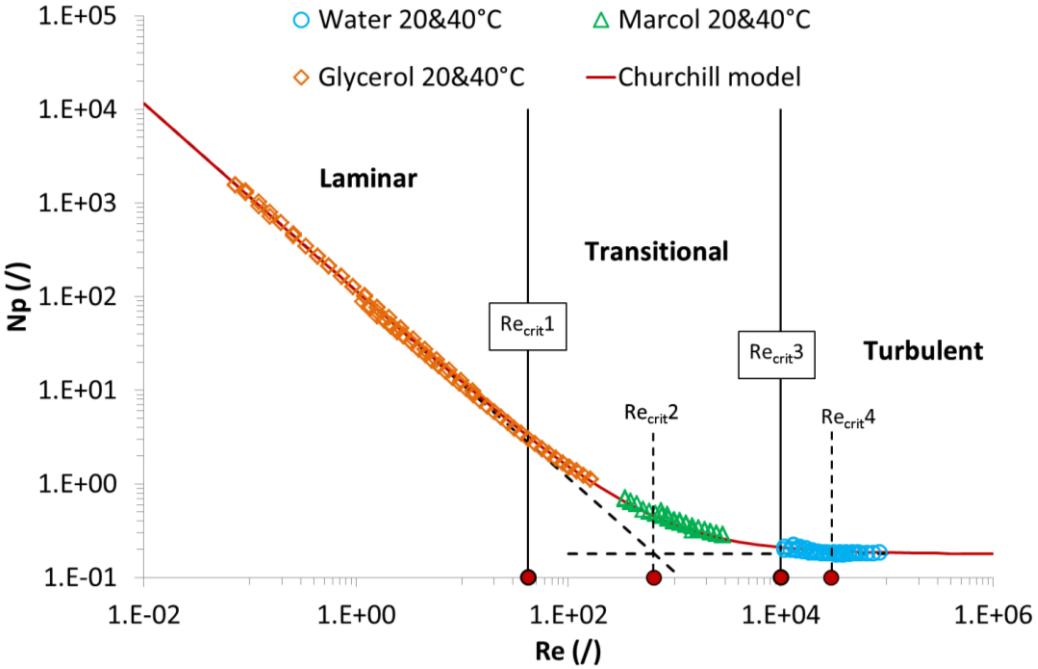

Figure 6-2. Power consumption curve, Np-Re of experimental set-up (Le, 2017)

In the non-Newtonian case, a generalized mixing Reynolds number has to be defined as the viscosity is not a constant. The well-known Metzner and Otto concept (Metzner and Otto, 1957) was used: an equivalent viscosity μ_{eq} is defined as the Newtonian viscosity leading to the same power number. Metzner and Otto (1957) showed that the equivalent shear rate $\dot{\gamma}_{eq}$ associated to this viscosity (through the rheological behavior of the fluid) is proportional to the rotation frequency, which introduced the Metzner-Otto parameter Ks:

$$\dot{\gamma}_{eq} = K_s \cdot N \qquad \textit{Eq. 6-13}$$

For the shear-thinning fluids described by a power-law, $\mu = k.\dot{\gamma}^{n-1}$ this leads to the generalized Reynolds number:

$$\mathrm{Re}_g = \frac{\rho \cdot N^{2-n} \cdot d^2}{k \cdot K_s^{n-1}} \qquad \textit{Eq. 6-14}$$

Ks is a constant depending only on the geometry of both the reactor and the impeller. The concept can be extended to the transition region using a power equation (Jahangiri et al., 2001). Xanthan solutions (0.04; 0.1; 0.4 $\%_{vol/vol}$) in glucose solution (650 g/L) and in sucrose solution (943 g/L) were used to determine the proportionality constant Ks. The corresponding

value of the shear rate, $\dot{\gamma}_{eq}$, was extracted from the rheogram of the Xanthan solutions. Rieger and Novak's approach (Yang et al., 2010) was used to determine the value of Ks:

Eq. *6-15* with the generalized Reynolds number Re^* is written in a similar form:

$$N_p \cdot Re^* = K_P(n) \qquad \textit{Eq. 6-15}$$

With $Re^* = \frac{\rho \cdot N^{2-n} \cdot d^2}{k}$ and $K_P(n) = K_P \cdot K_S^{n-1}$.

The value of Ks is directly deduced from the linear regression $Ln[K_p(n)] = f(n-1)$ using the previously determined Kp value. This leads to Ks ≈ 38.5 (Le, 2017).

- **Use of power consumption curve and extended Metzner and Otto concept.**

The *in-situ* viscometry was conducted throughout hydrolysis in order to estimate the suspension viscosity and establish a rheogram. During experiments, the torque measurement used in conjunction with the power consumption curve, allowed the determination of a Reynolds number, and then of the viscosity. This procedure is valid as long as the power consumption curve allows a one-to-one correspondence between Np and Re which is true in the laminar and transition regimes. However, the precision of the viscosity determination decreases when Reynolds number increases as Np is decreasing until it reaches a roughly constant value in the turbulent regime. For this reason, the calculation of viscosity, using

Eq. 6-16, was limited to Re < Re_{crit-4} = 30000 (beyond this value, Np was almost constant) even if between Re_{crit-4} and Re_{crit-3}, it was poorly reliable (± 200%). Detailed methodology was previously described (Nguyen et al., 2013) and all critical Re were illustrated in **Figure 6-2**.

$$\mu = \frac{\rho \cdot N \cdot d^2}{Re} \qquad \textit{Eq. 6-16}$$

- **Identification of power law index**

Shear-thinning (or pseudo-plastic) is a term used in rheology to describe non-Newtonian fluids which have a decreasing viscosity when subjected to increasing shear rates. For shear-thinning fluids, the relationship between shear stress and shear rate can be modeled by Ostwald-de Waele (or Power-law) formula:

$$\tau = k \cdot \dot{\gamma}^n \qquad \textit{Eq. 6-17}$$

Where k is flow consistency index (Pa.s^n), $\dot{\gamma}$ is the shear rate (s^{-1}) and n is the flow behavior index (dimensionless). By definition, apparent viscosity μ of a fluid can be described by:

$$\mu = \frac{\tau}{\dot{\gamma}} \qquad \textit{Eq. 6-18}$$

By replacing τ with the Ostwald formula, we obtain then $\mu = k \cdot \dot{\gamma}^{n-1}$

Following Metzner and Otto (1957), in laminar flow, the relation between equivalent shear stress and rotation speed can be represented by $\dot{\gamma} = Ks \cdot N$ where Ks is a coefficient depending only on the system geometry (for our reactor, Ks = 38.9). The concept can be extended to transitional flow (Jahangiri et al., 2001). In our case, this interpretation was limited to $Re < Re_{crit\text{-}2}$. The viscosity from **Eq. 6-18** can be written as:

$$\mu = k \cdot (K_s \cdot N)^{n-1} \qquad \textit{Eq. 6-19}$$

The flow behavior index (*n*) and the consistency index (*k*) were investigated every 15 minutes by adjusting mixing rates (mean shear rates) from 170 to 200 RPM and back to 150 RPM. It was thus possible to deduce from the relationship between viscosity and mixing rate, **Eq. 6-19**, the flow behavior index (*n*) and the consistency index (*k*).

6.4.3. Particle size and morphology analysis

In a first stage, basic concepts related to the definition and characterization of size distribution functions are introduced. In a second stage, different techniques dedicated to particle size analyses are described.

- **Theory associated with distribution functions**

Because of the non-uniform size of particles, the variation of population size is presented as a size distribution. These distribution profiles can be compared via distribution functions, E(x) and cumulative distributions functions, F(x) (**Eq. 6-20**). They can be represented as discrete or continuous functions (p_i is the probability corresponding to class i).

	Distribution	Cumulative distribution
Continuous function	$E(x) \cdot dx = \frac{dn}{n}$	$F(x) = \int_0^{\infty} E(x) \cdot dx = 1$
Discrete function	$p_i = \frac{dn}{n}$	$F = \sum_0^{n_c} p_i = 1$

Eq. 6-20

Each distribution function (E(x) can be characterized by a range of moments and centered moments of order j (**Eq. 6-21**) (Himmel et al., 2007; Mosier et al., 2005).

$$\Gamma^i = \int_0^\infty x^i \cdot E(x) \cdot dx \quad and \ \Gamma^{i'} = \int_0^\infty (x - \bar{x})^i \cdot E(x) \cdot dx \quad Eq.\ 6\text{-}21$$

There are various ways to define an "equivalent" diameter for a non-spherical particle that will be reduced to the diameter if the particle is a spherical one. The sphere is chosen as reference because of its unambiguous definition of the diameter. The most useful diameter is the sphere equivalent diameter, d_{se}, which corresponds to the diameter of the sphere having the same volume as the particle being examined.

Most existing techniques give the characterization of distributions based on the number, length, surface or volume of the particles. Depending on the definition of the classes of particle, four types of distributions are defined (**Table 6-3)**.

Table 6-3. Definitions of distributions in number, dimension, surface and volume.

Distribution	Signification	Formula
Distribution in number	Percentage in number associated with each class	$p_{n_i} = \frac{n_i}{\sum n_i}$
Distribution in dimension	Percentage in dimension associated with each class	$p_{d_i} = \frac{n_i \cdot d_i}{\sum n_i \cdot d_i}$
Distribution in surface	Percentage in surface associated with each class	$p_{s_i} = \frac{n_i \cdot d_i^2}{\sum n_i \cdot d_i^2}$
Distribution in volume	Percentage in volume associated with each class	$p_{v_i} = \frac{n_i \cdot d_i^3}{\sum n_i \cdot d_i^3}$

Considering the complexity of particle shape and morphology, it is convenient to consider a mean diameter (and its associated standard deviation describing the width of the distribution around the mean value) for a given particle population (Nguyen, 2014). For instance, the average diameter can be defined by:

$$d_{p,q} = \left[\frac{\sum n_i \cdot d_i^p}{\sum n_i \cdot d_i^q} \right]^{1/p-q} \qquad Eq.\ 6\text{-}22$$

With n_i: the number of particles of diameter d_i , and p, q are the integers ($p = q+1$ with $q = 0, 1, 2, 3$ for number-, length-, surface- and volume-weighted, respectively) (Le, 2017). Based on these notations: $d_{1,0}$ is the number-average diameter, $d_{2,0}$ is the quadratic mean diameter, $d_{3,0}$ is the cube average diameter, $d_{4,3}$ is the mass or volume mean diameter, and $d_{3,2}$ is the area-average diameter or Sauter diameter .

- **Ex-situ diffraction light scattering (DLS)**

The volume-weighted particle size distribution (PSD) was determined by diffraction light scattering (DLS, Mastersizer 2000, Malvern Inst., range from 0.02 to 2000 µm, red λ = 632.8 nm and blue λ = 470.0 nm light). The working principle is based on the time-resolved measurement of the scattered light intensity generated by the passage of a dispersed particle sample through a laser beam, as illustrated in **Figure 6-3**. The light scattering angle is directly related to the size of the particles. Large particles scatter light at small angles, whereas small particles scatter light at wider angles. The scattering data is then analyzed to determine the size of the particles responsible for creating the scattering pattern, by the application of the Mie theory. Mie theory predicts scattering intensity as a function of the angle at which light is scattered at the point of interaction with a spherical particle. The particle size is then reported as a volume equivalent sphere diameter.

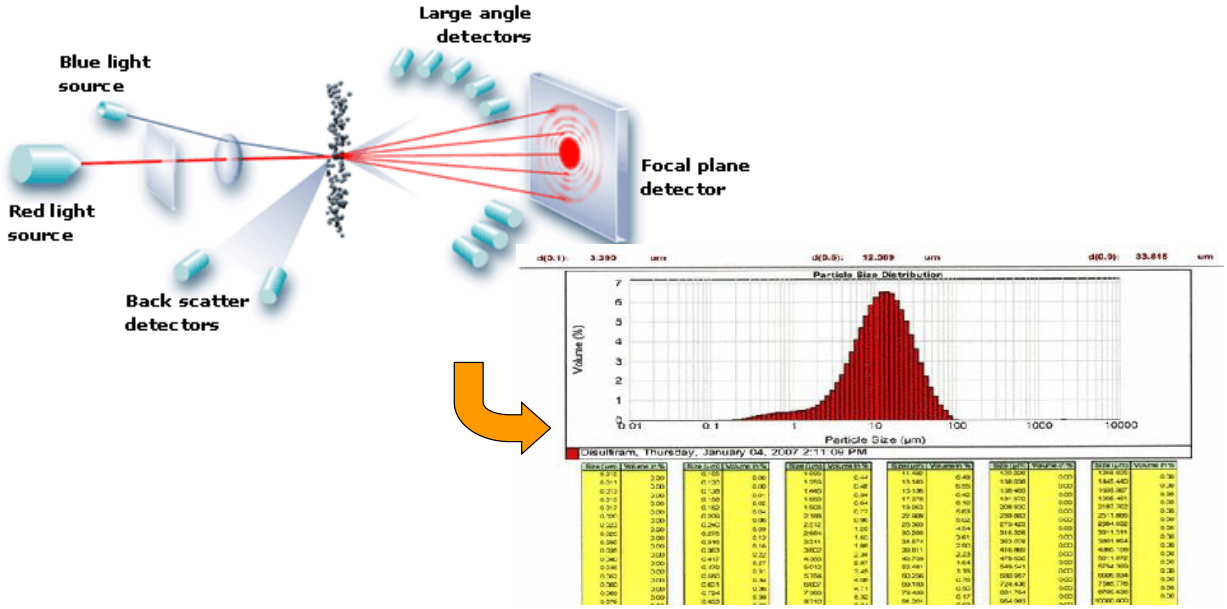

Figure 6-3. Operational principle of laser granulometer – Example of presentation of the data

A known volume of suspension (1 to 3 mL) was added to a water circulation loop in order to obtain laser obscuration between 5% and 40%. Whole suspension was mixed by a Heidolph magnetic stirrer at 200 RPM while the circulation loop was maintained by a Masterflex L/S model 7553-79 at pump speed 240 RPM. Analyses are conducted at room temperature (20 °C). The measurements of each sample were performed at three different dilution rates and in triplicate and the average data was taken. Particle size distribution $E_v(d_{se})$ during enzymatic hydrolysis was weighted by the suspension dry matter content in order to evaluate the impact of solubilization on suspended population.

- **In-situ focus beam reflectance measurement (FBRM)**

Focus beam reflectance measurements (FBRM) enables *in-situ* quantification and characterization of particles through the estimation of the chord length, (lc) and distribution of the chord length population, (CLD). *In-situ* CLD of particles was analyzed using an FBRM® G400 probe (Mettler Toledo, range: 0.1 to 1000 µm, laser light source λ = 795 nm, laser source rotation: 2 m/s). The principle of this method is illustrated in **Figure 6-4.** The solid-state laser light source provides a continuous beam of monochromatic light. An intricate set of lenses focuses the laser light to a small spot. This focal spot is carefully calibrated to be positioned at the interface between the probe window and the fluid. An electric motor is used to precisely rotate the optics at a constant speed (2 m/s). The focused beam scans a circular path at the interface between the probe window and the suspension. As the scanning focused beam sweeps across the face of the probe window, individual particles or particle structures (agglomerated or floc) will backscatter distinct pulses of reflected light. These pulses of backscattered light are detected by the probe and translated into chord lengths, based on the simple calculation of the scan speed (velocity) multiplied by the pulse width (time). A chord length is defined as the straight-line distance from one edge of a particle or particle structure to another edge.

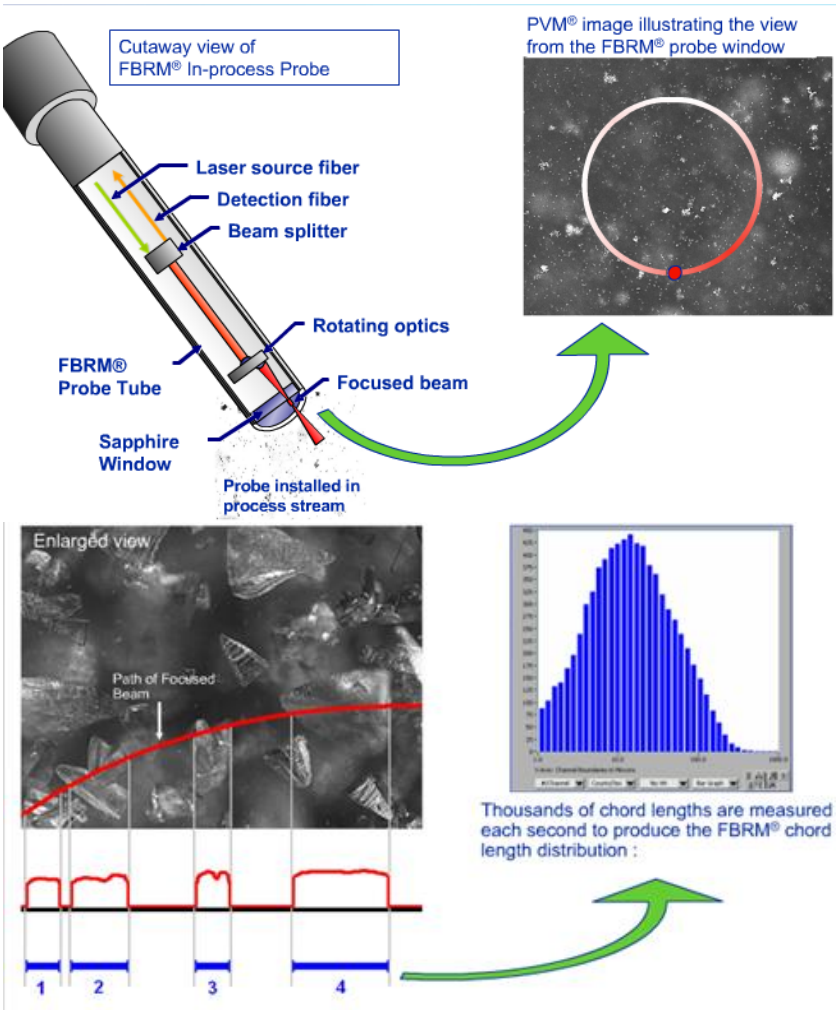

Figure 6-4. Operational principle of FBRM sensor from light signal up to CLD.

During enzymatic hydrolysis, this probe was placed in the reactor and allowed for real-time tracking of chord length and particle count. Acquisition time for all experiment was chosen equal to 30 sec, meaning 1 data point was calculated from the average chord count per second during 30 sec interval. The acquired raw data are treated with the FBRM software by dividing the size range from 0.1 to 1000 µm into 1000 class following a logarithm distribution then returned the average value as number of counts per sec for each class. Due to technical limitation, user can only export the pre-classified data with 100 classes ranging from 0.1 to 1000 µm.

At variance to DLS which allows to determine particle size distribution (PSD), the FBRM provides chord length distribution (CLD). The conversion from number weighted CLD into volume weighted PSD is possible under strict assumptions as described in (Nguyen et al., 2015). Therefore only raw data were considered in this study. To take into account

solubilization phenomenon that takes place during the process, the number chord length distribution (CLD) was multiplied by N_c.

- **Optical morpho-granulometry (MG)**

Changes in particle morphology were characterized using a morpho-granulometer (Mastersizer G3S, Malvern Instruments Ltd. SN: MAL1033756, software Morphologi v7.21). The instrument is composed of a system of lens (magnification: from x1 to x50, particle dimension: from 0.5 to 3000 µm), an optical device (Nikon CFI60 Bright/ Dark field) and a camera (IEEE1394a, Fire Wire^{TM}, 2592x1544 pixels). The morpho-granulometer is a particle size analyzer providing the ability to measure morphological characteristics of individual particles, and to report particle size distribution within a suspension sample. The main steps of a measurement/analysis procedure by the morpho-granulometer apparatus are presented in **Figure 6-5**. The measuring principle is based on the capture of composite image on defined sample area, the on-line image processing, and the identification and analysis of geometric properties of individual cells (such as diameter, aspect ratio, circularity). Multiple morphometric criteria were calculated for each cell particle and associated distributions (in number and in volume) were generated for each parameter.

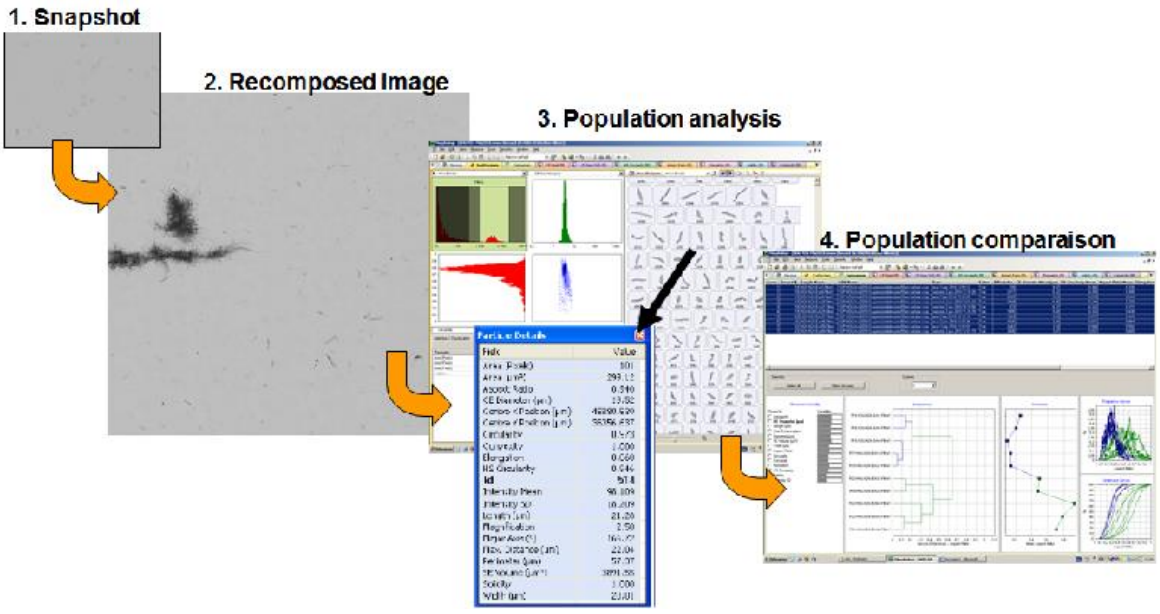

Figure 6-5. Main steps of a measurement procedure by the Malvern Morphology® G3 instrument

Samples analyzed in dry way were dispersed on a glass plate using the dispersion bell and an injection pressure of 3 bar. A surface of 20x20 mm was selected by the operator and

analyzed in bright field with a magnification x 2.5, under the standardized operating conditions (light intensity 64, threshold for particle detection 170).

For sample analyzed in wet way, 60 µL of suspension sample (diluted if necessary) were deposited between cover glass and slide. A surface of 5x5 mm was analyzed in dark field with a magnification x10, under the standardized operating conditions (light intensity 90, exposure time 400 ms, threshold for particle detection 30-100).

APPENDIX

Annex 1. Overview of the experiments performed during this PhD thesis. *Bold text represents the data presented in this manuscript. MG refers to morphogranulometry, FTIR to Fourier Transform Infrared Spectroscopy, Abf to an arabinofuranosidases (GH51) and EC to elementary composition*

Experiment	***Substrate***	***Enzymes***	***Pretreatment***	***Total matter***	***Sugars***	***Proteins***	***In-situ* viscosity**	***DLS***	***FBRM***	***Others***
Matrix - 1	Complete wheat meal	None					X			
Matrix – 2	Complete wheat meal	Rovabio					X			
Matrix – 3	Wheat bran	None					X		X	MG
Matrix – 4	Wheat bran	Rovabio – dose 1					X	X	X	MG
Matrix – 5	Wheat bran	Rovabio – dose 2					X	X	X	MG - FTIR
Matrix – 6	Maize bran	None					X		X	MG
Matrix – 7	Maize bran	Rovabio – dose 1					X	X	X	MG
Matrix – 8	Maize bran	Rovabio – dose 2					X	X	X	MG - FTIR
Starch - 1	**Wheat meal**	**Rovabio**					**X**			
Starch – 2	Maize meal	Rovabio					X			
Starch – 3	**Wheat bran N°1**	**Amyloglucosidases α-amylases + Rovabio**					**X**			
Starch – 4	Wheat bran N°1	Spirizyme + None					X			
Starch – 5	Wheat bran N°1	Spirizyme + Rovabio (dose 1)					X			
Starch – 6	**Wheat bran N°1**	**Spirizyme + Rovabio (dose 2)**					**X**			
Starch – 7	Maize bran	Spirizyme + None					X			
Starch – 8	Maize bran	Spirizyme + None					X			
Starch – 9	Wheat brushed bran	Spirizyme + None					X			
Starch - 10	Wheat brushed bran	Spirizyme + Rovabio					X			

Experiment	*Substrate*	*Enzymes*	*Pretreatment*	*Total matter*	*Sugars*	*Proteins*	*In-situ viscosity*	*DLS*	*FBRM*	*Others*
Ratio – 1	**dWB**	**None**					**X**	**X**	**X**	MG
Ratio – 2	**dWB**	**Rovabio - dose 1**					**X**	**X**	**X**	MG
Ratio – 3	**dWB**	**Rovabio - dose 2**			**X**		**X**	**X**	**X**	MG
Ratio – 4	**dWB**	**Rovabio - dose 3**					**X**	**X**	**X**	MG - EC
Ratio - 5	**dWB**	**Rovabio - dose 4**			**X**		**X**	**X**	**X**	MG - EC - FTIR
Kinetic – 1	**dWB**	**Rovabio (dose max)**					**X**	**X**		
Kinetic – 2	dWB	Rovabio					X			
Kinetic – 3	**dWB + supernatant Kinetic – 2**	**Rovabio**					**X**			
Kinetic – 4	**dWB 6h-treated**	**Rovabio**					**X**			
Comparison - 1	dWB	Rovabio Excel		X		X	X	X	X	
Comparison – 2	dWB	Rovabio Advance		X		X	X	X	X	
Comparison – 4	dWB	XynC	Thermic	X		X	X	X	X	
Comparison – 5	dWB	AeXynM	Thermic	X		X	X	X	X	
Comparison – 6	dWB	XynC + Abf51	Thermic	X	X	X	X	X	X	
Comparison – 7	**dWB**	**Rovabio Advance**	**Thermic**	**X**	**X**	**X**	**X**	**X**	**X**	
Comparison – 8	**dWB**	**None**	**Thermic**	**X**	**X**	**X**	**X**	**X**	**X**	
Comparison – 9	dWB	Rovabio Excel	Thermic	X	X	X	X	X	X	
Comparison – 10	**dWB**	**XynC**	**Thermic**	**X**	**X**	**X**	**X**	**X**	**X**	
Limitation 1	**Milled dWB**	**Rovabio**		**X**	**X**	**X**	**X**	**X**	**X**	MG
Limitation 2	**dWB**	**Rovabio + Rovabio**		**X**	**X**	**X**	**X**	**X**	**X**	
Limitation 3	**dWB**	**Rovabio + Pectinases**		**X**	**X**	**X**	**X**	**X**	**X**	
Limitation 4	**dWB**	**Rovabio + Proteases**		**X**	**X**	**X**	**X**	**X**	**X**	
Limitation 5	**dWB**	**Rovabio + Ctec2**		**X**	**X**	**X**	**X**	**X**	**X**	

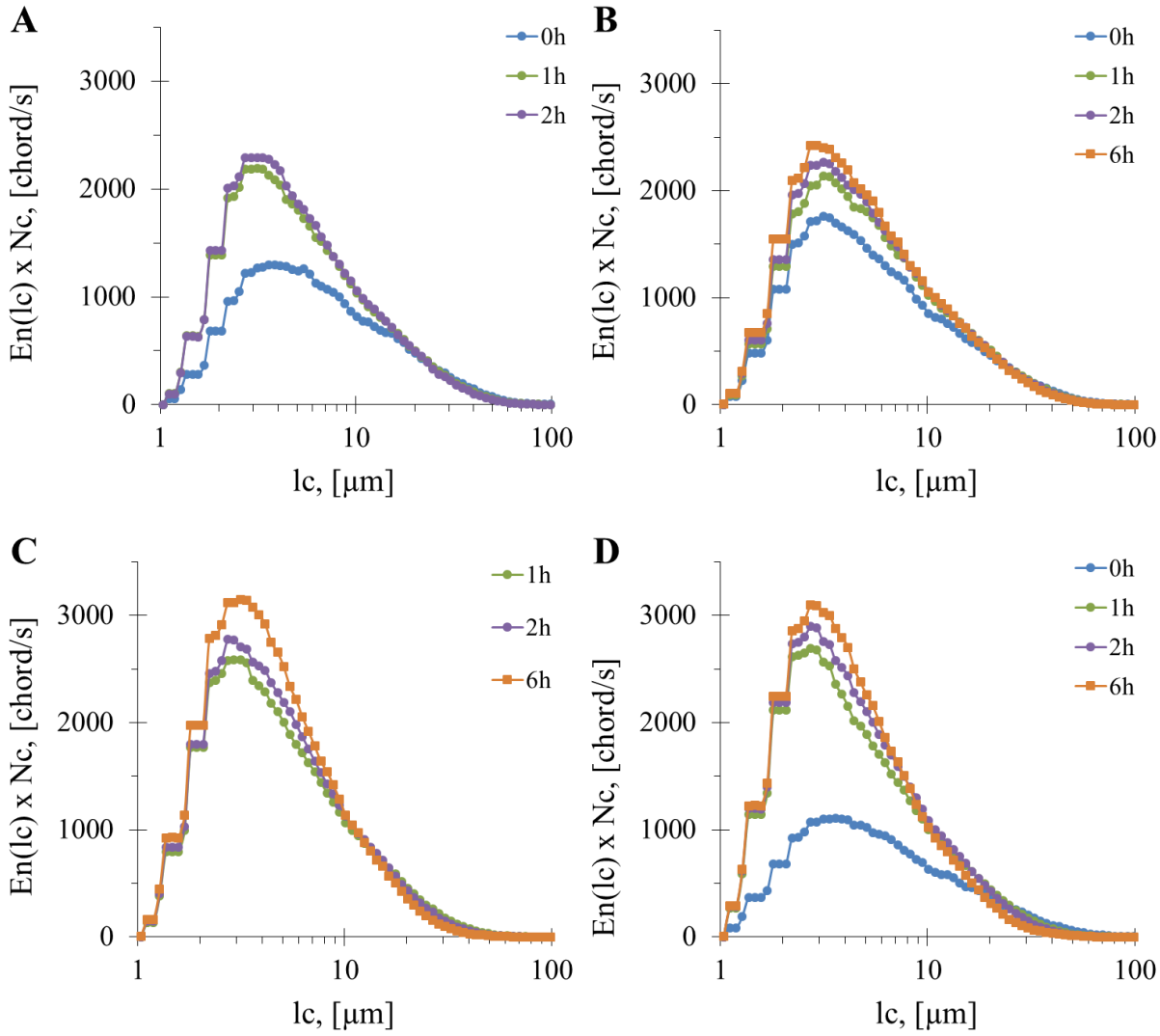

Annex 2. Number distribution of lc multiplied by Nc, for different hydrolysis times with 1.1 U/gdm (A), 11 U/gdm (B), 380 U/gdm (C) and 1100 U/gdm (D)

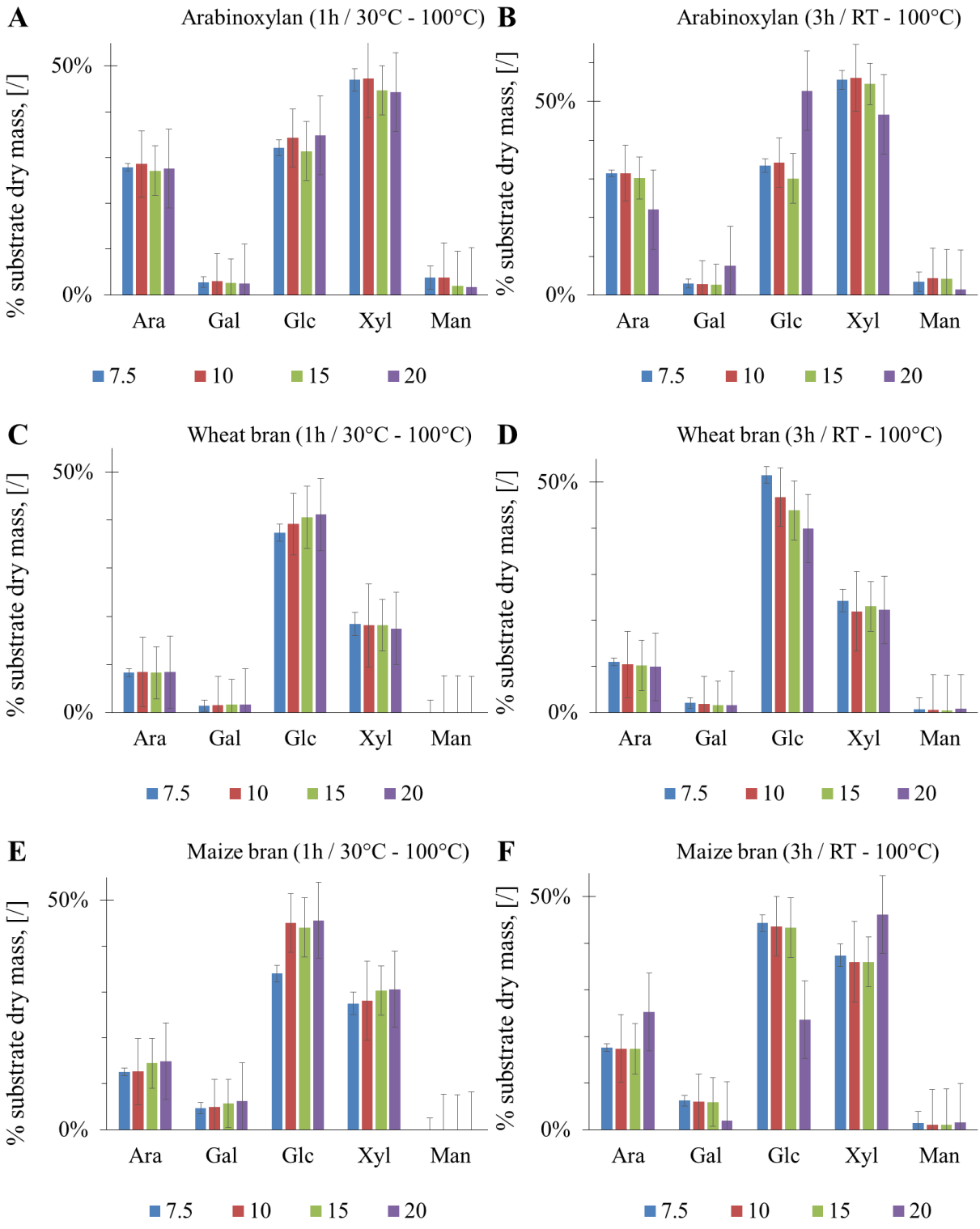

Annex 3. Soluble monosaccharides released after acid hydrolysis of insoluble AX, WB and MB and expressed as the % of the initial dry matter mass treated (% intakes)

REFERENCES

Rocha, V., N. Maeda, R., Pereira, N., F. Kern, M., Elias, L., Simister, R., Steele-King, C., Gómez, L.D., McQueen-Mason, S.J., 2016. Characterization of the cellulolytic secretome of *Trichoderma harzianum* during growth on sugarcane bagasse and analysis of the activity boosting effects of swollenin. Biotechnol. Prog. 32, 327–336. https://doi.org/10.1002/btpr.2217

Abudabos, A.M., Al-Atiyat, R.M., Stanley, D., Aljassim, R., Albatshan, H.A., 2017. The effect of corn distiller's dried grains with solubles (DDGS) fortified with enzyme on growth performance of broiler. Environ. Sci. Pollut. Res. 24, 21412–21421. https://doi.org/10.1007/s11356-017-9808-5

Aftab, U., 2009. Utilization of alternative protein meals with or without multiple-enzyme supplementation in broilers fed low-energy diets. J. Appl. Poult. Res 18, 292–296. https://doi.org/10.3382/japr.2008-00103

Alloui-Lombarkia, O., Zemmouri, F., Smulikowska, S., Alloui, N., 2003. *In-vitro* effects of enzymes on the viscosity and non-starch polysaccharides of barley. Br. Poult. Sci. 44, 800–801.

Almirall, M., Esteve-Garcia, E., 1995. *In-vitro* stability of a β-glucanase preparation from Trichoderma longibrachiatum and its effect in a barley based diet fed to broiler chicks. Anim. Feed Sci. Technol. 54, 149–158. https://doi.org/10.1016/0377-8401(94)00757-Z

Alves, E.F., Bose, S.K., Francis, R.C., Colodette, J.L., Iakovlev, M., Van Heiningen, A., 2010. Carbohydrate composition of eucalyptus, bagasse and bamboo by a combination of methods. Carbohydr. Polym. 82, 1097–1101. https://doi.org/10.1016/j.carbpol.2010.06.038

Amerah, A.M., 2015. Interactions between wheat characteristics and feed enzyme supplementation in broiler diets. Anim. Feed Sci. Technol. 199, 1–9. https://doi.org/10.1016/j.anifeedsci.2014.09.012

Andberg, M., Penttilä, M., Saloheimo, M., 2015. Swollenin from *Trichoderma reesei* exhibits hydrolytic activity against cellulosic substrates with features of both endoglucanases and cellobiohydrolases. Bioresour. Technol. 181, 105–113. https://doi.org/10.1016/j.biortech.2015.01.024

Antoine, C., Peyron, S., Mabille, F., Lapierre, C., Bouchet, B., Abecassis, J., Rouau, X., 2003. Individual contribution of grain outer layers and their cell wall structure to the mechanical properties of wheat bran. J. Agric. Food Chem. 51, 2026–2033. https://doi.org/10.1021/jf0261598

Ao, T., Cantor, A.H., Pescatore, A.J., Pierce, J.L., 2008. *In-vitro* evaluation of feed-grade enzyme activity at pH levels simulating various parts of the avian digestive tract. Anim. Feed Sci. Technol. 140, 462–468. https://doi.org/10.1016/j.anifeedsci.2007.04.004

Apprich, S., Tirpanalan, Ö., Hell, J., Reisinger, M., Böhmdorfer, S., Siebenhandl-Ehn, S., Novalin, S., Kneifel, W., 2014. Wheat bran-based biorefinery 2: Valorization of products. LWT - Food Sci. Technol. 56, 222–231. https://doi.org/10.1016/j.lwt.2013.12.003

Aulrich, K., Flachowsky, G., 2001. Studies on the mode of action of non- starch-polysaccharides (NSP)- degrading enzymes *in vitro*. Arch. für Tierernaehrung 54, 19–32. https://doi.org/10.1080/17450390109381963

Banerjee, G., Scott-Craig, J.S., Walton, J.D., 2010. Improving Enzymes for Biomass Conversion: A Basic Research Perspective. https://doi.org/10.1007/s12155-009-9067-5

Bayod, E., Bolmstedt, U., Innings, F., Tornberg, E., 2005. Rheological characterization of fiber suspensions prepared from vegetable pulp and dried fiber: A comparative study. Annu. Trans. Nord. Rheol. Soc. 13, 249–253.

Beaugrand, J., Crônier, D., Debeire, P., Chabbert, B., 2004. Arabinoxylan and hydroxycinnamate content of wheat bran in relation to endoxylanase susceptibility. J. Cereal Sci. 40, 223–230. https://doi.org/10.1016/j.jcs.2004.05.003

Bedford, M., Classen, H., 1993. An in vitro assay for prediction of broiler intestinal viscosity and growth when fed rye-based diets in the presence of exogeneous enzymes. Poult. Sci. 72, 137–143. https://doi.org/10.3382/ps.0720137

Bedford, M.R., Partridge, G.G., 2011. Enzymes in farm animal nutrition. CABI Pub., Wallingford, Oxfordshire, UK; Cambridge, MA.

Beldman, G., Schols, H.A., Pitson, S.M., Searle-van Leeuwen, M.J.F., Voragen, A.G.J., 1997. Arabinans and arabinan degrading enzymes.

Biely, P., 2012. Microbial carbohydrate esterases deacetylating plant polysaccharides. Biotechnol. Adv. 30, 1575–1588. https://doi.org/10.1016/j.biotechadv.2012.04.010

Biely, P., Singh, S., Puchart, V., 2016. Towards enzymatic breakdown of complex plant xylan structures: State of the art. Biotechnol. Adv. 34, 1260–1274. https://doi.org/10.1016/j.biotechadv.2016.09.001

Boisen, S., Fernández, J.A., 1997. Prediction of the total tract digestibility of energy in feedstuffs and pig diets by *in vitro* analyses. Anim. Feed Sci. Technol. 68, 277–286. https://doi.org/10.1016/S0377-8401(97)00058-8

Boisen, S., Fernández, J.A., 1995. Prediction of the apparent ileal digestibility of protein and amino acids in feedstuffs and feed mixtures for pigs by *in vitro* analyses. Anim. Feed Sci. Technol. 51, 29–43. https://doi.org/10.1016/0377-8401(94)00686-4

Boraston, A.B., Bolam, D.N., Gilbert, H.J., Davies, G.J., 2004. Carbohydrate-binding modules: fine-tuning polysaccharide recognition. Biochem. J. 382, 769–781. https://doi.org/10.1042/BJ20040892

Bradford, M.M., 1976. A rapid and sensitive method for the quantitation of microgram quantities of protein utilizing the principle of protein-dye binding. Anal. Biochem. 72, 248–254. https://doi.org/10.1016/0003-2697(76)90527-3

Brillouet, J.-M., Mercier, C., 1981. Fractionation of wheat bran carbohydrates. J. Sci. Food Agric. 32, 243–251. https://doi.org/10.1002/jsfa.2740320307

Brufau, J., Francesch, M., Pérez-Vendrell, A.M., 2006. The use of enzymes to improve cereal diets for animal feeding. J. Sci. Food Agric. 86, 1705–1713. https://doi.org/10.1002/jsfa.2557

Burton, R.A., Fincher, G.B., 2014. Plant cell wall engineering: applications in biofuel

production and improved human health. Curr. Opin. Biotechnol. 26, 79–84. https://doi.org/10.1016/j.copbio.2013.10.007

Burton, R.A., Gidley, M.J., Fincher, G.B., 2010. Heterogeneity in the chemistry, structure and function of plant cell walls. Nat. Chem. Biol. 6, 724–732. https://doi.org/10.1038/nchembio.439

Call, H.P., Mücke, I., 1997. History, overview and applications of mediated lignolytic systems, especially laccase-mediator-systems (Lignozym®-process). J. Biotechnol. https://doi.org/10.1016/S0168-1656(97)01683-0

Cengiz, O., Koksal, B.H., Onol, A.G., Tatli, O., Sevim, O., Avci, H., Bilgili, S.F., 2012. Influence of dietary enzyme supplementation of barley-based diets on growth performance and footpad dermatitis in broiler chickens exposed to early high-moisture litter. J. Appl. Poult. Res. 21, 117–125. https://doi.org/10.3382/japr.2011-00447

Choct, M., Hughes, R.J., Trimble, R.P., Angkanaporn, K., Annison, G., 1995. Non-starch polysaccharide-degrading enzymes increase the performance of broiler chickens fed wheat of low apparent metabolizable energy. J. Nutr. 125, 485–92. https://doi.org/10.1093/jn/125.3.485

Chotěborská, P., Palmarola-Adrados, B., Galbe, M., Zacchi, G., Melzoch, K., Rychtera, M., 2004. Processing of wheat bran to sugar solution. J. Food Eng. 61, 561–565. https://doi.org/10.1016/S0260-8774(03)00216-4

Chundawat, S.P.S., Beckham, G.T., Himmel, M.E., Dale, B.E., 2011. Deconstruction of Lignocellulosic Biomass to Fuels and Chemicals. Annu. Rev. Chem. Biomol. Eng. 2, 121–145. https://doi.org/10.1146/annurev-chembioeng-061010-114205

Churchill, S.W., 1977. Friction factor equation spans all fluid flow regimes. Chem. Eng. Sci. 84, 91–92.

Classen, H.L., Apajalahti, J., Svihus, B., Choct, M., 2016. The role of the crop in poultry production. Worlds. Poult. Sci. J. https://doi.org/10.1017/S004393391600026X

Cosgrove, D.J., 2017. Microbial Expansins. Annu. Rev. Microbiol. 71, 479–497. https://doi.org/10.1146/annurev-micro-090816-093315

Cosgrove, D.J., 2000. Expansive growth of plant cell walls. Plant Physiol. Biochem. 38, 109–24. https://doi.org/10.1038/35030000

Cozannet, P., Preynat, A., Noblet, J., 2012. Digestible energy values of feed ingredients with or without addition of enzymes complex in growing pigs. J. Anim. Sci 90, 209–211. https://doi.org/10.2527/jas53938

Crepin, V.F., Faulds, C.B., Connerton, I.F., 2004. Functional classification of the microbial feruloyl esterases. Appl. Microbiol. Biotechnol. https://doi.org/10.1007/s00253-003-1476-3

Danicke, S., Vahjen, W., Simon, O., Jeroch, H., 1999. Effects of dietary fat type and xylanase supplementation to rye-based broiler diets on selected bacterial groups adhering to the intestinal epithelium, on transit time of feed, and on nutrient digestibility. Poult. Sci. 78, 1292–1299. https://doi.org/10.1093/ps/78.9.1292

Dasari, R.K., Eric Berson, R., 2007. The effect of particle size on hydrolysis reaction rates and rheological properties in cellulosic slurries. Appl. Biochem. Biotechnol. 137-140, 289–

299. https://doi.org/10.1007/s12010-007-9059-x

Dashtban, M., Schraft, H., Qin, W., 2009. Fungal bioconversion of lignocellulosic residues; Opportunities & perspectives. Int. J. Biol. Sci. 5, 578–595. https://doi.org/10.7150/ijbs.5.578

De La Mare, M., Guais, O., Bonnin, E., Weber, J., Francois, J.M., 2013. Molecular and biochemical characterization of three GH62 α-l-arabinofuranosidases from the soil deuteromycete *Penicillium funiculosum*. Enzyme Microb. Technol. 53, 351–358. https://doi.org/10.1016/j.enzmictec.2013.07.008

de Vries, R.P., Kester, H.C.M., Poulsen, C.H., Benen, J. a E., Visser, J., 2000. Synergy between accessory enzymes from *Aspergillus* in the degradation of plant cell wall polysaccharides. Carbohydr. Res. 327, 401–410. https://doi.org/10.1016/S0008-6215(00)00066-5

de Vries, R.P., Visser, J., Ronald, P., de Vries, R., P., 2001. *Aspergillus* Enzymes Involved in Degradation of Plant Cell Wall Polysaccharides. Microbiol. Mol. Biol. Rev. 65, 497–522. https://doi.org/10.1128/MMBR.65.4.497

Dibble, C.J., Shatova, T.A., Jorgenson, J.L., Stickel, J.J., 2011. Particle Morphology Characterization and Manipulation in Biomass Slurries and the Effect on Rheological Properties and Enzymatic Conversion 1751–1759. https://doi.org/10.1002/btpr.669

Dunaway, K.W., Dasari, R.K., Bennett, N.G., Eric Berson, R., 2010. Characterization of changes in viscosity and insoluble solids content during enzymatic saccharification of pretreated corn stover slurries. Bioresour. Technol. 101, 3575–3582. https://doi.org/10.1016/j.biortech.2009.12.071

Ebringerová, A., Hromádková, Z., Heinze, T., 2005. Hemicellulose 1–67. https://doi.org/10.1007/b136816

Eibinger, M., Sigl, K., Sattelkow, J., Ganner, T., Ramoni, J., Seiboth, B., Plank, H., Nidetzky, B., 2016. Functional characterization of the native swollenin from *Trichoderma reesei*: study of its possible role as C1 factor of enzymatic lignocellulose conversion. Biotechnol. Biofuels 9, 178. https://doi.org/10.1186/s13068-016-0590-2

FAO, 2017. Food outlook, biannual report on global food markets, FAO.

Fardet, A., 2017. New hypotheses for the health-protective mechanisms of whole-grain cereals: what is beyond fibre? https://doi.org/10.1017/S0954422410000041

Fässler, C., Arrigoni, E., Venema, K., Hafner, V., Brouns, F., Amadò, R., 2006. Digestibility of resistant starch containing preparations using two *in-vitro* models. Eur. J. Nutr. 45, 445–453. https://doi.org/10.1007/s00394-006-0618-7

Faulds, C.B., Mandalari, G., Lo Curto, R.B., Bisignano, G., Christakopoulos, P., Waldron, K.W., 2006. Synergy between xylanases from glycoside hydrolase family 10 and family 11 and a feruloyl esterase in the release of phenolic acids from cereal arabinoxylan. Appl. Microbiol. Biotechnol. 71, 622–629. https://doi.org/10.1007/s00253-005-0184-6

François, J.-M., 2007. A simple method for quantitative determination of polysaccharides in fungal cell walls 1, 2995–3000. https://doi.org/10.1038/nprot.2006.457

Fuente, J.M., De Ayala, P.P., Flores, A., Villamide, M.J., 1998. Effect of storage time and dietary enzyme on the metabolizable energy and digesta viscosity of barley-based diets for poultry. Poult. Sci. 77, 90–97. https://doi.org/10.1093/ps/77.1.90

Fuente, J.M., De Ayala, P.P., Villamide, M.J., 1995. Effect of dietary enzyme on the metabolizable energy of diets with increasing levels of barley fed to broilers at different ages. Anim. Feed Sci. Technol. 56, 45–53. https://doi.org/10.1016/0377-8401(95)00815-5

Furniss, C.S.M., Belshaw, N.J., Alcocer, M.J.C., Williamson, G., Elliott, G.O., Gebruers, K., Haigh, N.P., Fish, N.M., Kroon, P.A., 2002. A family 11 xylanase from *Penicillium funiculosum* is strongly inhibited by three wheat xylanase inhibitors. Biochim. Biophys. Acta - Proteins Proteomics 1598, 24–29. https://doi.org/10.1016/S0167-4838(02)00366-7

Gao, X., Kumar, R., Wyman, C.E., 2014. Fast hemicellulose quantification via a simple one-step acid hydrolysis. Biotechnol. Bioeng. 111, 1088–96. https://doi.org/10.1002/bit.25174

Geddes, C.C., Peterson, J.J., Mullinnix, M.T., Svoronos, S.A., Shanmugam, K.T., Ingram, L.O., 2010. Optimizing cellulase usage for improved mixing and rheological properties of acid-pretreated sugarcane bagasse. Bioresour. Technol. 101, 9128–9136. https://doi.org/10.1016/j.biortech.2010.07.040

Georgelis, N., Nikolaidis, N., Cosgrove, D.J., 2015. Bacterial expansins and related proteins from the world of microbes. Appl. Microbiol. Biotechnol. 99, 3807–3823. https://doi.org/10.1007/s00253-015-6534-0

Goacher, R.E., Selig, M.J., Master, E.R., 2014. Advancing lignocellulose bioconversion through direct assessment of enzyme action on insoluble substrates. Curr. Opin. Biotechnol. 27, 123–133. https://doi.org/10.1016/j.copbio.2014.01.009

Goldbeck, R., Damásio, A.R.L., Gonçalves, T.A., Machado, C.B., Paixão, D.A.A., Wolf, L.D., Mandelli, F., Rocha, G.J.M., Ruller, R., Squina, F.M., 2014. Development of hemicellulolytic enzyme mixtures for plant biomass deconstruction on target biotechnological applications. Appl. Microbiol. Biotechnol. 98, 8513–8525. https://doi.org/10.1007/s00253-014-5946-6

Gopalan, N., Rodríguez-Duran, L. V, Saucedo-Castaneda, G., Nampoothiri, K.M., 2015. Review on technological and scientific aspects of feruloyl esterases: A versatile enzyme for biorefining of biomass. https://doi.org/10.1016/j.biortech.2015.06.117

Gourlay, K., Hu, J., Arantes, V., Andberg, M., Saloheimo, M., Penttil, M., Saddler, J., 2013. Swollenin aids in the amorphogenesis step during the enzymatic hydrolysis of pretreated biomass. Bioresour. Technol. 142, 498–503. https://doi.org/10.1016/j.biortech.2013.05.053

Gourlay, K., Hu, J., Arantes, V., Penttilä, M., Saddler, J.N., 2015. The use of carbohydrate binding modules (CBMs) to monitor changes in fragmentation and cellulose fiber surface morphology during cellulase- And swollenin-induced deconstruction of lignocellulosic substrates. J. Biol. Chem. 290, 2938–2945. https://doi.org/10.1074/jbc.M114.627604

Guais, O., Borderies, G., Pichereaux, C., Maestracci, M., Neugnot, V., Rossignol, M., François, J.M., 2008. Proteomics analysis of "Rovabio™ Excel", a secreted protein cocktail from the filamentous fungus *Penicillium funiculosum* grown under industrial process fermentation. J. Ind. Microbiol. Biotechnol. 35, 1659–1668. https://doi.org/10.1007/s10295-008-0430-x

Guais, O., Tourrasse, O., Dourdoigne, M., Parrou, J.L., Francois, J.M., 2010. Characterization of the family GH54 α-l-arabinofuranosidases in *Penicillium funiculosum*, including a

novel protein bearing a cellulose-binding domain. Appl. Microbiol. Biotechnol. 87, 1007–1021. https://doi.org/10.1007/s00253-010-2532-4

Guillén, D., Sánchez, S., Rodríguez-Sanoja, R., 2010. Carbohydrate-binding domains: Multiplicity of biological roles. Appl. Microbiol. Biotechnol. 85, 1241–1249. https://doi.org/10.1007/s00253-009-2331-y

Gunawardana, P., Roland, D.A., Bryant, M.M., 2009. Effect of dietary energy, protein, and a versatile enzyme on hen performance, egg solids, egg composition, and egg quality of Hy-line W-36 hens during second cycle, phase two. J. Appl. Poult. Res. 18, 43–53. https://doi.org/10.3382/japr.2008-00047

Gupta, V.K., Kubicek, C.P., Berrin, J.-G., Wilson, D.W., Couturier, M., Berlin, A., Filho, E.X.F., Ezeji, T., 2016. Fungal Enzymes for Bio-Products from Sustainable and Waste Biomass. https://doi.org/10.1016/j.tibs.2016.04.006

Haraldsson, A.-K., Rimsten, L., Alminger, M., Andersson, R., Åman, P., Sandberg, A.-S., 2005. Digestion of barley malt porridges in a gastrointestinal model: Iron dialysability, iron uptake by Caco-2 cells and degradation of β-glucan. J. Cereal Sci. 42, 243–254. https://doi.org/10.1016/j.jcs.2005.04.002

Hell, J., Kneifel, W., Rosenau, T., Böhmdorfer, S., 2014. Analytical techniques for the elucidation of wheat bran constituents and their structural features with emphasis on dietary fiber - A review. Trends Food Sci. Technol. 35, 102–113. https://doi.org/10.1016/j.tifs.2013.10.012

Henrissat, B., Bairoch, A., 1993. New families in the classification of glycosyl hydrolases based on amino acid sequence similarities. Biochem. J. 293 (Pt 3), 781–8.

Heuzé, V., Tran, G., Baumont, R., Noblet, J., Renaudeau, D., Lessire, M., Lebas, F., 2015. Wheat bran. Feed. a Program. by INRA, CIRAD, AFZ FAO.

Heuzé, V., Tran, G., Suavant, D., Lebas, F., 2016. Maize bran and hominy feed. Feed. a Program. by INRA, CIRAD, AFZ FAO.

Himmel, M.E., Ding, S.-Y., Johnson, D.K., Adney, W.S., Nimlos, M.R., Brady, J.W., Foust, T.D., 2007. Biomass Recalcitrance: Engineering Plants and Enzymes for Biofuels Production. Science (80-.). 315, 804–807. https://doi.org/10.1126/science.1137016

Hoebler, C., Barry, J.L., David, A., Delort-Laval, J., 1989. Rapid acid hydrolysis of plant cell wall polysaccharides and simplified quantitative determination of their neutral monosaccharides by gas-liquid chromatography. J. Agric. Food Chem. 37, 360–367. https://doi.org/10.1021/jf00086a020

Hossain, K., Ulven, C., Glover, K., Ghavami, F., Simsek, S., Alamri, M.S., Kumar, A., Mergoum, M., 2013. Interdependence of cultivar and environment on fiber composition in wheat bran. Aust. J. Crop Sci. 7, 525–531. https://doi.org/10.1007/s11934-014-0462-x

Hu, J., Saddler, J.N., 2018. Why does GH10 xylanase have better performance than GH11 xylanase for the deconstruction of pretreated biomass? Biomass and Bioenergy 110, 13–16. https://doi.org/10.1016/j.biombioe.2018.01.007

Inal, F., Coskun, B., Balevi, T., 2000. The determination of viscosity in barley and using possibilities of barleys, having different viscosity, supplemented with enzyme in layer diets. Indian J. Anim. Sci. 70, 1250–1254.

Jäger, G., Girfoglio, M., Dollo, F., Rinaldi, R., Bongard, H., Commandeur, U., Fischer, R., Spiess, A.C., Büchs, J., 2011. How recombinant swollenin from *Kluyveromyces lactis* affects cellulosic substrates and accelerates their hydrolysis. Biotechnol. Biofuels 4, 33. https://doi.org/10.1186/1754-6834-4-33

Jahangiri, M., Golkar-Narenji, M.R., Montazerin, N., Savarmand, S., 2001. Investigation of the viscoelastic effect on the Metzner and Otto coefficient through LDA velocity measurements. Chin. J. Chem. Eng. 9, 77–83.

Juge, N., 2006. Plant protein inhibitors of cell wall degrading enzymes. Trends Plant Sci. 11, 359–367. https://doi.org/10.1016/j.tplants.2006.05.006

Kang, K., Wang, S., Lai, G., Liu, G., Xing, M., 2013. Characterization of a novel swollenin from *Penicillium oxalicum* in facilitating enzymatic saccharification of cellulose. BMC Biotechnol. 13, 42. https://doi.org/10.1186/1472-6750-13-42

Khanizadeh, S., Buszard, D., Zarkadas, C.G., 1995. Misues of the Kjeldahl method for estimating protein content in plant tissue. HortScience 30, 1341–1342. https://doi.org/10.1021/i560137a008

Knudsen, K.E.B., 2014. Fiber and nonstarch polysaccharide content and variation in common crops used in broiler diets. Poult. Sci. 93, 2380–2393. https://doi.org/10.3382/ps.2014-03902

Kroon, P.A., Williamson, G., 1996. Release of ferulic acid from sugar-beet pulp by using arabinanase, arabinofuranosidase and an esterase from *Aspergillus niger*. Biotechnol. Appl. Biochem. 23, 263–267. https://doi.org/10.1111/j.1470-8744.1996.tb00382.x

Kubicek, C.P., Kubicek, E.M., 2016. Enzymatic deconstruction of plant biomass by fungal enzymes. Curr. Opin. Chem. Biol. https://doi.org/10.1016/j.cbpa.2016.08.028

Kumar, P., Barrett, D.M., Delwiche, M.J., Stroeve, P., 2009. Methods for Pretreatment of Lignocellulosic Biomass for Efficient Hydrolysis and Biofuel Production. Ind. Eng. Chem. (Analytical Ed. 48, 3713–3729. https://doi.org/10.1021/ie801542g

Lafond, M., Bouza, B., Eyrichine, S., Bonnin, E., Crost, E.H., Geraert, P.A., Giardina, T., Ajandouz, E.H., 2011. An integrative *in vitro* approach to analyse digestion of wheat polysaccharides and the effect of enzyme supplementation. Br. J. Nutr. 106, 264–73. https://doi.org/10.1017/S0007114511000134

Lafond, M., Bouza, B., Eyrichine, S., Rouffineau, F., Saulnier, L., Giardina, T., Bonnin, E., Preynat, A., 2015. *In vitro* gastrointestinal digestion study of two wheat cultivars and evaluation of xylanase supplementation. J. Anim. Sci. Biotechnol. 6, 5. https://doi.org/10.1186/s40104-015-0002-7

Lafond, M., Guais, O., Maestracci, M., Bonnin, E., Giardina, T., 2014. Four GH11 xylanases from the xylanolytic fungus *Talaromyces versatilis* act differently on (arabino)xylans. Appl. Microbiol. Biotechnol. 98, 6339–6352. https://doi.org/10.1007/s00253-014-5606-x

Lamp, A.E., Evans, A.M., Moritz, J.S., 2015. The effects of pelleting and glucanase supplementation in hulled barley based diets on feed manufacture, broiler performance, and digesta viscosity. J. Appl. Poult. Res. 24, 295–303. https://doi.org/10.3382/japr/pfv028

Le, T., 2017. Investigation of physical mechanisms during deconstruction of pretreated

lignocellulosic matrix and its ability to liberate a fermentable carbon substrate in a bio-process. INSA. https://doi.org/10.1017/CBO9781107415324.004

Le, T., Anne-Archard, D., Coma, V., Cameleyre, X., Lombard, E., To, K.A., Pham, T.A., Nguyen, T.C., Fillaudeau, L., 2017. Using in-situ viscosimetry and morphogranulometry to explore hydrolysis mechanisms of filter paper and pretreated sugarcane bagasse under semi-dilute suspensions. Biochem. Eng. J. 127, 9–20. https://doi.org/10.1016/j.bej.2017.07.006

Lee, S.Y., Kim, J.S., Kim, J.M., An, B.K., Kang, C.W., 2010. Effects of multiple enzyme (ROVABIO®Max) containing carbohydrolases and phytase on growth performance and intestinal viscosity in broiler chicks fed corn-wheat-soybean meal based diets. Asian-Australasian J. Anim. Sci. https://doi.org/10.5713/ajas.2010.90592

Lei, Z., Shao, Y., Yin, X., Yin, D., Guo, Y., Yuan, J., 2016. Combination of Xylanase and Debranching Enzymes Specific to Wheat Arabinoxylan Improve the Growth Performance and Gut Health of Broilers. J. Agric. Food Chem. 64, 4932–4942. https://doi.org/10.1021/acs.jafc.6b01272

Lequart, C., Nuzillard, J.M., Kurek, B., Debeire, P., 1999. Hydrolysis of wheat bran and straw by an endoxylanase: Production and structural characterization of cinnamoyl-oligosaccharides. Carbohydr. Res. 319, 102–111. https://doi.org/10.1016/S0008-6215(99)00110-X

Levasseur, A., Saloheimo, M., Navarro, D., Andberg, M., Monot, F., Nakari-Setälä, T., Asther, M., Record, E., 2006. Production of a chimeric enzyme tool associating the *Trichoderma reesei* swollenin with the Aspergillus niger feruloyl esterase A for release of ferulic acid. Appl. Microbiol. Biotechnol. 73, 872–880. https://doi.org/10.1007/s00253-006-0546-8

Li, H.-Q., Xu, J., 2013. A new correction method for determination on carbohydrates in lignocellulosic biomass. Bioresour. Technol. 138, 373–6. https://doi.org/10.1016/j.biortech.2013.03.148

Li, W.F., Sun, J.Y., Xu, Z.R., 2004. Effects of NSP Degrading Enzyme on *In vitro* Digestion of Barley. Asian-Australasian J. Anim. Sci. 17, 122–126. https://doi.org/2004.17.1.122

Lide, D., 2000. CRC handbook of chemistry and physics: A ready-reference book of chemical and physical data.

Liu, D., Chen, X., Yue, Y., Chen, M., Wu, Q., 2011. Structure and rheology of nanocrystalline cellulose. Carbohydr. Polym. 84, 316–322. https://doi.org/10.1016/j.carbpol.2010.11.039

Lombard, V., Golaconda Ramulu, H., Drula, E., Coutinho, P.M., Henrissat, B., 2014. The carbohydrate-active enzymes database (CAZy) in 2013. Nucleic Acids Res. 42. https://doi.org/10.1093/nar/gkt1178

Lu, H., Adedokun, S.A., Preynat, A., Legrand-Defretin, V., Geraert, P.A., Adeola, O., Ajuwon, K.M., 2013. Impact of exogenous carbohydrases and phytase on growth performance and nutrient digestibility in broilers. Can. J. Anim. Sci. 93, 243–249. https://doi.org/10.4141/cjas2012-138

Lu, H., Preynat, A., Legrand-Defretin, V., Geraert, P.A., Adeola, O., Ajuwon, K.M., 2016. Effects of dietary supplementation of exogenous multi-enzyme mixture containing carbohydrases and phytase on growth performance, energy and nutrient digestibility, and selected mucosal gene expression in the small intestine of weanling pigs fed nutrient

deficient diets. J. Anim. Sci 96, 243–251. https://doi.org/10.1139/cjas-2015-0078

Luo, D., Yang, F., Yang, X., Yao, J., Shi, B., Zhou, Z., 2009. Effects of Xylanase on Performance, Blood Parameters, Intestinal Morphology, Microflora and Digestive Enzyme Activities of Broilers Fed Wheat-based Diets. Asian-Australasian J. Anim. Sci. 22, 1288–1295. https://doi.org/10.5713/ajas.2009.90052

Maes, C., Delcour, J.A., 2002. Structural Characterisation of Water-extractable and Water-unextractable Arabinoxylans in Wheat Bran. J. Cereal Sci. 35, 315–326. https://doi.org/10.1006

Maisonnier-Grenier, S., Clavurier, K., Saulnier, L., Bonnin, E., Geraert, P.-A., 2006. Biochemical characteristics of wheat and their relation with apparent metabolisable energy value in broilers with or without non-starch polysaccharide enzyme. J. Sci. Food Agric. 86, 1714–1721. https://doi.org/10.1002/jsfa.2555

Makhdum, Z., Habib ur, R., Larik, J.M., Bux, P., Hameed, A., 2013. Crude enzymes supplementation in fibrous diet improves performance of commercial broilers. J. Appl. Anim. Res. 41, 218–222. https://doi.org/10.1080/09712119.2012.742439

Malathi, V., Devegowda, G., 2001. *In Vitro* Evaluation of Nonstarch Polysaccharide Digestibility of Feed Ingredients by Enzymes. Poult. Sci. 80, 302–305. https://doi.org/10.1093/ps/80.3.302

Mangat, M., Kalra, K.L., Kocher, G.S., Phutela, R., Sharma, S., 2010. Comparative ethanol production for two corn varieties by commercial enzymes. Starch/Staerke 62, 647–651. https://doi.org/10.1002/star.200900253

Marketsandmarkets.com, 2015. Feed Enzymes Market by Type (Phytase, Protease, and Carbohydrase), Livestock (Ruminants, Swine, Poultry, and Aquatic Animals), Source (Microorganism, Plant, and Animal), Form (Liquid and Dry), and Region - Global Forecast to 2022.

Martens-Uzunova, E.S., Schaap, P.J., 2009. Assessment of the pectin degrading enzyme network of *Aspergillus niger* by functional genomics. Fungal Genet. Biol. 46 Suppl 1, S170–S179. https://doi.org/10.1016/j.fgb.2008.07.021

McCleary, B. V., Matheson, N.K., 1983. Action patterns and substrate-binding requirements of β-d-mannanase with mannosaccharides and mannan-type polysaccharides. Carbohydr. Res. 119, 191–219. https://doi.org/10.1016/0008-6215(83)84056-7

Metzner, A.B., Otto, R.E., 1957. Agitation of non-Newtonian fluids. AIChE J. 3, 3–10. https://doi.org/10.1002/aic.690030103

Meunier, J.P., Manzanilla, E.G., Anguita, M., Denis, S., Perez, J.F., Gasa, J., Cardot, J.-M., Garcia, F., Moll, X., Alric, M., 2007. Evaluation of a dynamic *in vitro* model to simulate the porcine ileal digestion of diets differing in carbohydrate composition. J. Anim. Sci. 86, 1156–1163. https://doi.org/10.2527/jas.2007-0145

Milne, T.A., Chum, H.L., Agblevor, F., Johnson, D.K., 1992. Standardized analytical methods. Biomass and Bioenergy 2, 341–366. https://doi.org/10.1016/0961-9534(92)90109-4

Min, Y.N., Yan, F., Liu, F.Z., Coto, C., Waldroup, P.W., 2009. Effect of various dietary enzymes on energy digestibility of diets high in distillers dried grains with solubles for broilers. J. Appl. Poult. Res 18, 734–740. https://doi.org/10.3382/japr.2009-00046

Minekus, M., Marteau, P., Havenaar, R., Huis in 't Veld, J.H.J., 1995. A multicompartmental dynamic computer-controlled model simulating the stomach and small intestine. Altern. to Lab. Anim. 23, 197–209.

Mohnen, D., 2008. Pectin structure and biosynthesis. Curr. Opin. Plant Biol. 11, 266–277. https://doi.org/10.1016/j.pbi.2008.03.006

Mosier, N., Wyman, C., Dale, B., Elander, R., Lee, Y.Y., Holtzapple, M., Ladisch, M., 2005. Features of promising technologies for pretreatment of lignocellulosic biomass. Bioresour. Technol. 96, 673–686. https://doi.org/10.1016/J.BIORTECH.2004.06.025

Mottet, A., Tempio, G., 2017. Global poultry production: current state and future outlook and challenges. Worlds. Poult. Sci. J. 1–12. https://doi.org/10.1017/S0043933917000071

Mushtaq, T., Sarwar, M., Ahmad, G., Nisa, M.U., Jamil, A., 2006. The influence of exogenous multienzyme preparation and graded levels of digestible lysine in sunflower meal-based diets on the performance of young broiler chicks two weeks posthatching. Poult. Sci. 85, 2180–2185. https://doi.org/10.1093/ps/85.12.2180

Nahas, J., Lefrancois, M.R., 2001. Effects of feeding locally grown whole barley with or without enzyme addition and whole wheat on broiler performance and carcass traits. Poult. Sci. 80, 195–202. https://doi.org/10.1093/ps/80.2.195

Newman, R.H., Hill, S.J., Harris, P.J., 2013. Wide-Angle X-Ray Scattering and Solid-State Nuclear Magnetic Resonance Data Combined to Test Models for Cellulose Microfibrils in Mung Bean Cell Walls. Plant Physiol. 163, 1558–1567. https://doi.org/10.1104/pp.113.228262

Nguyen, T.C., 2014. *In-situ* and *ex-situ* multi-scale physical metrologies to investigate the destructuration mechanisms of lignocellulosic matrices and release kinetics of fermentescible cellulosic carbon. INSA Toulouse.

Nguyen, T.-C., Anne-Archard, D., Coma, V., Cameleyre, X., Lombard, E., Binet, C., Nouhen, A., Kim Anh, T., Fillaudeau, L., 2013. *In situ* rheometry of concentrated cellulose fibre suspensions and relationships with enzymatic hydrolysis. Bioresour. Technol. 133, 563–572. https://doi.org/10.1016/j.biortech.2013.01.110

Nguyen, T.C., Anne-Archard, D., Fillaudeau, L., 2015. Rheology of Lignocellulose Suspensions and Impact of Hydrolysis : A Review Paper pulp. https://doi.org/10.1007/10

Noblet, J., Jaguelin-Peyraud, Y., 2007. Prediction of digestibility of organic matter and energy in the growing pig from an *in vitro* method. Anim. Feed Sci. Technol. 134, 211–222. https://doi.org/10.1016/j.anifeedsci.2006.07.008

Onipe, O.O., Jideani, A.I.O., Beswa, D., 2015. Composition and functionality of wheat bran and its application in some cereal food products. Int. J. Food Sci. Technol. 50, 2509–2518. https://doi.org/10.1111/ijfs.12935

Osei, S.A., Oduro, S., 2000. Effects of dietary enzyme on broiler chickens fed diets containing wheat bran. J. Anim. Feed Sci. 9, 681–686. https://doi.org/10.22358/jafs/68118/2000

Park, K.R., Park, C.S., Kim, B.G., 2016. An enzyme complex increases *in vitro* dry matter digestibility of corn and wheat in pigs. Springerplus 5, 598. https://doi.org/10.1186/s40064-016-2194-5

Parker, M.L., Ng, A., Waldron, K.W., 2005. The phenolic acid and polysaccharide composition

of cell walls of bran layers of mature wheat (Triticum aestivum L. cv. Avalon) grains. J. Sci. Food Agric. 85, 2539–2547. https://doi.org/10.1002/jsfa.2304

Parkkonen, T., Tervilä- Wilo, A., Hopeakoski- Nurminen, M., Morgan, A., Poutanen, K., Autio, K., 1997. Changes in wheat micro structure following *in vitro* digestion. Acta Agric. Scand. Sect. B - Soil Plant Sci. 47, 43–47. https://doi.org/10.1080/09064719709362437

Peng, F., Peng, P., Xu, F., Sun, R.C., 2012. Fractional purification and bioconversion of hemicelluloses. Biotechnol. Adv. 30, 879–903. https://doi.org/10.1016/j.biotechadv.2012.01.018

Pettersen, R.C., 1991. Wood Sugar Analysis by Anion Chromatography. J. Wood Chem. Technol. 11, 495–501. https://doi.org/10.1080/02773819108051089

Pettersen, R.C., 1984. The Chemical Composition of Wood. pp. 57–126. https://doi.org/10.1021/ba-1984-0207.ch002

Pollegioni, L., Tonin, F., Rosini, E., 2015. Lignin-degrading enzymes. FEBS J. 282, 1190–1213. https://doi.org/10.1111/febs.13224

Prückler, M., Siebenhandl-Ehn, S., Apprich, S., Höltinger, S., Haas, C., Schmid, E., Kneifel, W., 2014. Wheat bran-based biorefinery 1: Composition of wheat bran and strategies of functionalization. LWT - Food Sci. Technol. https://doi.org/10.1016/j.lwt.2013.12.004

Quemada, D., 2006. Modélisation rhéologique structurelle: dispersions concentrées et fluides complexes. Editions TEC & DOC.

Rahman, S.H.A., Choudhury, J.P., Ahmad, A.L., Kamaruddin, A.H., 2007. Optimization studies on acid hydrolysis of oil palm empty fruit bunch fiber for production of xylose. Bioresour. Technol. 98, 554–559. https://doi.org/10.1016/j.biortech.2006.02.016

Ravindran, V., 2013. Feed enzymes: The science, practice, and metabolic realities. J. Appl. Poult. Res. 22, 628–636. https://doi.org/10.3382/japr.2013-00739

Raynal-Ioualalen, R., 1996. Procédé de fractionnement des sons de blé. Extraction et étude des propriétés fonctionnelles des arabinoxylanes. http://www.theses.fr.

Roberto, I.C., Mussatto, S.I., Rodrigues, R.C.L.B., 2003. Dilute-acid hydrolysis for optimization of xylose recovery from rice straw in a semi-pilot reactor. Ind. Crops Prod. 17, 171–176. https://doi.org/10.1016/S0926-6690(02)00095-X

Rodrigues, A.C., Haven, M.Ø., Lindedam, J., Felby, C., Gama, M., 2015. Celluclast and Cellic® CTec2: Saccharification/fermentation of wheat straw, solid–liquid partition and potential of enzyme recycling by alkaline washing. Enzyme Microb. Technol. 79-80, 70–77. https://doi.org/10.1016/j.enzmictec.2015.06.019

Rosgaard, L., Andric, P., Dam-Johansen, K., Pedersen, S., Meyer, A.S., 2007. Effects of substrate loading on enzymatic hydrolysis and viscosity of pretreated barley straw. Appl. Biochem. Biotechnol. 143, 27–40. https://doi.org/10.1007/s12010-007-0028-1

Saeman, J.F., Moore, W.E., Mitchell, R.L., Millett, M.A., 1954. Techniques for the determination of pulp constituents by quantitiative paper chromatography. TAPPI J. 37, 336–343. https://doi.org/10.10371/RD04030

Saha, B.C., 2000. α-L-Arabinofuranosidases: Biochemistry, molecular biology and application in biotechnology. Biotechnol. Adv. https://doi.org/10.1016/S0734-9750(00)00044-6

Saloheimo, M., Paloheimo, M., Hakola, S., Pere, J., Swanson, B., Nyyssönen, E., Bhatia, A., Ward, M., Penttilä, M., 2002. Swollenin, a *Trichoderma reesei* protein with sequence similarity to the plant expansins, exhibits disruption activity on cellulosic materials. Eur. J. Biochem. 269, 4202–4211. https://doi.org/10.1046/j.1432-1033.2002.03095.x

Santos, C.A., Ferreira‐filho, J.A., O 'donovan, A., Gupta, V.K., Tuohy, M.G., Souza, A.P., 2017. Production of a recombinant swollenin from *Trichoderma harzianum* in *Escherichia coli* and its potential synergistic role in biomass degradation. Microb. Cell Fact. 16. https://doi.org/10.1186/s12934-017-0697-6

Saulnier, L., Sado, P.E., Branlard, G., Charmet, G., Guillon, F., 2007. Wheat arabinoxylans: Exploiting variation in amount and composition to develop enhanced varieties. J. Cereal Sci. 46, 261–281. https://doi.org/10.1016/j.jcs.2007.06.014

Scheller, H.V., Ulvskov, P., 2010. Hemicelluloses. Annu. Rev. Plant Biol. 61, 263–289. https://doi.org/10.1146/annurev-arplant-042809-112315

Schulze, E., 1891. Zur Kenntniss der chemischen Zusammensetzung der pflanzlichen Zellmembranen. Berichte der Dtsch. Chem. Gesellschaft 24, 2277–2287. https://doi.org/10.1002/cber.18910240210

Seskeviciene, J., Jeroch, H., Danicke, S., Gruzauskas, R., Volker, L., Broz, J., 1999. Feeding value of wheat and wheat-based diets with different content of soluble pentosans when fed to broiler chickens without or with enzyme supplementation. Arch. Fur Geflugelkd. 63, 129–132.

Shirzadi, H., Moravej, H., Shivazad, M., 2009. Comparison of the effects of different kinds of NSP enzymes on the performance, water intake, litter moisture and jejunal digesta viscosity of broilers fed barley-based diet. J. Food Agric. Environ. 7, 615–619.

Shoseyov, O., Shani, Z., Levy, I., 2006. Carbohydrate Binding Modules: Biochemical Properties and Novel Applications. Microbiol. Mol. Biol. Rev. 70, 283–295. https://doi.org/10.1128/MMBR.00028-05

Simbaya, J., Slominski, B.A., Guenter, W., Morgan, A., Campbell, L.D., 1996. The effects of protease and carbohydrase supplementation on the nutritive value of canola meal for poultry: *In vitro* and *in vivo* studies. Anim. Feed Sci. Technol. 61, 219–234. https://doi.org/10.1016/0377-8401(95)00939-6

Slavin, J.L., Marlett, J.A., 1983. Evaluation of High-Performance Liquid Chromatography for Measurement of the Neutral Saccharides in Neutral Detergent Fiber. J. Agric. Food Chem. 31, 467–471. https://doi.org/10.1021/jf00117a001

Smeets, N., Nuyens, F., Van Campenhout, L., Niewold, T., 2014. Variability in the *in vitro* degradation of non-starch polysaccharides from wheat by feed enzymes. Anim. Feed Sci. Technol. 187, 110–114. https://doi.org/10.1016/j.anifeedsci.2013.10.020

Smith, P.K., Krohn, R.I., Hermanson, G.T., Mallia, A.K., Gartner, F.H., Provenzano, M.D., Fujimoto, E.K., Goeke, N.M., Olson, B.J., Klenk, D.C., 1985. Measurement of protein using bicinchoninic acid. Anal. Biochem. 150, 76–85. https://doi.org/10.1016/0003-2697(85)90442-7

Spanghero, M., Volpelli, L.., 1999. A comparison of the predictions of digestible energy content of compound feeds for pigs by chemical or *in vitro* analysis. Anim. Feed Sci. Technol. 81, 151–159. https://doi.org/10.1016/S0377-8401(99)00076-0

Sumner, J.B., Howell, S.F., 1935. A method for determination of saccharase activity. J. Biol. Chem. 111, 371–378.

Sun, R., Fang, J.M., Tomkinson, J., 2000. Characterization and esterification of hemicelluloses from rye straw. J. Agric. Food Chem. 48, 1247–1252. https://doi.org/10.1021/jf990570m

Svihus, B., 2014. Function of the digestive system. J. Appl. Poult. Res. 23, 306–314. https://doi.org/10.3382/japr.2014-00937

Svihus, B., Sacranie, A., Denstadli, V., Choct, M., 2010. Nutrient utilization and functionality of the anterior digestive tract caused by intermittent feeding and inclusion of whole wheat in diets for broiler chickens. Poult. Sci. 89, 2617–2625. https://doi.org/10.3382/ps.2010-00743

Szijarta, N., Siika-aho, M., Sontag-Strohm, T., Viikari, L., 2011. Liquefaction of hydrothermally pretreated wheat straw at high-solids content by purified Trichoderma enzymes. Bioresour. Technol. 102, 1968–1974. https://doi.org/10.1016/j.biortech.2010.09.012

Tapingkae, W., Yachai, M., Visessanguan, W., Pongtanya, P., Pongpiachan, P., 2008. Influence of crude xylanase from *Aspergillus niger* FAS128 on the *in vitro* digestibility and production performance of piglets. Anim. Feed Sci. Technol. 140, 125–138. https://doi.org/10.1016/j.anifeedsci.2007.02.001

Tekeli, A., Bilgeçli, K., Çelen, F., Kurbal, Ö.F., Bitigiç, M., 2014. Effects of Multi-Enzyme Supplementation in Wheat Based Quail (Coturnix coturnix japonica) Rations an Egg Production, Egg Quality and Some Blood Parameters. Anim. Nutr. Feed Technol. 14. 9-18.

Templeton, D., Ehrman, T., 1995. Determination of Acid Insoluble Lignin in Biomass. Natl. Renew. Energy Lab. L. 003 2011, 2. https://doi.org/NREL/TP-510-42618

Tervilä-Wilo, A., Parkkonen, T., Morgan, A., Hopeakoski-Nurminen, M., Poutanen, K., Heikkinen, P., Autio, K., 1996. *In-Vitro* Digestion of Wheat Microstructure with Xylanase and Cellulase from *Trichoderma reesei*. J. Cereal Sci. 24, 215–225. https://doi.org/10.1006/jcrs.1996.0054

Tuckey, R., March, B.E., Biely, J., 1958. Diet and the Rate of Food Passage in the Growing Chick. Poult. Sci. 37, 786–792. https://doi.org/10.3382/ps.0370786

Vahjen, W., Busch, T., Simon, O., 2005. Study on the use of soya bean polysaccharide degrading enzymes in broiler nutrition. Anim. Feed Sci. Technol. 120, 259–276. https://doi.org/10.1016/j.anifeedsci.2005.02.020

Vahjen, W., Simon, O., 1999. Biochemical characteristics of non starch polysaccharide hydrolyzing enzyme preparations designed as feed additives for poultry and piglet nutrition. Arch. Anim. Nutr. https://doi.org/10.1080/17450399909386147

van den Brink, J., de Vries, R.P., 2011. Fungal enzyme sets for plant polysaccharide degradation. Appl. Microbiol. Biotechnol. 91, 1477–1492. https://doi.org/10.1007/s00253-011-3473-2

van der Klis, J.D., Kwakernaak, C., de Wit, W., 1995. Effects of endoxylanase addition to wheat-based diets on physico-chemical chyme conditions and mineral absorption in broilers. Anim. Feed Sci. Technol. 51, 15–27. https://doi.org/10.1016/0377-

8401(95)00687-I

Van Dyk, J.S., Pletschke, B.I., 2012. A review of lignocellulose bioconversion using enzymatic hydrolysis and synergistic cooperation between enzymes-Factors affecting enzymes, conversion and synergy. Biotechnol. Adv. 30, 1458–1480. https://doi.org/10.1016/j.biotechadv.2012.03.002

Várnai, A., Viikari, L., Marjamaa, K., Siika-aho, M., 2011. Adsorption of monocomponent enzymes in enzyme mixture analyzed quantitatively during hydrolysis of lignocellulose substrates. Bioresour. Technol. 102, 1220–1227. https://doi.org/10.1016/j.biortech.2010.07.120

Viamajala, S., McMillan, J.D., Schell, D.J., Elander, R.T., 2009. Rheology of corn stover slurries at high solids concentrations - Effects of saccharification and particle size. Bioresour. Technol. 100, 925–934. https://doi.org/10.1016/j.biortech.2008.06.070

von Schantz, L., Gullfot, F., Scheer, S., Filonova, L., Cicortas Gunnarsson, L., Flint, J., Daniel, G., Nordberg-Karlsson, E., Brumer, H., Ohlin, M., 2009. Affinity maturation generates greatly improved xyloglucan-specific carbohydrate binding modules. BMC Biotechnol. 9, 92. https://doi.org/10.1186/1472-6750-9-92

Walsh, M.C., Geraert, P.A., Maillard, R., Kluess, J., Lawlor, P.G., 2012. The effect of a non-starch polysaccharide-hydrolysing enzyme (Rovabio® Excel) on feed intake and body condition of sows during lactation and on progeny growth performance. Animal 6, 1627–1633. https://doi.org/10.1017/S1751731112000237

Wang, M., Cai, J., Huang, L., Lv, Z., Zhang, Y., Xu, Z., 2010. High-level expression and efficient purification of bioactive swollenin in *Aspergillus oryzae*. Appl. Biochem. Biotechnol. 162, 2027–2036. https://doi.org/10.1007/s12010-010-8978-0

Wang, Y., Tang, R., Tao, J., Gao, G., Wang, X., Mu, Y., Feng, Y., 2011. Quantitative investigation of non-hydrolytic disruptive activity on crystalline cellulose and application to recombinant swollenin. Appl. Microbiol. Biotechnol. 91, 1353–1363. https://doi.org/10.1007/s00253-011-3421-1

Wertz, J.L., 2010. La lignine.

Wertz, J.-L., 2011. Les hémicelluloses.

West, M.L., Corzo, A., Dozier, W.A., Blair, M.E., Kidd, M.T., 2007. Assessment of dietary rovabio excel in practical united states broiler diets. J. Appl. Poult. Res. 16, 313–321. https://doi.org/10.1093/japr/16.3.313

Wijaya, Y.P., Dhimas, R., Putra, D., Widyaya, V.T., Ha, J., Suh, D.J., Kim, C.S., 2014. Bioresource Technology Comparative study on two-step concentrated acid hydrolysis for the extraction of sugars from lignocellulosic biomass. Bioresour. Technol. 164, 221–231. https://doi.org/10.1016/j.biortech.2014.04.084

Wilfart, A., Jaguelin-Peyraud, Y., Simmins, H., Noblet, J., van Milgen, J., Montagne, L., 2008. Kinetics of enzymatic digestion of feeds as estimated by a stepwise *in vitro* method. Anim. Feed Sci. Technol. 141, 171–183. https://doi.org/10.1016/j.anifeedsci.2007.05.021

Wiman, M., Palmqvist, B., Tornberg, E., Lidén, G., 2011. Rheological characterization of dilute acid pretreated softwood. Biotechnol. Bioeng. 108, 1031–1041. https://doi.org/10.1002/bit.23020

Wong, D.W.S., 2006. Feruloyl esterase: A key enzyme in biomass degradation. Appl. Biochem. Biotechnol. https://doi.org/10.1385/ABAB:133:2:87

Woolridge, E., 2014. Mixed Enzyme Systems for Delignification of Lignocellulosic Biomass. Catalysts 4, 1–35. https://doi.org/10.3390/catal4010001

Yang, J., Zhang, X., Yong, Q., Yu, S., 2010. Three-stage hydrolysis to enhance enzymatic saccharification of steam-exploded corn stover. Bioresour. Technol. 101, 4930–4935. https://doi.org/10.1016/j.biortech.2009.09.079

Yasar, S., Forbes, J.M., 2000. Enzyme supplementation of dry and wet wheat-based feeds for broiler chickens: performance and gut responses. Br. J. Nutr. 84, 297–307. https://doi.org/10.1017/S0007114500001574

Yegani, M., Swift, M.L., Zijlstra, R.T., Korver, D.R., 2013. Prediction of energetic value of wheat and triticale in broiler chicks: A chick bioassay and an *in vitro* digestibility technique. Anim. Feed Sci. Technol. 183, 40–50. https://doi.org/10.1016/j.anifeedsci.2013.03.010

Yoon, S.-Y., Han, S.-H., Shin, S.-J., 2014. The effect of hemicelluloses and lignin on acid hydrolysis of cellulose. Energy 77, 19–24. https://doi.org/10.1016/j.energy.2014.01.104

Zhang, Z., Marquardt, R.R., Guenter, W., 2000. Evaluating the Efficacy of Enzyme Preparations and Predicting the Performance of Leghorn Chicks Fed Rye-Based Diets with a Dietary Viscosity Assay. Poult. Sci. 79, 1158–1167. https://doi.org/10.1093/ps/79.8.1158

Zhou, Q., Lv, X., Zhang, X., Meng, X., Chen, G., Liu, W., 2011. Evaluation of swollenin from Trichoderma pseudokoningii as a potential synergistic factor in the enzymatic hydrolysis of cellulose with low cellulase loadings. World J. Microbiol. Biotechnol. 27, 1905–1910. https://doi.org/10.1007/s11274-011-0650-5

Zhou, S., Runge, T.M., 2014. Validation of lignocellulosic biomass carbohydrates determination via acid hydrolysis. Carbohydr. Polym. 112, 179–185. https://doi.org/10.1016/j.carbpol.2014.05.088

RÉSUMÉ LONG

Les champignons filamenteux sécrètent naturellement une grande variété et quantité d'enzymes hydrolytiques afin de dégrader les polysaccharides complexes composant la biomasse végétale en sucres simples pour assurer leurs croissances. Depuis les années 80, ces cocktails enzymatiques sont utilisés en nutrition animale comme complément alimentaire pour augmenter l'assimilation de polysaccharides faiblement digestibles par les animaux, appelés communément 'fibres', et ainsi améliorer leur santé, leur croissance et leur performance tout en réduisant l'impact de l'élevage sur l'environnement. Ces travaux de thèse vont se concentrer sur un cocktail enzymatique d'origine fongique, Rovabio®, développé par la société Adisseo et contenant une large gamme d'enzymes hydrolytiques sécrétées par le champignon filamenteux *Talaromyces versatilis* dans des conditions de fermentation spécifiques. Plus précisément ils se concentreront sur une étude compréhensive de la manière dont ce cocktail enzymatique complexe décompose et dégrade ces fibres pour les rendre assimilables par les animaux.

En effet, si les effets positifs du cocktail enzymatique Rovabio® sur les performances animales ont été démontrées lors d'études *in-vivo*, son mode d'action et notamment les mécanismes par lesquels les fibres sont déconstruites et rendues accessibles restent encore mal caractérisés. Cette difficulté dans l'identification et la compréhension de ces mécanismes résulte de 3 points : (i) la complexité biochimique et structurelle du substrat, (ii) le nombre et la variété des enzymes composant le cocktail enzymatique et (iii) les conditions d'hydrolyses (suspension solide-liquide à haute teneur en matière sèche et hétérogène) qui limitent les transferts. A ce jour, les travaux se cantonnent à caractériser les activités enzymatiques capables d'agir sur des fibres complexes de manière « unitaire » et éventuellement en synergie avec d'autres enzymes, elles aussi bien caractérisées. Cependant aucune étude ne considère un cocktail dans son entièreté et ne caractérise son mode d'action global sur des substrats polysaccharidiques complexes, car il n'existe pas de méthodes définies pour la réaliser. L'originalité des travaux présentés dans ce manuscrit est donc d'aborder une telle étude rendue possible en s'appuyant sur l'utilisation d'un bioréacteur instrumenté combinant des analyses physiques *in-situ* (viscosimétrie et morphogranulométrie) et biochimiques *ex-situ* afin d'avoir un point de vue global sur ce phénomène de déconstruction des fibres. Cette approche multi-

échelle est par ailleurs originale car rarement considérée en nutrition animale où environ 85% des études sur les additifs alimentaires enzymatiques sont réalisées *in-vivo*.

Le substrat de référence de cette étude est le son de blé. En effet cette céréale compose principalement la ration alimentaire des animaux d'élevage en Europe. Le son représente la partie du grain majoritairement composée de fibres. Notre objectif étant d'étudier plus spécifiquement l'action de du cocktail enzymatique Rovabio® sur la dégradation des NSP (polysaccharides non amylacés), un protocole permettant de désamidonner la matrice a été adapté et permet d'éliminer plus de 70% de l'amidon présent dans le son de blé. Le comportement rhéologique de cette matrice en suspension a été préalablement caractérisé et montre une augmentation de la viscosité et des propriétés rhéofluidifiantes avec une augmentation de la concentration. Une concentration critique, Ccrit, de 50 gdm/L a été identifiée pour le son de blé désamidonné et représente le passage d'une suspension diluée au comportement Newtonien à une suspension semi-diluée au comportement non Newtonien.

Une fois le substrat caractérisé et l'approche expérimentale mise en place et validée nous avons cherché à comprendre quels sont les mécanismes sous-jacents à la déconstruction du son de blé par Rovabio®. Il a alors été mis en évidence que l'action du Rovabio® se caractérise par une première phase de fragmentation notamment des grosses particules, concomitante avec une forte solubilisation de la matière en suspension. La déconstruction du son de blé se poursuit ensuite par un phénomène de fragmentation, cette fois sans solubilisation des polysaccharides. Expérimentalement, une importante chute de la viscosité accompagnée d'une diminution des particules de grandes tailles et d'une augmentation des populations de plus petites tailles en contrepartie sont initialement mesurées. Le son de blé désamidonné est solubilisé en 73,2% de sucres et 26,8% de protéines et la solubilisation des sucres s'arrête après 2 h d'hydrolyse alors que la fragmentation des particules continue et conduit à l'apparition d'une population récalcitrante de taille moyenne. L'ajout d'une xylanase seule, en tant qu'enzyme la plus active du cocktail Rovabio®, solubilise quant à elle la même quantité d'arabinoxylane mais ne permet pas une fragmentation importante des particules. Ces résultats confirment donc l'importance de la richesse et de la diversité d'un cocktail enzymatique pour déconstruire efficacement des structures aussi complexes que le son de blé. Cependant, en dépit de cela, seulement 37% de matière sèche est solubilisée, même en excès de Rovabio®.

Dans un deuxième temps nous avons cherché à comprendre quels sont les facteurs limitant la déconstruction des fibres du son de blé par Rovabio®. Une série d'expérimentations complémentaires a mis en évidence que cette incapacité du cocktail enzymatique à dégrader complètement ces fibres n'avait pour origine ni l'inhibition ni l'inactivation des enzymes mais semblerait provenir d'une inaccessibilité des enzymes à leur substrat. Pour vérifier cette hypothèse, l'accessibilité du substrat a été accrue en augmentant la surface spécifique des particules par un processus de broyage aboutissant à la production d'une population homogène de particules plus fines. Nous avons ainsi pu montrer que ce traitement mécanique permet d'augmenter le rendement d'hydrolyse enzymatique de la fraction récalcitrante du son de blé et que l'accessibilité du substrat est donc le principal facteur limitant l'action du cocktail hydrolytique Rovabio®. En se replaçant dans le domaine de la nutrition animale, ce problème d'accessibilité pourrait difficilement être résolu par un traitement mécanique car, sauf dans le cas d'un processus de broyage intense coûteux en énergie et donc non compétitif sur le plan technico-économique. De plus, il restera toujours une fraction insoluble et non accessible aux enzymes dont les particules qui ne seront solubilisées qu'en surface. Cependant, ce processus se déroule en partie naturellement dans le gésier des volailles (ou estomac musculaire) et joue un rôle important dans le broyage des matières premières, ce qui n'est pas pris en compte dans cette étude.

Une approche physique n'étant pas industriellement compatible, nous avons recherché si cette augmentation de l'accessibilité du substrat pouvait être obtenue via une approche biochimique, c'est-à-dire en complémentant le cocktail Rovabio® en activités enzymatiques pouvant assurer cette fonction. Des cocktails de cellulases, de protéases et de pectinases ont alors été testés successivement. Au final, seule l'addition de pectinases à une suspension de son de blé déjà traitée par Rovabio® permettait d'en augmenter le rendement d'hydrolyse. On retrouve alors d'une part une fragmentation des grosses particules qui se traduit par une augmentation de leurs surfaces spécifiques et d'autre part une solubilisation des particules fines libérées exclusivement en sucres composés de glucose. Cette libération exclusive de glucose suite à l'action d'enzymes type « pectinase » montre clairement qu'elles permettent indirectement d'augmenter l'accessibilité de la cellulose aux cellulases présentes dans le cocktail Rovabio®. Dans l'ensemble, ces résultats mettent en évidence l'intérêt d'utiliser des enzymes déconstructrices attaquant les structures minoritaires de la biomasse mais qui assure la cohésion et la résistance de ce réseau complexe. Ainsi on parvient à fragiliser cette structure

et à augmenter l'accessibilité enzymatique des structures principales du réseau de lignocellulose.

En conclusion, ces résultats permettent une meilleure compréhension des modes d'actions d'un cocktail enzymatique industriel riche tel que Rovabio® et ouvre des pistes de réflexion pour l'optimiser. Ils fournissent des informations détaillées d'un point de vue physique et chimique sur les mécanismes de déconstruction de substrat complexe tel que le son de blé, en utilisant une approche expérimentale intégrée, ce qui est rarement considéré en nutrition animale. Malgré la richesse et la diversité enzymatique de Rovabio®, la déconstruction du son de blé reste limitée à 37%, même en excès d'enzyme. Nos données expérimentales ont montré que cette limitation, qui semble provenir d'une inaccessibilité du substrat, pourrait être surmontée en augmentant la surface spécifique du substrat (traitement mécanique) et/ou en désorganisant sa structure (traitement enzymatique). Cependant ces deux méthodes ne permettent toujours pas une hydrolyse complète du substrat. Au final, ce travail attire l'attention sur des enzymes de déconstruction telles que les pectinases, protéases, FAE (ferulic acide esterases), LPMO (polysaccharides monoxygénases), etc. Au-delà de ceci, on démontre ici la pertinence de combiner le génie des procédés à des approches biochimiques. La conception d'une installation expérimentale dédiée et multi-instrumentée, associée à une stratégie expérimentale bien définie, a permis la compréhension d'un phénomène complexe dépendant de nombreux paramètres qui pourront être modulés au fil des expériences (composition du cocktail, type de substrat, conditions d'hydrolyse, etc.).